1986

Fate and Transport of Low-Ph Hazardous Materials After Deep Well Disposal.

Winton G. Aubert
Louisiana State University and Agricultural & Mechanical College

INFORMATION TO USERS

While the most advanced technology has been used to photograph and reproduce this manuscript, the quality of the reproduction is heavily dependent upon the quality of the material submitted. For example:

- Manuscript pages may have indistinct print. In such cases, the best available copy has been filmed.

- Manuscripts may not always be complete. In such cases, a note will indicate that it is not possible to obtain missing pages.

- Copyrighted material may have been removed from the manuscript. In such cases, a note will indicate the deletion.

Oversize materials (e.g., maps, drawings, and charts) are photographed by sectioning the original, beginning at the upper left-hand corner and continuing from left to right in equal sections with small overlaps. Each oversize page is also filmed as one exposure and is available, for an additional charge, as a standard 35mm slide or as a 17"x 23" black and white photographic print.

Most photographs reproduce acceptably on positive microfilm or microfiche but lack the clarity on xerographic copies made from the microfilm. For an additional charge, 35mm slides of 6"x 9" black and white photographic prints are available for any photographs or illustrations that cannot be reproduced satisfactorily by xerography.

Aubert, Winton G.

FATE AND TRANSPORT OF LOW-PH HAZARDOUS MATERIALS AFTER DEEP WELL DISPOSAL

The Louisiana State University and Agricultural and Mechanical Col. PH.D. 1986

PLEASE NOTE:

In all cases this material has been filmed in the best possible way from the available copy. Problems encountered with this document have been identified here with a check mark __✓__.

1. Glossy photographs or pages _____
2. Colored illustrations, paper or print _____
3. Photographs with dark background _____
4. Illustrations are poor copy _____
5. Pages with black marks, not original copy __✓__
6. Print shows through as there is text on both sides of page _____
7. Indistinct, broken or small print on several pages __✓__
8. Print exceeds margin requirements _____
9. Tightly bound copy with print lost in spine _____
10. Computer printout pages with indistinct print _____
11. Page(s) _____ lacking when material received, and not available from school or author.
12. Page(s) _____ seem to be missing in numbering only as text follows.
13. Two pages numbered _____. Text follows.
14. Curling and wrinkled pages _____
15. Dissertation contains pages with print at a slant, filmed as received __✓__
16. Other _____

_____

_____

University
Microfilms
International

FATE AND TRANSPORT OF LOW-PH HAZARDOUS MATERIALS AFTER DEEP WELL DISPOSAL

A Dissertation

Submitted to the Graduate Faculty of the
Louisiana State University and
Agricultural and Mechanical College
in partial fulfillment of the
requirements for the degree of
Doctor of Philosophy

in

The Department of Petroleum Engineering

by
Winton G. Aubert
B.S., Louisiana State University, 1974
M.S., Louisiana State University, 1975
M.S., Louisiana State University, 1985
December, 1986

ACKNOWLEDGMENTS

I wish to express my most sincere appreciation to my major professor, Dr. William J. Bernard, of the Department of Petroleum Engineering. Timely completion of this work would have been impossible without Dr. Bernard's guidance.

I am very grateful to E. I. DuPont de Nemours and Company, Inc., and the Louisiana Chemical Association for providing funding for this study.

The contributions of Dr. Ralph D. Nelson, Jr., of DuPont, were invaluable and are especially appreciated.

I am thankful to the Department of Petroleum Engineering for affording me the opportunity to undertake this study.

I am grateful to the examining committee for its particiation: Dr. Robert C. McIlhenny of Industrial Engineering, Dr. Oscar K. Huh of the Department of Geology and the Coastal Studies Institute, Dr. Zaki A. Bassiouni, Chairman of the Department of Petroleum Engineering, Dr. Teresa G. Monger of the Department of Petroleum Engineering, and Dr. W. David Constant of the Department of Petroleum Engineering. Dr. Joanne M. Wolcott of the Department of Petroleum Engineering provided valuable advice and guidance, which is most appreciated.

TABLE OF CONTENTS

LIST OF TABLES

LIST OF FIGURES

ABSTRACT

The ultimate fate and chemical kinetics of low-pH hazardous wastes after deep well injection were studied. Two experimental approaches were taken. Chemical kinetics of reactions involving acids and typical formation clays was studied using a batch reaction scheme. The effects of reactions involving flowing acidic waste streams and disposal formations were characterized using sand packs of length one foot, four feet, and twenty feet. A numerical ground water flow simulator was used to model the interactions of flowing acidic wastes with linear sand packs and with a hypothetical waste disposal system.

Reaction rate coefficients and activation energies were determined for reactions of hydrochloric acid, nitric acid, and sulfuric acid with sodium montmorillonite, kaolinite, and illite. Reactions were studied at temperatures of fifty degrees Celsius (122 degrees Fahrenheit) and seventy degrees Celsius (158 degrees Fahrenheit). Values of rate coefficients and activation energies agree reasonably well with those obtained by a previous investigator using a different experimental approach.

Sand pack experimentation provided evidence of the neutralizing effect on acid of typical formation clays. Sand packs containing typical proportions of sodium montmorillonite, illite, and kaolinite were found to have a neutralizing effect on hydrochloric acid, nitric acid,

and sulfuric acid. Actual formation material from a waste disposal well in St. Bernard Parish, Louisiana (the "Kaiser" well), was found to neutralize hydrochloric acid. The Kaiser well material was the most effective at neutralizing acid, and kaolinite was the least effective at neutralizing acid.

The ground water flow simulator SUTRA was used to simulate flow of acidic fluids through sand packs containing Kaiser well material. Simulated results of one foot, four foot, and twenty foot sand pack runs agree reasonably well with experimental results. SUTRA was used to model a hypothetical but realistic low-pH waste disposal system in which wastes were injected for periods of time up to twenty years.

CHAPTER I.

Introduction

Waste disposal by deep well injection has been practiced for more than thirty years. Disposal of liquid, hazardous industrial waste by underground injection has become for waste generators a widely favored method of waste disposal, primarily due to the low cost of this method relative to other means of waste disposal. However, the injection well disposal method has been attacked by critics as a technology of questionable viability. Much of the skepticism directed at underground waste disposal arises from the paucity of information available on the fate and transport of hazardous materials after injection into disposal wells (Gordon and Bloom, 1986).

The United States Congress has actively sought to regulate and control all methods of hazardous waste disposal through such legislation as the Federal Clean Air Act, Toxic Substances Control Act, Safe Drinking Water Act, and the Clean Water Act. Legislation of particular note is RCRA, the Resource Conservation and Recovery Act of 1976 (Public Law 94-580) which, among other provisions, authorized the Environmental Protection Agency (EPA) to list and identify hazardous wastes and regulate deep well disposal. Section 3000 4 (f) and (g) of RCRA provides for banning of underground waste injection beginning in

August, 1988, unless the Environmental Protection Agency can determine that waste injection is not detrimental to environmental quality or to human health.

Louisiana legislation aimed at controlling production and disposal of hazardous wastes includes the following: La. Act 334 of 1978, La. Act 449 of 1979, and La. Acts 795 and 803 of 1984. The latter prohibit well disposal of hazardous wastes after Jan. 1, 1991, except in cases where the hazardous nature of the waste cannot be reduced by technology, the waste cannot be reclaimed, disposal will not endanger the population or the environment, and no reasonable alternative exists to well injection of the wastes.

Possibly the most important activity in designing a waste disposal well is the site selection. Fortunately, an extensive body of geologic information exists, provided by the petroleum industry, on virtually all areas where underground waste disposal is feasible. A disposal formation can be chosen based on subsurface data for a particular area, and then the following criteria, established by the EPA, can be applied: (1) uniformity of disposal medium, (2) large areal extent, (3) substantial thickness, (4) high porosity and permeability, (5) low pressure, (6) saline connate water, (7) separation from potable water, (8) adequate barriers to water above and below the zone of interest, (9) no inadequately plugged wells nearby, and (10) compatibility of the mineralogy and

fluids of the reservoir with the injected wastes.

Five categories of injection wells have been established by the Underground Injection Control program of the Federal Safe Drinking Water Act (Collins and Kayser, 1985). The categories are:

Class I - industrial and municipal hazardous waste disposal wells, excluding Class IV wells;

Class II - brine injection wells, enhanced oil recovery injection wells, and liquid hydrocarbon storage wells;

Class III - solution mining wells;

Class IV - disposal wells for hazardous and radioactive wastes, which inject into or above formations which contain sources of drinking water (these are now banned);

Class V - any injection well not included in Classes I through IV.

Enormous volumes of liquid wastes have been disposed underground. Even if this disposal practice were stopped immediately, a sufficient volume of hazardous waste has accumulated underground over more than thirty years to justify an examination of the fate of these wastes. It is possible, even likely, that some hazardous waste materials will react ionically with sandstone or with clay impurities within sandstone. Such reactions could render the waste immobile, thus permanently confining the waste. Also, reactions could chemically change the waste, making

it non-hazardous. It is unlikely that injected waste streams will be rendered more hazardous by interaction with subsurface environments.

Part of the justification for this study is the possibility of providing information which may aid the EPA in developing guidelines to implement the appropriate sections of the law. Forty one percent of all injected wastes are classified as acidic by the EPA (Gordon and Bloom, 1986). This study will quantitatively examine interactions of a specific hazardous waste, namely acids with a pH below 2.0, with disposal reservoir rocks and assess the characteristics of transport of this hazardous waste after well injection.

This research describes interactions involving acids and sandstone matrices and clay minerals within the rock matrices. A quantitative assessment is made of the extent of the interactions. This information is used to verify and improve existing mathematical models of the processes. A liquid-solid adsorption model developed from experimental results has been included in a numerical fluid-flow simulator. This simulator in conjunction with laboratory sand pack experiments can be used to predict the behavior of acid-sandstone systems and should be a valuable aid in assessing long-term effects of injection of low-pH materials into sandstone formations.

CHAPTER II.

Review of Literature

1. Disposal Well Technology

According to several authors (Galley, 1968, Martinez, 1979, Pojasek, 1980, Reeder, 1977, Smith, 1979, and Warner, 1968), the main concern in planning a hazardous waste disposal well is protection of fresh water supplies from contamination by the waste. Hazardous wastes, usually in aqueous form, are injected under pressure into wells penetrating porous and permeable sedimentary rock formations such as sandstone and limestone. The Resource Conservation and Recovery Act (RCRA) identifies hazardous wastes as low pH (pH < 2.0), high pH (pH > 12.5), material containing cyanide compounds in certain concentrations, and material containing specified concentrations of heavy metals. Aqueous solutions of organic compounds from specific manufacturing processes are also included as "Listed Wastes" (Scrivner, et al., 1986). The rock formations are separated from each other and from the surface by impermeable confining layers, such as shales. The wells are drilled and completed using technology proven through many years of application in the petroleum industry for production and injection wells. The disposal formations lie from about 1000 feet below the surface to more than 10,000 feet below the surface, depending on the geological characteristics of the area. The U.S. Bureau

of Mines has investigated underground waste disposal by observing operating installations at industrial and municipal plants and oilfields (Donaldson, 1976).

Waste streams must usually be pretreated before injection to prevent damage to surface equipment and subsurface tubulars, and to prevent plugging of the injection zone. Pretreatment includes filtration to remove solids and chemical treatment to prevent formation of precipitates in the disposal zone. Salinity of injected fluid must sometimes be adjusted, as many disposal formations are sensitive to the introduction of fresh water. Mungan (1965) found that formation damage in the form of permeability reduction occurred in formations containing the clays illite and kaolinite. This was caused by clay contact with water which was less saline than the native water of the formation. Changes in pH also resulted in permeability damage. The reduction in permeability resulted from small pore channels in the formations being blocked by fine particles such as dispersed clays and cementation material. Particles became dislodged by clay dispersion due to changes in salinity or by dissolution of cement by acids or bases.

One example of fluid treatment for a well used for acid disposal was the use of a polymer compatible with the waste stream. This polymer was degraded by contact with hydrochloric acid and minimized damage to the disposal formation due to its stabilizing effect on formation clays

which had become mobilized (Davis and Jarrell, 1983). In another instance, alkaline waste water was treated with gasoline to remove hydrocarbons before the waste was injected (Athavaley, et al., 1981). Coffey, et al. (1981) described the design of a facility for disposing of caustic wastewater. Their design included the use of a buffer solution injected prior to the waste stream to delay contact of the injected waste with formation water. It was felt that this method would restrict any precipitates from forming near the wellbore. Another facility for underground disposal of effluent from a geothermal power plant was described by Owen, et al. (1979). This design removed supersaturated ionic species and residual suspended solids from brine prior to disposal. Chemical plant wastewater at another site was pretreated by removal of suspended solids and adjustment of pH (making this waste non-hazardous as per RCRA guidelines), then disposed of underground (Dugas and Reed, 1978).

Gordon and Bloom (1986) reported on a list of "potential contamination pathways" developed by the Congressional Office of Technology Assessment. Disposal wells must be designed to prevent the escape of wastes via (1) inadequate confining beds, (2) unplanned hydraulic fracturing of confining layers, (3) displacement of saline water into a potable aquifer, (4) migration of injection liquid into a potable water zone within the same aquifer,

(5) injection into a potable water source, (6) upward migration of waste liquid from the injection zone along the outside of well casing, (7) escape into a potable aquifer due to wellbore failure, or (8) vertical migration and leakage through abandoned or closed wells in the vicinity. Confining layer leaks such as dissolution channels and shrinkage cracks induced by geo-chemical reactions of wastes with injection formations must also be avoided.

EPA criteria for deep disposal wells address all aspects of the wells from design to operational monitoring (Smith, 1979, and Bouwer, 1976). The Federal Safe Drinking Water Act includes a portion on Underground Injection Control (UIC) to adequately safeguard present and future sources of drinking water. Whiteside and Raef (1986) interpreted the UIC regulations as follows: Disposal formations must be saline aquifers containing at least one percent (10,000 milligrams per liter) total dissolved solids (TDS). This criterion may be waived if (1) the aquifer contains greater than 3,000 milligrams per liter (mg/l) TDS and less than 10,000 mg/l TDS, (2) the aquifer is not currently a source of potable water, and (3) the aquifer cannot in the future serve as a source of potable water. A candidate aquifer must have adequate volume and petrophysical properties such as porosity and permeability. There must be adequate confining layers which restrict fluid movement into drinking water zones or

into hydrocarbon production zones. The area of the injection site should have minimal faulting and risk of seismic activity, and should contain no unplugged wells.

According to UIC, three casing strings usually should be used in waste disposal wells. UIC refers to these casings as conductor pipe, surface casing, and protection casing. All casings must be adequate to withstand stresses of drilling, reservoir pressure, workovers, and reservoir and injection fluids. The conductor casing has the largest diameter, and may be either cemented in a drilled wellbore or driven into the ground; it serves to seal shallow water zones and protect against loss of circulation during subsequent drilling. Surface casing is then cemented in a wellbore drilled to near the 3,000 mg/l TDS depth. Cement used to set the surface casing should extend to the surface and should be pressure tested upon curing. Protection casing must be cemented in a wellbore drilled to at least the depth of 10,000 mg/l TDS water. This casing provides some redundancy in protection of potential drinking water zones and is usually cemented back to the surface. George and Thomas (1986) compiled a comprehensive cementing technique for use in disposal wells. Injection tubing is installed inside the protection casing. Injection tubing may terminate at a packer, which provides a physical pressure-resistant barrier to the movement of injected fluids into the casing-tubing annulus. Figure 1 is a diagram of a

Figure 1: Schematic of a Disposal Well Utilizing a Packer Seal (Klemt, et al., 1986)

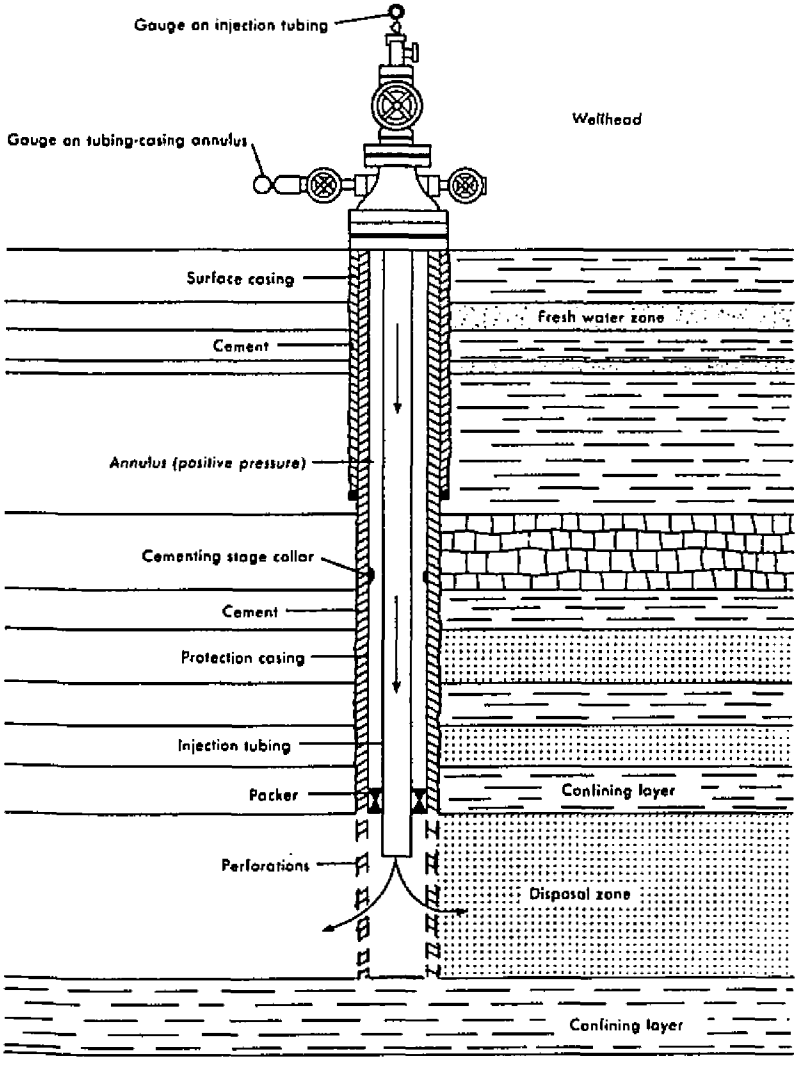

disposal well which utilizes a packer seal. Some disposal wells utilize a fluid seal to provide the barrier to movement of injected fluids into the casing-tubing annulus (Figure 2). Before injection begins, completion techniques such as sand screen installation or gravel packing may be used to prevent the migration of formation solids into the disposal wellbore.

Monitoring of disposal wells during operation is also regulated by UIC. Continuous recordings must be made of injection pressure, flow rate, volume injected, and casing-tubing annulus pressure. Maximum allowable injection pressure is determined by fracture leak-off tests or by the use of fracture pressure correlations. Annulus pressure can be maintained above injection pressure so that any leaks occur from the annulus into the injection tubing rather than vice versa. Most disposal well installations use sacrificial corrosion-monitoring plugs in the injected stream to predict tubing replacement time and evaluate replacement materials.

Mechanical integrity of waste disposal wells must be demonstrated initially and every five years for the working life of the well. UIC mechanical integrity includes (1) no leaks in the casing, tubing, or packer, and (2) no vertical fluid movement into a source of drinking water. Leak detection can be accomplished by pressure tests on the annulus. Vertical migration can be detected or inferred by logging techniques such as

Figure 2: Schematic of a Disposal Well Utilizing a Fluid Seal (Klemt, et al., 1986)

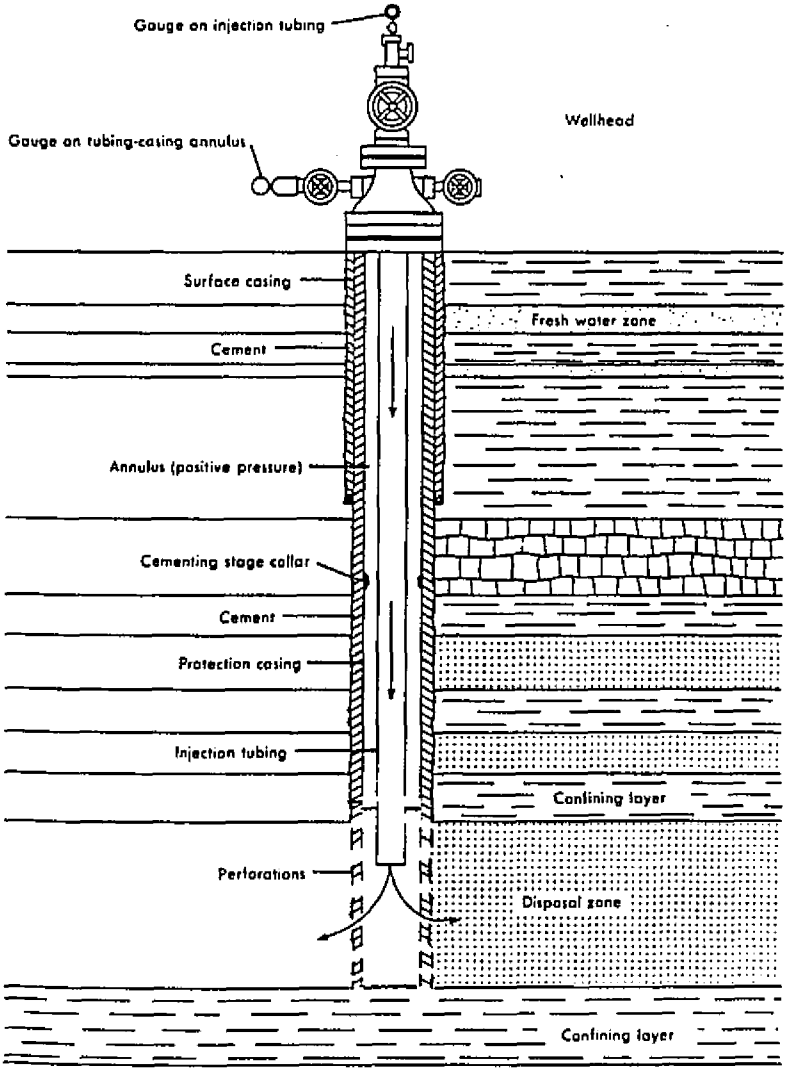

acoustic cement bond logging, temperature logging of deviations from an area's geothermal gradient due to fluid flow, and noise logging to detect casing leaks. One of the most common logging techniques for leak detection in the petroleum industry is the radioactive tracer log, but this method is not mentioned in the UIC regulations.

The U.S. Environmental Protection Agency conducted a survey of the hazardous waste injection industry and the results were reported by Brasier (1986). Salient statistics revealed by the EPA report are that the average disposal well depth is 4,000 feet, the average separation of the disposal zone from aquifers containing less than one percent total dissolved solids is 2,800 feet, and seventy six percent of injection zones are sand or sandstone with a shale confining layer. All disposal wells contain tubing and at least two casing strings. Most of the wells utilize a packer. The packerless wells rely on a fluid seal to separate the casing-tubing annulus and the injection fluid.

2. The Gulf Coast: An Active Underground Disposal Area

Virtually all types of hazardous wastes are being disposed of by deep well injection in the Gulf Coast area. Some general classes of compounds are organic acids, alcohols, and solvents, and inorganic acids, bases, and salts (Ciaccio, 1971, Green, 1983, Mackay, et al., 1985). Waste compounds are disposed of by injection because

incineration, for example, can produce an eventual greater waste volume. Some waste compounds are not biologically degradable or are difficult to decompose and are possibly better suited for underground disposal. Industries which contribute most to the volume of injected hazardous wastes are chemical and petrochemical plants, pharmaceutical producers, oil refineries, natural gas plants, and metals industries.

All the stated geological criteria for waste disposal wells, as well as many sources of industrial wastes, exist along the Gulf Coast (Jacobus, et al., 1985, and Brasier, 1986). Of the 195 deep waste injection wells active in the United States during 1983, more than sixty percent were in Louisiana and Texas. Most of the 195 disposal wells were located on sites where the wastes were generated. Eighty nine percent of injected volume was accounted for by the petro-chemical industry.

Subsurface geology of the Gulf Coast is characterized by alternating layers of sedimentary deposits (Eardley, 1981). These deposits are relatively young, geologically. More than twenty thousand feet of Tertiary and Quaternary sediments make up the Gulf Coast geosyncline, which is the principal geological structure underlying this area. Rocks in this area range in age from recent to about 65 million years old, and are frequently so unconsolidated that producing wells often must be modified to prevent the production of sand grains. Also common in the Gulf Coast

subsurface are salt domes. Salt domes, also known as salt diapirs, exist in various sizes and shapes, and these structures are often a basis of geologic traps for petroleum, as the salt has pierced and deformed nearby fluid-bearing sedimentary strata.

Waste disposal reservoirs in the Gulf Coast area are composed primarily of sandstone, which usually exhibits the necessary porosity and permeability to contain large quantities of fluid and to allow fluid flow (Latil, 1980). These reservoirs are not pure sandstone; the sandstone layer may be streaked with another sedimentary rock, usually shale, or the sandstone matrix may contain some concentration of impurities, such as clays. Van der Marel and Beutelspacher (1968, 1976) presented a detailed study of these materials. Some of the common clays and related minerals indigenous to Gulf Coast sandstone formations are listed in Table 1.

Some of the clays present in sandstone formations are active clays and react preferentially with certain ions and other molecules (Bourgoyne, et al., 1986). For example, sodium montmorillonite, the major mineral in bentonite, reacts with water, a polar molecule, as follows: When bentonite is brought into contact with fresh water, the water molecules hydrate the sodium ions and displace the ions from the surface or interlayers of the crystals in bentonite. The hydrated ions and water molecules are physically much larger and cause the

Table 1: Clays and related minerals common to sandstones

Kaolins - kaolinite

Smectites - montmorillonite

Micas - illite, potassium bentonite, vermiculite

Chlorites - hydrated chlorite

Irons - hematite

Silicas - quartz

Carbonates - Ca, dolomite

Sulphurs - sulfide,sulfate

Feldspars - Na, Ca

Organic matter - lignin, coke

bentonite structure to expand about ten to twelve times its unreacted size. This hydration process is reversible and responds differently to varied ions in solution, thus explaining why some sandstone formations are sensitive to the introduction of fresh water. Expansion or swelling of clays in the presence of fresh water inside a sandstone matrix can result in a drastic reduction in the permeability of the sandstone, as the physically larger clay molecules take up more space in the pore channels within the sandstone. Other reactions could cause the clay to become a "migratable fine" and physically plug pore throats. Inorganic ions which react to change the volume of bentonite are sodium, potassium, calcium, and some acids and bases. Organic molecules may produce similar effects dependent on the magnitude of their dielectric constant. Waste streams can contain all of these ionic species, various organic compounds, and heavy metal wastes.

Louisiana wells accounted for more than twenty one percent of the approximately 12.5 billion gallons of hazardous waste disposed of during 1983. Industries within seven La. parishes between Baton Rouge and New Orleans produced 13,465,944 tons of hazardous wastes during 1983. More than ninety eight percent of these wastes were retained on-site and were then handled by injection well disposal (73.3 percent) or surface impoundment (22.6 percent) prior to treatment. Table 2

Table 2: Compounds Injected into a Louisiana Disposal Well

Pesticide process water
Aqueous waste of toluene
Spent caustic
Sodium bromide solution
Adiponitrile of HI and ZN
Caustic sulfide
Acid cleaning solution
Allyl chloride
HCl of cobalt and zinc
HCl
Caustic
Herbicide waste water
Waste xylene
HCl of $AlCl_3$
Zinc water
Recycled styrene
Methanol waste
Propylene by-products
Waste glycol
Dinitrophenol
Alcohol waste
Metachloro and methyl benzoate
Plant water
Waste alcohol water
Salt water
Waste liquids of D.M.F.
Neutralized H_2SO_4
Ammonia wash water
Spent HCl
Spent acid
Ammonium bromate water

lists some of the compounds which were injected into a typical Louisiana waste disposal well (Martinez, 1979). However, over sixty percent of the net wastes produced in Louisiana in 1983 was water containing small concentrations of hazardous materials under EPA designator codes D002 (corrosive), D003 (reactive), and D007 (chromium > 5.0 mg/liter).

Figure 3 contrasts hazardous wastes with total produced wastes in Louisiana. Waste disposal distribution by parish is illustrated in Figure 4. Figures 5 and 6 represent produced waste distribution by EPA code sort and common classification.

The apparent popularity in Louisiana of waste disposal by deep well injection can be attributed in no small part to the extreme cost advantage enjoyed by well disposal relative to other methods of waste disposal (Jacobus, et al., 1985). As indicated in Figure 7, average disposal cost per ton for injection well disposal in Louisiana is $0.54, cost per ton for land fill/impoundment is $24.00, and cost per ton for incineration is $136.00. EPA estimates for average waste disposal costs are $8.00 per ton for well injection, $28.00 per ton for surface impoundment, and $50.00 per ton for landfilling (Gordon and Bloom, 1986).

Figure 3

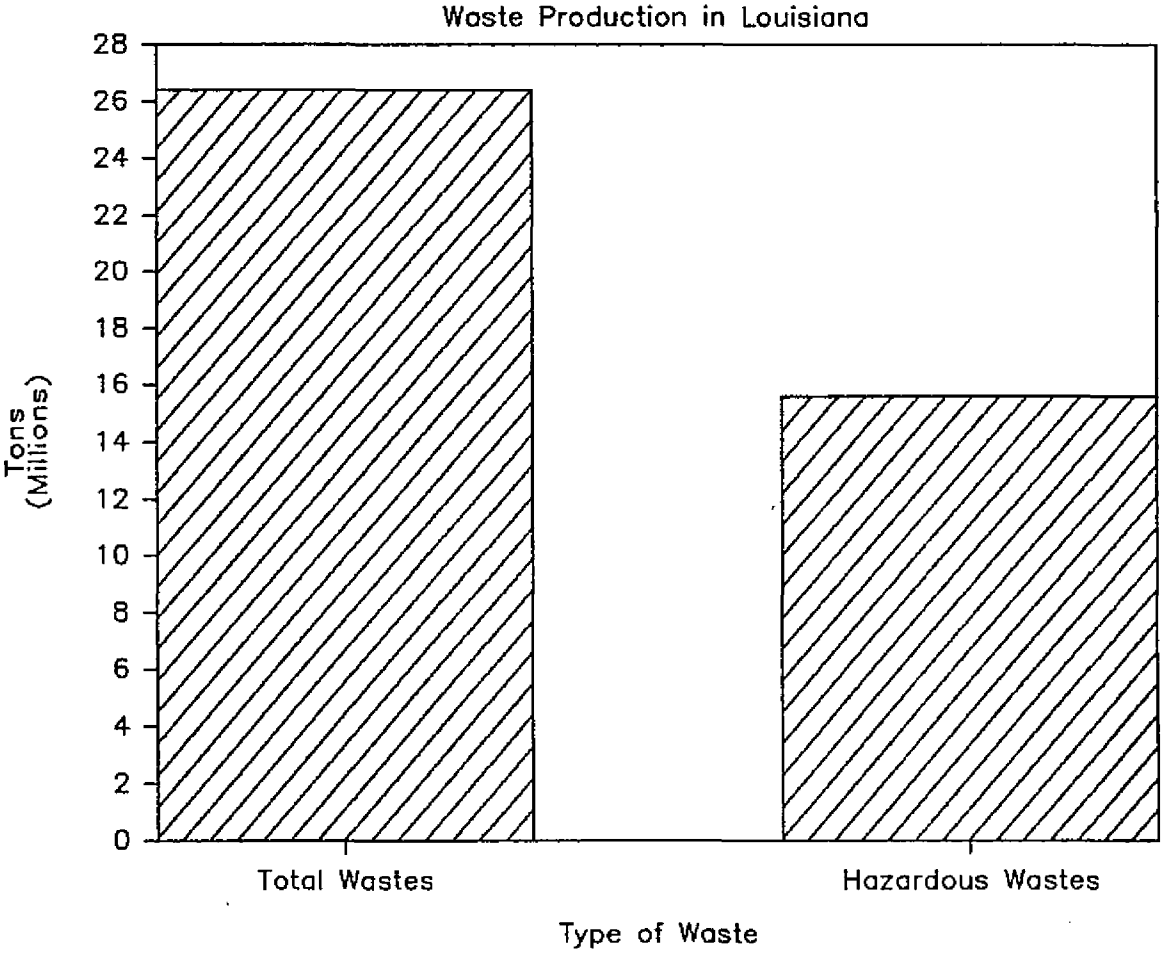
Waste Production in Louisiana
28
26
24
22
20
18
16
14
12
10
8
6
4
2
0
Tons (Millions)
Total Wastes
Hazardous Wastes
Type of Waste

Figure 4

Waste Disposal Distribution by Parish

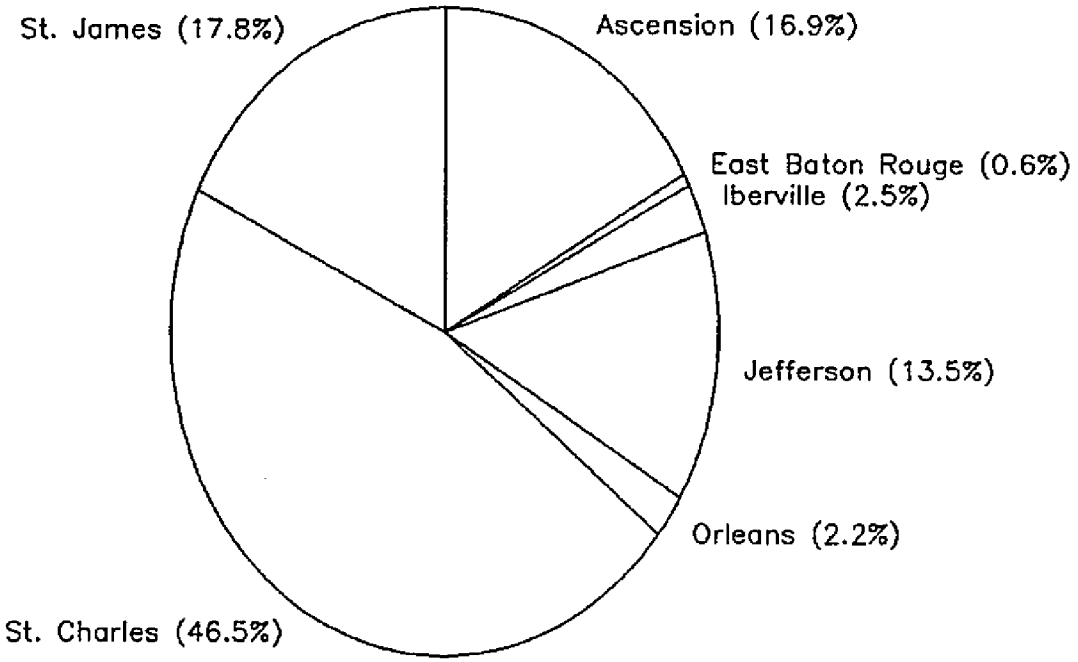

Figure 5

EPA Wastes (Jacobus, et al., 1985)

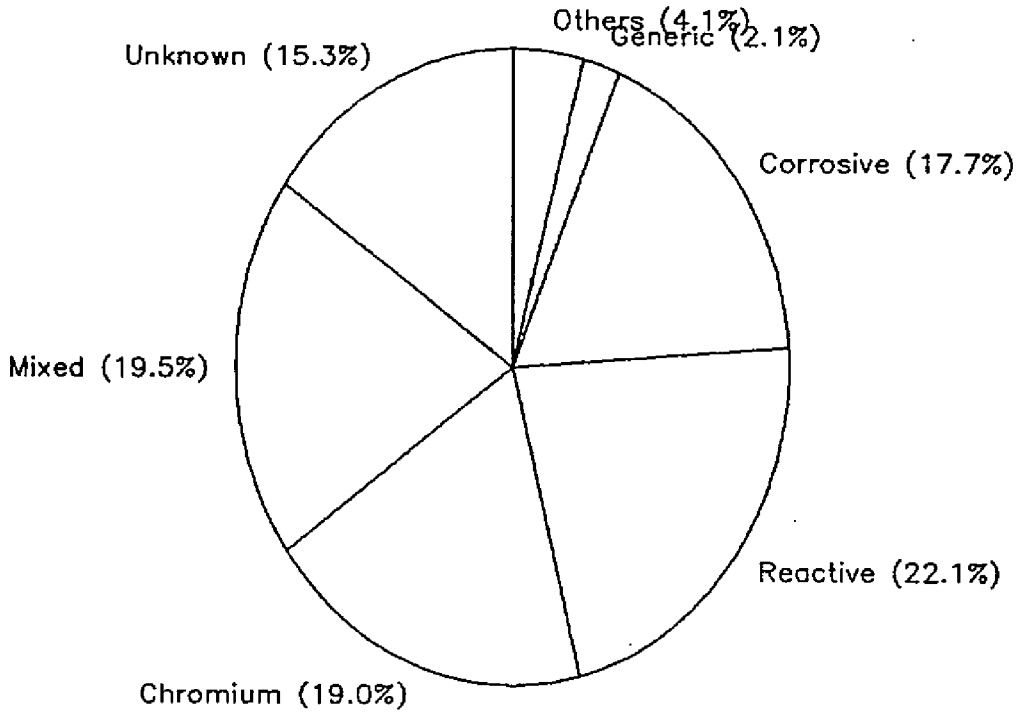

Figure 6

Common Names (Jacobus, et al., 1985)

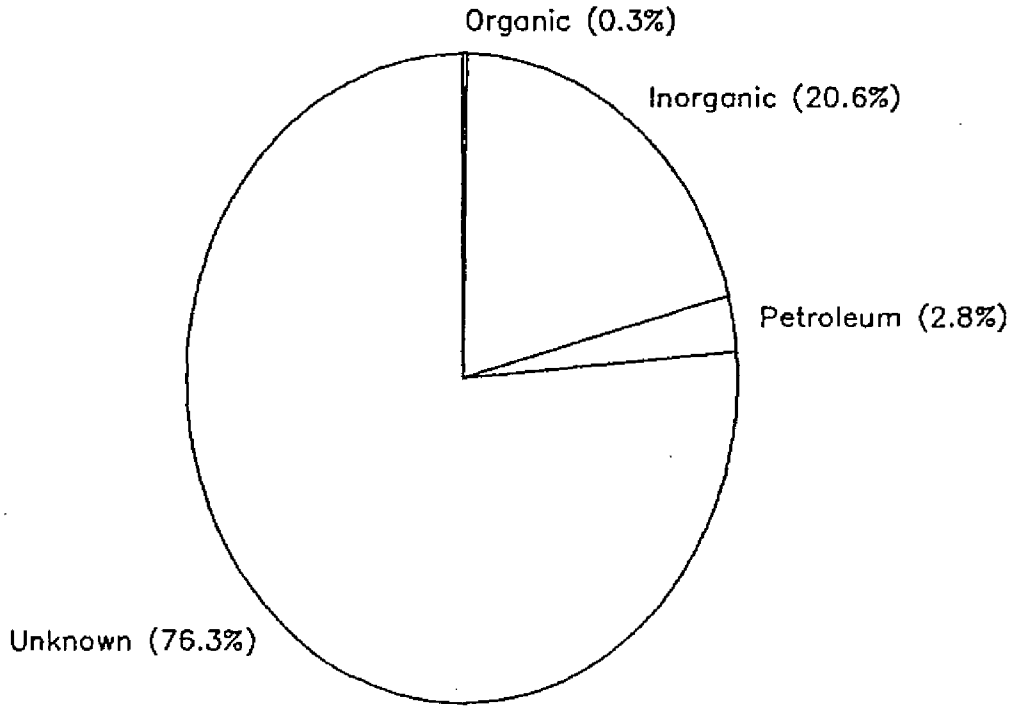

Figure 7

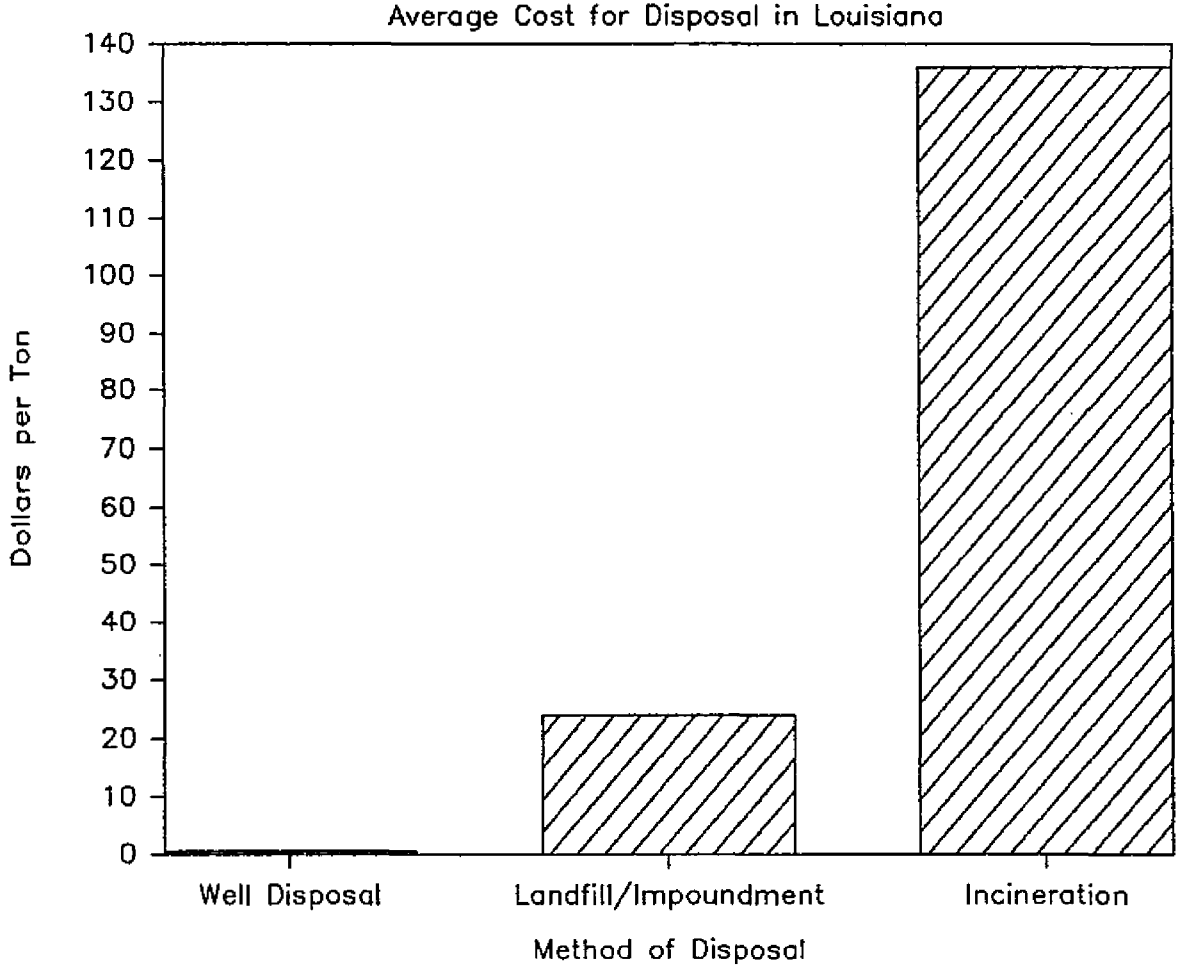
Average Cost for Disposal in Louisiana
Dollars per Ton
140
130
120
110
100
90
80
70
60
50
40
30
20
10
0
Well Disposal
Landfill/Impoundment
Incineration
Method of Disposal

3. Acid Dissolution of Clays

One of the mechanisms by which waste solutions interact with formation materials is by acid dissolution of clay minerals. Several researchers have addressed this phenomenon. The first report on the use of an acid dissolution technique to determine the chemical analysis of a clay was that of Brindley and Youell (1951). This often-quoted work states that dissolution rates of magnesium, iron, and hydrogen from magnesium chlorite are nearly equal. The aluminum dissolution rate was found to closely approximate that for magnesium, etc. at first, but then the rate decreased markedly. This phenomenon was explained by the initial dissolution rate representing aluminum in octahedral positions in the clay structure, and the slower rate reflecting dissolution of aluminum from tetrahedral locations.

Two studies by Osthaus (1954, 1956) have been very enlightening. In the first study, the clays nontronite and montmorillonite were reacted with dilute hydrochloric acid. Semilogarithmic plots of iron and aluminum in solution vs. time showed distinct changes in slope as the dissolution reaction proceeded. The initial rapid increase of aluminum and iron resulted from dissolution dominated by ions in the clays' octahedral layer. A less rapid increase of solution ions followed, from the tetrahedral layer. In the 1956 study, dissolution curves were generated for several montmorillonites and

nontronite. The plots were generally semilogarithmic straight lines or curves which could be resolved into two straight lines, which agreed with the results of Brindley and Youell (1951). Osthaus further determined that the acid dissolution of metal ions from clays is a first order reaction with the rate constant increasing proportional to acid concentration. Granquist and Sumner (1959) confirmed the kinetics results of Osthaus; they observed pseudo-first order reactions of a Texas bentonite with acid. Included in this study was a consideration of the effect of clay surface area changes on the reactions. (For a description of first order and pseudo first order reactions, see Chapter III.)

Turner (1964) studied the kinetics of acid dissolution of two common clay minerals, montmorillonite and kaolinite. He found that the acid dissolution of metal ions (iron, magnesium, aluminum) from the lattice structure of the clay followed pseudo first order kinetics regarding acid concentration and temperature. The rate constant for dissolution of aluminum, in a 30% HCl solution at 80 deg. C., from the octahedral layer of kaolinite, was determined to be 0.0083 $hr.^{-1}$ and the rate constants for dissolution of iron, magnesium, and aluminum from the octahedral structure of montmorillonite were nearly equal and found to be 0.0207 $hr.^{-1}$ This author further showed that the rates of dissolution of silica and alumina were about equal. However, Turner prepared his

clay samples by dispersing them in distilled water. Such preparation allows the clays to hydrate, or expand, thus rendering the clay structure more susceptible to entry by external ionic species such as hydrogen. The use of a brine solution in clay preparation would have better simulated the clays' native (subsurface) environment. Similar results were reported by Abdul-Latif and Weaver (1969) for the clays palygorskite and sepiolite. Reaction rate constants decreased from magnesium to iron to aluminum. The rate constant for magnesium in sepiolite was found to be about 240 times the rate constant for magnesium in sepiolite.

Acid dissolution of clays corresponds to a heterogeneous, or two-phase, system in which reactions occur involving a liquid (acid) phase and a solid (clay) phase. Often computations of chemical and phase equilibria are made simultaneously to include strong interaction effects. A nonlinear method for solving equilibrium, material balance, and phase relationships was presented by Sanderson and Chien (1973). The solution method was programmed for a large digital computer, and is a fast iterative solution method.

Another author, Miller (1965), reported similarly on the mechanisms by which hydrogen displaces aluminum from montmorillonite and kaolinite clays. His results indicated pseudo zero order kinetics for release of aluminum from kaolinite and pseudo first order kinetics

for release of aluminum from montmorillonite. He proposed two different mechanisms of reaction: for kaolinite, a diffusion controlled "edge" attack by hydrogen, and for montmorillonite, an "all surface" attack by which hydrogen released aluminum. Novak and Cicel (1978) studied fifteen smectites, the clay group which contains montmorillonite. The dissolution rate of the octahedral layer was found to be dependent on the substitution of Fe^{3+} and Mg^{2+} for Al^{3+} in octahedral positions.

Notwithstanding the previously mentioned authors' attempts to calculate structural formulae for montmorillonite and kaolinite clays, Ross (1969) determined that the acid dissolution technique of determining relative amounts of aluminum in octahedral and tetrahedral positions could not be used in the stated calculation. This study also indicated no preferential displacement of octahedral over tetrahedral aluminum by hydrogen in eight chlorites. Sand columns containing various amounts of clay were constructed by Griffin and Shimp (1978). They found that movement through the columns of magnesium and iron was restricted by cation exchange, while movement of heavy metals such as lead, mercury, and zinc was restricted by precipitation of the ions.

Laudelout, et al. (1968), presented a treatise in which free energy and enthalpy changes were measured and calculated for ion exchange processes of magnesium,

calcium, barium, sodium and other cations in montmorillonite clay. They achieved good agreement between experimental and mathematical techniques. Banin (1968) experimentally determined ion exchange isotherm curves for calcium-sodium, calcium-potassium, sodium-potassium, calcium-hydrogen, and sodium-hydrogen ion pairs, all in montmorillonite clay. The shape of the curves for ion exchange reactions of calcium-sodium and calcium-potassium were found to be identical, but the calcium-hydrogen exchange isotherm differed considerably.

Bromley (1973) analytically correlated data on concentrated electrolytes in aqueous solutions. His empirical expressions are reasonable approximations for activity coefficients of many salt solutions. Meissner and Kusik (1973) predicted activity coefficients of concentrated electrolytes in aqueous solutions, and developed a relationship for determining vapor pressure of water in aqueous solutions of more than one electrolyte.

Thermodynamics of electrolyte solutions has been treated by many authors. Pitzer (1973) presented a system of simplified equations describing the thermodynamic properties of electrolytes to concentrations of several molal. His equations appeared to agree well with experimental results.

Maes, et al. (1975), studied ion exchange adsorption of metal ions in sodium montmorillonite. A linear relationship of ion exchange and composition was found up

to an exchange level of about seventy percent. Huang (1973) presented thermodynamic stability diagrams of halloysite, kaolinite, sodium montmorillonite, and potassium mica. Stability diagrams have been used to represent natural geologic systems in equilibrium and to predict the eventual mineralogical characteristics of unstable geologic horizons. Geologic structures in which a transformation from predominantly montmorillonite clay to predominantly illite clay has recently occurred are important in exploration for hydrocarbons. Structural formulas for kaolinite and sodium montmorillonite are given as $Al_2Si_2O_5(OH)_4$ (kaolinite) and $Na_{0.33}Al_{2.33}Si_{3.67}O_{10}(OH)_2$ (montmorillonite). Inoue and Minato (1979), in observing cation exchange equilibria for calcium-potassium montmorillonite at various temperatures and normalities, found that montmorillonite showed a greater selectivity for the calcium ion. In 1953, Gaines and Thomas (1953) derived expressions for thermodynamic equilibrium constants of ion exchange for adsorption on montmorillonite clay. This mathematically rigorous work has limited applicability to the present research.

In phase equilibria calculations, non-ideal behavior of liquid reactants at a liquid-vapor interface is described by activity coefficients. Deviations from ideal gas behavior of gaseous reactants are taken into account by fugacity coefficients. Nothnagel, et al. (1973), reported association constants for 178 pure fluids and

established mixing rules for estimating constants for mixtures. These authors felt the information useful for calculating equilibria for non-ideal systems such as petrochemicals.

Ion exchange phenomena as affecting enhanced recovery of hydrocarbon fluids have been studied by several authors. Ionic hardness of formation fluids can render ineffective some chemical flooding processes. Smith (1978) treated laboratory cores by preflushing with brines of low ionic concentration to displace hard solutions. In some cases large volumes were required when the preflush contained relatively low concentrations of ions. More saline preflush was found to be effective at smaller preflush volumes. The effects of dispersion, cation exchange, and adsorption on chemical flooding were studied by Lake and Helfferich (1978). This work demonstrated that when small volumes of chemicals are used in a flood, dispersion effects modify calculated results. These authors described a new phenomenon in which cation exchange is initiated by dispersion. An extension of this 1978 study was carried out by Hill and Lake (1978). Surfactants, which modify surface tension between flood solutions and formation surfaces, complicated cation exchange and a divalent cation-surfactant "complex" was postulated. It was also found that surfactant adsorption on formation surfaces was reduced by twenty percent by reducing the cation concentration in the surfactant from

300 parts per million (ppm) to zero. The experimental results of Hill and Lake (1978) were compared to calculated values by Hirasaki (1982). The 1982 study showed that a surfactant system in which the concentration of sodium and calcium was constant in all components of the flood can undergo significant changes in calcium concentration due to ion exchange. Bunge and Radke (1983) presented a chromatographic theory for ion exchange during an alkaline flood. They showed that efficiency of alkaline preflushing is dependent on the exchange isotherm, size of the preflush, pH and salinity of the preflush, and the ionic character of the rock. Increasing injected pH and salinity was more efficient than increasing the size of the preflush, up to a critical volume approximating continuous injection. Lieu, et al. (1982) investigated the aspects of consumption of sodium hydroxide and sodium orthosilicate by reservoir sands during alkaline flooding. A long-term pulse study, in which reactants were pumped under pressure into a test well which communicated hydraulically with a monitor well, revealed that alkaline concentration decreased exponentially with time. After 120 days the concentration of one percent sodium hydroxide had dropped to zero. Similar results were observed for sodium orthosilicate. Sodium hydroxide concentration also decreased with increasing flow rate.

The reported experimental results pertaining to clay

minerals are inconclusive. Some report congruent dissolution, but other researchers report incongruent dissolution with pseudo-first order or zero order dissolution rates. Most reports fail to examine the possibility of other reaction products being present. All clay minerals are not the same, as kaolinite behaves differently, and is structurally different from, illite or montmorillonite.

4. Waste Movement and Transport

Attempts to assess underground waste transport have achieved mixed results. Leenheer, et al. (1976) , and Ehrlich, et al. (1979), sampled effluent from monitor wells which issued from injected organic waste streams. In the first case the organic wastes were unstable and reactive, producing iron compounds and acid precipitates which plugged the injection wells. Groundwater samples 1500 feet to 2000 feet away from the injection well contained methane and hydrogen sulfide gases, and samples fifty feet to 150 feet away showed evidence of dissolution of formation carbonates. In the other instance, organic carbon compounds were converted to carbon dioxide by subsurface bacteria. These studies yielded results which reflect a relative lack of experimental control and a necessarily large number of experimental variables. Pascale and Martin (1978) reported encouragingly on a Florida deep-well waste

injection system. Over thirteen billion gallons of acidic waste containing inorganic salts and organic compounds were injected into a limestone formation under a 220 feet thick confining layer. Three monitor wells were used for data collection, with two wells penetrating the injection zone 1.9 miles north and 1.5 miles south of the injection site. A shallow monitor well penetrated the first permeable zone above the confining layer. Pressures in the injection zone wells increased less than thirty psi over seven years, with no changes in the effluent water chemistry. Pressure in the shallow well decreased about four psi, but increases in the concentrations of HCO_3^- and organic carbon have been observed in the effluent. In another system, the Glyben-Herzberg, a bouyant plume of injected waste, which was clearly discernable from the aquifer liquids, rose vertically until it migrated down gradient with fresh water flowing over the injection zone, according to Heutmaker, et al. (1977).

There are many reports of successful long-term operation of underground disposal wells. Hanby (1986) discussed three wells which began operation in 1969, 1974, and 1982. Injection rates averaged fifty eight to seventy gallons per minute. Every two years the well casing is inspected, the tubing is pulled, and logs are run. The area of waste movement is estimated by comparing injected volume with reservoir volume, and increases in injection pressure are calculated. Davis and Hineline (1986) report

that less than two percent of all disposal wells have caused environmental damage. Plugging of the injection zone caused by biological activity, inadequate fluid pretreatment, or incompatibility of fluids is the most common operational problem. They also point out that most "well failures" are actually improper operation of monitoring equipment which does not result in any contamination. Walter (1986) researched the history of a disposal well which was completed in 1960. After injected fluids were discovered at the surface near the well, and the cause was determined to be shallow leaks in the well casing, a monitor well network was installed. Injected wastes were found in a shallow sand about 150 feet from the injection well. However, additional monitor wells penetrating the only heavily used aquifer in the area found no contamination. A large volume of fluid has since been removed from the contaminated sand, and the level of contamination has dropped considerably.

5. Reactions of Wastes and Disposal Formations

A wide variety of hazardous materials is disposed by underground injection. Low pH (acidic) and high pH (alkaline) wastes can be neutralized by various reactions which are likely to occur within specific disposal formations. Scrivner, et al. (1986) presented a summary of significant reactions which affect the hazardous nature of wastes.

Carbonate formations such as limestone and dolomite react with acidic wastes to raise the pH. A typical reaction (Scrivner, et al., 1986) is

$$2HCl + CaCO_3 \text{ -----> } CaCl_2 + H_2O + CO_2 \text{ (aqueous).}$$

Sandstone formations (SiO_2) undergo slow dissolution in aqueous alkaline solutions and lower the pH of the solution. The reactions followed in caustic sandstone dissolution are complex, but can be represented as

$$SiO_2 + 2OH^- \text{ -----> } Si(OH)_2O_2^{-2} \text{ (silicate).}$$

The silicate species can be a mixture of $Si(OH)_4$, $Si(OH)_3O^-$, $Si(OH)_2O_2^{-2}$, and $Si_4(OH)_4O_8^{-4}$. The kinetic equation which describes the neutralization of alkaline materials by sandstone is

$$\frac{d[OH^-]}{dt} = -k_s[OH^-]$$

where $k_s = 4.24E06\ e^{-9750/T}\ sec^{-1}$, with T in degrees Kelvin.

Acidic solutions also cause dissolution of sandstone, but at very slow rates (Iler, 1979). Typical reactions are

$$SiO_2 + 2H_2O \text{ -----> } H_4SiO_4 \text{ (silicic acid)}$$

and $$H_4SiO_4 + H^+ \text{ -----> } H_2O + Si(OH)^{+3}.$$

The concentration of total silica in solution is approximately

$$C_{Si} = \log^{-1} \{ 0.522 - 0.053 * pH - 1162/(T + 273) \}.$$

Reactions of acid with clay proceed faster than acid-sandstone reactions. Clay constituents such as aluminum, magnesium, and iron are more soluble in acid than is silica, so the acid neutralization process in a sandstone-clay system is dominated by clay. Clays contain a silica structure and an alumina or aluminosilicate structure. Clay dissolution by acid attack is an extraction of metal ions from the aluminosilicate or alumina lattice. The silica lattice is left intact and exhibits a very similar x-ray diffraction pattern to the original clay at metal extractions of up to fifty percent. Extraction of aluminum from octahedral positions in the aluminosilicate lattice occurs at a faster rate than extraction of tetrahedrally-positioned aluminum, as reported by Turner (1964) and Mathews, et al. (1955).

Clay dissolution can be significant for alkaline wastes. Reactions of clays and high pH solutions result in a tendency toward neutral pH. Organic compounds can

hydrolyze in aqueous solutions, which then usually become less hazardous. Metal ions can be removed from solution by co-precipitation after injection. Ion exchange between clays and metals can occur. Organic compounds can undergo microbial degradation to reduce their hazardous nature.

6. Clay Structure

Naturally occurring clay minerals are classified based on chemical composition or physical structure (Beutelspacher and van der Marel, 1968). Three types of clay which represent various configurations of aluminosilicate structure are smectites, micas, and kaolins. Common examples of each clay are montmorillonite (smectite), illite (mica), and kaolinite (kaolin). Each clay has structural features which contribute to its ion exchange characteristics. Iler (1979) presented a complete description of clay structures and structural formulas.

i) Sodium Montmorillonite (Smectite)

Smectites exhibit a tetrahedral-octahedral-tetrahedral (TOT) structure. The formula which represents this sheet-like structure is

$$2SiO_2 \cdot Al_2O_3 \cdot 2SiO_2.$$

Physically, smectite appears as a central layer of aluminum oxide in octahedral configuration holding

together two silica sheets in tetrahedral coordination. When aluminum ions plus surface sodium ions replace silicon in the tetrahedral structure, or magnesium ions plus surface sodium ions replace aluminum in the octahedral layer, other ionic species and water (an ion-like polar molecule) can readily penetrate between the sheets. This penetration causes a change in the relative positions of the layers, which is also referred to as "slippage". If water penetrates between the tetrahedral and octahedral layers, the water molecules interact with sodium ions and remove them from their positions as "replacements". Removal of monovalent sodium ions results in a net negative charge on the sheets from which sodium is removed. The entire structure is thus easily dispersed or expanded as the similarly-charged layers repel each other.

Sodium montmorillonite is a form of smectite that is often found in sandstone formations, and is sufficiently abundant to be mined for use in drilling muds. In sodium montmorillonite no silicon in tetrahedral positions is replaced by magnesium. In about one-sixth of the aluminum octahedra, magnesium ions plus surface sodium ions replace aluminum. Aluminum has a +3 oxidation state and magnesium has a +2 oxidation state. All the aluminum and magnesium ions then occupy positions in the octahedral layers while the sodium ions associated with the magnesium assume positions between the tetrahedral and octahedral

structures. Figure 8 is a schematic of one configuration of sodium montmorillonite. One means by which metal ions including sodium, aluminum, and magnesium are dissociated from sodium montmorillonite is via displacement by hydrogen. Acid compounds provide the concentration of ionic hydrogen necessary to accomplish clay dissolution. One reaction scheme by which acids "attack" sodium montmorillonite is

$$12SiO_2 \cdot (2MgO + 5Al_2O_3) \cdot 12SiO_2 \cdot Na_2O \cdot 6H_2O + 36H^+ \longrightarrow 2Na^+ + 2Mg^{+2} + 10Al^{+3} + 24SiO_2 + 24H_2O.$$

Thirty-six moles of acid thus react with one mole of sodium montmorillonite. One mole of sodium montmorillonite is

$$12*60 + 2*40 + 5*102 + 12*60 + 62 + 6*18 = 2200 \text{ grams.}$$

Or, one gram of sodium montmorillonite will neutralize 0.0164 moles of acid.

ii) Illite (Mica)

Micas also exhibit tetrahedral-octahedral-tetrahedral structure. In mica most of the tetrahedral silicon is replaced by aluminum plus surface sodium. Aluminum occupies tetrahedral and octahedral sites with sodium in positions between the layers. Figure 9 represents the structure of illite.

Figure 8: Structure of Sodium Montmorillonite (Grim, 1962)

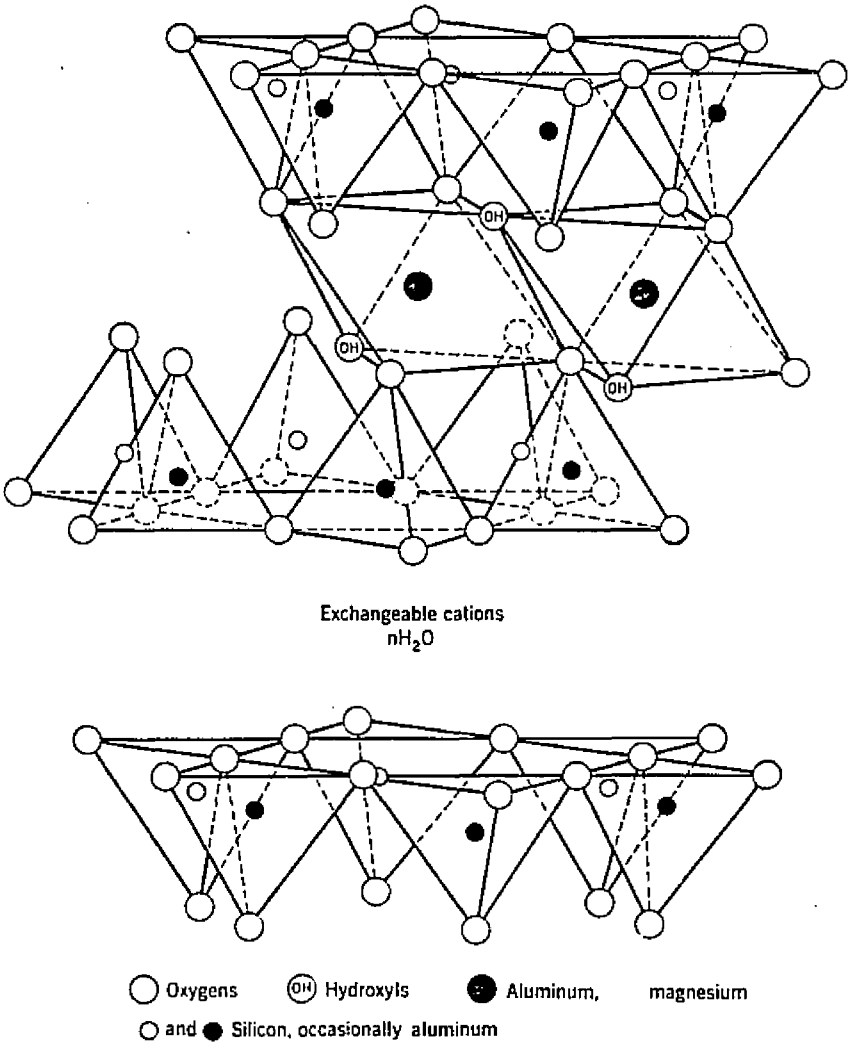

Figure 9: Structure of Illite (Grim, 1962)

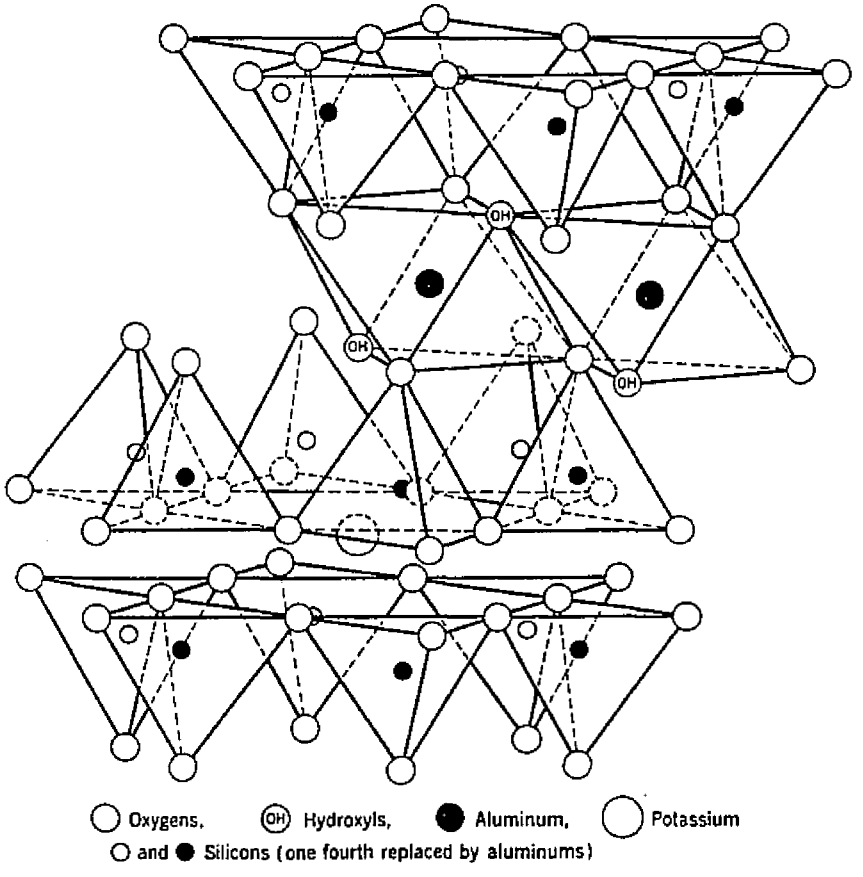

A naturally abundant form of mica is muscovite, in which about one fourth of the silicon in tetrahedral positions is replaced by aluminum. An associated potassium ion replaces an equal number of sodium ions in inter-layer sites. In warm environments some potassium ions are replaced by H_3O^- radicals. This resulting form of mica is known as illite, another clay often found in sandstones.

Illite undergoes acid dissolution similarly to montmorillonite. Aluminum in octahedral sites reacts faster than aluminum in tetrahedral positions. A typical acid-illite reaction is

$$(Al_2O_3 + 6SiO_2) \cdot 4Al_2O_3 \cdot (Al_2O_3 + 6SiO_2) \cdot 2K_2O \cdot 4H_2O + 40H^+ \longrightarrow 4K^+ + 12Al^{+3} + 12SiO_2 + 24H_2O.$$

Forty moles of acid react with one mole of illite. One mole of illite is

$$(102 + 6*60) + 4*102 + (102 + 6*60) + 2*94 + 4*18 = 1592 \text{ grams.}$$

One gram of illite can neutralize 0.0251 moles of acid.

iii) Kaolinite (Kaolin)

Kaolins differ from the previously discussed clays in that tetrahedral silica layers alternate with octahedral aluminum oxide layers. Very little ionic replacement

alters the structure in which the only metal ions contained in the tetrahedral layers are silicon and the only metal ions in the octahedral layers are aluminum. Figure 10 is a representation of kaolinite.

Acid dissolution of kaolinite can follow this scheme:

$$2Al_2O_3 \cdot 4SiO_2 \cdot 4H_2O + 12H^+ \longrightarrow 4Al^{+3} + SiO_2 + 10H_2O.$$

Twelve moles of acid react with 2*102 + 4*60 + 4*18 = 516 grams of kaolinite. One gram of kaolinite can neutralize 0.0233 moles of acid.

Figure 10: Structure of Kaolinite (Grim, 1962)

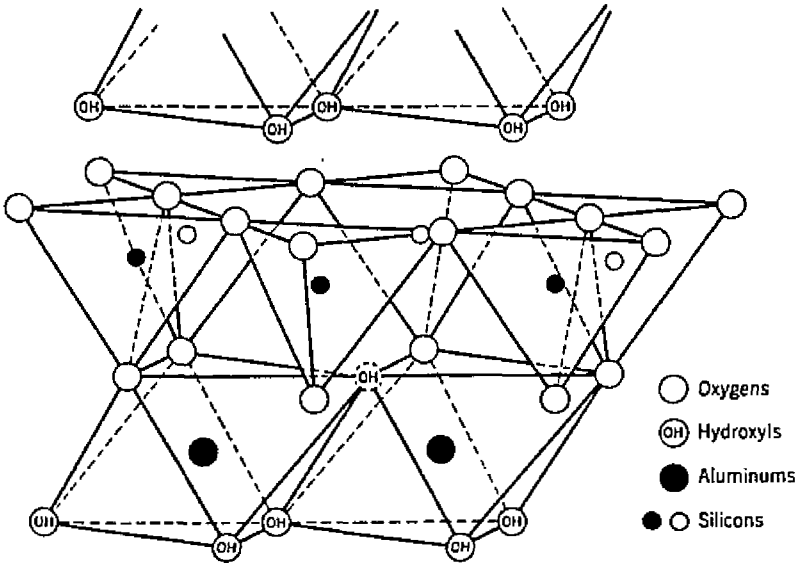

CHAPTER III.

Kinetics of Acid-Clay Reactions

1. Fundamental Relationships

Underground disposal of hazardous wastes involves injection of liquid materials such as aqueous wastes into disposal formations of solid materials such as sandstone and clay. Chemical reactions involving liquid wastes and solid formation materials thus involve two phases of matter. Such two-phase chemical reactions are known as heterogeneous reactions.

Acid dissolution of clay minerals occurs when hydrogen ions from acid displace metal ions from positions in the clays' structure, or lattice. In the clays montmorillonite, illite, and kaolinite, the lattice is composed of sheet-like tetrahedral and octahedral layers. The products of acid-clay reactions are free metal ions (aluminum, magnesium, iron, etc.) and altered clay structures which contain hydrogen. At some time after a system of acid and clay has reacted, the concentration of free metal ions becomes sufficient to displace hydrogen in clay lattices at the same rate hydrogen is displacing metals from the lattices. The acid-clay reaction has reached equilibrium when the "forward" reaction rate equals the "reverse" reaction rate. The nature of dissolution reactions is such that when equilibrium is reached, there are significant quantities of all reactants

present in the system. Such reactions are classified as reversible reactions.

In order for any reaction to occur between materials injected underground and subsurface disposal formations, molecules of liquid wastes must come into contact with formation surfaces in sufficient concentration. Hill (1977) defines adsorption as the preferential concentration of reactive species at the interface between two phases. Adsorption phenomena may be physical, in which intermolecular forces are involved, or chemical, which involve a transfer of electrons between reactants. The latter type of adsorption is called chemisorption.

Several physical and chemical processes must occur in the correct sequence when heterogeneous reactions take place. Seven steps on a molecular level which make up heterogeneous reactions were delineated by Hill (1977):

(1) Mass transfer of reactants from the fluid bulk to the gross exterior surface of the solid.

(2) Molecular diffusion of reactants from the exterior solid surface into its pore sturcture.

(3) Chemisorption of at least one reactant on the solid surface.

(4) Reaction on the solid surface (may be several steps).

(5) Desorption of the adsorbed reactant from the solid surface.

(6) Transfer of reaction products from the interior

of the solid to its gross external surface.

(7) Mass transfer of products from the external surface of the solid to the fluid bulk.

The net rate of chemical reaction is influenced by each of these processes. The overall rate of reaction is determined by the slowest process, which is the rate controlling step.

Energy is expended when an ion or molecule approaches a reactive surface or is removed from the surface. The observed energy exchanged in a heterogeneous reaction is a composite consisting of the true energy of activation and the heats of adsorption and/or desorption. The observed rate of heterogeneous reactions is determined by the amount of solid surface area covered by reactive ions and the specific velocity of the reaction (Turner, 1964). Other factors which contribute to rates of reaction are concentrations of reactants and temperature of reaction, which is the most important variable.

The Arrhenius equation (Smith, 1970) relates temperature with the rate coefficient of heterogeneous reactions:

$$k = A\, e^{-E_t/RT},$$

where k = reaction rate coefficient,

E_t = true energy of activation,

A = frequency factor for reaction,

which may also include steric factors,

R = gas constant, and

T = absolute temperature.

The reaction rate coefficient, k, includes the combined effects of all experimental variables.

Arrhenius' relationship can be written as

$$\ln (k) = \ln (A) - E_t/(RT).$$

Differentiation of this expression with respect to temperature yields

$$\frac{d \ln(k)}{dT} = \frac{E_t}{RT^2} .$$

If reaction rate coefficients for two temperatures are known, and activation energy (E) is assumed to be constant over the temperature range in question, then

$$\ln \frac{k_2}{k_1} = -\frac{E_t}{R} \{ T_2^{-1} - T_1^{-1} \}.$$

A semi-logarithmic plot of rate coefficient against reciprocal temperature thus yields a straight line with negative slope.

Since the observed activation energy of heterogeneous reactions includes heats of adsorption and/or desorption, an "apparent energy of activation", E_a, replaces the true energy of activation, E_t, in the Arrhenius relationship:

$$k = A\, e^{-E_a/RT}$$

and $$\ln \frac{k_2}{k_1} = \frac{-E_a}{R} \{ T_2^{-1} - T_1^{-1} \},$$

with other variables defined as before.

In reactions such as acid dissolution of clays, hydrogen ions must come into contact with reactive sites. Reactive sites may contain sodium, magnesium, or aluminum, and these metals are replaced by hydrogen upon reaction. Reaction rate expressions are usually written in the form of binary reactions involving hydrogen and reactive sites. An expression for reaction of octahedral aluminum in ideal sodium montmorillonite with acid (Iler, 1955) is

$$12SiO_2 \cdot (2MgO + 5Al_2O_3) \cdot 12SiO_2 \cdot Na_2O \cdot 6H_2O + 30H^+ \longrightarrow 10Al^{+3} + 12SiO_2 \cdot (2MgO + 15H_2O) \cdot 12SiO_2 \cdot Na_2O \cdot 6H_2O \cdot$$

Thirty H^+ ions replace ten Al^{+3} ions. For reaction of octahedral magnesium in sodium montmorillonite with acid,

$$12SiO_2 \cdot (2MgO + 5Al_2O_3) \cdot 12SiO_2 \cdot Na_2O \cdot 6H_2O + 4H^+ \longrightarrow 2Mg^{+2} + 12SiO_2 \cdot (2H_2O + 5Al_2O_3) \cdot 12SiO_2 \cdot Na_2O \cdot 6H_2O \cdot$$

Four H^+ ions replace $2Mg^{+2}$ ions. The acid-sodium reaction for montmorillonite is

$$12SiO_2 \cdot (2MgO + 5Al_2O_3) \cdot 12SiO_2 \cdot Na_2O \cdot 6H_2O + 2H^+ \longrightarrow$$
$$2Na^+ + 12SiO_2 \cdot (2MgO + 5Al_2O_3) \cdot 12SiO_2 \cdot 7H_2O \cdot$$

Two H^+ ions replace 2 Na^+ ions. In summary, thirty six H^+ ions replace two Na^+ ions, two Mg^{+2} ions, and ten Al^{+3} ions. Three types of sites are involved in the reaction: Na^+ in interlayer positions, Mg^{+2} in octahedral positions, and Al^{+3} in octahedral positions (Iler, 1955).

In order to model acid dissolution of clay, some assumptions (Turner, 1964) are necessary about reactions involving hydrogen ions and various sites. The assumptions are:

(1) reactions at sodium sites are instantaneous,

(2) all Mg^{+2} and Al^{+3} reaction sites behave similarly,

(3) the release of Mg^{+2} into solution involves a single, slow, rate-limiting step, and

(4) the release of Al^{+3} into solution involves a single, slow, rate-limiting step.

Four fast intermediate reactions occur for which reaction rates and kinetic constants cannot be determined. The fast reactions are displacement of sodium by hydrogen, displacement of magnesium sites by hydrogen yielding an intermediate monovalent magnesium ion, and two displacements of aluminum sites by hydrogen which yield intermediate monovalent and divalent aluminum, respectively. Two slow reactions for which reaction rates

and kinetic constants can be determined are

$$(MgO)_{Mg\ site} + 2H^{+} \text{ -----> } (H_2O)_{Mg\ site} + Mg^{+2}$$

and $(Al_2O_3)_{Al\ site} + 6H^{+} \text{ -----> } 3(H_2O)_{Al\ site} + 2Al^{+3}$.

2. Reaction Rate Expressions

A formulation of rate expressions for acid dissolution of clay must focus on specific ion exchange phenomena. For the clays montmorillonite, illite, and kaolinite, the focus is on displacement of aluminum and magnesium by hydrogen. Rate coefficients, k, can be experimentally determined for hydrogen-magnesium reactions and for hydrogen-aluminum reactions. Activation energies, E, can also be determined for the stated reactions.

A general form of chemical kinetics equations which represents reaction involving two species, A and B, is (Smith, 1970)

$$r = k\ [C_A]^a\ [C_B]^b$$

where r = rate of reaction,

k = rate coefficient,

C_A = concentration of species A,

C_B = concentration of species B,

a = order of reaction with respect to species A, and

b = order of reaction with respect to species B.

For a reaction which is first-order with respect to each of two reactants, the exponents a and b are unity and the expression for reaction rate can be simplified. In terms of the concentration of reactant A, the rate equation above can be written

$$r = - \frac{\partial [C_A]}{\partial t} = k\ [C_A]^a\ [C_B]^b\ .$$

The Arrhenius relationship allows a substitution for the rate coefficient k, in the general rate equation:

$$\frac{\partial [C_A]}{\partial t} = - A\ e^{-E/RT}\ [C_A]^a\ [C_B]^b\ .$$

The over-all "order" of a reaction is the sum of the individual reactant exponents.

If an excess of one reactant is available in a reaction system, and it is assumed that the concentration of the excess reactant does not appreciably change during the reaction, then second-order reactions can be simplified to "pseudo first-order" conditions (Turner, 1964):

$$- \frac{\partial [C_A]}{\partial t} = (k[C_B]^b) \cdot [C_A]^a$$

$$= k'[C_A]\ ,$$

where a = 1 and $[C_B]$ is constant.

Pseudo first-order reactions were observed by Osthaus (1956) for acid dissolution of montmorillonite. The

excess reactant was acid. Turner (1964) showed that acid dissolution of metal ions from the lattice structures of montmorillonite and kaolinite follows pseudo first-order kinetics with respect to acid concentration and temperature. The current research also assumes pseudo first-order behavior of acid/clay reaction systems, and is restricted to acid concentrations and temperatures near the ranges addressed by Turner (1964). Even though the acid-clay system is heterogeneous, a further assumption is that pseudo-homogeneous rate expressions may be used to describe the kinetics. This implies that acid-clay reactions are not limited by bulk diffusion, but an investigation confirming the limiting mechanism of acid-clay reactions is beyond the scope of this study. Adsorption phenomena were not investigated in the batch reaction study.

Kinetic equations can contain terms for both forward and reverse reactions. Forward reactions in acid dissolution of clays are those in which H^{+} ions replace Mg^{+2} ions or Al^{+3} ions from their lattice positions. Reverse reactions are those in which Mg^{+2} ions and Al^{+3} ions replace H^{+} ions from "new" lattice positions. At equilibrium, the forward reaction rates equal the reverse reaction rates (for each metal-hydrogen combination). Early in the reaction period, clays will be depleted of relatively little of their magnesium and aluminum (Turner, 1964), so relatively little free Mg^{+2} and Al^{+3} ions will

be available to contribute to the reverse reaction. Terms representing reverse reaction rates can then be neglected.

Variables in the kinetic equations are defined as follows:

C_{H+} = concentration of H^+ (acid) in solution,

C_{Mg+2} = concentration of Mg^{+2} in solution,

C_{Al+3} = concentration of Al^{+3} in solution,

$C_{Mg(clay)}$ = concentration of Mg^{+2} in clay sites,

$C_{Al(clay)}$ = concentration of Al^{+3} in clay sites,

$C_{H(Mg-clay)}$ = concentration of H^+ in magnesium sites (after reaction),

$C_{H(Al-clay)}$ = concentration of H^+ in aluminum sites (after reaction),

$k_{Mg}\ exp\{-E_{Mg}/RT\}$ = forward rate coefficient for slow magnesium-hydrogen reaction,

$k_{Al}\ exp\{-E_{Al}/RT\}$ = forward rate coefficient for slow aluminum-hydrogen reaction,

$k_{Mg(rev)}\ exp\{-E_{Mg(rev)}/RT\}$ = reverse rate coefficient for slow hydrogen-magnesium reaction,

$k_{Al(rev)}\ exp\{-E_{Al(rev)}/RT\}$ = reverse rate coefficient for slow hydrogen-aluminum reaction,

E_{Mg} = activation energy for slow forward magnesium-hydrogen reaction,

E_{Al} = activation energy for slow forward aluminum-hydrogen reaction,

$E_{Mg(rev)}$ = activation energy for reverse hydrogen-magnesium reaction,

$E_{Al\,(rev)}$ = activation energy for reverse hydrogen-aluminum reaction,

R = gas constant, and

T = absolute temperature.

A rate expression for magnesium-hydrogen reactions is

$$\frac{d\,C_{Mg+2}}{dt} = -C_{H+}\,C_{Mg\,(clay)}\,k_{Mg}\exp\{-E_{Mg}/RT\}$$

$$- C_{Mg+2}\;C_{H\,(Mg-clay)}\;k_{Mg\,(rev)}\;\exp\{-E_{Mg\,(rev)}/RT\},$$

where the frequency factor A is replaced by k_{Mg}. A rate expression for aluminum-hydrogen reactions is

$$\frac{d\,C_{Al+3}}{dt} = -C_{H+}\,C_{Al\,(clay)}\,k_{Al}\exp\{-E_{Al}/RT\}$$

$$- C_{Al+3}\,C_{H\,(Al-clay)}\,k_{Al\,(rev)}\exp\{-E_{Al\,(rev)}/RT\}.$$

The second term on the right side of both equations (reverse reaction terms) can be neglected early in a reaction period, as there is little depletion of aluminum and magnesium.

Further simplification is possible if it is assumed, as per pseudo first-order constraints, (1) that the acid concentration (and the H^+ concentration) is in excess so that little concentration change occurs during reaction, (2) constant temperature exists, and (3) that the quantities of aluminum and magnesium remaining in clay

sites is the difference between total original aluminum and magnesium and amounts currently in solution.

The rate expressions for magnesium-hydrogen and aluminum-hydrogen reactions can be modified using these variables:

$k'_{Mg} = C_{H+}\, k_{Mg}$,

$k'_{Al} = C_{H+}\, k_{Al}$, (assumption 1)

$C_{Mg(orig)} = C_{Mg(clay)} + C_{Mg+2}$,

$C_{Al(orig)} = C_{Al(clay)} + C_{Al+3}$, (assumption 3)

$k_{T(Mg)} = k'_{Mg} \exp\{ -E_{Mg}/RT \}$, and

$k_{T(Al)} = k'_{Al} \exp\{ -E_{Al}/RT \}$. (assumption 2)

The rate expression for aluminum-hydrogen reactions becomes

$$\frac{d\, C_{Al+3}}{dt} = -C_{H+}\, C_{Al(clay)}\, k_{Al} \exp\{ -E_{Al}/RT \},$$

since $$\frac{d\, C_{Al+3}}{dt} = \frac{-\, d\, C_{Al(clay)}}{dt},$$

or $$\frac{d\,(C_{Al(orig)} - C_{Al+3})}{dt} = -(C_{Al(orig)} - C_{Al+3})\, k_{T(Al)}$$

$$d\,(C_{Al(orig)} - C_{Al+3}) = -(C_{Al(orig)} - C_{Al+3})\, k_{T(Al)}\, dt$$

$$\frac{d\,(C_{Al(orig)} - C_{Al+3})}{(C_{Al(orig)} - C_{Al+3})} = -k_{T(Al)}\, dt$$

Integration of this expression between concentration limits $C_{Al(orig)}$ and $(C_{Al(orig)} - C_{Al+3})$, and between time limits zero and t, yields

$$\ln \{ C_{Al(orig)} - C_{Al+3} \} = -k_{T(Al)}\, t$$

$$\ln \{ 1 - C_{Al+3}/C_{Al(orig)} \} = -k_{T(Al)}\, t \ .$$

From a series of measurements of C_{Al+3} and time, a semi-logarithmic plot of log $\{ 1-C_{Al+3}/C_{Al(orig)} \}$ against time results in a straight line with slope $-k_{T(Al)}$. Since

$$k_{T(Al)} = k'_{Al} \exp \{ -E_{Al}/RT \}$$

$$= C_{H+}\, k_{Al} \exp \{ -E_{Al}/RT \} \ ,$$

$$\frac{k_{T(Al)}}{C_{H+}\, k_{Al}} = \exp \{ -E_{Al}/RT \}$$

or

$$\ln \frac{k_{T(Al)}}{C_{H+}\, k_{Al}} = \frac{-E_{Al}}{R} \frac{1}{T} \ .$$

Measurements of $k_{T(Al)}$ at various temperatures can be plotted on a semi-logarithmic graph as log $k_{T(Al)}$ against 1/T. The result is a straight line with slope $-E_{Al}/R$. R and T are known, and $k_{T(Al)}$ is determined from the previous plot. Then

$$k'_{Al} = \frac{k_{T(Al)}}{\exp \{-E_{Al}/RT\}}$$

$$k_{Al} = \frac{k'_{Al}}{C_{H+}} \ .$$

Measurements of C_{Al+3} and time for two temperatures thus allow determination of k_{Al} and E_{Al}. An analogous treatment of magnesium-hydrogen reactions allows determination of k_{Mg} and E_{Mg}. These coefficients help satisfy industrial requirements for parameters used in sophisticated mathematical simulators.

3. Measurement Precision

There is some uncertainty in calculation of reaction rate coefficients and activation energies (Hill, 1977). Sufficient measurements must be taken to establish a functional form for the variables in question. Errors in measurement of the physical quantities time, concentration, and temperature contribute to the degree of imprecision of the calculated rate constants and activation energies.

For a system that obeys first-order kinetics, the following independent variables are defined:

t_1 = time of measurement 1,

Δt_1 = error in t_1,

t_2 = time of measurement 2,

Δt_2 = error in t_2,

C_1 = concentration measured at t_1,

ΔC_1 = error in C_1,

C_2 = concentration measured at t_2, and

ΔC_2 = error in C_2 .

The calculated value of rate coefficient, k, will be expected to have a random error, Δk, expressed as

$$\left[\frac{\Delta k}{k}\right]^2 = \left[\frac{\Delta t_1}{t_2 - t_1}\right]^2 - \left[\frac{\Delta t_2}{t_2 - t_1}\right]^2$$

$$+ \frac{\left[\frac{\Delta C_1}{C_1}\right]^2}{\left[\ln \frac{C_1}{C_2}\right]^2} + \frac{\left[\frac{\Delta C_2}{C_2}\right]^2}{\left[\ln \frac{C_1}{C_2}\right]^2} .$$

The following independent variables are defined as:

T_1 = temperature measurement 1,

ΔT_1 = error in T_1,

T_2 = temperature measurement 2,

ΔT_2 = error in T_2,

k_1 = rate coefficient calculated at T_1,

Δk_1 = error in k_1,

k_2 = rate coefficient calculated at T_2, and

Δk_2 = error in k_2 .

The expected random error in calculated activation energy, ΔE, is given by

$$\left[\frac{\Delta E}{E}\right]^2 = \left[\frac{T_2}{(T_2 - T_1)}\right]^2 \left[\frac{\Delta T_1}{T_1}\right]^2 + \left[\frac{T_1}{(T_2 - T_1)}\right]^2 \left[\frac{\Delta T_2}{T_2}\right]^2$$

$$+ \frac{\left[\frac{\Delta k_1}{k_1}\right]^2 + \left[\frac{\Delta k_2}{k_2}\right]^2}{\left[\ln \frac{k_2}{k_1}\right]^2}$$

CHAPTER IV.

Experimental Procedure

1. Safety Considerations

Some of the procedures followed in this research required precise handling of concentrated acids. All hazardous materials were handled in a laboratory hood. Safety glasses and protective gloves and clothing were used by all personnel handling concentrated acids. First aid materials were readily available at all times and personnel were briefed regarding administration of first aid. Appropriate emergency procedures to be followed in case of an accident were discussed. All waste material was disposed of following recommended procedures: solid wastes were bagged in plastic and deposited in appropriate containers, and liquid wastes were highly diluted and flushed with water.

2. Simulation of Subsurface Environment

Waste disposal formations are rock matrices with impurities occupying interstitial positions within the matrices. In Gulf Coast areas the rock matrices are usually sandstone. Impurities within sandstone include clay minerals, some of which actively undergo ion exchange with aqueous solutions.

Subsurface disposal formations were simulated in this research by non-reactive columns packed with (1) a mixture of 80 - 120 mesh (0.125 - 0.180 millimeter) Ottawa sand and representative concentrations of clay, and (2) actual formation material (including sand and clay) washed from the injection zone of a disposal well located in St. Bernard Parish, Louisiana. A complete description of the sand pack apparatus is included in a later section on sand pack reactions. Energy dispersive x-ray analysis (EDXA) was performed on all solid materials used in the present research. EDXA is discussed in detail in a later section describing analytical methods. Table 3 is an analysis of the Ottawa sand. An analysis of the formation sand is presented in Table 4. Laboratory mixtures of sand and clay contained eighty-five percent by weight sand and fifteen percent by weight clay. Clay mineral concentration of about fifteen percent corresponds well to published analyses of typical sandstones (Pettijohn, 1957).

Formation clays were represented by three commonly occurring species: illite, kaolinite, and sodium montmorillonite. Cambrian Shale illite from Silver Hill, Montana, and kaolinite from Washington County, Georgia, were used. These clays were obtained from the University of Missouri, Department of Geology, Source Clay Minerals Repository, Columbia, Missouri. Tables 5 and 6 present analyses of this illite and kaolinite. Wyoming

Table 3: Analysis of Ottawa Sand

Component	Fraction of Total
Quartz	0.96
Kaolinite	0.018
Illite	0.022

Table 4: Analysis of Kaiser Sand

Component	Fraction of Total
Quartz	0.95
K-Feldspar	0.01
Plagioclase	0.01
Halite	0.01
Kaolinite	0.0066
Illite	0.0052
Smectite	0.0082

Table 5: Composition of Illite

Component	Fraction of Total
SiO_2	0.5174
Al_2O_3	0.2398
Fe_2O_3	0.0457
FeO	0.0109
MgO	0.0229
CaO	0.0097
Na_2O	0.0036
K_2O	0.0550
TiO_2	0.0068
H_2O^-	0.0692
H_2O^+	0.0240

Table 6: Composition of Kaolinite

Component	Fraction of Total
SiO_2	0.4384
Al_2O_3	0.3885
Fe_2O_3	0.0046
FeO	0.0000
MgO	0.0036
CaO	0.0000
Na_2O	0.0000
K_2O	0.0000
TiO_2	0.0103
H_2O^-	0.1354
H_2O^+	0.0000

sodium montmorillonite, available from Ward's Natural Science Supplies, Rochester, New York, was also used in this research. Table 7 is an analysis of this sodium montmorillonite.

Waste disposal formations typically contain native brines of at least 10,000 milligrams per liter (mg/L) total dissolved solids (TDS) (Whiteside and Raef, 1986). Sodium montmorillonite, a common formation clay, swells considerably as it undergoes hydration with fresh water (Bourgoyne, et al., 1986). In the current research dry sand packs were flooded to saturation with 50,000 mg/L sodium chloride brine. Use of brine with the stated concentration of salt minimized clay swelling. No problems were experienced with plugging of sand packs by swollen clays.

3. Simulation of Waste Streams

The U.S. Environmental Protection Agency (EPA) reports that forty one percent of injected wastes are acidic (Gordon and Bloom, 1986). Low pH materials are classified as hazardous if their pH is less than two (Scrivner, et al., 1986). The present research examines low pH hazardous waste streams.

For the batch reactions, hydrochloric acid, nitric acid, and sulfuric acid were used. Batch reactions are described in detail in a later section. Each batch

Table 7: Composition of Sodium Montmorillonite

Component	Fraction of Total
SiO_2	0.6230
Al_2O_3	0.2350
Fe_2O_3	0.0335
FeO	0.0037
MgO	0.0195
CaO	0.0031
Na_2O	0.0040
K_2O	0.0063
TiO_2	0.0000
H_2O^-	0.0645
H_2O^+	0.0000

reaction mixture contained 750 grams water, twenty two grams NaCl, twenty grams of a particular clay, and various types and concentrations of acid. The stated concentrations were achieved by diluting concentrated acid with distilled, deionized water. All concentrated acids were reagent grade materials from Mallinckrodt.

Hydrogen ion concentration was calculated on a molal, or gram moles of hydrogen per kilogram of water, basis. For each acid, two H^+ molalities were used. For hydrochloric acid, H^+ molality was calculated as

$$\frac{216 \text{ g acid added}}{.75 \text{ kg } H_2O + (.216)(1 - .38) \text{ kg } H_2O} \cdot \frac{.38 \text{ g HCl}}{1 \text{ g acid}}$$

$$\cdot \frac{1 \text{ g mole HCl}}{36.5 \text{ g HCl}} \cdot \frac{1 \text{ g mole } H^+}{1 \text{ g mole HCl}}$$

$$= 2.55 \frac{\text{mole } H^+}{\text{kg } H_2O} = 2.55 \text{ Molal (M) } H^+, \text{ and}$$

$$\frac{21.6 \text{ g acid added}}{.75 \text{ kg } H_2O + (.0216)(1 - .38) \text{ kg } H_2O} \cdot \frac{.38 \text{ g HCl}}{1 \text{ g acid}}$$

$$\cdot \frac{1 \text{ g mole HCl}}{36.5 \text{ g HCl}} \cdot \frac{1 \text{ g mole } H^+}{1 \text{ g mole HCl}}$$

$$= .295 \text{ M } H^+ .$$

For nitric acid, H^+ molality was calculated as

$$\frac{202.5 \text{ g acid added}}{.75 \text{ kg } H_2O + (.2025)(1 - .7) \text{ kg } H_2O} \cdot \frac{.7 \text{ g } HNO_3}{1 \text{ g acid}}$$

$$\cdot \frac{1 \text{ g mole } HNO_3}{63 \text{ g } HNO_3} \cdot \frac{1 \text{ g mole } H^+}{1 \text{ g mole } HNO_3}$$

$$= 2.78 \text{ M } H^+, \text{ and}$$

$$\frac{20.3 \text{ g acid added}}{.75 \text{ kg } H_2O + (.0203)(1 - .7) \text{ kg } H_2O} \cdot \frac{.7 \text{ g } HNO_3}{1 \text{ g acid}}$$

$$\cdot \frac{1 \text{ g mole } HNO_3}{63 \text{ g } HNO_3} \cdot \frac{1 \text{ g mole } H^+}{1 \text{ g mole } HNO_3}$$

$$= .298 \text{ M } H^+ .$$

For sulfuric acid, H^+ molality was calculated as

$$\frac{115 \text{ g acid added}}{.75 \text{ kg } H_2O + (.115)(1 - .957) \text{ kg } H_2O} \cdot \frac{.957 \text{ g } H_2SO_4}{1 \text{ g acid}}$$

$$\cdot \frac{1 \text{ g mole } H_2SO_4}{98 \text{ g } H_2SO_4} \cdot \frac{2 \text{ g mole } H^+}{1 \text{ g mole } H_2SO_4}$$

$$= 2.98 \text{ M } H^+, \text{ and}$$

$$\frac{11.5 \text{ g acid added}}{.75 \text{ kg } H_2O + (.0115)(1 - .957) \text{ kg } H_2O} \cdot \frac{.957 \text{ g } H_2SO_4}{1 \text{ g acid}}$$

$$\cdot \frac{1 \text{ g mole } H_2SO_4}{98 \text{ g } H_2SO_4} \cdot \frac{2 \text{ g mole } H^+}{1 \text{ g mole } H_2SO_4}$$

$$= .30 \text{ M } H^+ .$$

The sand pack experiments used diluted hydrochloric acid, nitric acid, and sulfuric acid. Concentrated acids were diluted to a pH of 1.0 using distilled, deionized water. The dilute acid mixtures were pumped through sand packs, which are detailed in a later section.

4. Batch Reactions

A batch reaction apparatus was used to provide data required in the determination of reaction rate coefficients, k, and energies of activation, E. The

apparatus consisted of a shaker bath containing four one-liter reaction flasks. In the flasks were various combinations of water, acid, clay, and salt. The shaker bath provided variable reciprocating agitation. Selected temperatures were maintained by water heated by a thermostatically controlled element. Hollow polyethylene balls floating on the surface of the bath were used to provide insulation against heat loss and inhibit evaporation of water. Figure 11 is an illustration of the batch reaction apparatus.

The variables of reactants and conditions studied included:

(1) Three acids - hydrochloric acid, nitric acid, and sulfuric acid;

(2) Two hydrogen concentrations;

(3) One salt concentration - five molal sodium chloride;

(4) Three clays - sodium montmorillonite, illite, and kaolinite, at fixed acid-clay ratio; and

(5) Two temperatures of reaction were used - fifty degrees Celsius (122 deg. F.) and seventy degrees Celsius (158 deg. F.).

Table 8 displays the specific combinations of reactants for each experimental run.

Reactions were allowed to proceed for fixed time intervals at constant temperature. Reactions were terminated after approximately five days. Reaction flasks

Figure 11: Batch Reaction Apparatus

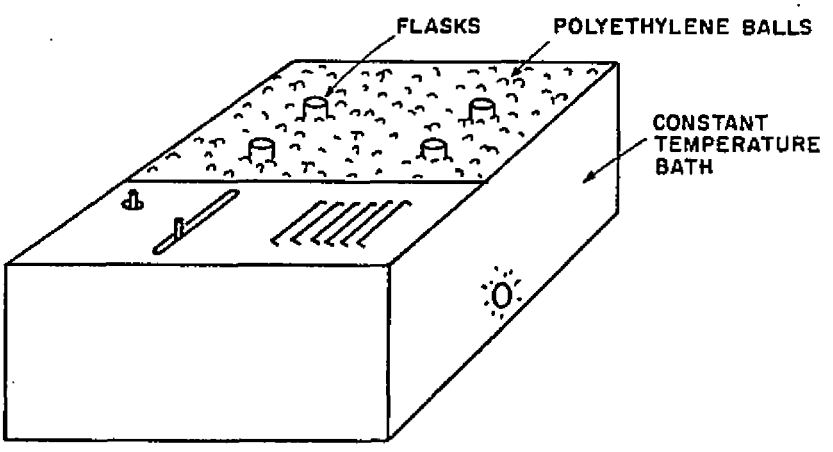

Table 8: Batch Reaction Mixtures

Clay	Acid	H^+ Molality	Temp., deg. C.
Sodium Montmorillonite	HCl	2.55	50
Sodium Montmorillonite	HNO_3	2.78	50
Sodium Montmorillonite	H_2SO_4	2.98	50
Sodium Montmorillonite	HCl	2.55	70
Sodium Montmorillonite	HNO_3	2.78	70
Sodium Montmorillonite	H_2SO_4	2.98	70
Sodium Montmorillonite	HCl	.295	50
Sodium Montmorillonite	HNO_3	.298	50
Sodium Montmorillonite	H_2SO_4	.300	50
Sodium Montmorillonite	HCl	.295	70
Sodium Montmorillonite	HNO_3	.298	70
Sodium Montmorillonite	H_2SO_4	.300	70
Kaolinite	HCl	2.55	50
Kaolinite	HNO_3	2.78	50
Kaolinite	H_2SO_4	2.98	50
Kaolinite	HCl	2.55	70
Kaolinite	HNO_3	2.78	70
Kaolinite	H_2SO_4	2.98	70
Kaolinite	HCl	.295	50
Kaolinite	HNO_3	.298	50
Kaolinite	H_2SO_4	.300	50
Kaolinite	HCl	.295	70
Kaolinite	HNO_3	.298	70
Kaolinite	H_2SO_4	.300	70
Illite	HCl	2.55	50
Illite	HNO_3	2.78	50
Illite	H_2SO_4	2.98	50
Illite	HCl	2.55	70
Illite	HNO_3	2.78	70
Illite	H_2SO_4	2.98	70
Illite	HCl	.295	50
Illite	HNO_3	.298	50
Illite	H_2SO_4	.300	50
Illite	HCl	.295	70
Illite	HNO_3	.298	70
Illite	H_2SO_4	.300	70

were covered with parafilm during agitation to prevent evaporation of liquids. Samples of liquid were removed periodically from the flasks using a vacuum pipette. All samples were taken near the liquid surface. Sample volume was twenty five milliliters in each case, or about 2.5 percent of total volume. The samples were filtered under vacuum using a Buchner funnel and Whatman qualitative filter paper. All implements were washed with distilled, deionized water prior to each sampling procedure. Samples were collected in polyethylene vials with screw-on lids. The vials were washed with a ten percent solution of nitric acid prior to sample collection. All sample vials were labelled and uniquely numbered. Samples were stored in a refrigerator, then were analyzed for concentrations of aluminum ions and magnesium ions by atomic absorption spectrophotometry. This method is presented in detail in a later section on analytical methods.

5. Sand Pack Reactions

Simulation of flow of waste streams through disposal formations was performed with a single-pass sand pack reaction apparatus. Glass columns were packed with representative mixtures of sand and clay or with actual formation material. The glass columns were one foot and four feet long. A twenty foot long jacketted column of polyvinyl chloride (PVC) was packed with actual formation material. Temperature of the sand packs was maintained by

circulation of hot water from an insulated reservoir through water jackets surrounding the columns. The hot water reservoir was a fifty liter capacity pot. Insulation was provided by styrofoam packing material surrounding the outside of the pot and by hollow polyethylene balls floating on the surface of the water. A submersible, thermostatically controlled heater was the source of heat, and water was circulated to the water jackets by an aquarium pump. Tygon tubing connected the hot water reservoir and the water jackets. Figure 12 is an illustration of the sandpack apparatus.

The columns were packed with dry sand and clay or actual formation material as follows. A small amount of dry solid material (approximately ten grams) were placed in a vertically supported column. The columns were agitated as the dry material was added. This process was repeated until the columns were filled. The dry material density was approximately 2.6 grams per cubic centimeter (g/cc) (Bourgoyne, et al., 1986). The porosity of the sand pack was calculated by: (1) dividing the mass of solid material in the column by the density of the solid, yielding the grain volume of the sand pack, (2) subtracting the grain volume of solids from the bulk volume of the column, yielding the pore volume, and (3) dividing the pore volume by the bulk volume, resulting in porosity. Typical porosities of the packed columns were approximately forty percent.

Figure 12: Sand Pack Apparatus

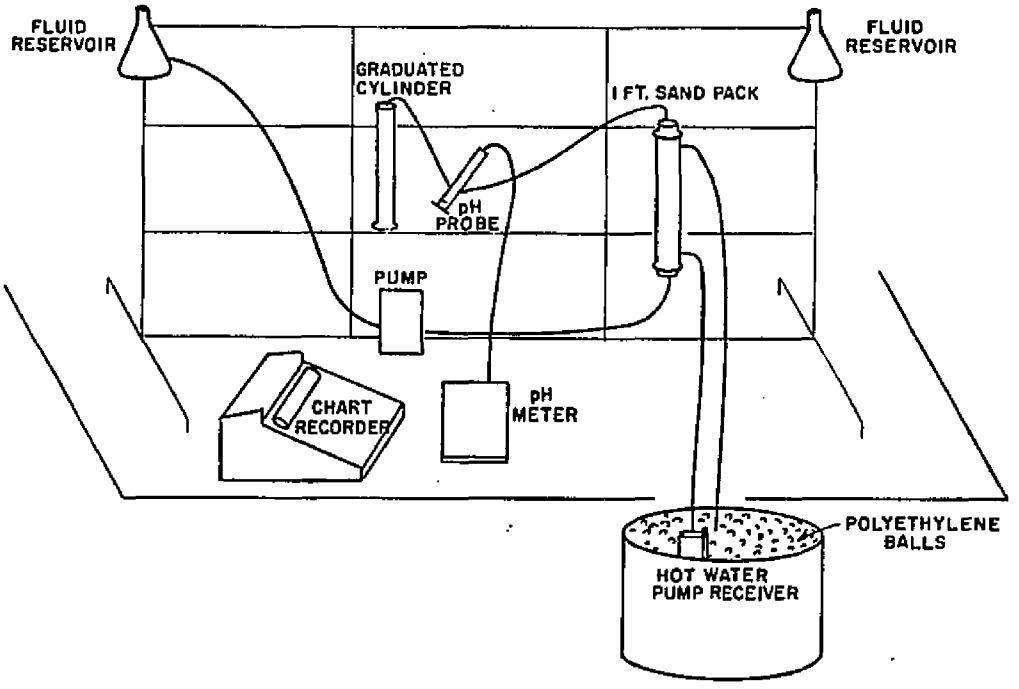

A low-volume, positive-displacement, reciprocating pump was used to circulate simulated low-pH wastes through the sand packs. A detailed description of the fluid mixtures used is presented in a previous section dealing with simulation of waste streams. Flow rates corresponded to fluid velocities of from approximately one foot per day to approximately four feet per day. The rates are somewhat representative of actual disposal systems.

The fluid end of the pump, as well as all connecting tubing, was made of teflon; no metal parts were exposed to waste streams. Polyethylene bottles of ten liter capacity were used as reservoirs for brine and acid solutions. An in-line pH probe was used to make real-time measurements of pH of the sandpack effluent. The pH probe was connected to an Orion digital pH meter, and pH vs. time was recorded with a strip chart recorder. The pH meter was calibrated using pH buffer solutions of four pH and seven pH to make low-pH measurements. The terminus of the flow stream was a parafilm-covered graduated cylinder in which sand pack effluent was collected. The sand pack apparatus was mounted on a rectangular laboratory rack.

6. Analytical Methods

Reactions of acids with clays generally result in dissolution of the clay structures as hydrogen ions from acid release metal ions from positions in clay lattices. The extent of acid-clay reactions is directly related to

the concentration of free metal ions in solution with acids and clays. After reaction, hydrogen ions occupy positions in the lattice structures of clays, so the acidity of the remaining solution is lessened. Acid-clay reactions thus also result in neutralization of acid.

In this research, batch reactions involved acids and clays in known concentrations, in solution with distilled, deionized water. Samples of solution were removed from reaction flasks at known time intervals and analyzed by atomic absorption spectrophotometry for free metal ions which were released from clay structures. Sodium montmorillonite, illite, and kaolinite contribute metal ions upon reaction with acid.

Atomic absorption spectrophotometry (AA) was the analytical method used to determine concentrations of aluminum ions and magnesium ions in solution. In atomic absorption spectrophotometry, a flame is used to atomize a solution sample (Franson, et al., 1985). For detection of magnesium the flame is produced by oxidation of a mixture of air and acetylene. Aluminum ions in solution are directly aspirated into a flame produced by nitrous oxide and acetylene. In each case a light beam is directed through the flame and a detector measures the amount of light absorbed by the atomized ions in the flame. The light is produced by a source lamp which is made of the element in question, as each element has a characteristic absorption wavelength. The concentration of an element

(ion) in solution is proportional to the amount of light of a characteristic wavelength absorbed in the flame. The atomic absorption spectrometer displays the concentration of an ion in parts per million (ppm). If the concentration of an ion in a particular sample is greater than expected, dilution of the sample is necessary. The ionic concentration determined by the spectrometer must be multiplied by the dilution factor. A permanent record of measurement results is also produced by the spectrometer. AA analysis was performed for this study by the Louisiana State University Department of Civil Engineering.

Energy dispersive x-ray analysis (EDXA) was performed on sand and clay used in this research. EDXA involves the use of an electron beam to excite, or raise the energy levels of, electrons in elements of interest (Franson, et al., 1985). As excited electrons of an element return to their ground or lowest energy states, x-rays are emitted which are characteristic of the element. The EDXA phenomenon is a result of specific discrete quantum energy levels associated with electrons surrounding atoms. EDXA spectra represent numbers of x-rays detected corresponding to various energies. EDXA can be used for quantitative or qualitative analysis. A commercial firm specializing in materials evalution was used for the EDXA work.

CHAPTER V.

Numerical Simulation

Flow of low-pH hazardous waste streams through subsurface disposal zones was simulated using the ground water flow simulator SUTRA (Voss, 1984), which is an acronym for Saturated, Unsaturated TRAnsport. SUTRA is available from the United States Geological Survey (USGS) Open File Services Section, Denver, Colorado. SUTRA documentation is entitled "A Finite-Element Simulation Model for Saturated-Unsaturated, Fluid-Density-Dependent Ground-Water Flow with Energy Transport or Chemically-Reactive Single-Species Solute Transport".

1. Physical Aspects of SUTRA Simulation

Two basic physical models are utilized by SUTRA. One model simulates the flow of ground water, with fluid pressure being the primary variable upon which the flow model is based. Since variations in fluid density can also contribute to fluid flow, the effects of gravity are accounted for in the flow field. A second physical model is employed by SUTRA to simulate movement of either thermal energy or solute concentration in ground water. The mathematical expressions used to describe the physical mechanisms governing energy transport and solute transport are very similar. Fluid temperature is the significant variable which characterizes thermal energy distribution.

The distribution of solute concentration in a ground water system is characterized primarily by solute mass fraction, the ratio of solute mass to fluid mass. When simulating thermal energy transport with SUTRA, a constant solute concentration is assumed in the flow system. When simulating solute transport, a constant temperature is assumed.

Various parameters are required by SUTRA to model fluid flowing through porous media. Fluid parameters include pressure, temperature, density, solute mass fraction, and viscosity. Required solid matrix parameters are porosity, fluid saturation, compressibility, and permeability. Gravitational acceleration is also accounted for by SUTRA. Fluid density and viscosity can vary with temperature. A general form of Darcy's law is used by SUTRA to describe fluid flow in porous media. The flow expression is described in detail in a later section on mathematical aspects of SUTRA simulation.

SUTRA flow simulation is based on variations of fluid mass within discrete volumes. The model calculates changes with time of fluid mass within porous solid matrices by numerical solution of a fluid mass balance equation. This equation is described in detail in a later section. Factors which can affect total fluid mass present at a given time are changes in saturation, injection or production wells, natural ground water movement, or changes in fluid density due to temperature

or concentration variations.

A unified equation represents transport of either thermal energy or solute concentration. For thermal energy transport, a numerical solution of an energy balance equation is utilized. Thermal energy moves through porous media by flow of fluid or by thermal conduction through solid or fluid. Solute transport involves numerical solution of a solute mass balance equation. Solute mass can be transported by flow of fluid or by diffusion. Solute species can undergo equilibrium adsorption. The solute balance equation is presented in a later section.

SUTRA is a two-dimensional model. However, thickness of a two-dimensional region can vary, so that a three-dimensional effect is provided. Plane areas or cross-sections can be simulated. An area can be represented in radial or Cartesian coordinates. For example, a disposal zone which is to be simulated is divided into a single layer of contiguous "blocks" or finite elements. The relative sizes of the blocks with respect to the overall simulated volume should be small enough so that the subdivided region appears as a fine mesh. The finite element is the basic unit of a finite element mesh.

SUTRA elements are two-dimensional quadrilaterals in the x-y plane with finite thicknesses in the third dimension, z. Illustrations of a two-dimensional mesh and a quadrilateral element are included in Figure 13b. Each quadrilateral element has twelve straight edges, with four

Figure 13b: SUTRA Finite Element Mesh (Voss, 1984)

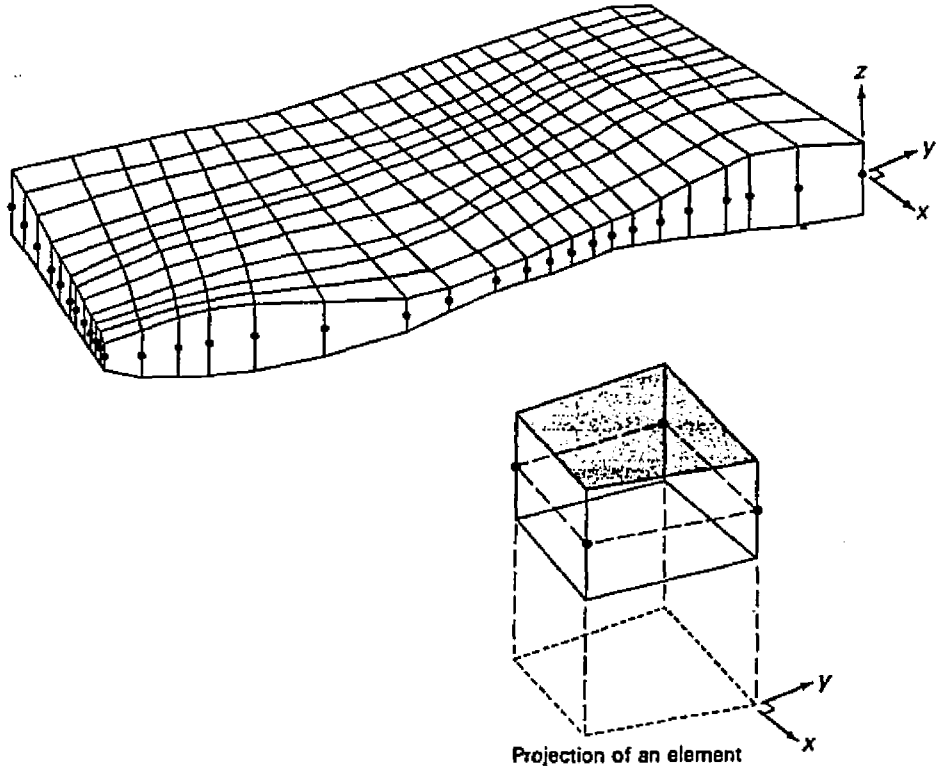

edges parallel to the z (thickness) direction. Each of the edges parallel to the z direction is bisected by the x-y plane. The point of intersection of the x-y plane and a z edge is the midpoint of that edge and is referred to as a node. The top and bottom surfaces of an element are mirror images about the x-y plane. Each quadrilateral element contains four nodes. Parameters can vary from node to node but cannot vary along a z edge. Nodes are shared by the elements adjoining the node, and only nodes at external corners of the mesh are contained in only one element. The thickness of the mesh, which is measured along the z edges, can vary smoothly from node to node. Thus, three-dimensional shapes are represented by a two-dimensional mesh of nodes and elements.

2. Mathematical Aspects of SUTRA Simulation

SUTRA employs algorithms based on standard finite-element approximations for terms in the flux balance equations of fluid mass, solute mass, and thermal energy. Other non-flux terms such as nodewise variations in porosity, permeability, fluid saturations, etc., are approximated with a finite-element mesh version of integrated finite differences. This "hybrid" method preserves mathematical elegance while being relatively efficient.

The general form of Darcy's law which is used by SUTRA to describe fluid flow in porous media is (Voss, 1984):

$$v = -\frac{k}{\varepsilon S \mu}(\nabla \cdot P - \rho g) \ ,$$

where v = average fluid velocity,

k = product of solid matrix permeability and relative permeability to fluid flow,

ε = porosity or pore space fraction,

S = fluid saturation,

μ = fluid viscosity,

$\nabla \cdot P$ = pressure gradient,

ρ = density of fluid, and

g = gravitational acceleration.

Gravitational acceleration is oriented along the direction in which vertical elevation is measured.

The fluid mass balance equation implemented by SUTRA (Voss, 1984) includes the above form of Darcy's law:

$$Q_p = \left[S \rho \Psi + \varepsilon \rho \frac{\partial S}{\partial P} \right] \frac{\partial P}{\partial t}$$

$$+ \varepsilon S \frac{\partial P}{\partial U} \frac{\partial U}{\partial t} - \nabla \cdot \left[\frac{k \rho}{\mu} (\nabla \cdot P - \rho g) \right] .$$

In addition to the variables defined for the flow equation,

Q_p = fluid mass source,

Ψ = volume of fluid released from pore space due to a drop in fluid pressure, and

U = solute concentration or temperature.

The SUTRA solute mass balance equation is

$$\frac{\partial}{\partial t} \left[\varepsilon S \rho C + (1-\varepsilon) \rho_s C_s \right] = - \nabla \cdot (\varepsilon S \rho v C)$$

$$+ \nabla \cdot \left[\varepsilon S \rho (D_m + D) \cdot \nabla C \right] + \varepsilon S \rho \Gamma_w + (1-\varepsilon) \rho_s \Gamma_s + Q_p C .$$

In this expression, f = adsorption factor,

D_m = apparent molecular diffusivity of solute,

D = dispersion coefficient,

Γ_w = source of solute mass in fluid,

C = solute concentration in fluid,

C_s = concentration of adsorbate on solid,

Γ_s = adsorbate mass source, and

and other variables are defined as above.

3. Input Data Requirements

SUTRA requires input from two FORTRAN "read" units. Output may be accomplished through a single "write" unit, or a second "write" unit may be used to store results of one simulation for use as initial conditions of a subsequent simulation. Complete details of SUTRA input and output data can be found in the reference (Voss, 1984).

Input data for SUTRA is arranged into twenty five datasets, where each dataset represents one or more lines on a terminal screen or one or more cards of data. Some datasets are optional depending on the type of simulation, such as solute or energy transport. A brief description of the input datasets follows:

Dataset one - specifies simulation of either solute transport or thermal energy transport.

Dataset two - used to provide headings and labels for output listings.

Dataset three - defines the finite element mesh by numbers of nodes and elements, specifies pressure, temperature, and concentration nodes, and specifies observation time steps and nodes.

Dataset four - specifies transient or steady-state flow and whether results will be stored for a subsequent simulation.

Dataset five - includes control parameters for limiting numerical dispersion.

Dataset six - specifies time step size, number of time steps, and solution cycling parameters.

Dataset seven - controls output, including whether plots are to be produced.

Dataset eight - specifies iterative or non-iterative solutions, and iteration convergence criteria.

Dataset nine - inputs fluid properties including compressibilities, specific heats, densities, viscosities, and solute concentrations.

Dataset ten - inputs rock matrix properties including compressibilities, specific heats, densities, and diffusivities.

Dataset eleven - specifies adsorption parameters.

Dataset twelve - allows inclusion of production or decay of thermal energy or solute mass.

Dataset thirteen - specifies direction of gravitational acceleration.

Dataset fourteen - inputs nodewise space coordinates, thicknesses, and porosities.

Dataset fifteen - inputs elementwise permeabilities and dispersivities.

Dataset sixteen - includes data required for plotting.

Dataset seventeen - includes fluid source or sink data.

Dataset eighteen - inputs thermal energy or solute mass source or sink data.

Dataset nineteen - specifies pressures at nodes.

Dataset twenty - specifies solute concentrations or temperatures at nodes.

Dataset twenty one - inputs observation node data.

Dataset twenty two - inputs element incidence data, which defines the shape of a finite element mesh.

Dataset twenty three - specifies simulation starting time.

Dataset twenty four - specifies nodewise initial pressures.

Dataset twenty five - specifies nodewise initial temperatures or concentrations.

4. Sand Pack Simulation

SUTRA was used in the current research to simulate flow of low-pH waste streams through sand packs. This configuration represented a linear flow regime. The sand packs were filled with actual formation material from a waste disposal well in St. Bernard Parish, Louisiana (the "Kaiser" well). Hydrogen ion concentration was the active chemical parameter; acid neutralization was directly indicated by a decrease in hydrogen ion concentration of sand pack effluent.

SUTRA was used to match the performance of a one foot long sand pack filled with Kaiser well material, at seventy degrees Celsius. The interaction process

involving hydrogen ions and material of the sand pack was adsorption. Adsorption of hydrogen ions on clay serfaces was approximated with a Langmuir adsortion isotherm (Hill, 1977), as this isotherm most closely matched the results of the sand pack experimentation.

The results of the simulated one foot sand pack run were used to predict the results of packs four feet and twenty feet long. SUTRA was also used to model a hypothetical but realistic (full scale) waste disposal system in which low-pH wastes were injected for periods of time ranging up to twenty years.

The simulated geometry of a sand pack system is illustrated in Figure 13. A complete SUTRA input dataset for simulation of flow through sand packs is included in Appendix A.

Figure 13: Simulated Sand Pack Geometry

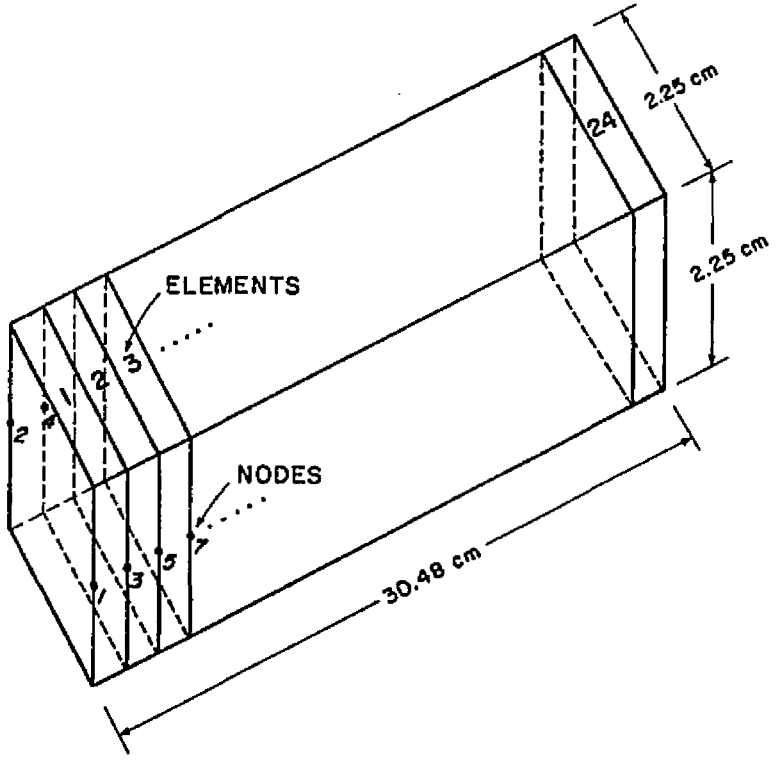

CHAPTER VI.

Results of Experimentation and Simulation

1. Results of Batch Reactions

Liquid samples of each batch reaction mixture were removed from the reaction flasks at known time intervals. Sample volume in each case was twenty five milliliters. The samples were filtered into polyethylene sample vials, as described in the experimental procedure. Samples were analyzed by atomic absorption spectrophotometry (AA) for concentrations of Al^{+3} ions and Mg^{+2} ions in solution. Tables 9 through 44 display the results of AA analysis for each of the reaction mixtures listed in Table 8, p. 71.

Batch reaction data for Al^{+3} and Mg^{+2} displaced from sodium montmorillonite and illite were plotted semi-logarithmically as log [1 - $C/C_{orig.}$] vs. time in hours, where C and $C_{(orig.)}$ are defined as in Chapter III. Only aluminum data for kaolinite were plotted, as only trace quantities of magnesium are present in kaolinite. Original metal concentrations in the batch mixtures were calculated for each combination of acid type, acid concentration, and metal ion. For sodium montmorillonite, the mass of aluminum originally in twenty grams of clay is

$$20 \text{ g clay} \cdot \frac{.235 \text{ g } Al_2O_3}{1 \text{ g clay}} \cdot \frac{1 \text{ g mole } Al_2O_3}{102 \text{ g } Al_2O_3} \cdot \frac{2 \text{ g mole Al}}{1 \text{ g mole } Al_2O_3} \cdot \frac{27 \text{ g Al}}{1 \text{ g mole Al}} = 2.49 \text{ g } Al^{+3} .$$

The concentration of aluminum originally in a batch mixture containing HCl is then

$$\frac{2.49 \text{ g } Al^{+3}}{884 \text{ g } H_2O} \cdot 10^6 = 2815 \text{ ppm } Al^{+3} ,$$

since 750 grams of distilled, deionized water were used and the HCl contributed 134 grams of water (884 g total).

The mass of magnesium originally in twenty grams of sodium montmorillonite is

$$20 \text{ g clay} \cdot \frac{.020 \text{ g MgO}}{1 \text{ g clay}} \cdot \frac{1 \text{ g mole MgO}}{40.3 \text{ g MgO}} \cdot \frac{1 \text{ g mole Mg}}{1 \text{ g mole MgO}} \cdot \frac{24.3 \text{ g } Mg^{+2}}{1 \text{ g mole Mg}} = 0.235 \text{ g } Mg^{+2} .$$

The concentration of magnesium originally in a batch mixture is then

$$\frac{.235 \text{ g } Mg^{+2}}{884 \text{ g } H_2O} \cdot 10^6 = 266 \text{ ppm } Mg^{+2} .$$

Similar calculations were made for each combination of reactants, and the results appear in Table 45. Plots of batch reaction data are Figures B1 through B60 in Appendix B.

Table 9: Batch Reaction of 2.55 Molal H^+ in HCl and Sodium Montmorillonite at Fifty Degrees Celsius.

Time, hrs.	Al Concentration, parts per million	Mg Concentration, parts per million
2	8	13
4	17	13
21	13	23
24	46	16
48	69	36
75	124	39
98	154	44

Table 10: Batch Reaction of 2.78 Molal H^+ in HNO_3 and Sodium Montmorillonite at Fifty Degrees Celsius.

Time, hrs.	Al Concentration, parts per million	Mg Concentration, parts per million
2	14	4
4	29	13
21	47	11
24	66	13
48	99	26
75	138	30
98	178	36

Table 11: Batch Reaction of 2.98 Molal H^+ in H_2SO_4 and Sodium Montmorillonite at Fifty Degrees Celsius.

Time, hrs.	Al Concentration, parts per million	Mg Concentration, parts per million
2	17	14
4	32	22
21	83	33
24	117	36
48	131	40
75	185	48
98	212	60

Table 12: Batch Reaction of 2.55 Molal H^+ in HCl and Sodium Montmorillonite at Seventy Degrees Celsius.

Time, hrs.	Al Concentration, parts per million	Mg Concentration, parts per million
5	49	29
21	138	50
28	177	55
47	445	99
53	485	111
69	630	127
98	1100	190

Table 13: Batch Reaction of 2.78 Molal H^+ in HNO_3 and Sodium Montmorillonite at Seventy Degrees Celsius.

Time, hrs.	Al Concentration, parts per million	Mg Concentration, parts per million
5	53	37
21	144	47
28	183	55
47	435	92
53	441	106
69	559	122
98	1010	198

Table 14: Batch Reaction of 2.98 Molal H^+ in H_2SO_4 and Sodium Montmorillonite at Seventy Degrees Celsius.

Time, hrs.	Al Concentration, parts per million	Mg Concentration, parts per million
5	67	44
21	222	67
28	283	87
47	713	140
53	725	162
69	923	171
98	1734	223

Table 15: Batch Reaction of 0.295 Molal H^+ in HCl and Sodium Montmorillonite at Fifty Degrees Celsius.

Time, hrs.	Al Concentration, parts per million	Mg Concentration, parts per million
3	3	
22	24	32
28	28	42
54	48	54
77	61	56
100	79	67

Table 16: Batch Reaction of 0.298 Molal H^+ in HNO_3 and Sodium Montmorillonite at Fifty Degrees Celsius.

Time, hrs.	Al Concentration, parts per million	Mg Concentration, parts per million
3	4	
22	22	51
28	31	51
54	49	53
77	65	56
100	86	57

Table 17: Batch Reaction of 0.3 Molal H^+ in H_2SO_4 and Sodium Montmorillonite at Fifty Degrees Celsius.

Time, hrs.	Al Concentration, parts per million	Mg Concentration, parts per million
3	4	
22	24	36
28	31	46
54	52	49
77	68	52
100	90	61

Table 18: Batch Reaction of 0.295 Molal H^+ in HCl and Sodium Montmorillonite at Seventy Degrees Celsius.

Time, hrs.	Al Concentration, parts per million	Mg Concentration, parts per million
5	23	33
21	68	51
28	90	57
47	176	76
53	190	78
69	207	87
98	317	105

Table 19: Batch Reaction of 0.298 Molal H^+ in HNO_3 and Sodium Montmorillonite at Seventy Degrees Celsius.

Time, hrs.	Al Concentration, parts per million	Mg Concentration, parts per million
2	8	33
24	63	63
47	107	65
72	153	68
96	191	75

Table 20: Batch Reaction of 0.3 Molal H^+ in H_2SO_4 and Sodium Montmorillonite at Seventy Degrees Celsius.

Time, hrs.	Al Concentration, parts per million	Mg Concentration, parts per million
2	10	27
24	62	51
47	110	57
72	139	64
96	161	84

Table 21: Batch Reaction of 2.55 Molal H^+ in HCl and Kaolinite at Fifty Degrees Celsius.

Time, hrs.	Al Concentration, parts per million	Mg Concentration, parts per million
3	2	
21	15	trace
28	19	--
54	31	--
77	43	--
100	50	--

Table 22: Batch Reaction of 2.78 Molal H^+ in HNO_3 and Kaolinite at Fifty Degrees Celsius.

Time, hrs.	Al Concentration, parts per million	Mg Concentration, parts per million
5	9	trace
29	27	--
53	42	--
76	55	--
100	69	--

Table 23: Batch Reaction of 2.98 Molal H^+ in H_2SO_4 and Kaolinite at Fifty Degrees Celsius.

Time, hrs.	Al Concentration, parts per million	Mg Concentration, parts per million
5	27	trace
29	49	--
53	86	--
76	112	--
100	136	--

Table 24: Batch Reaction of 2.55 Molal H^+ in HCl and Kaolinite at Seventy Degrees Celsius.

Time, hrs.	Al Concentration, parts per million	Mg Concentration, parts per million
2	3	trace
24	49	--
47	100	--
72	154	--
96	211	--

Table 25: Batch Reaction of 2.78 Molal H^+ in HNO_3 and Kaolinite at Seventy Degrees Celsius.

Time, hrs.	Al Concentration, parts per million	Mg Concentration, parts per million
2	1	trace
24	51	--
47	90	--
72	135	--
96	210	--

Table 26: Batch Reaction of 2.98 Molal H^+ in H_2SO_4 and Kaolinite at Seventy Degrees Celsius.

Time, hrs.	Al Concentration, parts per million	Mg Concentration, parts per million
4	22	trace
27	145	--
50	271	--
72	367	--
94	554	--

Table 27: Batch Reaction of 0.295 Molal H^+ in HCl and Kaolinite at Fifty Degrees Celsius.

Time, hrs.	Al Concentration, parts per million	Mg Concentration, parts per million
5	6	trace
29	19	--
53	24	--
76	27	--
100	36	--

Table 28: Batch Reaction of 0.298 Molal H^+ in HNO_3 and Kaolinite at Fifty Degrees Celsius.

Time, hrs.	Al Concentration, parts per million	Mg Concentration, parts per million
5	12	trace
29	18	--
53	23	--
76	28	--
100	35	--

Table 29: Batch Reaction of 0.3 Molal H^+ in H_2SO_4 and Kaolinite at Fifty Degrees Celsius.

Time, hrs.	Al Concentration, parts per million	Mg Concentration, parts per million
5	9	trace
28	22	--
51	32	--
76	41	--
100	54	--

Table 30: Batch Reaction of 0.295 Molal H^+ in HCl and Kaolinite at Seventy Degrees Celsius.

Time, hrs.	Al Concentration, parts per million	Mg Concentration, parts per million
4	7	trace
27	26	--
50	41	--
72	61	--
94	68	--

Table 31: Batch Reaction of 0.298 Molal H^+ in HNO_3 and Kaolinite at Seventy Degrees Celsius.

Time, hrs.	Al Concentration, parts per million	Mg Concentration, parts per million
4	8	trace
27	25	--
50	43	--
72	60	--
94	73	--

Table 32: Batch Reaction of 0.3 Molal H^+ in H_2SO_4 and Kaolinite at Seventy Degrees Celsius.

Time, hrs.	Al Concentration, parts per million	Mg Concentration, parts per million
4	12	trace
27	47	--
50	82	--
72	110	--
94	140	--

Table 33: Batch Reaction of 2.55 Molal H^+ in HCl and Illite at Fifty Degrees Celsius.

Time, hrs.	Al Concentration, parts per million	Mg Concentration, parts per million
5	31	44
28	96	93
51	118	96
76	146	105
100	160	110

Table 34: Batch Reaction of 2.78 Molal H^+ in HNO_3 and Illite at Fifty Degrees Celsius.

Time, hrs.	Al Concentration, parts per million	Mg Concentration, parts per million
5	44	49
28	114	81
51	138	87
76	149	88
100	178	89

Table 35: Batch Reaction of 2.98 Molal H^+ in H_2SO_4 and Illite at Fifty Degrees Celsius.

Time, hrs.	Al Concentration, parts per million	Mg Concentration, parts per million
5	33	48
28	103	76
51	142	78
76	167	86
100	187	109

Table 36: Batch Reaction of 2.55 Molal H^+ in HCl and Illite at Seventy Degrees Celsius.

Time, hrs.	Al Concentration, parts per million	Mg Concentration, parts per million
4	55	16
28	219	57
51	299	64
76	424	86
100	505	94

Table 37: Batch Reaction of 2.78 Molal H^+ in HNO_3 and Illite at Seventy Degrees Celsius.

Time, hrs.	Al Concentration, parts per million	Mg Concentration, parts per million
4	79	37
28	206	69
51	282	71
76	399	85
100	546	92

Table 38: Batch Reaction of 2.98 Molal H^+ in H_2SO_4 and Illite at Seventy Degrees Celsius.

Time, hrs.	Al Concentration, parts per million	Mg Concentration, parts per million
4	55	24
28	207	60
51	297	82
76	382	86
100	402	88

Table 39: Batch Reaction of 0.295 Molal H^+ in HCl and Illite at Fifty Degrees Celsius.

Time, hrs.	Al Concentration, parts per million	Mg Concentration, parts per million
4	7	39
28	28	47
53	49	52
76	62	57
100	79	64

Table 40: Batch Reaction of 0.298 Molal H^+ in HNO_3 and Illite at Fifty Degrees Celsius.

Time, hrs.	Al Concentration, parts per million	Mg Concentration, parts per million
4	10	36
28	40	50
53	67	66
76	79	71
100	92	76

Table 41: Batch Reaction of 0.3 Molal H^+ in H_2SO_4 and Illite at Fifty Degrees Celsius.

Time, hrs.	Al Concentration, parts per million	Mg Concentration, parts per million
4	11	39
28	28	50
53	48	56
76	60	60
100	69	69

Table 42: Batch Reaction of 0.295 Molal H^+ in HCl and Illite at Seventy Degrees Celsius.

Time, hrs.	Al Concentration, parts per million	Mg Concentration, parts per million
4	23	1
28	88	28
51	136	47
76	157	47
100	174	57

Table 43: Batch Reaction of 0.298 Molal H^+ in HNO_3 and Illite at Seventy Degrees Celsius.

Time, hrs.	Al Concentration, parts per million	Mg Concentration, parts per million
2	13	1
25	84	31
48	119	42
73	164	53
98	177	65

Table 44: Batch Reaction of 0.3 Molal H^+ in H_2SO_4 and Illite at Seventy Degrees Celsius.

Time, hrs.	Al Concentration, parts per million	Mg Concentration, parts per million
2	18	1
25	80	28
48	119	33
73	161	40
98	193	41

Table 45: Original Metal Concentrations in Batch Mixtures

Clay	Acid	H^+ Molality	$C_{Al\,(orig.)}$, ppm	$C_{Mg\,(orig.)}$, ppm
Na Mont.	HCl	2.55	2815	266
Na Mont.	HCl	.295	3263	308
Na Mont.	HNO_3	2.78	3071	291
Na Mont.	HNO_3	.298	3293	312
Na Mont.	H_2SO_4	2.98	3298	312
Na Mont.	H_2SO_4	0.30	3318	314
Kaolinite	HCl	2.55	4649	49
Kaolinite	HCl	.295	5387	57
Kaolinite	HNO_3	2.78	5068	54
Kaolinite	HNO_3	.298	5437	57
Kaolinite	H_2SO_4	2.98	5443	59
Kaolinite	H_2SO_4	0.30	5476	58
Illite	HCl	2.55	2876	312
Illite	HCl	.295	3332	361
Illite	HNO_3	2.78	3136	341
Illite	HNO_3	.298	3363	365
Illite	H_2SO_4	2.98	3367	365
Illite	H_2SO_4	0.30	3387	367

2. Discussion and Comparison of Batch Reaction Results

As illustrated by the Figures in Appendix B, scattering of data resulted in some deviations from the expected straight lines. A linear least-squares curve fit was performed for the results of each batch reaction combination. A few data points appeared to be erroneous and were omitted from the curve fit. The resulting slope of each straight line is then $-k^*$, which, when multiplied by the factor ln(10) to change logarithmic bases, yielded the rate coefficient $-k_T$, as defined in Chapter III. The results of calculations of k_T for each metal in each batch reaction combination are displayed in Tables 46 through 48. The units of k_T are reciprocal hours.

There are some similarities in the batch reaction experimentation of this research and the work by Turner (1964), except that generally higher temperatures of reaction were used in the Turner study. Other differences in the present research and that of Turner are discussed later in this section.

Turner (1964) examined the effect of acid concentration on the rate coefficient k for dissolution of aluminum in kaolinite. He reported that as HCl concentration increased from ten percent to thirty percent, a threefold increase, there was a threefold increase in rate coefficient. Measurement temperature was ninety degrees Celsius. Ten percent HCl is equivalent to 1.08 molal H^+ and thirty percent HCl is equivalent to 3.53

Table 46: Observed Values of k_T for Sodium Montmorillonite

Acid	Temp., deg. C.	$k_{T(Al)}$, hr^{-1}	$k_{T(Mg)}$, hr^{-1}
2.55M H^+, HCl	50	5.5×10^{-4}	1.4×10^{-3}
2.78M H^+, HNO_3	50	5.2×10^{-4}	1.2×10^{-3}
2.98M H^+, H_2SO_4	50	6.6×10^{-4}	1.3×10^{-3}
2.55M H^+, HCl	70	3.7×10^{-3}	8.4×10^{-3}
2.78M H^+, HNO_3	70	2.9×10^{-3}	6.4×10^{-3}
2.98M H^+, H_2SO_4	70	4.8×10^{-3}	1.2×10^{-2}
.295M H^+, HCl	50	2.1×10^{-4}	1.7×10^{-3}
.298M H^+, HNO_3	50	2.5×10^{-4}	5.1×10^{-4}
.300M H^+, H_2SO_4	50	3.2×10^{-4}	1.2×10^{-3}
.295M H^+, HCl	70	9.0×10^{-4}	4.0×10^{-3}
.298M H^+, HNO_3	70	5.9×10^{-4}	1.8×10^{-3}
.300M H^+, H_2SO_4	70	6.8×10^{-4}	3.5×10^{-3}

Table 47: Observed Values of k_T for Kaolinite

Acid	Temp., deg. C.	$k_{T(Al)}$, hr^{-1}
2.55M H^+, HCl	50	1.1×10^{-4}
2.78M H^+, HNO_3	50	1.4×10^{-4}
2.98M H^+, H_2SO_4	50	2.5×10^{-4}
2.55M H^+, HCl	70	4.9×10^{-4}
2.78M H^+, HNO_3	70	3.5×10^{-4}
2.98M H^+, H_2SO_4	70	1.0×10^{-3}
.295M H^+, HCl	50	5.8×10^{-5}
.298M H^+, HNO_3	50	4.4×10^{-5}
.300M H^+, H_2SO_4	50	9.2×10^{-5}
.295M H^+, HCl	70	1.5×10^{-4}
.298M H^+, HNO_3	70	1.4×10^{-4}
.300M H^+, H_2SO_4	70	2.8×10^{-4}

Table 48: Observed Values of k_T for Illite

Acid	Temp., deg. C.	$k_{T(el)}$, hr^{-1}	$k_{T(mo)}$, hr^{-1}
2.55M H^+, HCl	50	6.8×10^{-4}	1.2×10^{-3}
2.78M H^+, HNO_3	50	6.7×10^{-4}	3.0×10^{-3}
2.98M H^+, H_2SO_4	50	7.2×10^{-4}	7.4×10^{-4}
2.55M H^+, HCl	70	1.9×10^{-3}	3.7×10^{-3}
2.78M H^+, HNO_3	70	1.7×10^{-3}	4.6×10^{-3}
2.98M H^+, H_2SO_4	70	1.6×10^{-3}	4.0×10^{-3}
.295M H^+, HCl	50	2.3×10^{-4}	8.1×10^{-4}
.298M H^+, HNO_3	50	2.6×10^{-4}	1.4×10^{-3}
.300M H^+, H_2SO_4	50	1.8×10^{-4}	9.3×10^{-4}
.295M H^+, HCl	70	7.4×10^{-4}	2.9×10^{-3}
.298M H^+, HNO_3	70	7.0×10^{-4}	5.7×10^{-4}
.300M H^+, H_2SO_4	70	6.6×10^{-4}	7.5×10^{-4}

molal H^+. The current research revealed a twofold increase in rate coefficient for an eightfold increase in H^+ concentration at fifty degrees Celsius. At seventy degrees Celsius, an eightfold increase in H^+ concentration resulted in a threefold increase in rate coefficient. It is believed that the differences of rate coefficient increase with acid concentration increase between this research and that of Turner are due to the higher temperatures of the previous study.

Turner also determined rate coefficients for dissolution of aluminum in kaolinite for temperatures ranging from sixty five degrees Celsius to ninety five degrees Celsius. To compare results of the current research to those of Turner, k_T at seventy degrees Celsius from the current research must be divided by the acid concentration to yield k. This k is then equivalent to Turner's k', which was found to be 8.867×10^{-4} liters per mole-hour (L/mole-hr). The current research found values of k to be 1.906×10^{-4} L/mole-hr at fifty degrees Celsius and 5.014×10^{-4} L/mole-hr at seventy degrees Celsius.

Apparent energy of activation (E_a) was determined by Turner to be 24.3 kilocalories per mole (kcal/mole) for dissolution of aluminum from kaolinite. For dissolution of magnesium and aluminum from sodium montmorillonite, apparent energies of activation were determined by Turner to be 17.5 kcal/mole. In the current research only two temperatures of reaction were examined. Apparent energies

of activation determined from the slope of the log (k_T) vs. 1/T plots, based on two points, are used for comparison purposes and should not be interpreted as absolute without verification by data from at least one additional temperature. For dissolution of aluminum from sodium montmorillonite, apparent energies of activation ranged from 9.3 kcal/mole to 21.8 kcal/mole, with an average value of 16.4 kcal/mole. For dissolution of magnesium from sodium montmorillonite, E_a's ranged from 9.3 kcal/mole to 24.5 kcal/mole, with an average value of 16.1 kcal/mole. For dissolution of aluminum from kaolinite, E_a's ranged from 10.3 kcal/mole to 16.6 kcal/mole, with an average value of 13.0 kcal/mole. The stated values used for comparison are averages for each metal in each clay over all acids and concentrations.

Turner also determined rate coefficients for dissolution of aluminum and magnesium from sodium montmorillonite. He observed that an increase of ten degrees Celsius in the range seventy degrees Celsius to ninety five degrees Celsius resulted in a twofold increase in rate coefficient. In the curent research, rate coefficients for aluminum and magnesium in sodium montmorillonite were found to undergo a fivefold to sevenfold increase due to a twenty degree Celsius increase in temperature, for 2.55M to 2.98M H^+ concentrations. Rate coefficients underwent twofold to fourfold increases due to a twenty degree Celsius temperature increase for

0.295M to 0.30M H^+ concentrations.

For dissolution of aluminum and magnesium from sodium montmorillonite at seventy degrees Celsius, Turner found rate coefficient k' to be 8.556 x 10^{-3} L/mole-hr. The current research found equivalent values of rate coefficient to range from 1.366 x 10^{-2} L/mole-hr to 1.432 x 10^{-3} L/mole-hr, with an average value of 5.361 x 10^{-3} L/mole-hr . Comparison values of k_T were obtained by averaging observed values for all metals over all concentrations of HCl at seventy degrees Celsius.

Rate coefficients for dissolution of aluminum and magnesium from illite are displayed in Table 48. Measured apparent energy of activation for dissolution of aluminum from illite varied from 8.8 kcal/mole to 14.1 kcal/mole, with an average of 11.5 kcal/mole. For dissolution of magnesium from illite, E_a's varied from 2.4 kcal/mole to 18.4 kcal/mole, with an average E_a of 10.3 kcal/mole.

Deviation of the current results from those of Turner can be attributed to several possible reasons. The "sodium montmorillonite" used in the previous study was Clay Spur, Wyoming, bentonite, which is about ninety percent sodium montmorillonite. The current research utilized a more pure form of sodium montmorillonite. Bentonite contains components with appreciable iron content, and displacement of iron by hydrogen is a clay dissolution mechanism not considered here or by Turner. Measurements made in the 1964 study were over a range of

temperatures which were higher than those here. Extension of results of clay dissolution by acid to temperatures outside the range of measurement is at best a questionable practice. Turner pretreated his clays by dispersing them in distilled water. This procedure undoubtedly caused the clay structures to expand upon hydration. The resulting effect on interaction of hydrated clays with acid is unknown. In the current research all fluids exposed to clays contained at least 50,000 mg/L NaCl. Kinetics mechanisms are quite complex and are dependent upon large numbers of variables. Inconsistent assumptions regarding some variables can cause deviation of results.

3. Results and Discussion of Sand Pack Experiments

Sand pack runs were made using packed columns one foot, four feet, and twenty feet in length. The packs were filled with either (1) Ottawa sand, (2) Ottawa sand and either sodium montmorillonite, kaolinite, and illite in ratios of eighty five mass percent sand and fifteen mass percent clay, and (3) sand from a waste disposal formation that was back-washed from a disposal well in St. Bernard Parish, Louisiana (the "Kaiser" well). During the runs sand pack temperature was maintained at fifty degrees Celsius or seventy degrees Celsius by circulating hot water through a water jacket. After saturating the sand packs with 50,000 mg/L brine, acid solution containing 100,000 mg/L NaCl at a pH of 1.0 was displaced through the

packs with a positive displacement pump. Acid type was varied from run to run. Hydrochloric acid, nitric acid, and sulfuric acid were used. Effluent pH was measured and recorded continuously for the one foot and four foot sand packs. The pH for the twenty foot sand pack was measured periodically, rather than continuously. The effluent pH measurements of the sand pack runs were digitized and plotted as shown in Figures 14 through 20.

Figure 14 is a plot of pH vs. pore volume injected for a sand pack containing only Ottawa sand at fifty degrees Celsius. The injected HCl has a pH of 1.0 . If there were no neutralization by the Ottawa sand pack and if there were no mixing between the injected acid and the displaced brine, then it would be expected that the effluent pH remain at about seven until one pore volume had been injected. Then the pH would suddenly change to 1.0, reflecting the emergence of the acid, and remain there from then on. In this sand pack run, rather than a sharp drop in pH, about one-half pore volume of injected acid exited the sand pack before the pH returned to 1.0. This indicates that the Ottawa sand, or its impurities, did neutralize the acid to some extent and/or there was some dispersion-caused mixing of acid and brine as the acid displaced the brine.

Figure 15 represents pH vs. pore volume injected for a pack containing eighty five mass percent Ottawa sand and fifteen mass percent sodium montmorillonite. The pH of

Figure 14

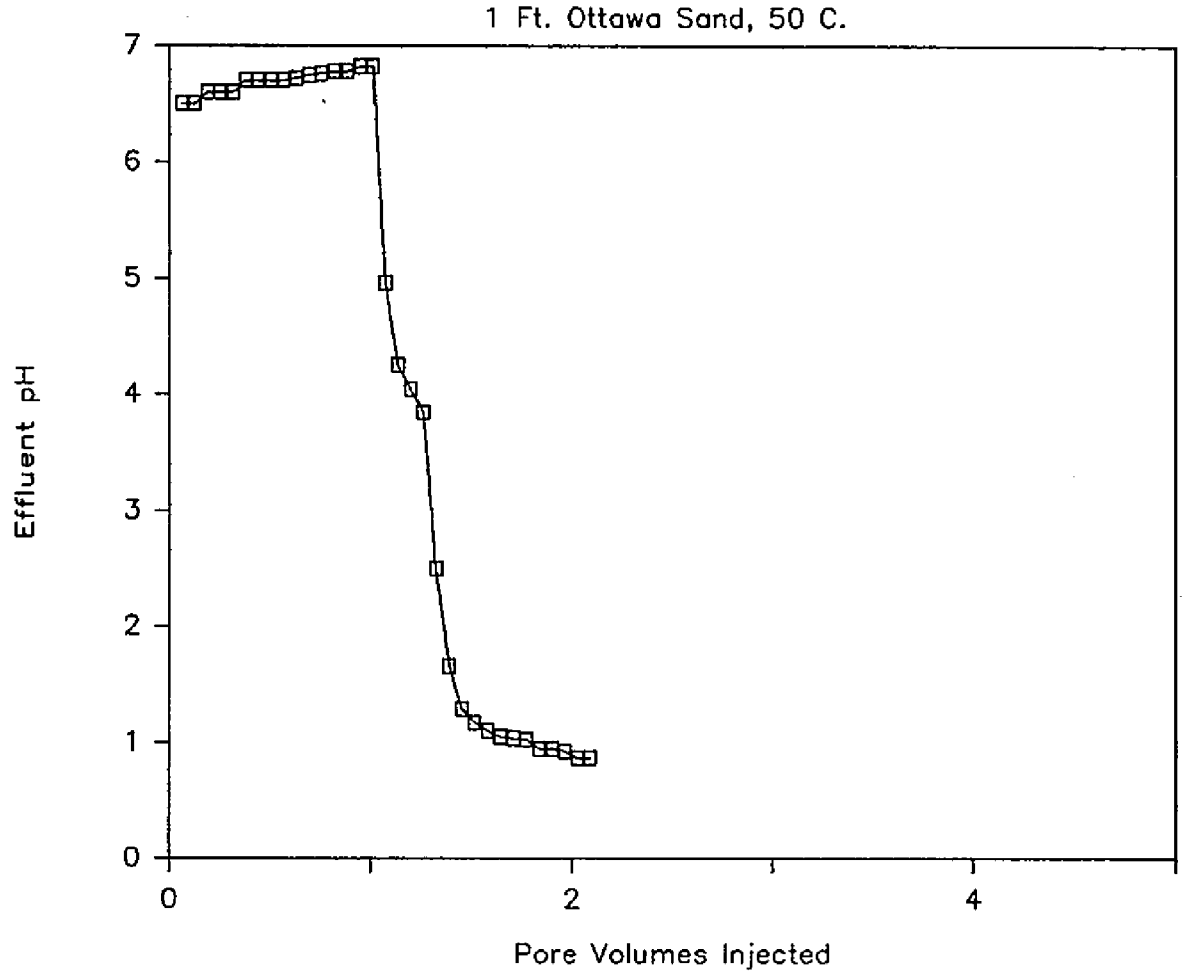
1 Ft. Ottawa Sand, 50 C.
Effluent pH
7
6
5
4
3
2
1
0
0
2
4
Pore Volumes Injected

Figure 15

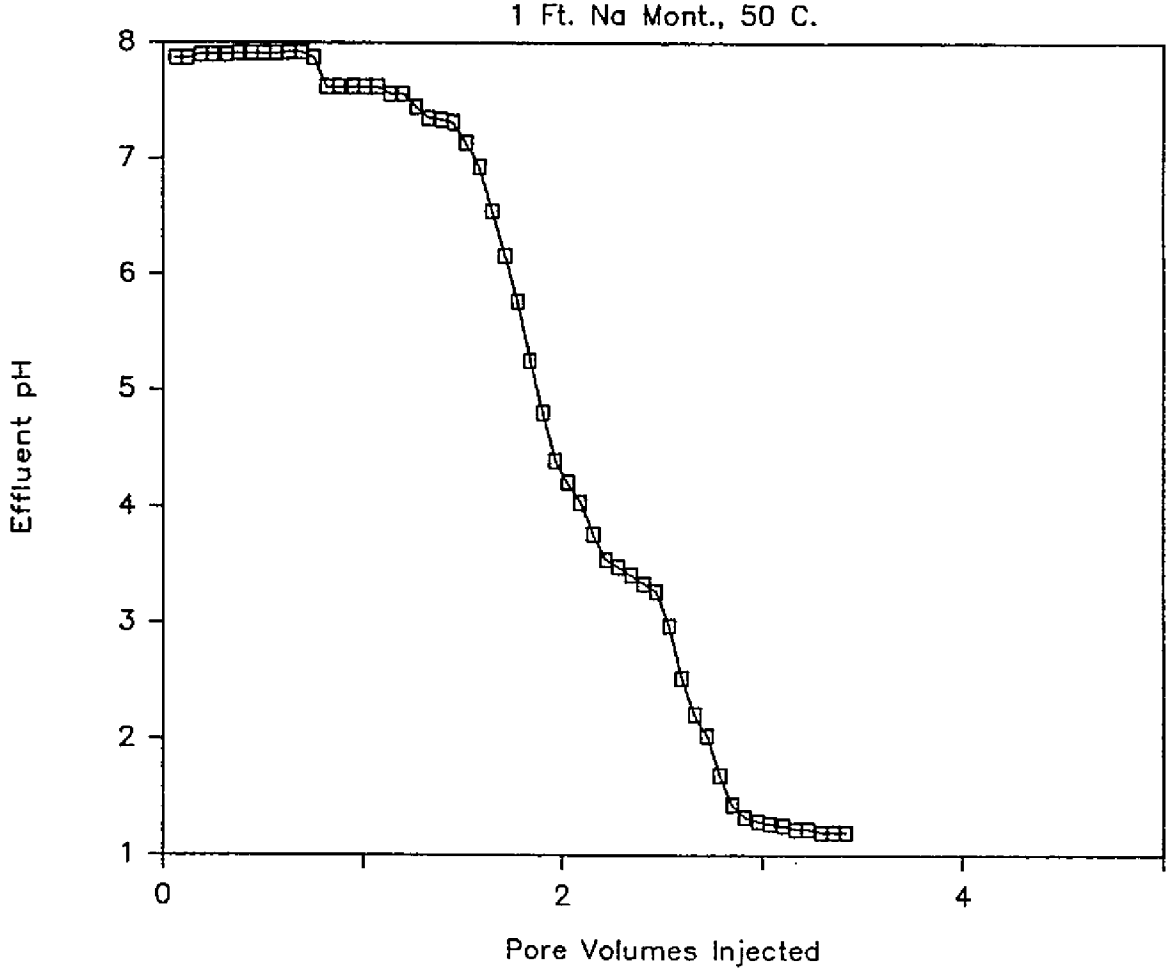
1 Ft. Na Mont., 50 C.
Effluent pH
8
7
6
5
4
3
2
1
0
2
4
Pore Volumes Injected

the effluent did not return to that of the injected fluid until about two and one-half pore volumes of injected acid had exited the sand pack. The effluent pH did not reach a value of two, which is the RCRA hazardous material criterion, until almost two pore volumes of injected acid had exited the pack. This clearly shows that a significant neutralization of acid had occurred. The flow rate of the injected acid was about four feet per day.

Figure 15 illustrates a characteristic common to all the sand pack runs of this study. At about two to two and one half pore volumes of injection, a plateau of pH occurred. This plateau can be explained as a deviation of the sand pack/acid system from pseudo first order behavior because first order behavior implies a smooth transition in pH. One of the assumptions necessary for pseudo first order treatment of acid dissolution of clay is a large excess of hydrogen ions. As acid solution first enters the sand pack, virtually all hydrogen ions react with metal sites in the clay, so there is no over-abundance of hydrogen ions remaining in solution, thus the pseudo first order assumption is not met.

Figure 16 illustrates the effect of varying flow rate through a one foot sand pack filled with sand and sodium montmorillonite. The injected acid was HCl at a pH of 1.0. The acid neutralization was more pronounced when the flow rate was one foot per day than when the flow rate was four feet per day. At one foot per day, over three pore

Figure 16

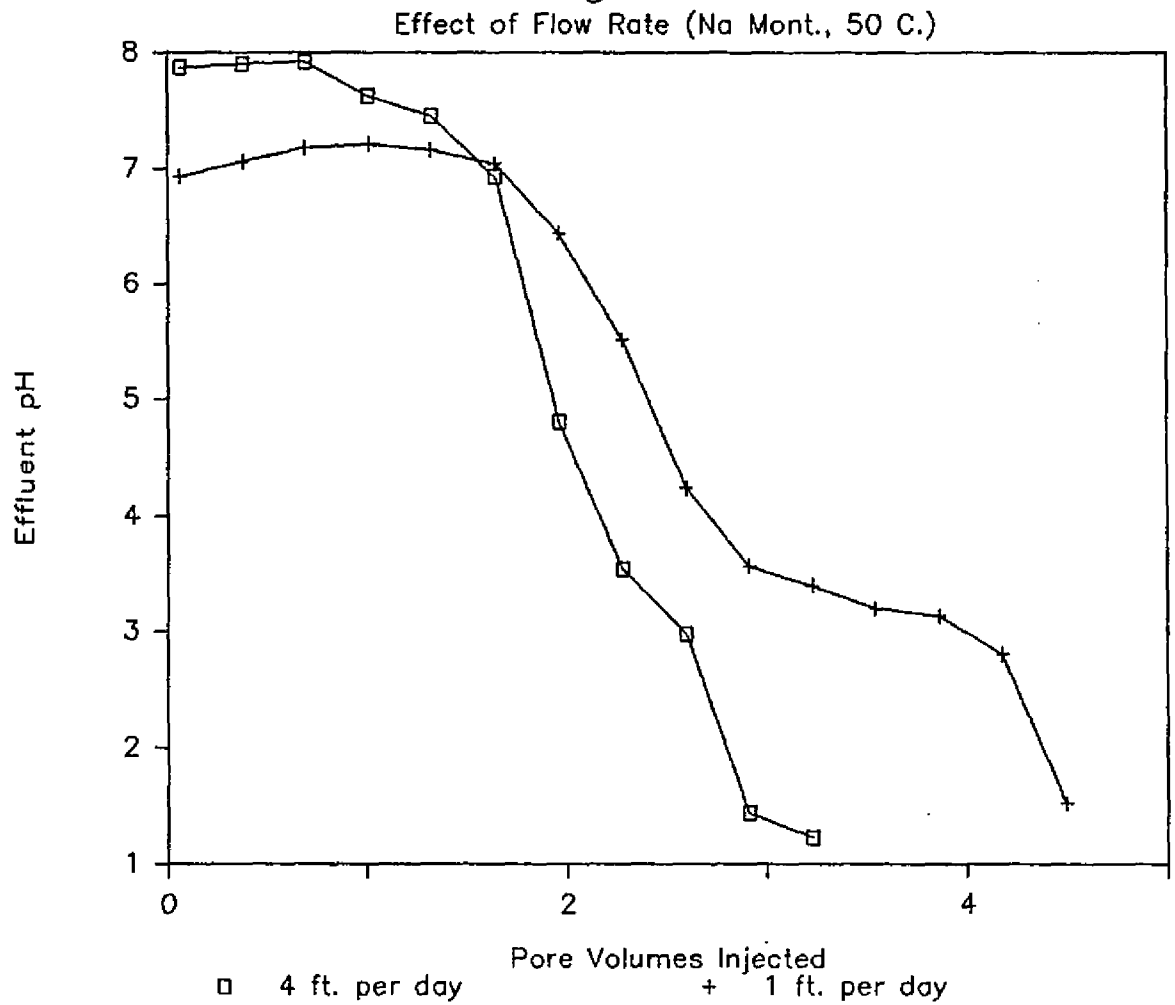
Effect of Flow Rate (Na Mont., 50 C.)
Effluent pH
8
7
6
5
4
3
2
1
0
2
4
Pore Volumes Injected
4 ft. per day
1 ft. per day

volumes of injected acid exited the sand pack before the pH returned to that of the injected acid. At four feet per day, about two pore volumes of injected acid exited the sand pack before the pH returned to that of the injected fluid. This implies that there is more neutralization occurring as the acid residence time increases. It is not believed that this effect of residence time is important in actual disposal operations. At the slow rate, it took one day for the acid to move through the pack. At the fast rate, it took six hours for acid to move through the pack. In actual operations, disposal wells are expected to last at least twenty years. Residence time will surely be long enough for all reactions to have proceeded to equilibrium. An experimental limitation that could affect measured values of pH is as follows. During sand pack runs, some solid material was flushed from the packs and deposited around the pH probe. This solid material could continue to react with acid. Low flow rates may have been insufficient to move the solid material from around the pH probe during runs.

The effect of temperature on acid neutralization by sand packs is displayed in Figure 17. The injected acid was HCl at a pH of 1.0. The pack was Ottawa sand and sodium montmorillonite. Acid neutralization was more pronounced at seventy degrees Celsius than at fifty degrees Celsius.

Figure 17

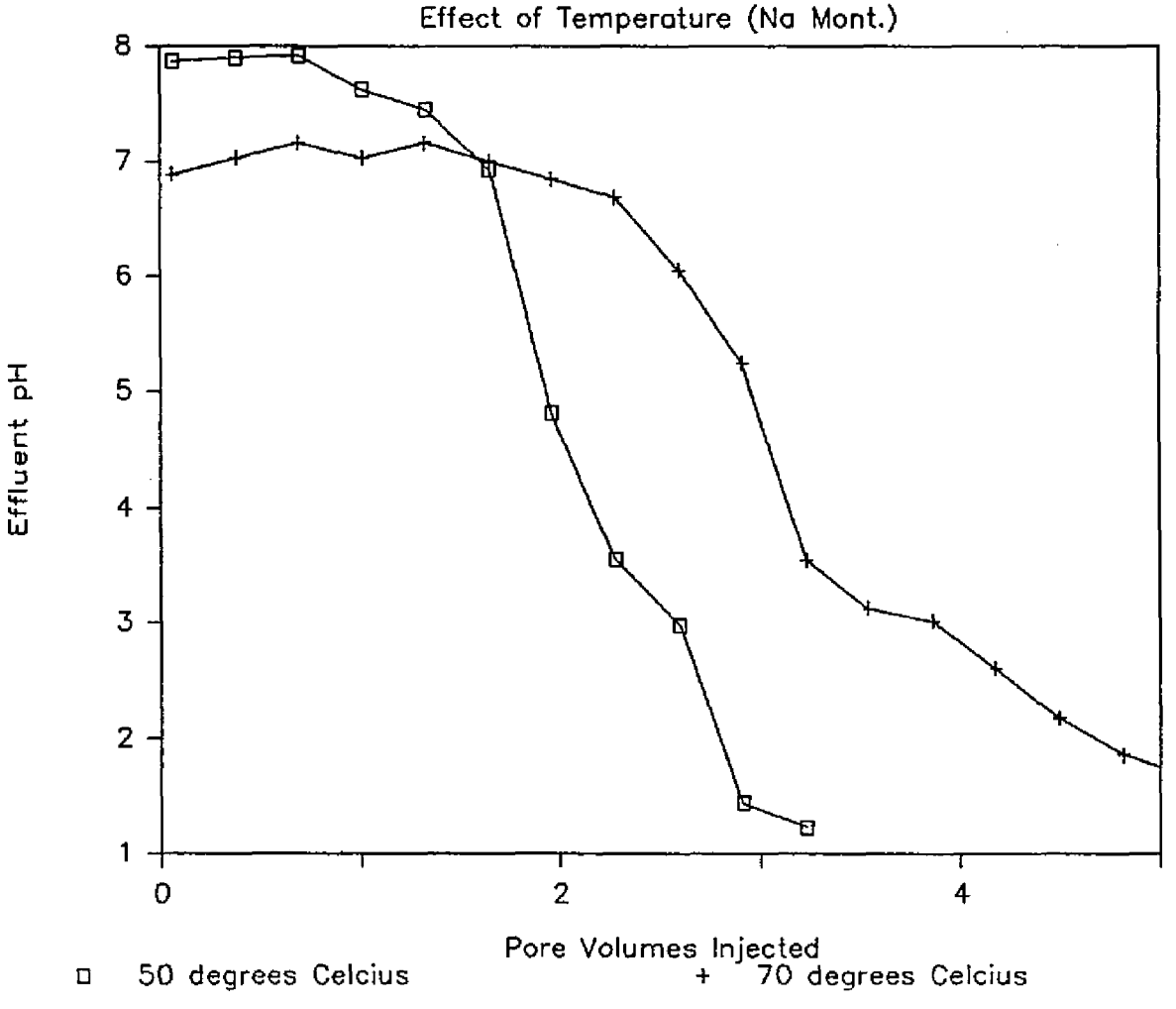
Effect of Temperature (Na Mont.)
Effluent pH
8
7
6
5
4
3
2
1
0
2
4
Pore Volumes Injected
50 degrees Celcius
70 degrees Celcius

The injected acid type was varied for the runs represented by Figure 18. Solutions of HCl, HNO_3, and H_2SO_4 were each injected into a pack containing Ottawa sand and sodium montmorillonite at seventy degrees Celsius. The pH of the injected acid was 1.0 in each case. The curves for nitric acid and sulfuric acid are very similar. More hydrochloric acid was neutralized by the sand pack relative to the other two acids.

Sand packs containing (1) sand and sodium montmorillonite, (2) sand and kaolinite, (3) sand and illite, and (4) Kaiser well material were used for the runs illustrated in Figure 19. The injected acid was HCl at a pH of 1.0 and the temperature was seventy degrees Celsius. The sand pack containing kaolinite neutralized the least acid. Comparable amounts of acid were neutralized by sand packs containing sodium montmorillonite and illite. The sand pack containing Kaiser well material neutralized the most acid.

Figure 19 shows that the pH of the sand pack effluent did not always begin at seven. Initial pH of the effluent from packs containing Kaiser well material was highest at about 8.5. Initial pH of effluent from sand packs containing kaolinite was about four. Reasons for this variation are unknown.

Figure 20 displays the effect of varying the length of sand packs containing Kaiser well material. The injected acid was HCl at a pH of 1.0, and the temperature

Figure 18

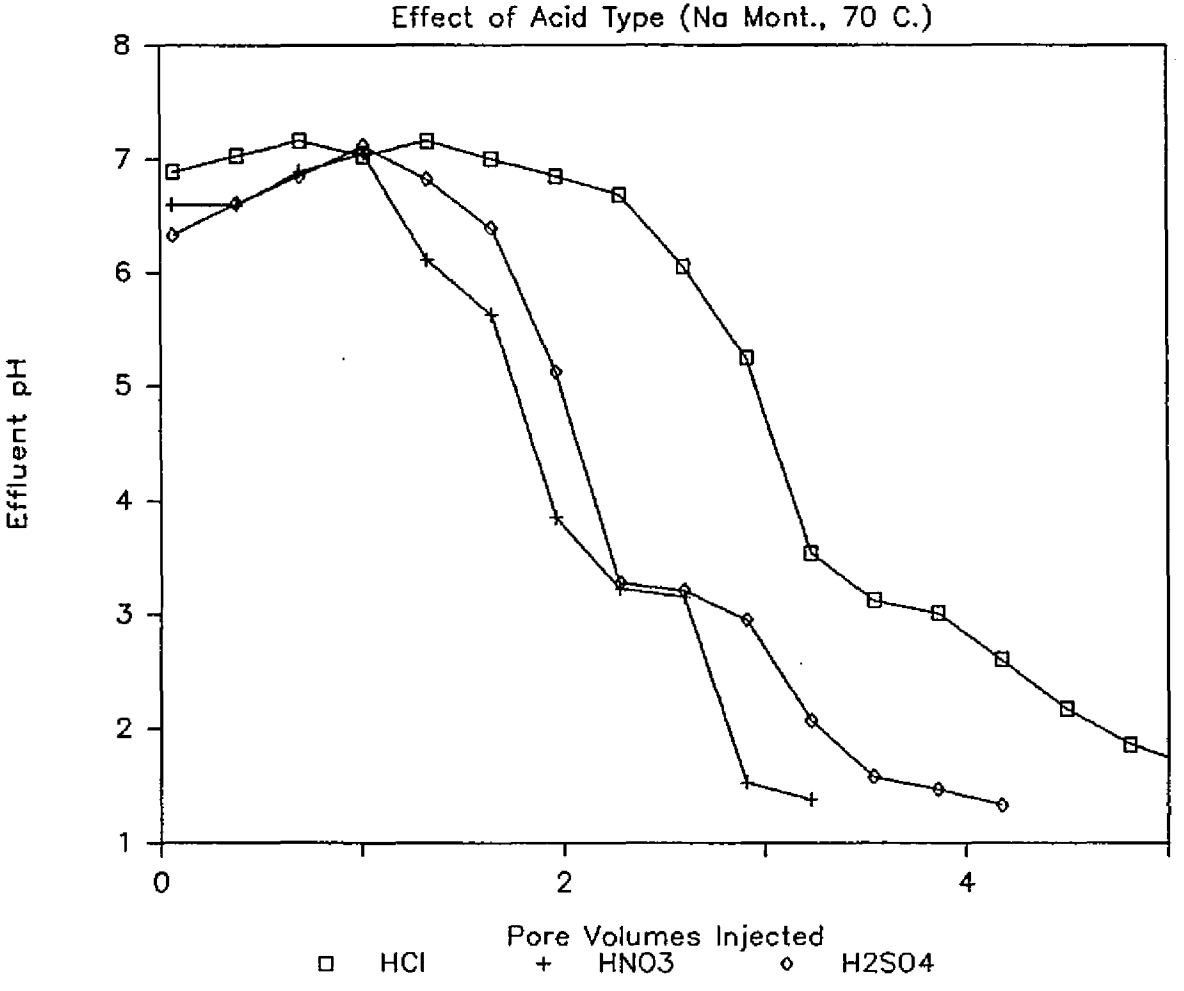
Effect of Acid Type (Na Mont., 70 C.)
Effluent pH
8
7
6
5
4
3
2
1
0
2
4
Pore Volumes Injected
□ HCl
+ HNO3
◇ H2SO4

Figure 19

Effect of Mineralogy (70 C.)

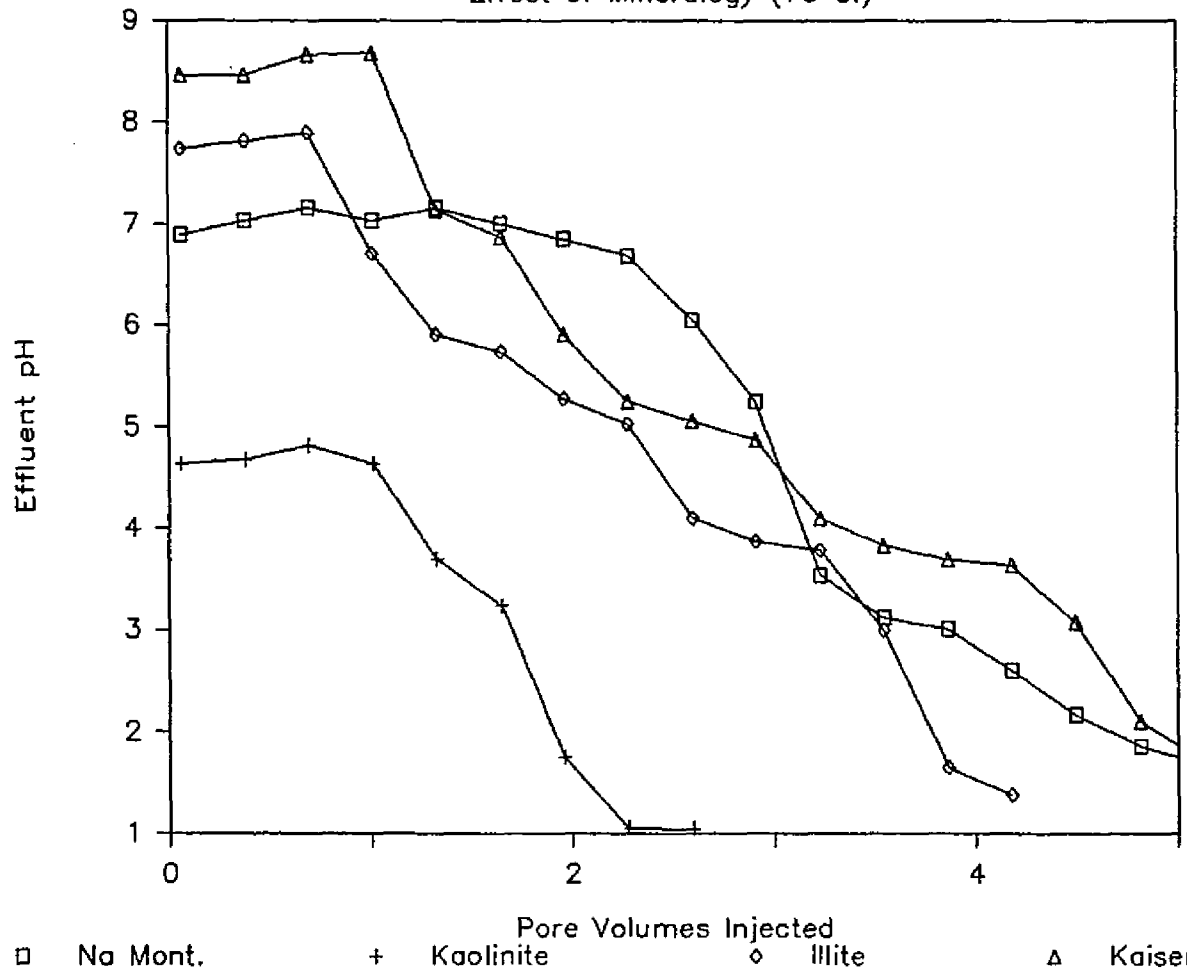

Figure 20

Effect of Pack Length (Kaiser, 70 C.)

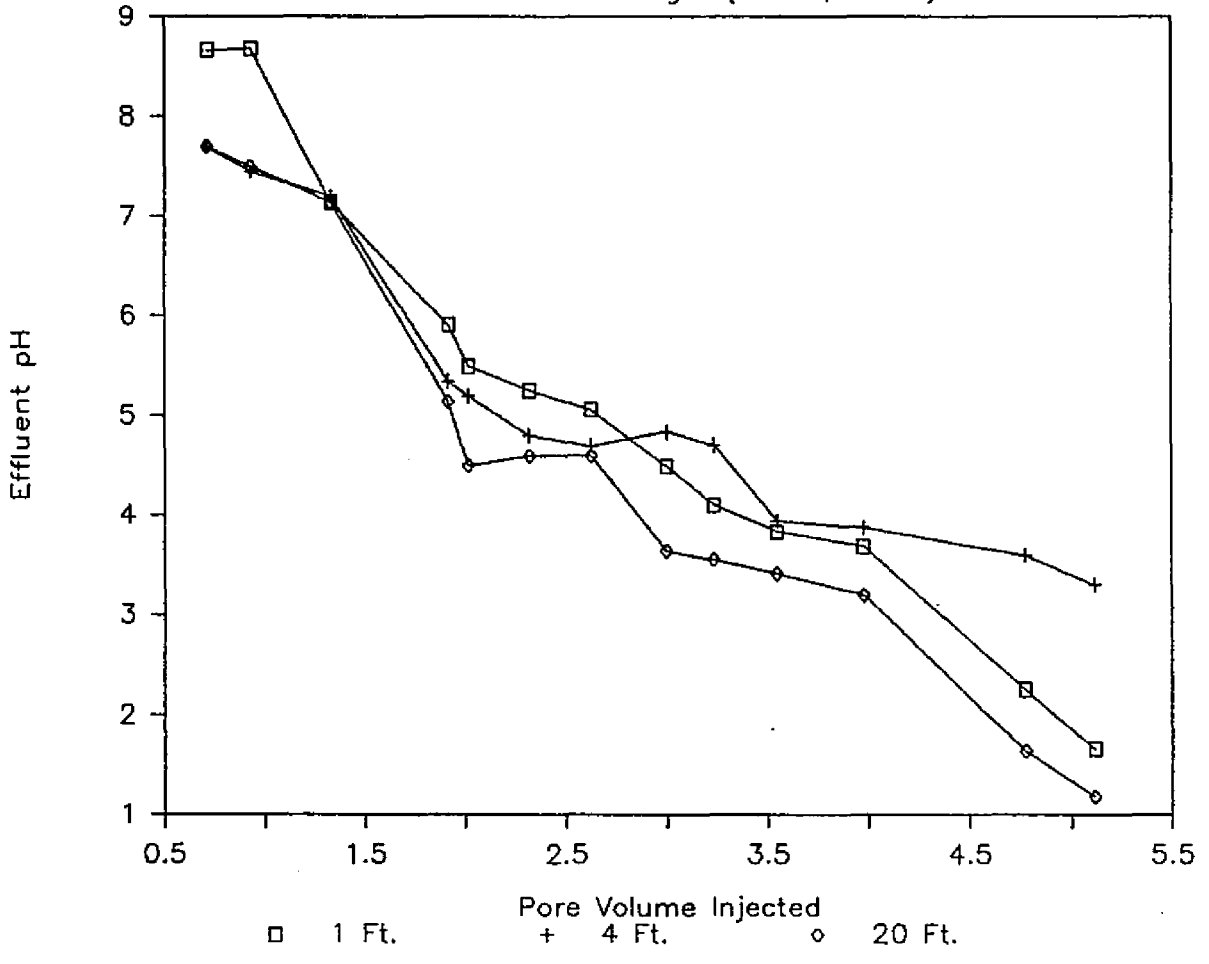

was seventy degrees Celsius. The acid neutralization based on pore volumes of acid injected was similar for one foot, four foot, and twenty foot sand packs. The injection rate was four feet per day for the one foot and four foot packs. The injection rate for the twenty foot sand pack was intermittent because of equipment problems, but averaged about ten feet per day.

4. Results and Discussion of Numerical Simulation

A ground water flow simulator, SUTRA (Voss, 1984), was used to model the flow of acidic solutions through the sand packs. In the interest of realism SUTRA was used to model flow of acidic fluids through packs containing Kaiser well sand, rather than the synthetic formation material.

The reaction of acid with actual formation material is very complex and is difficult to describe mathematically. The batch experiments performed in this research involved carefully controlled conditions and known mineral compositions. Therefore the batch experimental results could not be readily used for describing flow through the Kaiser sand. It was believed that relatively simple mathematical descriptions of adsorption, while not being rigorously correct, could be used to reasonably model these complex processes. The reactions of acid and formation material at least have the appearance of adsorption, in that the hydrogen ions are

retained on the solid clay surfaces much like classic liquid-solid adsorption. Hydrogen ions which adsorb on the clay surfaces or react with the clay are then not available for further reaction.

SUTRA was used to model a single reactive species, hydrogen, undergoing adsorption on the surface of formation material. The aim of the simulation was to match the overall effect of Kaiser well material on acidic fluid flowing through a linear sand pack. The experimental variable of interest was the pH of the effluent from the sand pack. The pack was modelled geometrically as discussed in Chapter V. Adsorption of hydrogen was approximated with a Langmuir adsorption isotherm (Hill, 1977).

Two parameters are used by SUTRA to characterize adsorption. The parameters are coefficients of terms in the Langmuir isotherm (Voss, 1984). The relationship of the adsorption coefficients to known quantities is

$$C_s = \frac{\chi_1(\rho_o C)}{1 + \chi_2(\rho_o C)}$$

$$\frac{\partial C_s}{\partial t} = \frac{\chi_1 \rho_o}{(1 + \chi_2 \rho_o C)^2} \frac{\partial C}{\partial t}$$

C_s = concentration of adsorbate on solid grains,

C = solute concentration as mass fraction,

ρ_o = constant fluid density,

χ_1 = Langmuir distribution coefficient, and

χ_2 = second Langmuir coefficient.

A match of the one foot sand pack experiment was made by adjusting the parameters affecting adsorption, chi_1 and chi_2, and by adjusting the parameter affecting dispersion, the dispersivity. Other parameters such as porosity, viscosity, density, and permeability remained fixed. It was found that the best value of dispersivity was zero. Even with a dispersivity of zero, SUTRA cannot model a perfectly sharp interface between injected and displaced fluid because of the numerical dispersion inherent with these models. The best values of chi_1 and chi_2 were 1.5×10^{-3} and 1.0×10^{-3}. Figure 21 shows this match of the SUTRA model with the one foot sand pack experiment. The values describing adsorption and dispersion were then used to model the performance of four foot and twenty foot Kaiser sand packs. Figures 22 and 23 show these results. The simulated results agree reasonably well with the measured results. The simulator generally underestimates the adsorptive ability of Kaiser well material. A SUTRA input dataset modelling the one foot sand pack is included in Appendix A.

SUTRA was also used to simulate a hypothetical, but realistic, system for disposal of low-pH hazardous wastes into a single disposal well in an infinitely large formation. Although SUTRA did a reasonably good job of matching the linear sand pack runs, it cannot be said that using SUTRA will adequately model an actual disposal system. The implication is that it will, but further

Figure 21

One Foot Kaiser Sand Pack

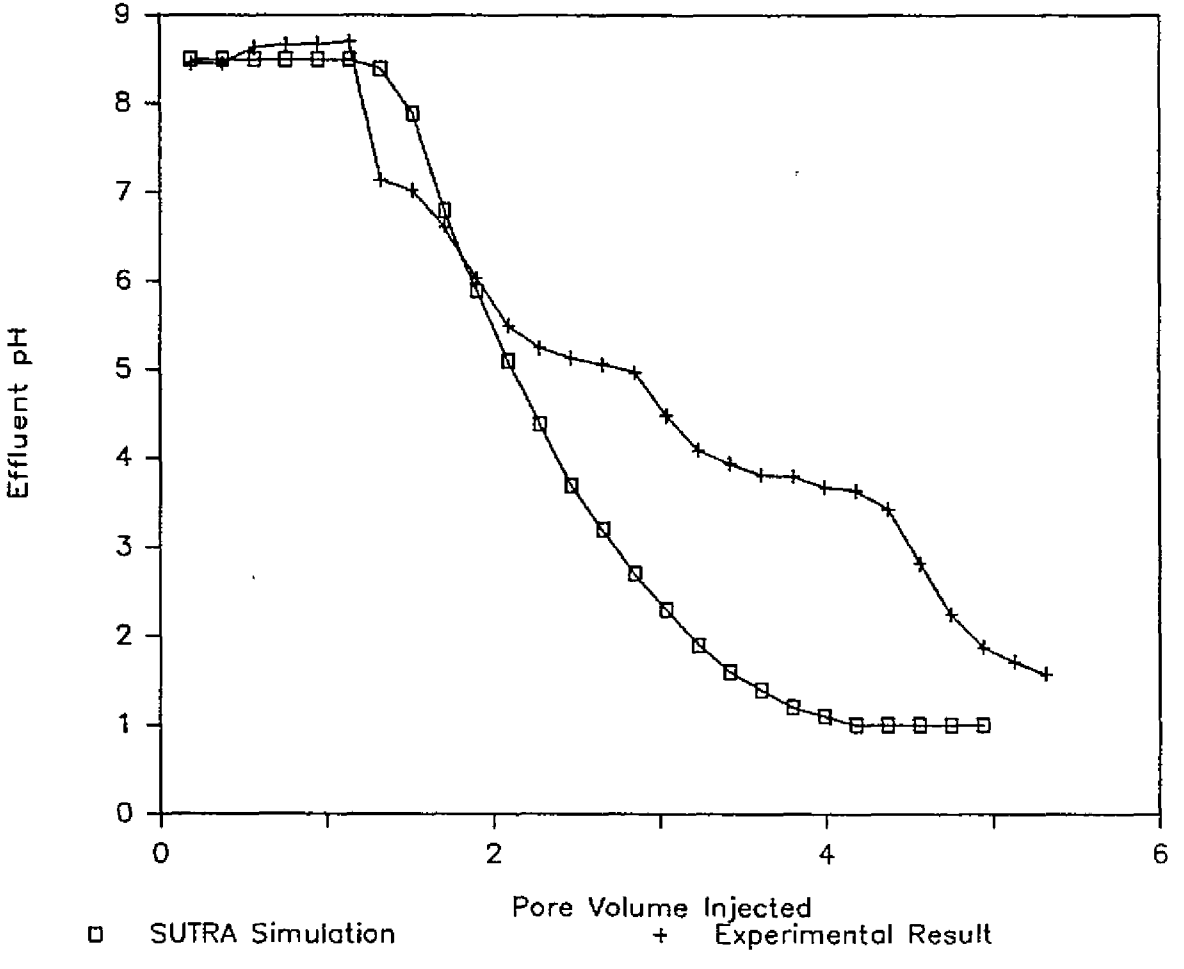

Figure 22

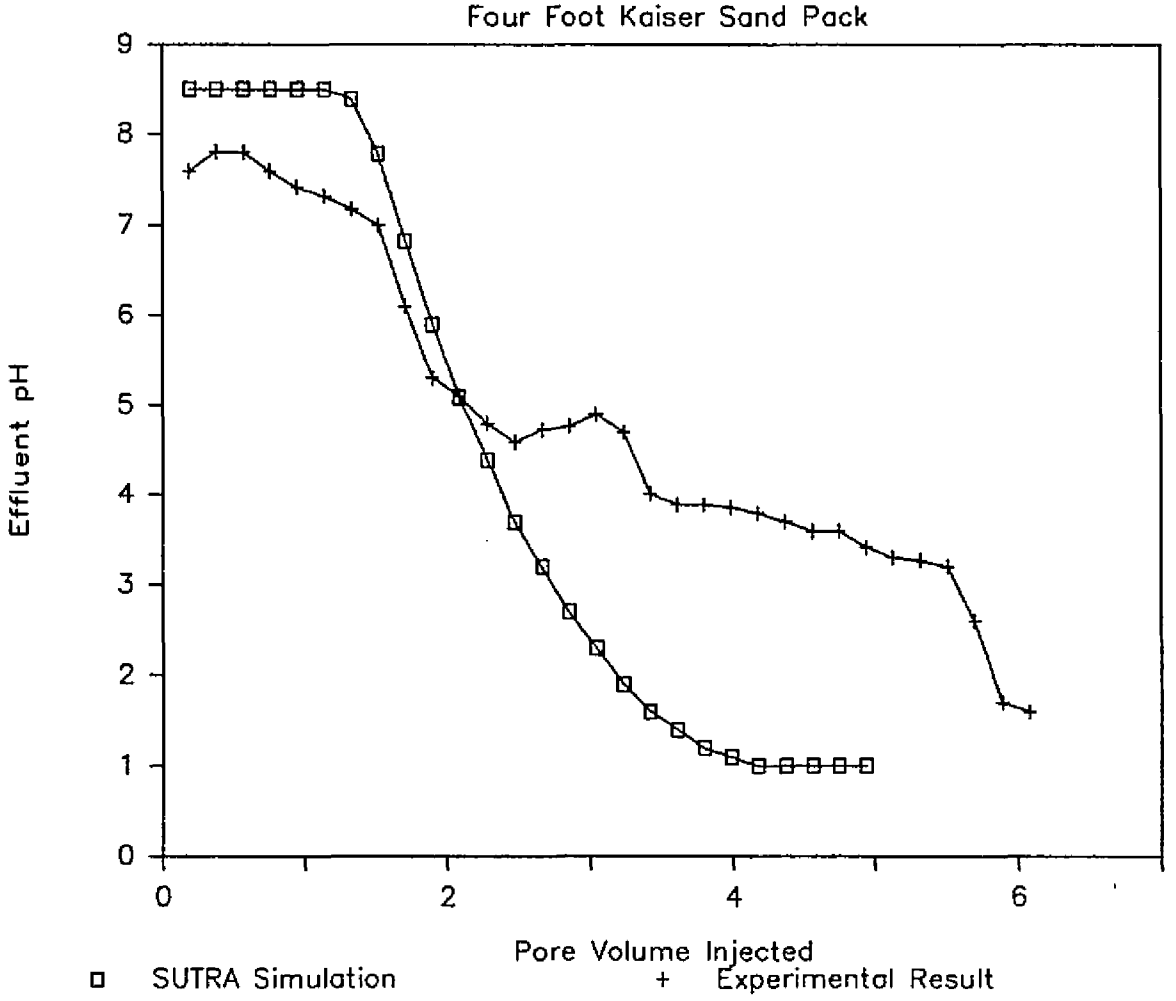
Four Foot Kaiser Sand Pack
Effluent pH
9
8
7
6
5
4
3
2
1
0
0
2
4
6
Pore Volume Injected
SUTRA Simulation
Experimental Result

Figure 23

Twenty Foot Kaiser Sand Pack

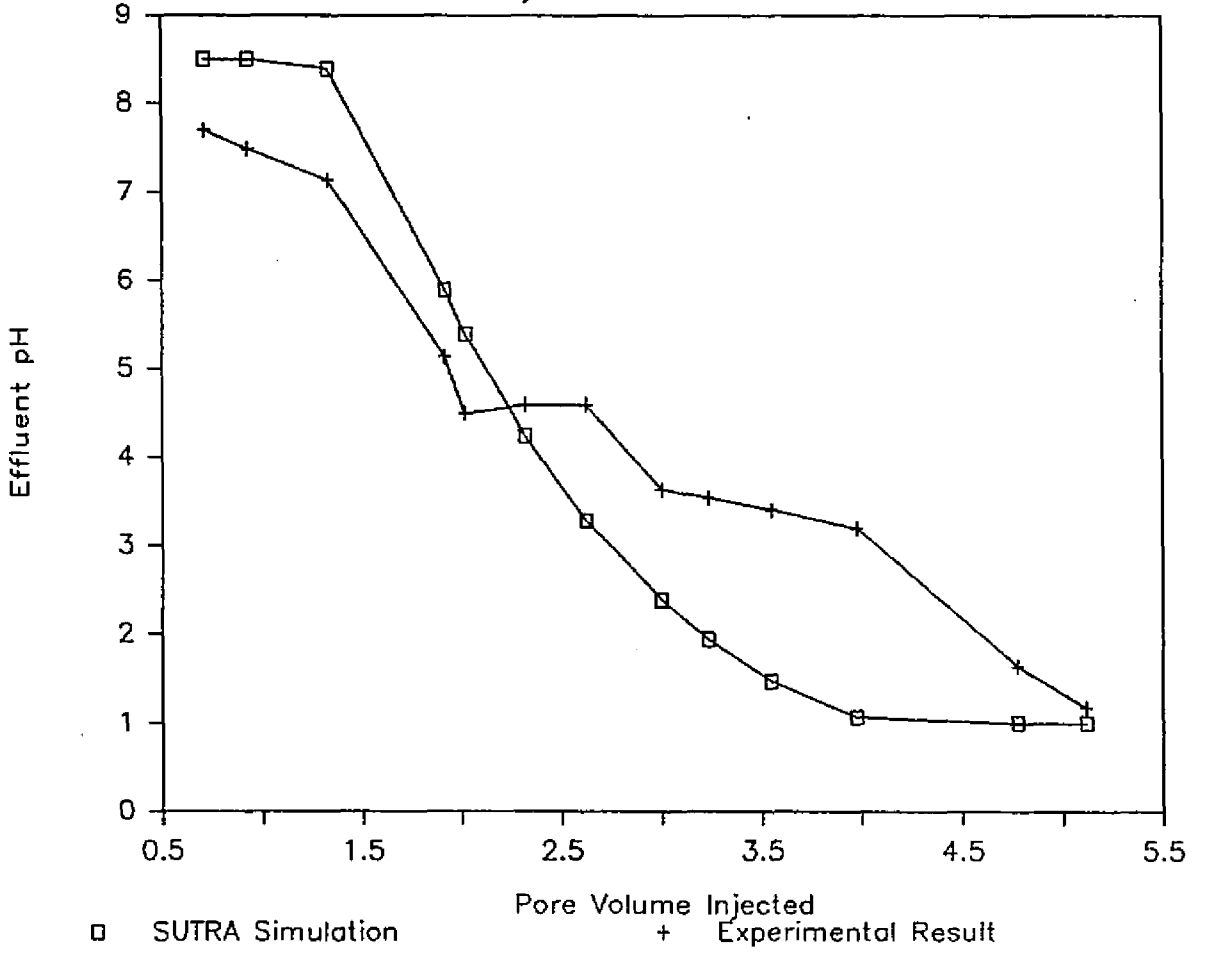

verification is recommended. The disposal system had the following characteristics:

Depth = 5000 ft.,

Formation thickness = 100 ft.,

Porosity = 0.30,

Permeability = 1000 millidarcies,

Fluid viscosity = 0.6 centipoise,

Injection rate = 10,000 barrels per day,

Injection fluid = acid brine (pH = 1),

Injection life = 20 years,

Wellbore radius = 0.5 ft.,

Aquifer radius = 250,000 ft., and

Dispersion = negligible (except for inherent numerical dispersion of the model).

The SUTRA input dataset for this simulation is listed in Appendix A.

Results of this simulation are presented in Figures 24 and 25. Figure 24 is a plot of pH vs. radial distance in feet away from the center of the injection wellbore. The individual curves on the plot represent time elapsed after the commencement of injection. Elapsed times from one year to twenty years are included. An interpretation of Figure 24 is as follows. The waste front after some time of injection, for example twenty years, is found by calculation:

$$\text{volume injected} = 10{,}000 \frac{\text{bbl}}{\text{d}} \times 5.616 \frac{\text{ft}^3}{\text{bbl}} \times 365 \frac{\text{d}}{\text{yr}} \times 20 \text{ yr}$$

Figure 24

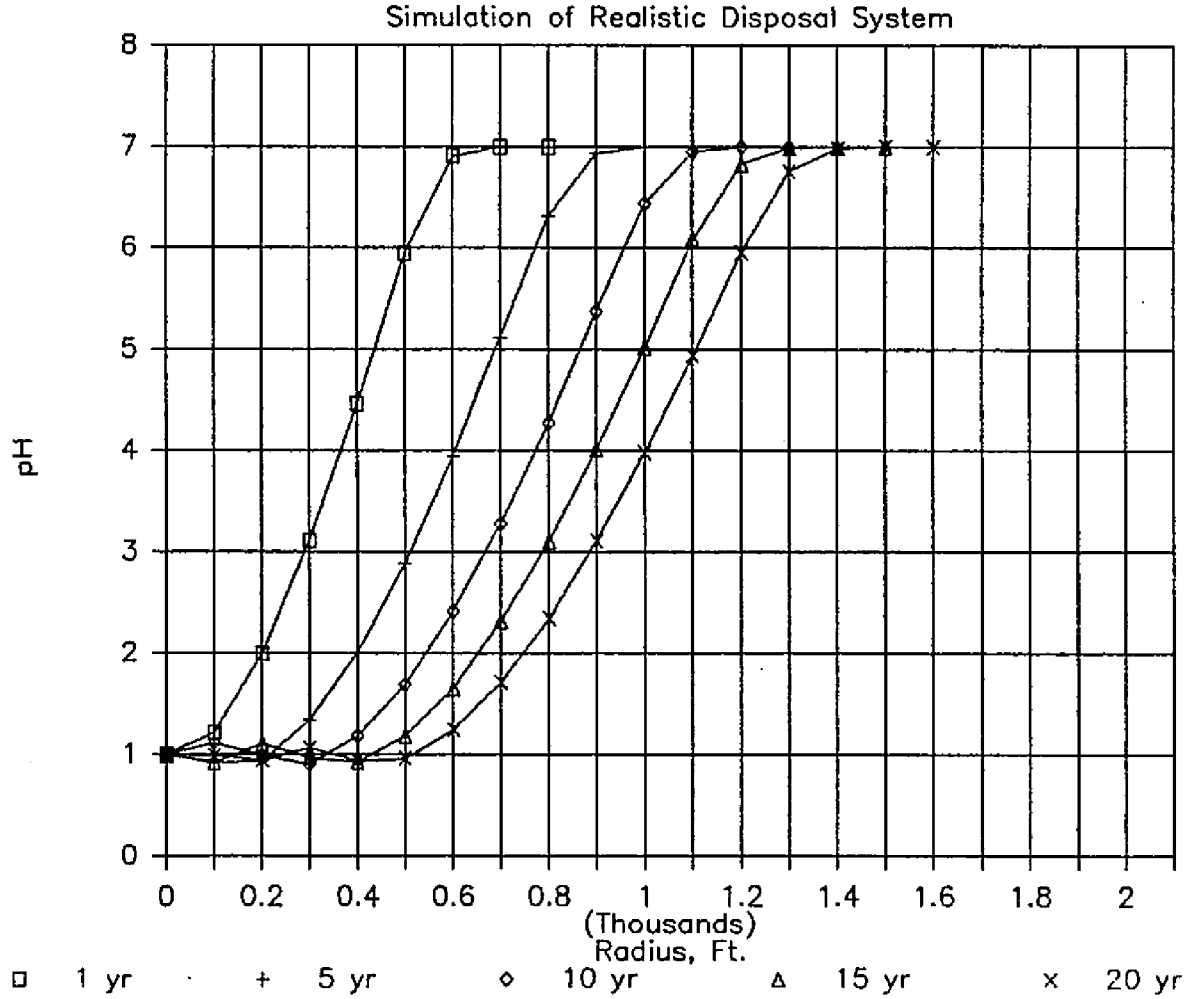
Simulation of Realistic Disposal System
pH
8
7
6
5
4
3
2
1
0
0
0.2
0.4
0.6
0.8
1
1.2
1.4
1.6
1.8
2
(Thousands)
Radius, Ft.
1 yr
5 yr
10 yr
15 yr
20 yr

Figure 25

Simulated Effect of Dispersion

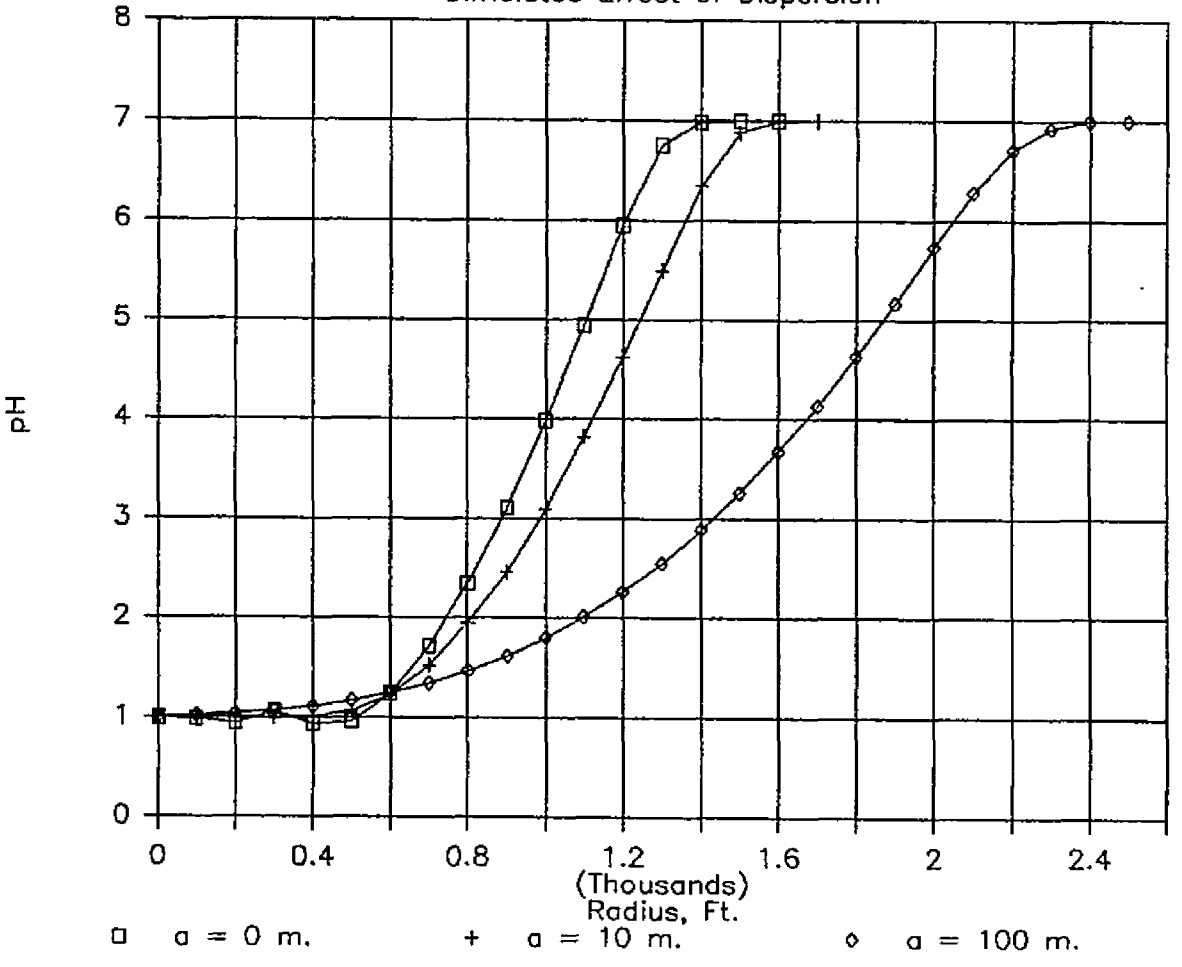

$$= 4.1 \times 10^{8} \text{ ft}^3 .$$

$$\text{Then} \quad (\text{radius})^2 = \frac{\text{volume injected}}{(\text{pi}) \times (\text{thickness}) \times (\text{porosity})}$$

$$= \frac{4.1 \times 10^{8} \text{ ft}^3}{(3.1416) \times (100 \text{ ft}) \times (.30)}$$

$$\text{radius} = 2085 \text{ ft.}$$

The waste front is 2085 feet away from the injection wellbore after twenty years of injection, ignoring dispersion. From Figure 24, after twenty years of injection, the acid is completely neutralized past a radius of 1400 feet. At 750 feet, the pH is two. This means that the injected acid is no longer hazardous past 750 feet. Fluid with a pH of 1.0, which is the acidity of the injected fluid, fills the formation to a radius of about 500 feet from the wellbore. Thus, out to a radius of 500 feet, the formation is depleted of its ability to neutralize acid. In summary, although the injected waste has traveled radially out to a distance of 2085 feet, the hazardous zone extends out to only 750 feet. A further implication is that when injection stops, and if the zone of waste begins to migrate, the acid would contact fresh formation material and eventually become completely non-hazardous.

Figure 25 depicts the results of a simulation of the hypothetical disposal system with the effects of dispersion shown for three values of dispersivity, zero

meters, ten meters, and 100 meters. Only the twenty year profiles are shown. Increasing values of dispersivity cause the waste fronts to become less sharp, as expected. The hazardous zone extends further out as dispersion increases.

Figure 26 depicts a SUTRA simulation of the hypothetical disposal system in which zero adsorption and zero dispersivity were used in the model. This Figure illustrates that the expected sharp interface between waste acid and native brine is instead smeared. This is caused by numerical dispersion, which is inherent in these types of models. The amount of numerical dispersion can be changed by modifying the grid block spacing and the time step size. An investigation into this is beyond the scope of the current research, but should be the subject of future work.

A reasonable approach to the use of the SUTRA model for actual disposal systems is to measure the effluent pH from a linear sand pack using actual formation material. The adsorption parameters for SUTRA can then be adjusted until a match of the sand pack results is achieved. These same parameters can then be used in SUTRA to model the actual system.

Figure 26

Effect of Numerical Dispersion

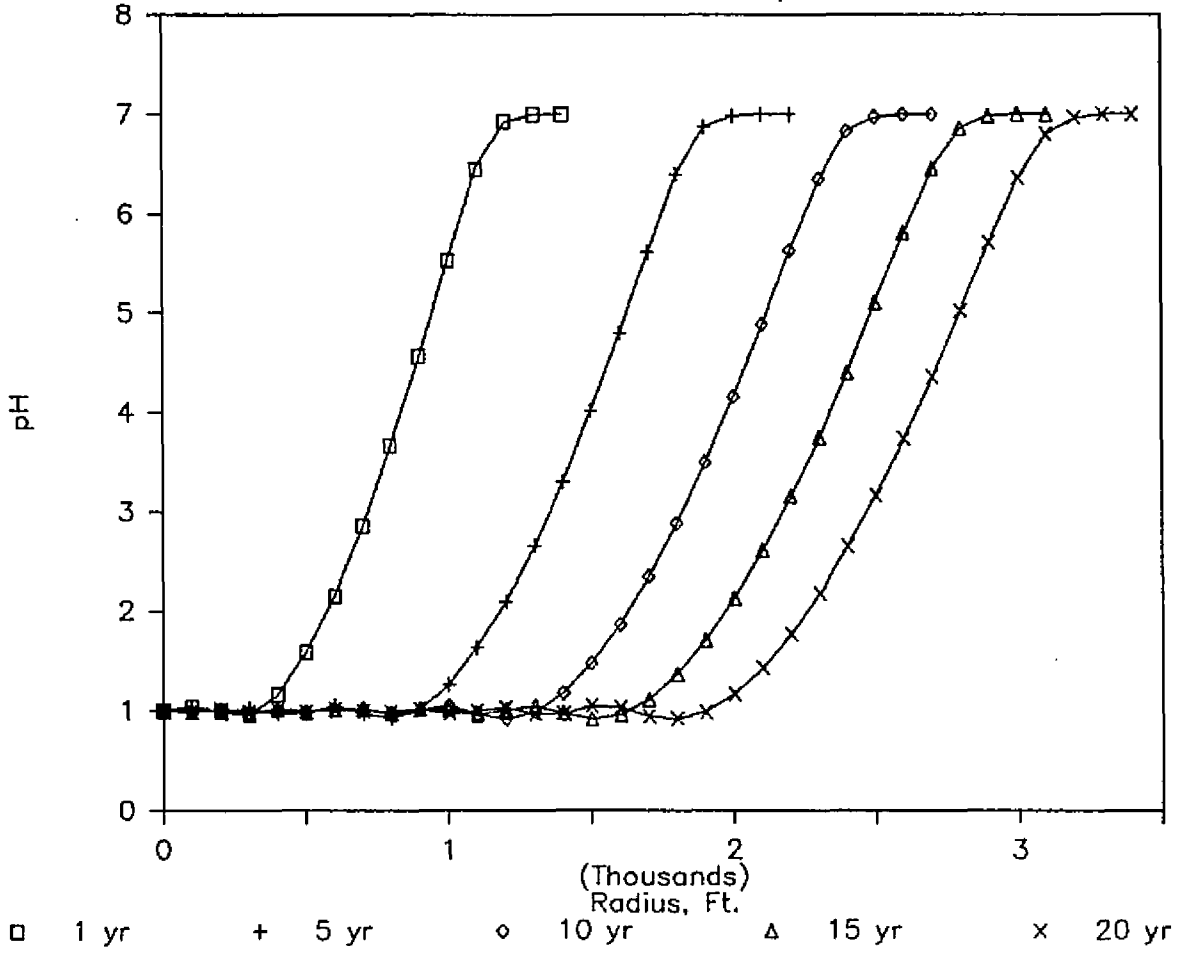

CHAPTER VII.

Conclusions and Recommendations

1. Conclusions

The conclusions of this study are presented relative to each experimental method and are enumerated as follows.

(1) Reaction rate coefficients and apparent energies of activation determined with the batch reaction technique agree reasonably well with those which the current research has in common with a previous study. It is concluded that the batch reaction technique is a valid method for analyzing the chemical kinetics of acid dissolution of clays, and that the coefficients determined will help satisfy industrial requirements for parameters used in sophisticated mathematical simulators.

(2) The sand pack technique appears to be a simple, inexpensive method of determining the acid neutralizing capabilities of material in waste injection formations.

(3) Sand pack experimentation illustrates that neutralization of hydrochloric acid, nitric acid, and sulfuric acid occurs due to interaction of acid with synthetic sand packs and packs containing actual formation material. Neutralization of more acid, on a pore volume basis, occurs at seventy degrees Celsius than at fifty degrees Celsius.

(4) A one foot long sand pack is as informative regarding acid neutralization as is a sand pack twenty

feet long, if the phenomenon of interest is the relative change in acidity.

(5) Type and quantity of clay minerals present in a disposal formation are important criteria in evaluating the effectiveness of the formation for acid neutralization.

(6) Underground movement of injected low-pH wastes serves to further neutralize the waste, as more fresh clay sites are encountered in the disposal formation.

(7) The SUTRA model matches the acid neutralization performance of short, linear sand pack systems relatively well. The SUTRA model appears to be a good tool for modelling acid neutralization of real low-pH waste injection systems.

2. Recommendations

The recommendations of this research are:

(1) Other classes of chemical compounds, such as organics, heavy metals, and bases, should be analyzed regarding their applicability for underground disposal using the techniques described here.

(2) The SUTRA model can now be used to predict the fate of low-pH waste streams disposed of in underground sandstone formations which contain clay minerals. However, the sensitivity of underground waste disposal to environmental conditions may warrant field tests of the

model. Such field tests involve considerable expense and are recommended only if mandated by regulatory bodies such as the EPA.

(3) The experimental approach described by this study provides a basis for further studies of acid-clay interaction mechanisms such as adsorption and diffusion.

REFERENCES

Abdul-Latif, N. and C. E. Weaver: "Kinetics of Acid-Dissolution of Palygorskite (Attapulgite) and Sepiolite", Clays and Clay Minerals, v. 17, 1969.

Athavaley, A. S., R. J. Funk, R. G. Sweet, and W. A. Coffey: "Deep Well Injection of Industrial Wastes", Ind. Wastes, 27(3), 1981.

Banin, A.: "Ion Exchange Isotherms of Montmorillonite and Structural Factors Affecting Them", Israel Journal of Chemistry, v. 6, 1968.

Beutelspacher, H., and van der Marel, H. W.: Atlas of Electron Microscopy of Clay Minerals and Their Admixtures, Am. Elsevier Publishing Co., 1968.

Bourgoyne, A. T., Jr., K. K. Millheim, M. E. Chenevert, and F. S. Young, Jr.: Applied Drilling Engineering, SPE Monograph, 1986.

Bouwer, H.: "Use of the Earth's Crust for Treatment or Storage of Sewage Effluent and Other Waste Fluids", CRC Crit. Rev. Environ. Control, 6(2), 1976.

Brasier, F.: "Injection of Hazardous Wastes - EPA Overview", Proceedings of the International Symposium on Subsurface Injection of Liquid Wastes, 1986, p. 1.

Brindley, G. W. and R. F. Youell: "A Chemical Determination of 'Tetrahedral' and 'Octahedral' Aluminum Ions in a Silicate", Acta. Cryst., 1951.

Bromley, L. A.: "Thermodynamic Properties of Strong Electrolytes in Aqueous Solutions", AIChE Journal, v. 19, no. 2, 1973.

Bunge, A. L., and C. J. Radke: "Divalent Ion Exchange With Alkali", Society of Petroleum Engineers Journal, 1983.

Ciaccio, L. L.: Water and Water Pollution Handbook, M. Decker, Inc., 1971.

Coffey, W. A., A. S. Athavaley, R. J. Funk, and R. G. Sweet: "Deep Well Injection of Industrial Wastes: A State-of-the-Arts Case History", Proc. Ind. Waste Conf., Vol. Date 1980, 35.

Collins, G. and M. B. Kayser: Interaction, Compatibilities, and Long-Term Environmental Fate of Deep -Well-Injected EOR Fluids and/or Waste Fluids with Reservoir Fluids and Rocks - State-of-the-Art, U.S. Dept. of Energy, Contract No. FC01-83FE60149, NIPER-70 (DE85000146), 1985.

Davis, K. E. and T. L. Hineline: "Two Decades of Successful Hazardous Waste Disposal Well Operation - A Compilation of Case Histories", Proceedings of the International Symposium on Subsurface Injection of Liquid Wastes, 1986.

Davis, K. E. and M. D. Jarrell: "Multiuse Polymer Protects Injection Well During Drilling, Underreaming, and Gravel Packing", Oil and Gas Journal, 81(50), 1983.

Donaldson, E. C.: "Subsurface Injection of Industrial Waste in the U.S.", Bur. Mines, Geol. Appl. Idrogeol., 11(2), 1976.

Dugas, R. S. and P. E. Reed: "Successful Pretreatment and Deep-Well Injection of Chemical Plant Wastewater", Proc. Ind. Waste Conf., Vol. Date 1977, 32.

Eardley, A. J.: Structural Geology of North America, Harper & Brothers, 1951.

Eaton, H. C., F. K. Cartledge, and M. E. Tittlebaum: "The Interaction of Parachlorophenol with Clay Minerals", Louisiana State University Hazardous Waste Research Center, Presented to EPA, 1986.

Ehrlich, G. G., E. M. Godsy, C. A. Pascale, and J. Vecchioli: "Chemical Changes in an Industrial Waste Liquid During Post-Injection Movement in a Limestone Aquifer, Pensacola, Fla.", Ground Water, v. 17, no. 6, 1979.

Eitel, W.: The Physical Chemistry of the Silicates, University of Chicago Press, 1954.

Franson, M. A. H., A. E. Greenburg, R. R. Trussill, and L. S. Clesceri: Standard Methods for the Examination of Water and Wastewater, 16th Eidtion, American Public Health Association, Washington, D.C., 1985.

Gaines, G. L., Jr., and H. C. Thomas: "Adsorption Studies on Clay Minerals. II. A Formulation oof the Thermodynamics of Exchange Adsorption", The Journal of Chemical Physics, v. 21, no. 4, 1953.

Galley, J. E.: "Subsurface Disposal in Geologic Basins - A study of Reservoir Strata", American Association of Petroleum Geologists Memoir 10, 1968.

George, C. and B. Thomas: "Cementing to Achieve Zone Isolation in Disposal Wells", Proceedings of the International Symposium on Subsurface Injection of Liquid Wastes, 1986.

Gordon, W. and J. Bloom: "Deeper Problems - Limits to Underground Injection as a Hazardous Waste Disposal Method", Proceedings of the International Symposium on Subsurface Injection of Liquid Wastes, 1986.

Granquist, W. T. and G. G. Sumner: "Acid Dissolution of a Texas Bentonite", Clays and Clay Minerals, 1959.

Green, W. J., et. al.: "Interaction of Clay Soils with Water and Organic Solvents: Implications for the Disposal of Hazardous Wastes", Environmental Science and Technology, 1983.

Greenberg, A. E., R. R. Trussell, L. S. Clesceri, and M. A. H. Franson: Standard Methods for the Examination of Water and Wastewater, 16th ed., American Public Health Association, 1985.

Griffin R. A., and J. F. Shimp: "Attenuation of Pollutants in Municiple Landfill Leachate by Clay Minerals", Report, EPA/600/2-78/157, Order No. PB-287140, 1978.

Grim, R. E.: Applied Clay Mineralogy, McGraw-Hill, Inc., 1962.

Hanby, K. P.: "Sixteen Successful Years - A History of Stauffer Chemical Company's Underground Injection at Bucks, Alabama", Proceedings of the International Symposium on Subsurface Injection of Liquid Wastes, 1986.

Heutmaker, D. L., F. L. Peterson, and S. W. Wheatcraft: "A Laboratory Study of Waste Injection into a Glyben-Herzberg Groundwater System Under Dynamic Conditions", Tech. Rep.-Univ. of Hawaii, Water Res. Research Center, 1977.

Hill, Jr., C.: An Introduction to Chemical Engineering Kinetics and Reactor Design, John Wiley & Sons, 1977.

Hill, H. J. and L. W. Lake: "Cation Exchange in Chemical Flooding: Part 3 - Experimental", Society of Petroleum Engineers Journal, 1978.

Hirasaki, G. J.: "Ion Exchange With Clays in the Presence of Surfactant", Society of Petroleum Engineers Journal, 1982.

Hower, W. F.: "Influence of Formation Clays on the Flow of Aqueous Fluids", ASTM Special Tech. Publication, 735 (Water Subsurf. Injection), 1981.

Huang, W. H.: "New Stability Diagrams of Some Clay Minerals in Aqueous Solution", Nature Physical Science, v. 243, 1973.

Iler, R. K.: The Chemistry of Silica: Solubility, Polymerization, Colloid and Surface Properties, and Biochemistry, John Wiley & Sons, Inc., 1979.

Iler, R. K.: The Colloid Chemistry of Silica and Silicates, Cornell University Press, 1955.

Inoue, A. and H. Minato: "Ca - K Exchange Reaction and Interstratification in Montmorillonite", Clays and Clay Minerals, v. 27, no. 6, 1979.

Jacobus, J., Englande, Jr., A. J., Reimers, R. S., and D'Amour, G.: "Louisiana Industry-Resource Recovery and By-Product Conversion Survey and Disposal Technologies", Tulane University, Contract No. 84-TUU/DNR(2)-B17, 1985.

Klemt, B., S. Pole, and R. MacKinnon: "Industrial Waste Disposal Wells Mechanical Integrity", Proceedings of the International Symposium on Subsurface Injection of Liquid Wastes, 1986.

Lake, L. W. and R. Helfferich: "Cation Exchange In Chemical Flooding: Part 2 - The Effect of Dispersion, Cation Exchange, and Polymer/Surfactant Adsorption on Chemical Flood Environment", Society of Petroleum Engineers Journal, 1978.

Latil, M., C. Bardon, J. Burger, and P. Sourieau: Enhanced Oil Recovery, Editions Technip, 1980.

Laudelout, H., R. Van Bladel, G. H. Bolt, and A. L. Page: "Thermodynamics of Heterovalent Cation Exchange Reactions in a Montmorillonite Clay", Transactions of the Faraday Society, v. 64, no. 6, 1968.

Leenheer, J. A., R. L. Malcolm, and W. R. White: "Physical, Chemical, and Biological Aspects of Subsurface Organic Waste Infection Near Wilmington, N.C.", U.S. Geol. Surv. Prof. Paper (U.S.), 1976.

Leenheer, J. A., R. L. Malcolm, and W. R. White: "Investigation of the Reactivity and Fate of Certain Organic Components of an Industrial Waste after Deep-Well Injection", Environmental Science and Technology, v. 10, no. 5, May, 1976.

Levenspiel, O.: Chemical Reaction Engineering, 2nd Ed., John Wiley & Sons, 1972.

Lieu, V. T., S. G. Miller, and S. J. Staphanos: "Long-Term Consumption of Caustic and Silicate Solutions by Petroleum Reservoir Sands", in "Soluble Silicates", edited by J. S. Falcone, Jr., ACS Symposium Series 194, Am. Chem. Society, 1982.

Mackay, D. M., Roberts, P. V., and Cherry, J. A.: "Transport of Organic Contaminants in Groundwater", Environmental Science and Technology, May, 1985.

Maes, A., P. Peigneur, and A. Cremers: "Thermodynamics of Transition Metal Ion Exchange in Montmorillonite", Proc. of the International Clay Conf., 1975.

Martinez, J. D.: "Waste Disposal Requirements and Louisiana's Environmental Quality", Proceedings, American Institute of Professional Geologists, 1979.

Mathews, A. C., S. B. Weed, and N. T. Coleman: "The Effect of Acid and Heat Treatment on Montmorillonoids", Clays and Clay Minerals, 1955.

Meissner, H. P. and C. L. Kusik: "Aqueous Solutions of Two or More Strong Electrolytes", Ind. Eng. Chem. Process Des. Devel., v. 12, no. 2, 1973.

Miller, R. J.: "Mechanisms for Hydrogen to Aluminum Transformations in Clays", Soil Science Society Proceedings, 29, 1965.

Mungan, N.: "Permeability Reduction Through Changes in pH and Salinity", Journal of Petroleum Technology, 1965.

Nothnagel, K. H., D. S. Abrams, and J. M. Prausnitz: "Generalized Correlation for Fugacity Coefficients in Mixtures at Moderate Pressures", Ind. Eng. Chem. Process Des. Devel., v. 12, no. 1, 1973.

Novak, I. and B. Cicel: "Dissolution of Smectites in Hydrochloric Acid: II. Dissolution Rate as a Function of Crystallochemical Composition", Clays and Clay Minerals, v. 26, no. 5, 1978.

Osthaus, B. B.: "Chemical Determination of Tetrahedral Ions in Nontronite and Montmorillonite", Clays and Clay Minerals, 1954.

Osthaus, B. B.: "Kinetic Studies on Montmorillonites and Nontronite by the Acid-Dissolution Technique", Clays and Clay Minerals, 1956.

Owen, L. B., E. Raber, C. Otto, R. Netherton, R. Neurath, and L. Allen: "Assessment of the Injectability of Conditioned Brine Produced by a Reaction Clarification: Gravity Filtration System in Operation at the Salton Sea Geothermal Field, Southern California", Report, UCID-18488, Energy Res. Abstracts, Abst. No. 10079, 5(7), 1980.

Pascale, C. A. and J. B. Martin: "Hydrologic Monitoring of a Deep-Well Waste-Injection System Near Pensacola, Fla., March 1970-Mar. 1977", Report, USGS/WRD/WRI-78/040, USGS/WRI-78-27, Order No. PB-284086, 1978.

Pettijohn, F. J.: Sedimentary Rocks, Harper and Row, Inc., 1957.

Pitzer, K. S.: "Thermodynamics of Electrolytes. I. Theoretical Basis and General Equations", The Journal of Physical Chemistry, v. 77, no. 2, 1973.

Pojasek, R. B.: Toxic and Hazardous Waste Disposal, v. 4, Ann Arbor Science, 1980.

Ponder, G. F.: "Groundwater Contaminant Transport Modeling", Environmental Science and Technology, Apr., 1984.

Ratliff, W.: "Dissolution of Silicate Minerals by Concentrated NaOH Solutions: Implications for Subsurface Waste Disposal", M.S. Thesis, Louisiana State University, 1985.

Reeder, L. R., et. al.: "Review and Assessment of Deepwell Injection of Hazardous Waste", U.S. EPA, EPA/600/2-77/029A, 1977.

Ross, G. J.: "Acid Dissolution of Chlorites: Release of Magnesium, Iron, and Aluminum and Mode of Acid Attack", Clays and Clay Minerals, v. 17, 1969.

Sanderson, R. V. and H. H. Chien: "Simultaneous Chemical and Phase Equilibrium Calculation", Ind. Eng. Chem. Process Des. Devel., v. 12, no. 1, 1973.

Scrivner, N. C., K. E. Bennett, R. A. Pease, A. Kopatsis, S. J. Sanders, D. M. Clark, and M. Rafal: "Chemical Fate of Injected Wastes", Proceedings of the International Symposium on Subsurface Injection of Liquid Wastes, 1986.

Sherwood, T. K., R. L. Pigford, and C. R. Wilke: Mass Transfer, McGraw Hill, Inc., 1975.

Smith, F. W.: "Ion-Exchange Conditioning of Sandstones for Chemical Flooding", Journal of Petroleum Technology, 1978.

Smith, J. M.: Chemical Engineering Kinetics, McGraw-Hill, Inc., 1970.

Smith, M. E.: "Solid Waste Disposal: Deepwell Injection", Chemical Engineering, 1979.

Spraggs, L. D. and Street, R. L.: "Three Dimensional Simulation of Thermally-Influenced Hydrodynamic Flows", U.S. Department of the Interior, 1975, Technical Report No. 190.

Turner, R.: "Kinetic Studies of Acid Dissolution of Montmorillonite and Kaolinite", U. Cal., Davis, Ph.D. Thesis, 1964.

Van der Marel, H. W., and Beutelspacher, H.: Atlas of Infrared Spectroscopy of Clay Minerals and Their Admixtures, Am. Elsevier Publishing Co., 1976.

Van Everdingen, A. F.: "Fluid Mechanics of Deepwell Disposal", Am. Assoc. Petroleum Geologists Memoir 10, 1968.

Voss, C. I.: "A Finite-Element Simulation Model for Saturated-Unsaturated, Fluid-Density-Dependent Ground Water Flow with Energy Transport or Chemically-Reactive Single-Species Solute Transport", U.S. Geological Survey Water Resources Investigations Report 84-4369, 1984.

Walter, B.: "Remediation of Ground-Water Contamination Resulting from the Failure of a Class I Injection Well: A Case History", Proceedings of the International Symposium on Subsurface Injection of Liquid Wastes, 1986.

Warner, D. L.: "Subsurface Disposal of Liquid Industrial Waste by Deepwell Injection", Am. Assoc. Petroleum Geologists Memoir 10, 1968.

Whiteside, R. F. and S. F. Raef: "Mechanical Integrity of Class I Injection Wells", Proceedings of the International Symposium on Subsurface Injection of Liquid Wastes, 1986.

"How Safe is Deep-Well Disposal of Waste?", Chemical Week, Nov. 21, 1984, editorial. (Latil, 1980).

APPENDIX A

The ground water flow simulator SUTRA (Voss, 1984) was used to model the flow of low-pH waste streams through linear sand packs. Adsorption coefficients in SUTRA which resulted in close matches with the performance of linear sand packs were used to model a full scale waste disposal system. The value of the Langmuir distribution coefficient was 1.0 x 10^{-3} and the second Langmuir coefficient was 1.0 x 10^{-3}.

The SUTRA input dataset used to model a linear sand pack is as follows:

```
SUTRA SOLUTE TRANSPORT
..... STEADY LINEAR FLOW WITH SOLUTE TRANSPORT
+++++++++ LINEAR SANDPACK MODEL - NA MONT., HCL
   50     24      7      0      2     2      2      0      4   9999
 0000             +01             +0             +1             +0
    0.00D0                                                1.000D-02
 1800          12.00D02          3.2D07          01       1.0D00
12.00D02  01     1
        +1
    0.00D0                   0.0D00     1000.D00         0.00D0
0.00D0    1.0D-03
    0.00D0                                              2650.D00
LANGMUIR       1.50D-03                  1.00D-03
    0.00D0                                               -0.00D0
NODE           001.D0         020.D0        1.00D0         0.40D0
    1         0.0000         0.0000        0.0225          1.000
    2     0.0225     0.0000     0.0225      1.000
    3     0.0000     0.0127     0.0225      1.000
    4     0.0225     0.0127     0.0225      1.000
    5     0.0000     0.0254     0.0225      1.000
    6     0.0225     0.0254     0.0225      1.000
    7     0.0000     0.0381     0.0225      1.000
    8     0.0225     0.0381     0.0225      1.000
    9     0.0000     0.0508     0.0225      1.000
   10     0.0225     0.0508     0.0225      1.000
   11     0.0000     0.0635     0.0225      1.000
   12     0.0225     0.0635     0.0225      1.000
   13     0.0000     0.0762     0.0225      1.000
   14     0.0225     0.0762     0.0225      1.000
   15     0.0000     0.0889     0.0225      1.000
   16     0.0225     0.0889     0.0225      1.000
```

17	0.0000	0.1016	0.0225	1.000
18	0.0225	0.1016	0.0225	1.000
19	0.0000	0.1143	0.0225	1.000
20	0.0225	0.1143	0.0225	1.000
21	0.0000	0.1270	0.0225	1.000
22	0.0225	0.1270	0.0225	1.000
23	0.0000	0.1397	0.0225	1.000
24	0.0225	0.1397	0.0225	1.000
25	0.0000	0.1524	0.0225	1.000
26	0.0225	0.1524	0.0225	1.000
27	0.0000	0.1651	0.0225	1.000
28	0.0225	0.1651	0.0225	1.000
29	0.0000	0.1778	0.0225	1.000
30	0.0225	0.1778	0.0225	1.000
31	0.0000	0.1905	0.0225	1.000
32	0.0225	0.1905	0.0225	1.000
33	0.0000	0.2032	0.0225	1.000
34	0.0225	0.2032	0.0225	1.000
35	0.0000	0.2159	0.0225	1.000
36	0.0225	0.2159	0.0225	1.000
37	0.0000	0.2286	0.0225	1.000
38	0.0225	0.2286	0.0225	1.000
39	0.0000	0.2413	0.0225	1.000
40	0.0225	0.2413	0.0225	1.000
41	0.0000	0.2540	0.0225	1.000
42	0.0225	0.2540	0.0225	1.000
43	0.0000	0.2667	0.0225	1.000
44	0.0225	0.2667	0.0225	1.000
45	0.0000	0.2794	0.0225	1.000
46	0.0225	0.2794	0.0225	1.000
47	0.0000	0.2921	0.0225	1.000
48	0.0225	0.2921	0.0225	1.000
49	0.0000	0.3048	0.0225	1.000
50	0.0225	0.3048	0.0225	1.000

ELEMENT	1.02-11	1.02-11	1.0D0	0.00
0.00	0.0			
	1 1.00E+00	1.00E+00	90.E+00	1.0
1.00	1.000			
	2 1.00E+00	1.00E+00	90.E+00	1.0
1.00	1.000			
	3 1.00E+00	1.00E+00	90.E+00	1.0
1.00	1.000			
	4 1.00E+00	1.00E+00	90.E+00	1.0
1.00	1.000			
	5 1.00E+00	1.00E+00	90.E+00	1.0
1.00	1.000			
	6 1.00E+00	1.00E+00	90.E+00	1.0
1.00	1.000			
	7 1.00E+00	1.00E+00	90.E+00	1.0
1.00	1.000			
	8 1.00E+00	1.00E+00	90.E+00	1.0
1.00	1.000			
	9 1.00E+00	1.00E+00	90.E+00	1.0

```
1.00      1.000
          10     1.00E+00     1.00E+00      90.E+00          1.0
1.00      1.000
          11     1.00E+00     1.00E+00      90.E+00          1.0
1.00      1.000
          12     1.00E+00     1.00E+00      90.E+00          1.0
1.00      1.000
          13     1.00E+00     1.00E+00      90.E+00          1.0
1.00      1.000 #
15B
          14     1.00E+00     1.00E+00      90.E+00          1.0
1.00      1.000
          15     1.00E+00     1.00E+00      90.E+00          1.0
1.00      1.000
          16     1.00E+00     1.00E+00      90.E+00          1.0
1.00      1.000
          17     1.00E+00     1.00E+00      90.E+00          1.0
1.00      1.000
          18     1.00E+00     1.00E+00      90.E+00          1.0
1.00      1.000
          19     1.00E+00     1.00E+00      90.E+00          1.0
1.00      1.000
          20     1.00E+00     1.00E+00      90.E+00          1.0
1.00      1.000
          21     1.00E+00     1.00E+00      90.E+00          1.0
1.00      1.000
          22     1.00E+00     1.00E+00      90.E+00          1.0
1.00      1.000
          23     1.00E+00     1.00E+00      90.E+00          1.0
1.00      1.000
          24     1.00E+00     1.00E+00      90.E+00          1.0
1.00      1.000
           1                   3.17D-6                 1.0000D-4
           2                   3.17D-6                 1.0000D-4
0000000000000000000000000000000000000000000000000000000000000000
   49               9.80D02
   50               9.80D02
0000000000000000000000000000000000000000000000000000000000000000
    1               1.00D-4
    2               1.00D-4
0000000000000000000000000000000000000000000000000000000000000000
10
1   35   49   00
     3     5     6     8     7
     4     7     8    10     9
     5     9    10    12    11
     6    11    12    14    13
     7    13    14    16    15
     8    15    16    18    17
     9    17    18    20    19
    10    19    20    22    21
    11    21    22    24    23
    12    23    24    26    25
```

```
    13     25     26     28     27
    14     27     28     30     29
    15     29     30     32     31
    16     31     32     34     33
    17     33     34     36     35
    18     35     36     38     37
    19     37     38     40     39
    20     39     40     42     41
    21     41     42     44     43
    22     43     44     46     45
    23     45     46     48     47
    24     47     48     50     49
```

The SUTRA input dataset used to model a hypothetical disposal is:

```
SUTRA SOLUTE TRANSPORT
#1 INPUT DATA
 HEADING
..... STEADY RADIAL FLOW WITH SOLUTE TRANSPORT
+++++++++ RADIAL FORMATION
  112     55      7      0      2     2      2      0     10   9999
 0000             +01             +0             +1             +0
    0.50D0                                                1.000D-02
  240        2.6298D06      6.31152D08          01       1.0D00
2.6298D06
 01     1
   12         1         1         1      +0      +0         1        01
         +1
    0.00D0                      0.0D00     1000.D00         0.00D0
0.00D0    6.0D-04
    0.00D0                                                2650.D00
NONE
  -0.00D+0            0.00D0          -0.00D+0             -0.00D0
    0.00D0                                                -0.00D0
NODE           0.3048         0.3048         1.9151         0.30D0
    1         0.5000         0.0000         0.5000          1.000
    2     0.5000    50.0000     0.5000      1.000
    3       100.0000         0.0000       100.0000          1.000
    4   100.0000    50.0000   100.0000      1.000
    5       200.0000         0.0000       200.0000          1.000
    6   200.0000    50.0000   200.0000      1.000
    7       300.0000         0.0000       300.0000          1.000
    8   300.0000    50.0000   300.0000      1.000
    9       400.0000         0.0000       400.0000          1.000
   10   400.0000    50.0000   400.0000      1.000
   11       500.0000         0.0000       500.0000          1.000
   12   500.0000    50.0000   500.0000      1.000
   13       600.0000         0.0000       600.0000          1.000
   14   600.0000    50.0000   600.0000      1.000
```

```
          15      700.0000        0.0000     700.0000          1.000
          16  700.0000   50.0000  700.0000      1.000
          17      800.0000        0.0000     800.0000          1.000
          18  800.0000   50.0000  800.0000      1.000
          19      900.0000        0.0000     900.0000          1.000
          20  900.0000   50.0000  900.0000      1.000
          21 1000.0000    0.0000 1000.0000      1.000
          22    1000.0000       50.0000    1000.0000          1.000
          23 1100.0000    0.0000 1100.0000      1.000
          24    1100.0000       50.0000    1100.0000          1.000
          25 1200.0000    0.0000 1200.0000      1.000
          26    1200.0000       50.0000    1200.0000          1.000
          27 1300.0000    0.0000 1300.0000      1.000
          28    1300.0000       50.0000    1300.0000          1.000
          29 1400.0000    0.0000 1400.0000      1.000
          30    1400.0000       50.0000    1400.0000          1.000
          31 1500.0000    0.0000 1500.0000      1.000
          32    1500.0000       50.0000    1500.0000          1.000
          33 1600.0000    0.0000 1600.0000      1.000
          34    1600.0000       50.0000    1600.0000          1.000
          35 1700.0000    0.0000 1700.0000      1.000
          36    1700.0000       50.0000    1700.0000          1.000
          37 1800.0000    0.0000 1800.0000      1.000
          38    1800.0000       50.0000    1800.0000          1.000
39 1900.0000    0.0000 1900.0000      1.000
          40    1900.0000       50.0000    1900.0000          1.000
          41 2000.0000    0.0000 2000.0000      1.000
          42    2000.0000       50.0000    2000.0000          1.000
          43 2100.0000    0.0000 2100.0000      1.000
          44    2100.0000       50.0000    2100.0000          1.000
          45 2200.0000    0.0000 2200.0000      1.000
          46    2200.0000       50.0000    2200.0000          1.000
          47 2300.0000    0.0000 2300.0000      1.000
          48    2300.0000       50.0000    2300.0000          1.000
          49 2400.0000    0.0000 2400.0000      1.000
          50    2400.0000       50.0000    2400.0000          1.000
          51 2500.0000    0.0000 2500.0000      1.000
          52    2500.0000       50.0000    2500.0000          1.000
          53 2600.0000    0.0000 2600.0000      1.000
          54    2600.0000       50.0000    2600.0000          1.000
          55 2700.0000    0.0000 2700.0000      1.000
          56    2700.0000       50.0000    2700.0000          1.000
          57 2800.0000    0.0000 2800.0000      1.000
          58    2800.0000       50.0000    2800.0000          1.000
          59 2900.0000    0.0000 2900.0000      1.000
          60    2900.0000       50.0000    2900.0000          1.000
          61 3000.0000    0.0000 3000.0000      1.000
          62    3000.0000       50.0000    3000.0000          1.000
          63 3100.0000    0.0000 3100.0000      1.000
          64    3100.0000       50.0000    3100.0000          1.000
          65 3200.0000    0.0000 3200.0000      1.000
          66    3200.0000       50.0000    3200.0000          1.000
          67 3300.0000    0.0000 3300.0000      1.000
          68    3300.0000       50.0000    3300.0000          1.000
```

```
   69 3400.0000     0.0000 3400.0000      1.000
   70    3400.0000       50.0000    3400.0000          1.000
   71 3500.0000     0.0000 3500.0000      1.000
   72     3500.0000       50.0000    3500.0000          1.000
   73 3600.0000     0.0000 3600.0000      1.000
   74    3600.0000       50.0000    3600.0000          1.000
   75 3700.0000     0.0000 3700.0000      1.000
   76     3700.0000       50.0000    3700.0000          1.000
   77 3800.0000     0.0000 3800.0000      1.000
   78    3800.0000       50.0000    3800.0000          1.000
   79 3900.0000     0.0000 3900.0000      1.000
   80     3900.0000       50.0000    3900.0000          1.000
   81 4000.0000     0.0000 4000.0000      1.000
   82    4000.0000       50.0000    4000.0000          1.000
   83 4100.0000     0.0000 4100.0000      1.000
   84     4100.0000       50.0000    4100.0000          1.000
   85 4200.0000     0.0000 4200.0000      1.000
   86    4200.0000       50.0000    4200.0000          1.000
   87 4300.0000     0.0000 4300.0000      1.000
   88     4300.0000       50.0000    4300.0000          1.000
   89 4400.0000     0.0000 4400.0000      1.000
   90    4400.0000       50.0000    4400.0000          1.000
   91 4500.0000     0.0000 4500.0000      1.000
   92     4500.0000       50.0000    4500.0000          1.000
   93 4600.0000     0.0000 4600.0000      1.000
   94    4600.0000       50.0000    4600.0000          1.000
   95 4700.0000     0.0000 4700.0000      1.000
   96     4700.0000       50.0000    4700.0000          1.000
   97 4800.0000     0.0000 4800.0000      1.000
   98    4800.0000       50.0000    4800.0000          1.000
   99 4900.0000     0.0000 4900.0000      1.000
  100     4900.0000       50.0000    4900.0000          1.000
  101 5000.0000     0.0000 5000.0000      1.000
  102    5000.0000       50.0000    5000.0000          1.000
  103 54000.000     0.0000 54000.000      1.000
  104     54000.000       50.0000    54000.000          1.000
  105 103000.00     0.0000 103000.00      1.000
  106    103000.00       50.0000    103000.00          1.000
  107 152000.00     0.0000 152000.00      1.000
  108     152000.00       50.0000    152000.00          1.000
  109 201000.00     0.0000 201000.00      1.000
  110    201000.00       50.0000    201000.00          1.000
  111 250000.00     0.0000 250000.00      1.000
  112     250000.00       50.0000    250000.00          1.000
ELEMENT        9.87D-13    9.87D-13        1.0D0          00.00
          1    1.00E+00    1.00E+00      00.E+00            1.0
1.00      1.000 #
          2    1.00E+00    1.00E+00      00.E+00            1.0
1.00      1.000
          3    1.00E+00    1.00E+00      00.E+00            1.0
1.00      1.000
          4    1.00E+00    1.00E+00      00.E+00            1.0
1.00      1.000
```

	5	1.00E+00	1.00E+00	00.E+00	1.0
1.00	1.000				
	6	1.00E+00	1.00E+00	00.E+00	1.0
1.00	1.000				
	7	1.00E+00	1.00E+00	00.E+00	1.0
1.00	1.000				
	8	1.00E+00	1.00E+00	00.E+00	1.0
1.00	1.000				
	9	1.00E+00	1.00E+00	00.E+00	1.0
1.00	1.000				
	10	1.00E+00	1.00E+00	00.E+00	1.0
1.00	1.000				
	11	1.00E+00	1.00E+00	00.E+00	1.0
1.00	1.000				
	12	1.00E+00	1.00E+00	00.E+00	1.0
1.00	1.000				
	13	1.00E+00	1.00E+00	00.E+00	1.0
1.00	1.000 #				
	14	1.00E+00	1.00E+00	00.E+00	1.0
1.00	1.000				
	15	1.00E+00	1.00E+00	00.E+00	1.0
1.00	1.000				
	16	1.00E+00	1.00E+00	00.E+00	1.0
1.00	1.000				
	17	1.00E+00	1.00E+00	00.E+00	1.0
1.00	1.000				
	18	1.00E+00	1.00E+00	00.E+00	1.0
1.00	1.000				
	19	1.00E+00	1.00E+00	00.E+00	1.0
1.00	1.000				
	20	1.00E+00	1.00E+00	00.E+00	1.0
1.00	1.000				
	21	1.00E+00	1.00E+00	00.E+00	1.0
1.00	1.000				
	22	1.00E+00	1.00E+00	00.E+00	1.0
1.00	1.000				
	23	1.00E+00	1.00E+00	00.E+00	1.0
1.00	1.000				
	24	1.00E+00	1.00E+00	00.E+00	1.0
1.00	1.000				
	25	1.00E+00	1.00E+00	00.E+00	1.0
1.00	1.000 #				
	26	1.00E+00	1.00E+00	00.E+00	1.0
1.00	1.000				
	27	1.00E+00	1.00E+00	00.E+00	1.0
1.00	1.000				
	28	1.00E+00	1.00E+00	00.E+00	1.0
1.00	1.000				
	29	1.00E+00	1.00E+00	00.E+00	1.0
1.00	1.000				
	30	1.00E+00	1.00E+00	00.E+00	1.0
1.00	1.000				
	31	1.00E+00	1.00E+00	00.E+00	1.0

```
1.00      1.000
          32     1.00E+00     1.00E+00      00.E+00          1.0
1.00      1.000
          33     1.00E+00     1.00E+00      00.E+00          1.0
1.00      1.000
          34     1.00E+00     1.00E+00      00.E+00          1.0
1.00      1.000
          35     1.00E+00     1.00E+00      00.E+00          1.0
1.00      1.000
          36     1.00E+00     1.00E+00      00.E+00          1.0
1.00      1.000
          37     1.00E+00     1.00E+00      00.E+00          1.0
1.00      1.000 #
          38     1.00E+00     1.00E+00      00.E+00          1.0
1.00      1.000
          39     1.00E+00     1.00E+00      00.E+00          1.0
1.00      1.000
          40     1.00E+00     1.00E+00      00.E+00          1.0
1.00      1.000
          41     1.00E+00     1.00E+00      00.E+00          1.0
1.00      1.000
          42     1.00E+00     1.00E+00      00.E+00          1.0
1.00      1.000
          43     1.00E+00     1.00E+00      00.E+00          1.0
1.00      1.000
          44     1.00E+00     1.00E+00      00.E+00          1.0
1.00      1.000
          45     1.00E+00     1.00E+00      00.E+00          1.0
1.00      1.000
          46     1.00E+00     1.00E+00      00.E+00          1.0
1.00      1.000
          47     1.00E+00     1.00E+00      00.E+00          1.0
1.00      1.000
          48     1.00E+00     1.00E+00      00.E+00          1.0
1.00      1.000
          49     1.00E+00     1.00E+00      00.E+00          1.0
1.00      1.000
          50     1.00E+00     1.00E+00      00.E+00          1.0
1.00      1.000
          51     1.00E+00     1.00E+00      00.E+00          1.0
1.00      1.000
          52     1.00E+00     1.00E+00      00.E+00          1.0
1.00      1.000
          53     1.00E+00     1.00E+00      00.E+00          1.0
1.00      1.000
          54     1.00E+00     1.00E+00      00.E+00          1.0
1.00      1.000
          55     1.00E+00     1.00E+00      00.E+00          1.0
1.00      1.000
          1                   9.380D+0                  1.0000D-4
          2                   9.380D+0                  1.0000D-4
0000000000000000000000000000000000000000000000000000000000000000
  111              1.602D07
```

```
  112                1.602D07
0000000000000000000000000000000000000000000000000000000000000000
    1                1.00D-4
    2                1.00D-4
0000000000000000000000000000000000000000000000000000000000000000
        12
    1    5     9    13    17    21    25    29    33    37    00
     1                1                3                4              2
     2     3     5     6     4
     3     5     7     8     6
     4     7     9    10     8
     5     9    11    12    10
     6    11    13    14    12
     7    13    15    16    14
     8    15    17    18    16
     9    17    19    20    18
    10    19    21    22    20
    11    21    23    24    22
    12    23    25    26    24
    13    25    27    28    26
    14    27    29    30    28
    15    29    31    32    30
    16    31    33    34    32
    17    33    35    36    34
    18    35    37    38    36
    19    37    39    40    38
    20    39    41    42    40
    21    41    43    44    42
    22    43    45    46    44
    23    45    47    48    46
    24    47    49    50    48
    25    49    51    52    50
    26    51    53    54    52
    27    53    55    56    54
    28    55    57    58    56
    29    57    59    60    58
    30    59    61    62    60
    31    61    63    64    62
    32    63    65    66    64
    33    65    67    68    66
    34    67    69    70    68
    35    69    71    72    70
    36    71    73    74    72
    37    73    75    76    74
    38    75    77    78    76
    39    77    79    80    78
    40    79    81    82    80
    41    81    83    84    82
    42    83    85    86    84
    43    85    87    88    86
    44    87    89    90    88
    45    89    91    92    90
    46    91    93    94    92
```

47	93	95	96	94
48	95	97	98	96
49	97	99	100	98
50	99	101	102	100
51	101	103	104	102
52	103	105	106	104
53	105	107	108	106
54	107	109	110	108
55	109	111	112	110

APPENDIX B

Reaction rate coefficients, k_T, were determined from the slopes of plots of log [1 - $C/C_{(orig.)}$] for each metal ion. The plots are displayed in Figures B1 through B60. A linear least-squares curve fit was performed on the data of the Figures and the slopes were determined from the first order coefficients. Multiplication of the values of the slopes by ln(10) resulted in k_T.

Figure B1

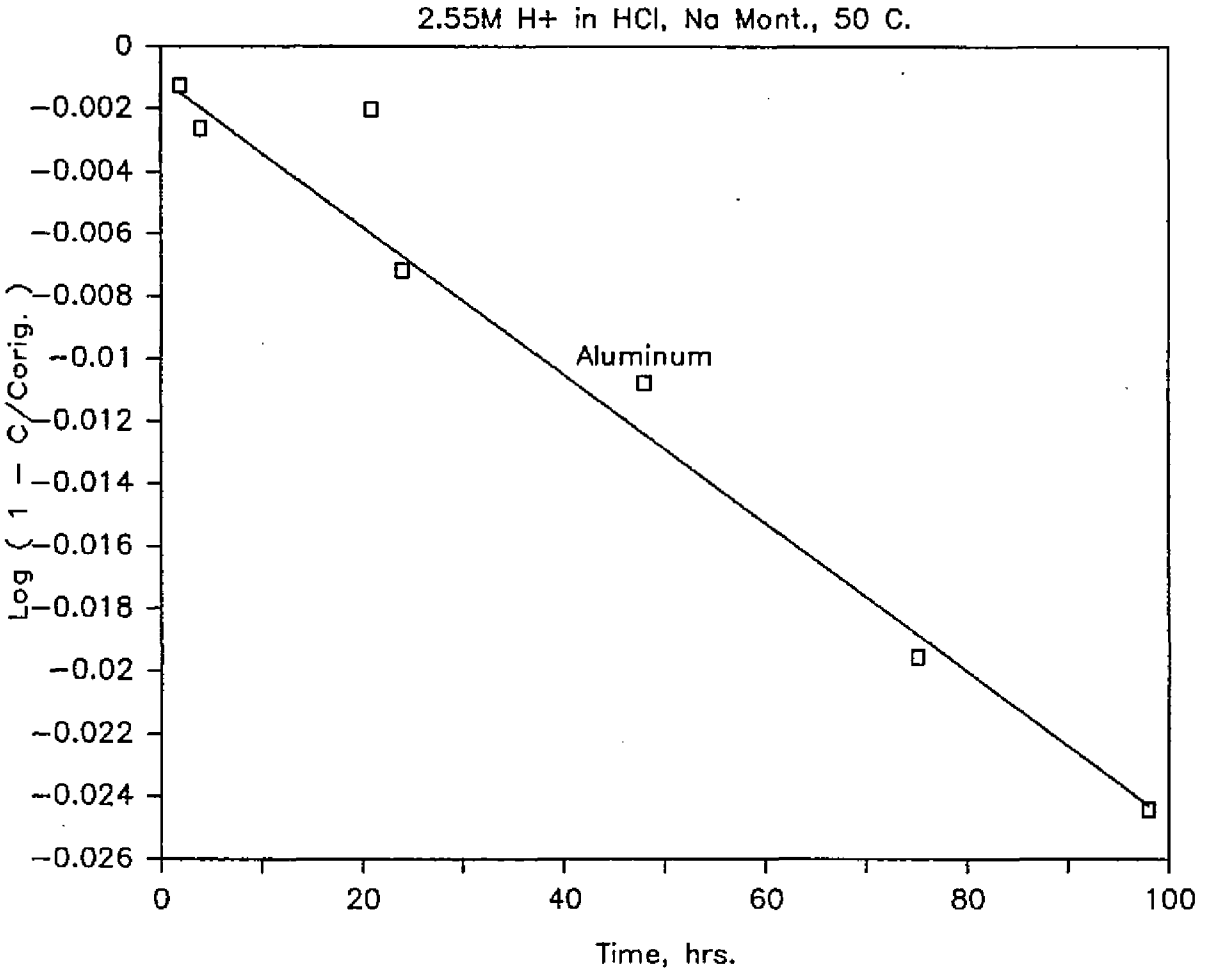
2.55M H+ in HCl, Na Mont., 50 C.
0
−0.002
−0.004
−0.006
−0.008
−0.01
−0.012
−0.014
−0.016
−0.018
−0.02
−0.022
−0.024
−0.026
Log (1 − C/Corig.)
Aluminum
0
20
40
60
80
100
Time, hrs.

Figure B2

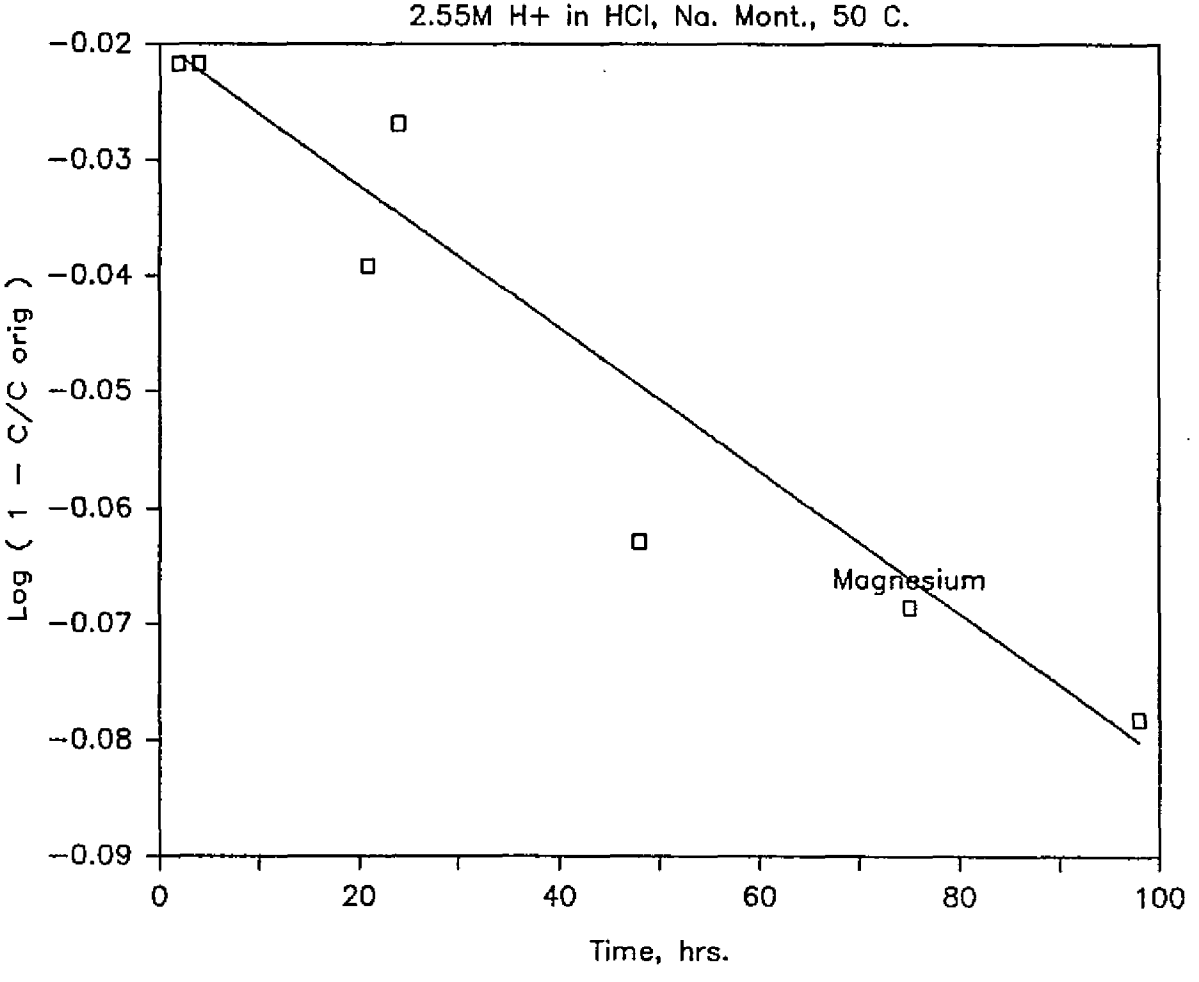
2.55M H+ in HCl, Na. Mont., 50 C.
Log (1 − C/C orig)
−0.02
−0.03
−0.04
−0.05
−0.06
−0.07
−0.08
−0.09
0
20
40
60
80
100
Time, hrs.
Magnesium

Figure B3

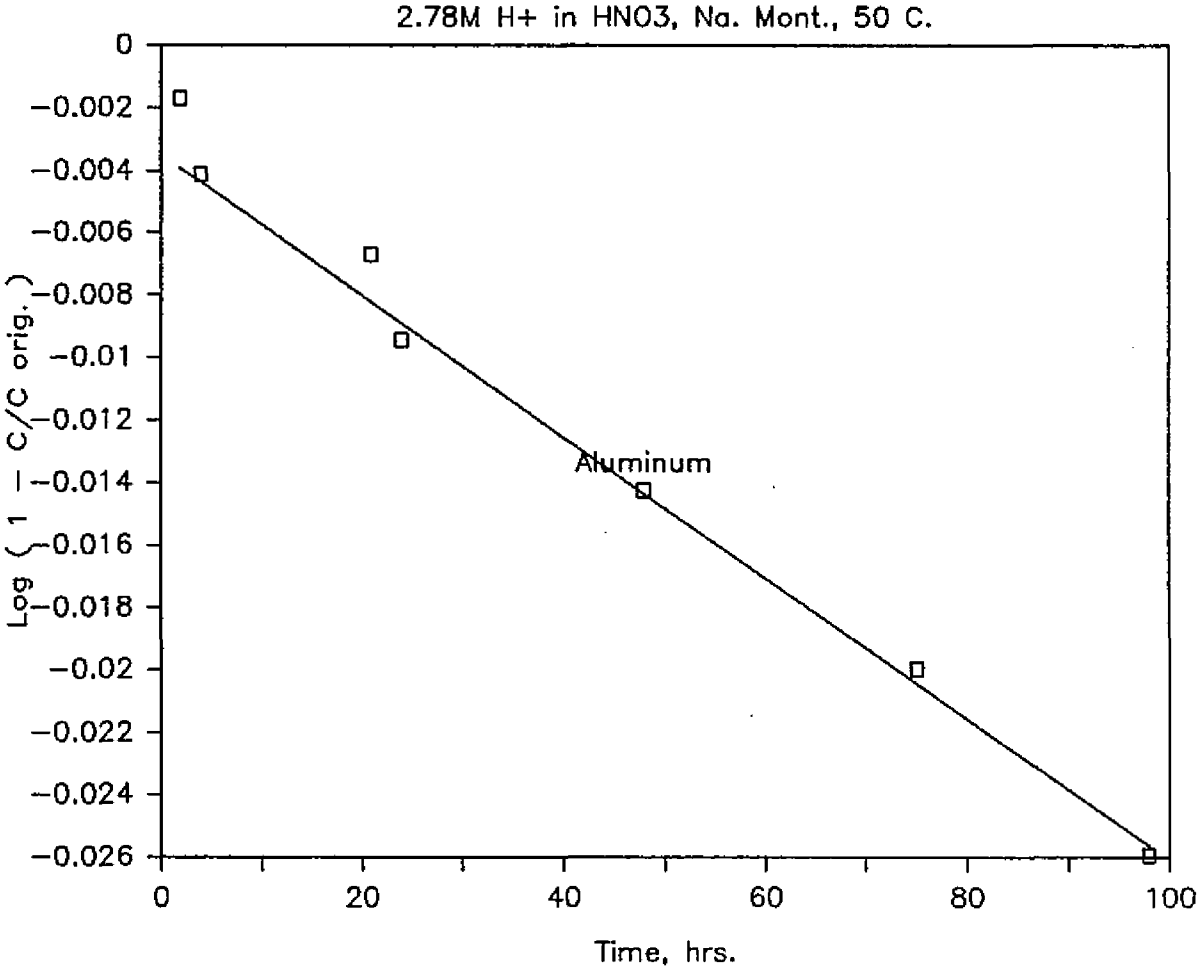
2.78M H+ in HNO3, Na. Mont., 50 C.
0
−0.002
−0.004
−0.006
−0.008
−0.01
−0.012
−0.014
−0.016
−0.018
−0.02
−0.022
−0.024
−0.026
Log (1 − C/C orig.)
Aluminum
0
20
40
60
80
100
Time, hrs.

Figure B4

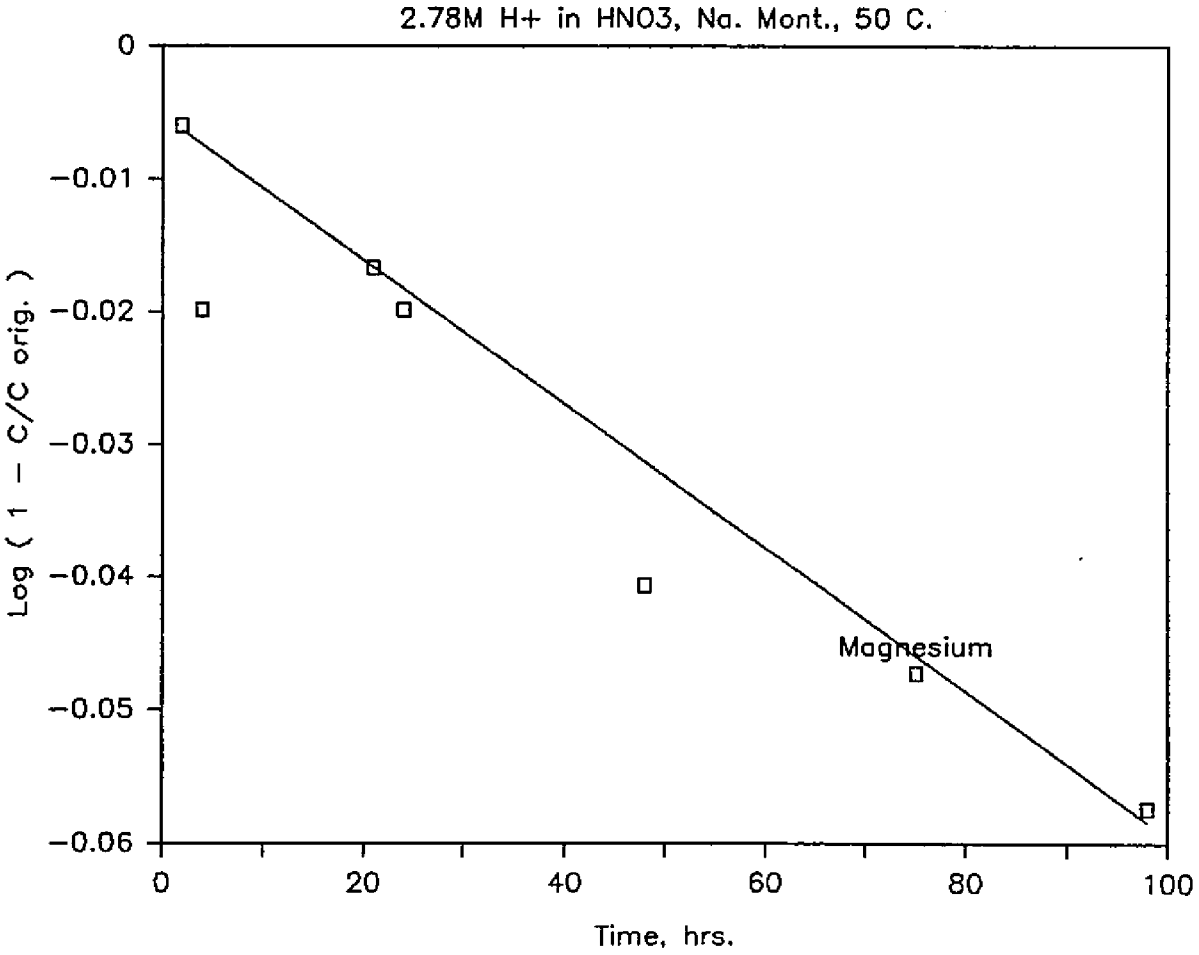
2.78M H+ in HNO3, Na. Mont., 50 C.
0
−0.01
−0.02
−0.03
−0.04
−0.05
−0.06
Log (1 − C/C orig.)
Magnesium
0
20
40
60
80
100
Time, hrs.

Figure B5

2.98M H+ in H2SO4, Na. Mont., 50 C.

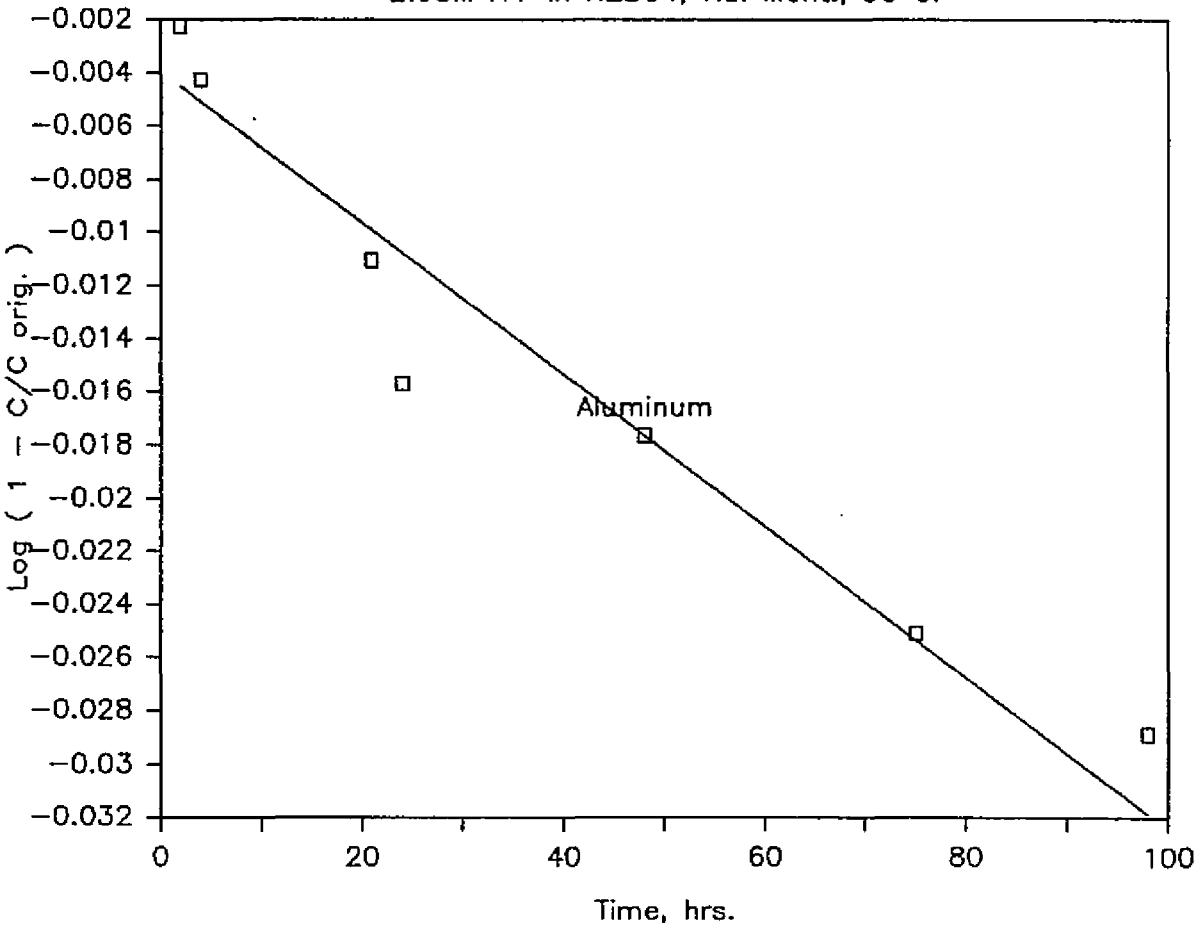

Figure B6

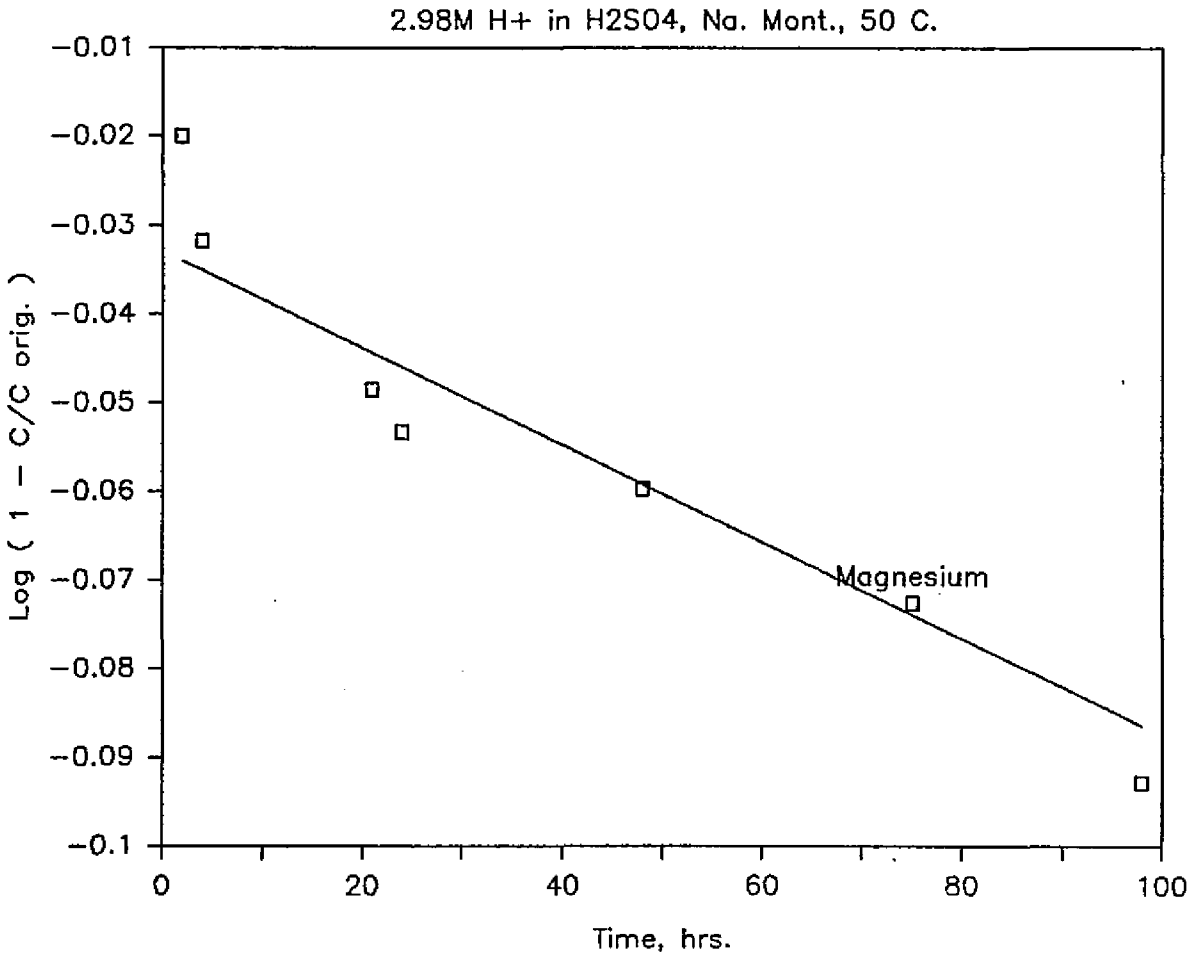
2.98M H+ in H2SO4, Na. Mont., 50 C.
Log (1 − C/C orig.)
−0.01
−0.02
−0.03
−0.04
−0.05
−0.06
−0.07
−0.08
−0.09
−0.1
0
20
40
60
80
100
Time, hrs.
Magnesium

Figure B7

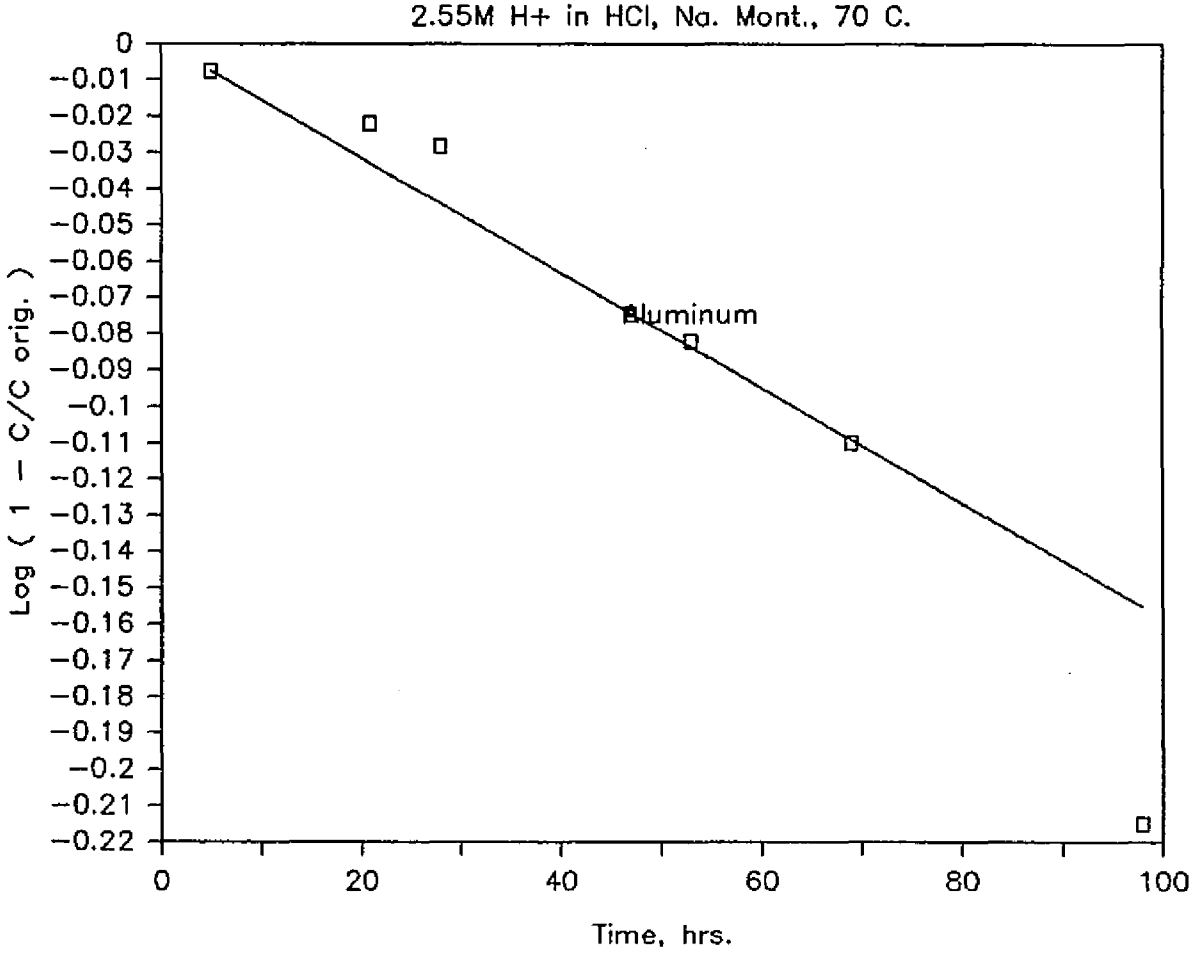
2.55M H+ in HCl, Na. Mont., 70 C.
Log (1 − C/C orig.)
0
−0.01
−0.02
−0.03
−0.04
−0.05
−0.06
−0.07
−0.08
−0.09
−0.1
−0.11
−0.12
−0.13
−0.14
−0.15
−0.16
−0.17
−0.18
−0.19
−0.2
−0.21
−0.22
Aluminum
0
20
40
60
80
100
Time, hrs.

Figure B8

2.55M H+ in HCl, Na Mont., 70 C.

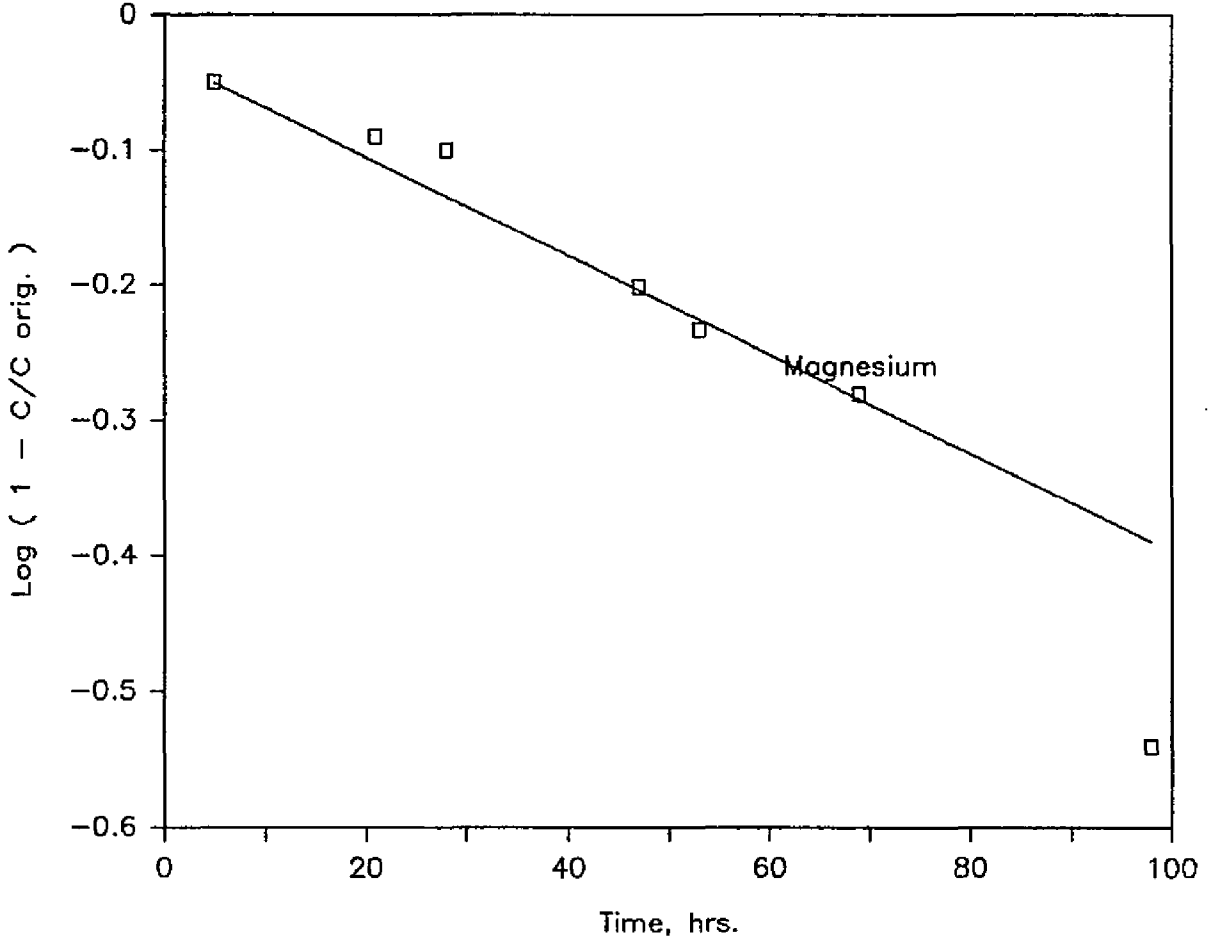

Figure B9

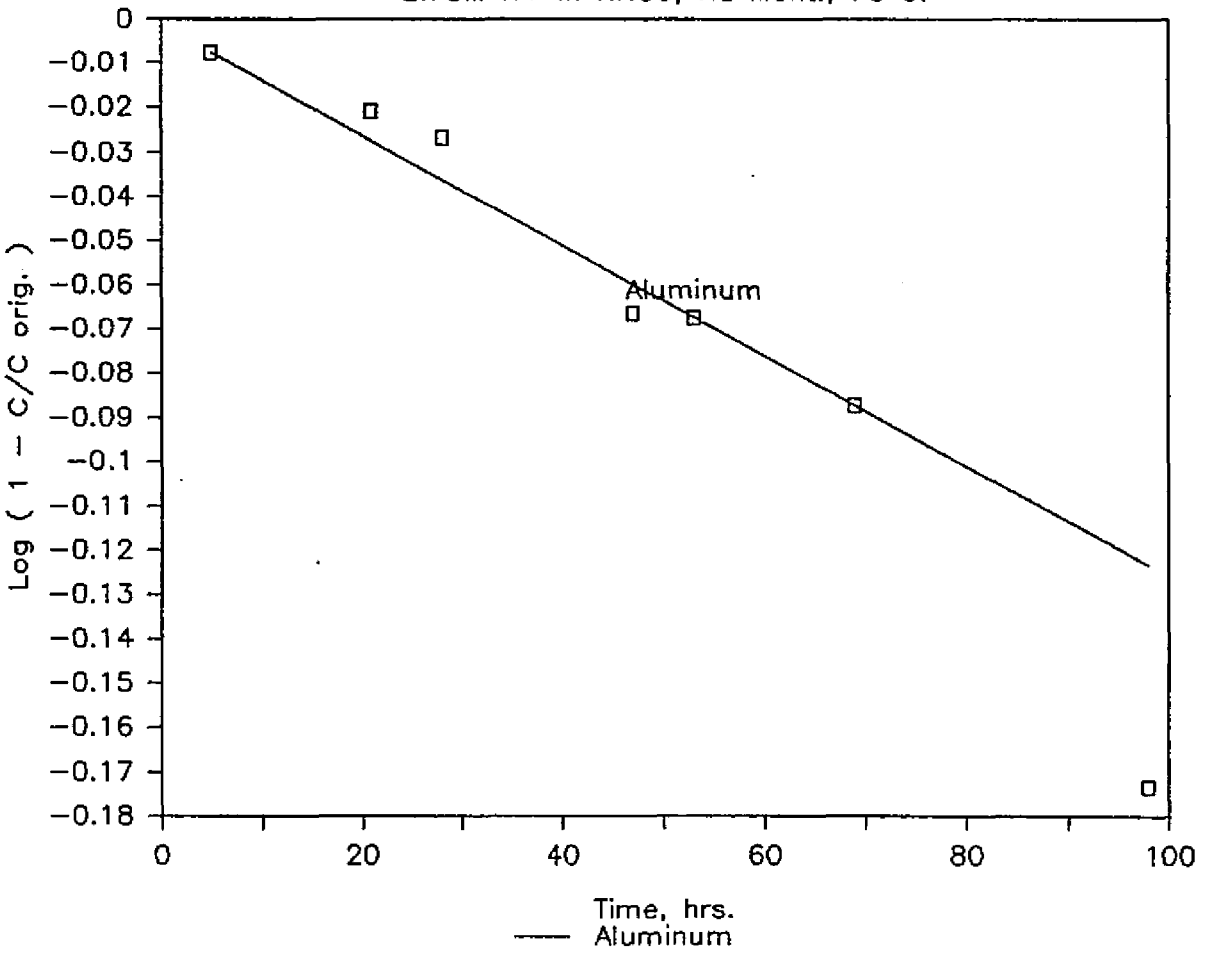
2.78M H+ in HNO3, Na Mont., 70 C.
Log (1 − C/C orig.)
0
−0.01
−0.02
−0.03
−0.04
−0.05
−0.06
−0.07
−0.08
−0.09
−0.1
−0.11
−0.12
−0.13
−0.14
−0.15
−0.16
−0.17
−0.18
Aluminum
0
20
40
60
80
100
Time, hrs.
Aluminum

Figure B10

2.78M H+ in HNO3, Na Mont., 70 C.

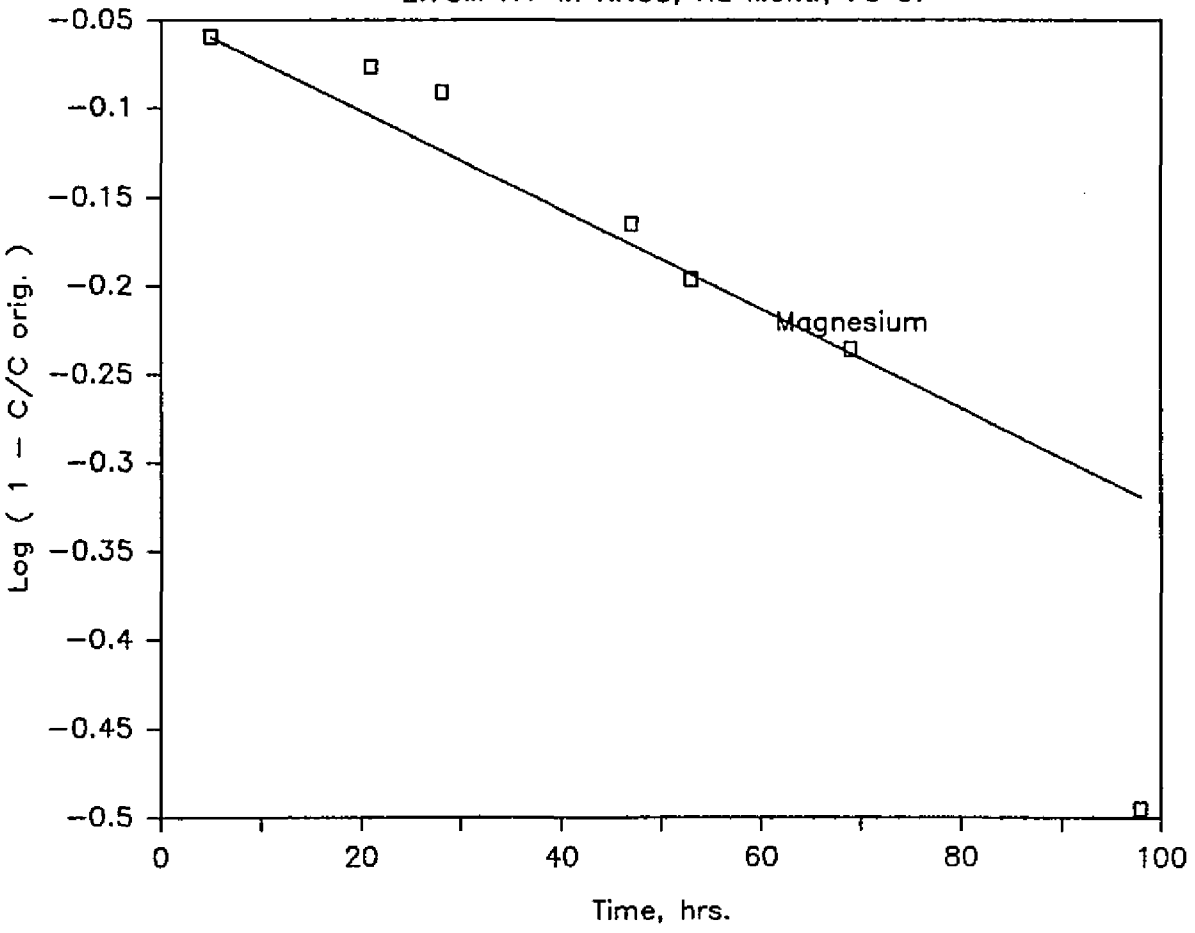

Figure B11

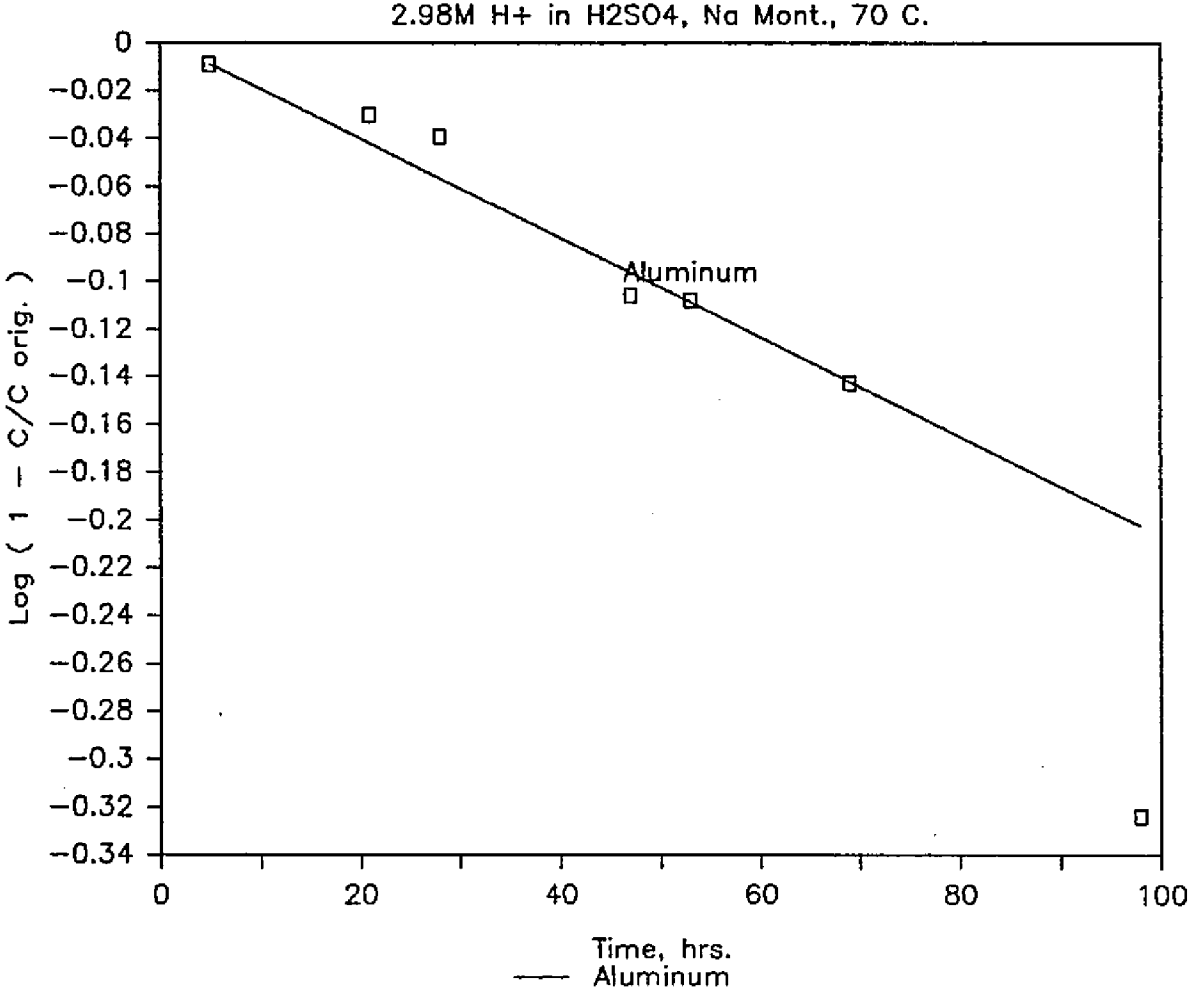
2.98M H+ in H2SO4, Na Mont., 70 C.
Log (1 - C/C orig.)
0
-0.02
-0.04
-0.06
-0.08
-0.1
-0.12
-0.14
-0.16
-0.18
-0.2
-0.22
-0.24
-0.26
-0.28
-0.3
-0.32
-0.34
Aluminum
0
20
40
60
80
100
Time, hrs.
Aluminum

Figure B12

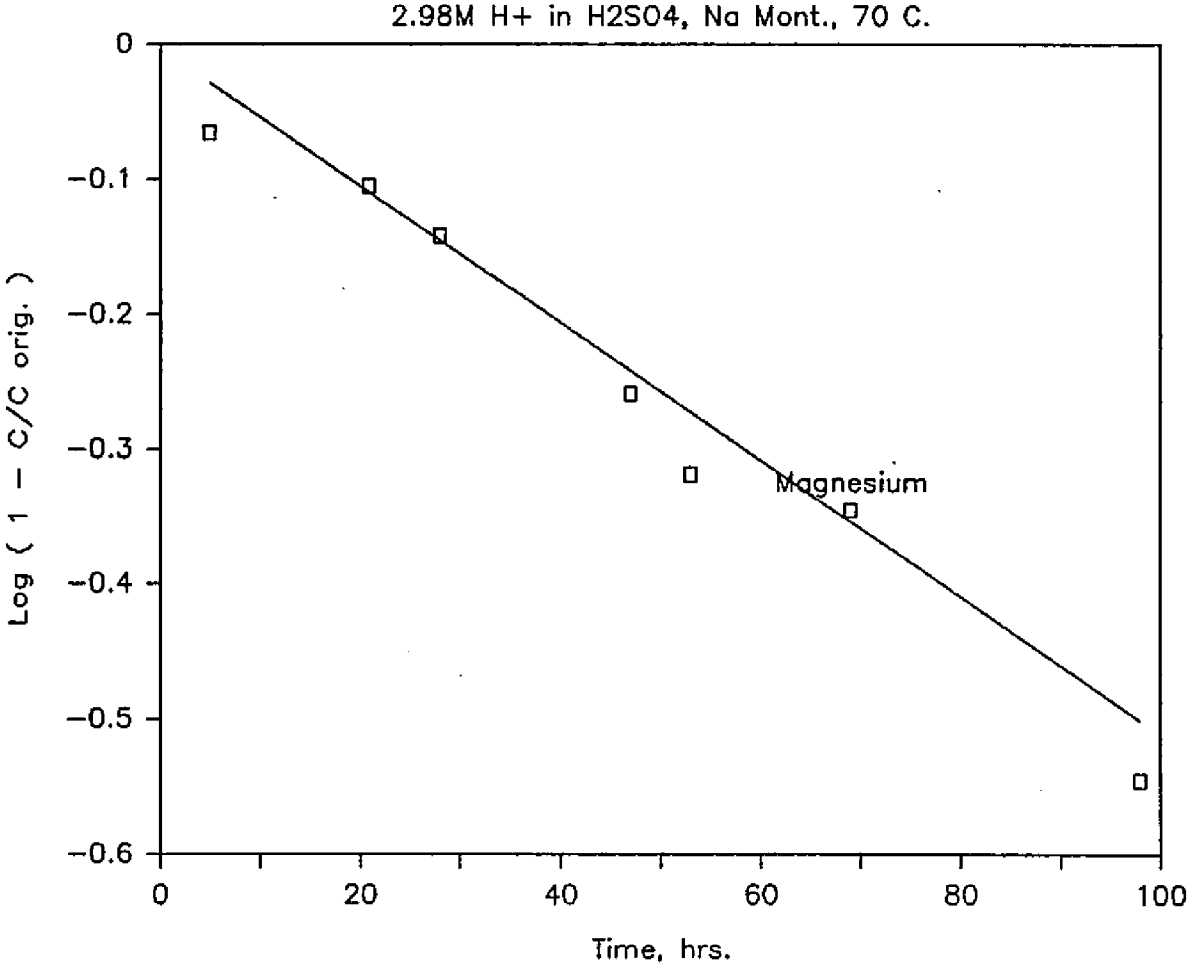
2.98M H+ in H2SO4, Na Mont., 70 C.
0
−0.1
−0.2
−0.3
−0.4
−0.5
−0.6
Log (1 − C/C orig.)
Magnesium
0
20
40
60
80
100
Time, hrs.

Figure B13

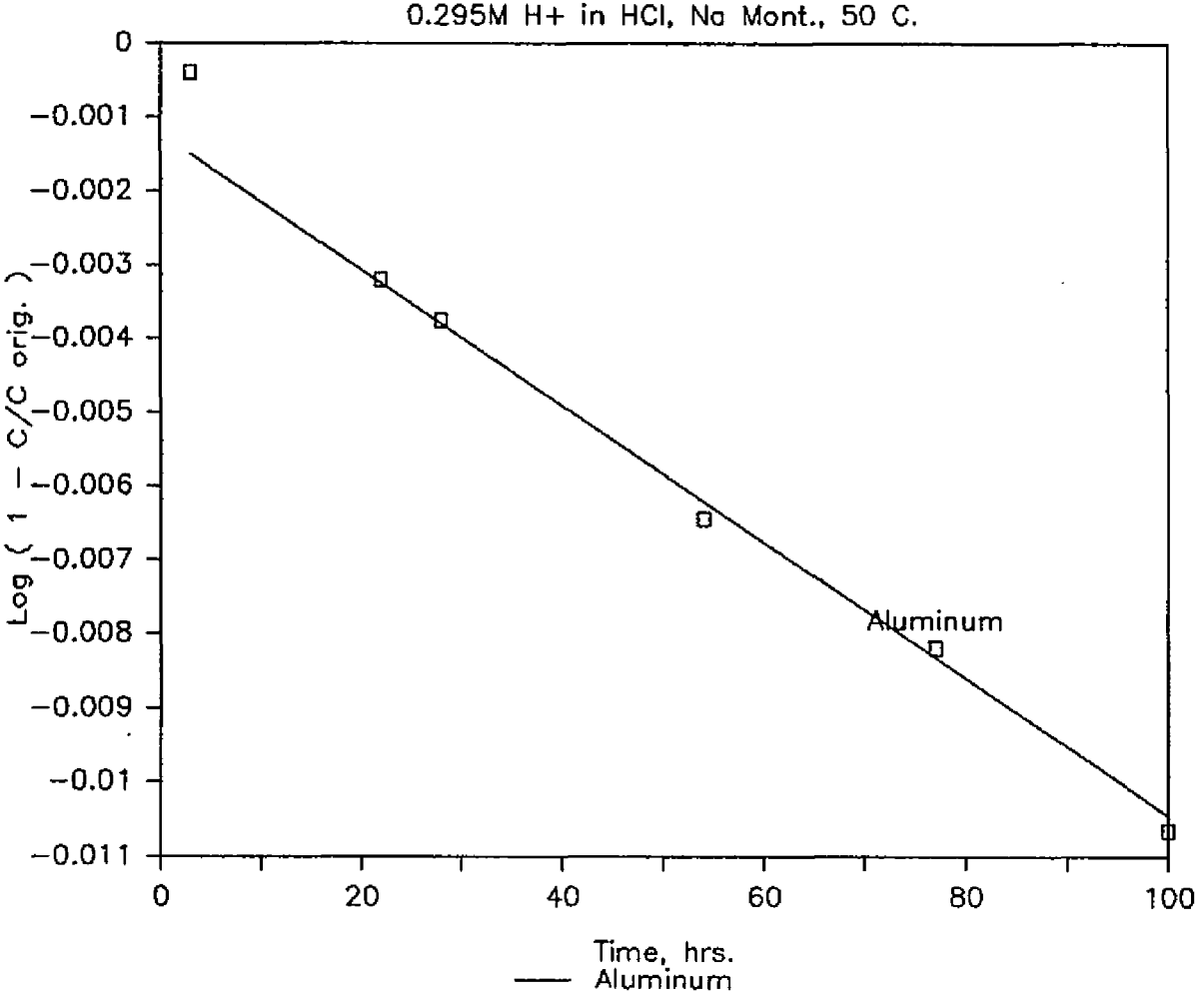
0.295M H+ in HCl, Na Mont., 50 C.
0
−0.001
−0.002
−0.003
−0.004
−0.005
−0.006
−0.007
−0.008
−0.009
−0.01
−0.011
Log (1 − C/C orig.)
0
20
40
60
80
100
Time, hrs.
Aluminum
Aluminum

Figure B14

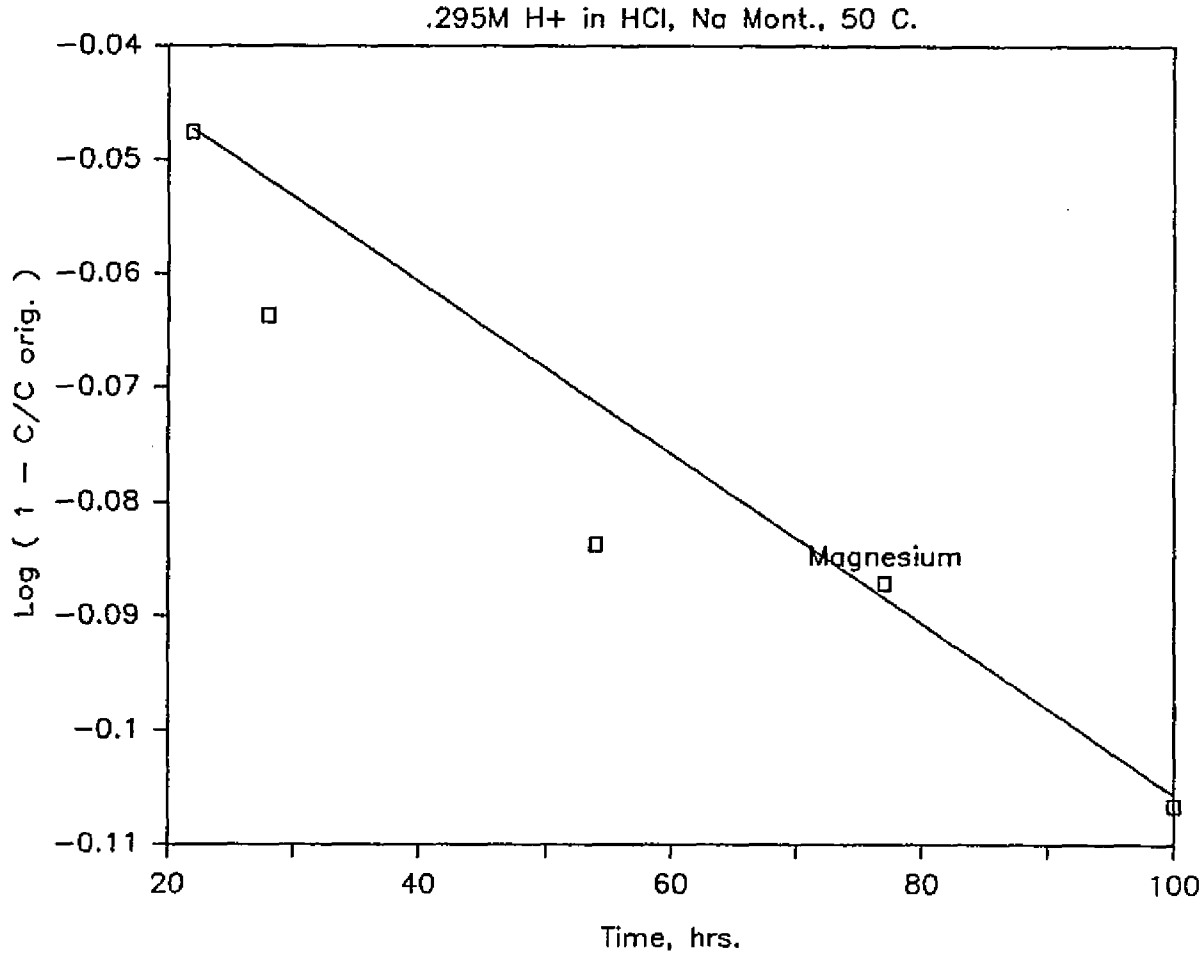
.295M H+ in HCl, Na Mont., 50 C.
−0.04
−0.05
−0.06
−0.07
−0.08
−0.09
−0.1
−0.11
Log (1 − C/C orig.)
Magnesium
20
40
60
80
100
Time, hrs.

Figure B15

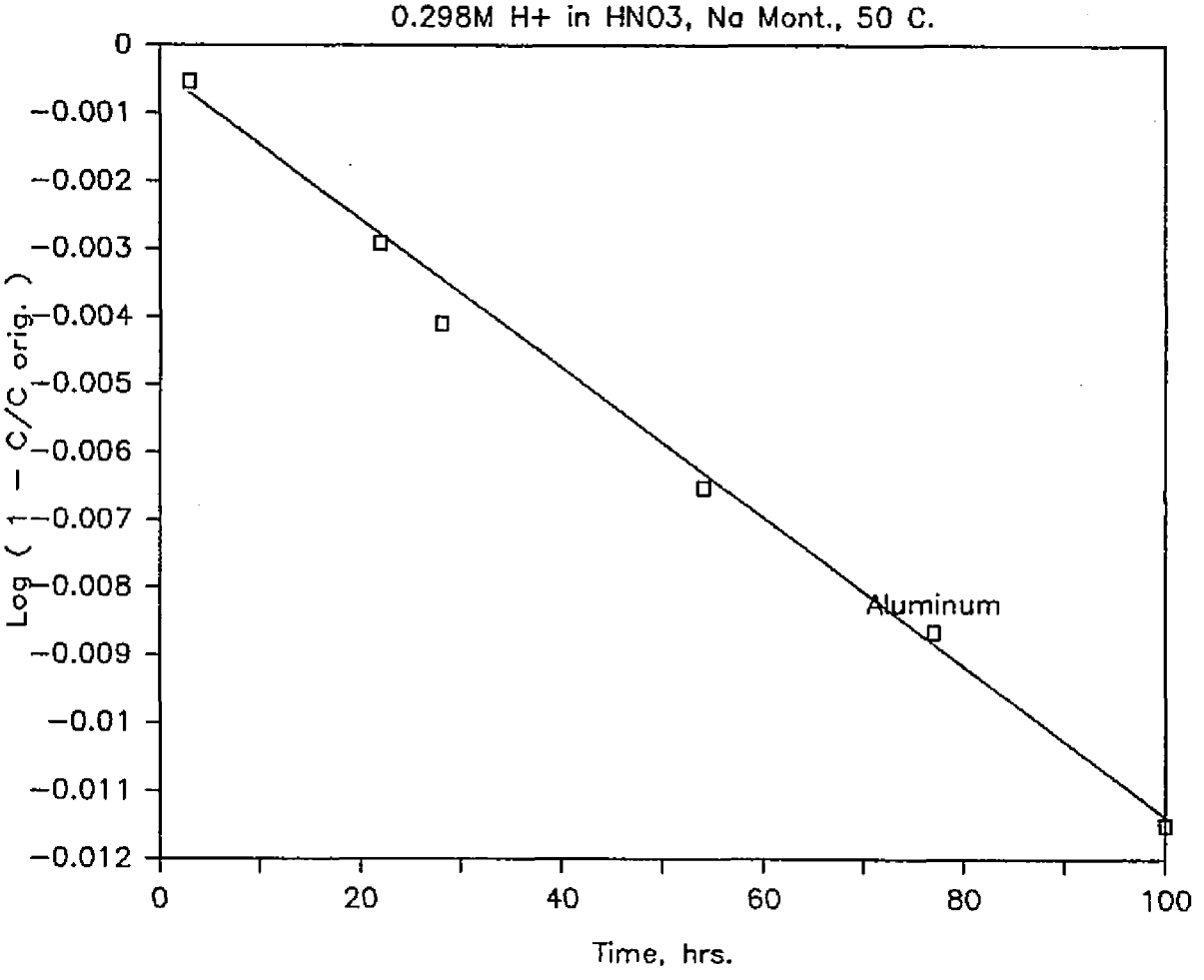
0.298M H+ in HNO3, Na Mont., 50 C.
0
−0.001
−0.002
−0.003
−0.004
−0.005
−0.006
−0.007
−0.008
−0.009
−0.01
−0.011
−0.012
Log (1 − C/C orig.)
0
20
40
60
80
100
Time, hrs.
Aluminum

Figure B16

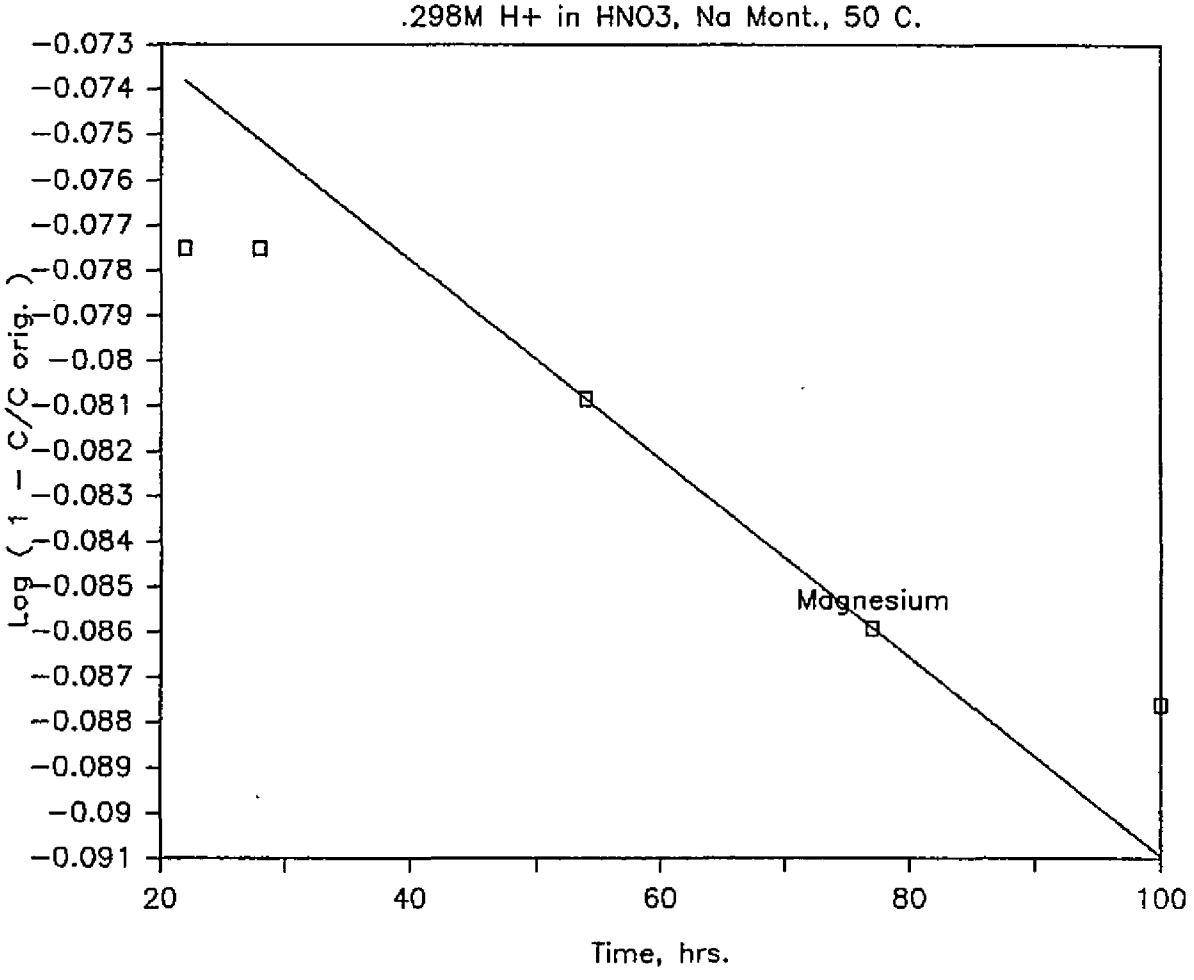
.298M H+ in HNO3, Na Mont., 50 C.
−0.073
−0.074
−0.075
−0.076
−0.077
−0.078
−0.079
−0.08
−0.081
−0.082
−0.083
−0.084
−0.085
−0.086
−0.087
−0.088
−0.089
−0.09
−0.091
Log (1 − C/C orig.)
Magnesium
20
40
60
80
100
Time, hrs.

Figure B17

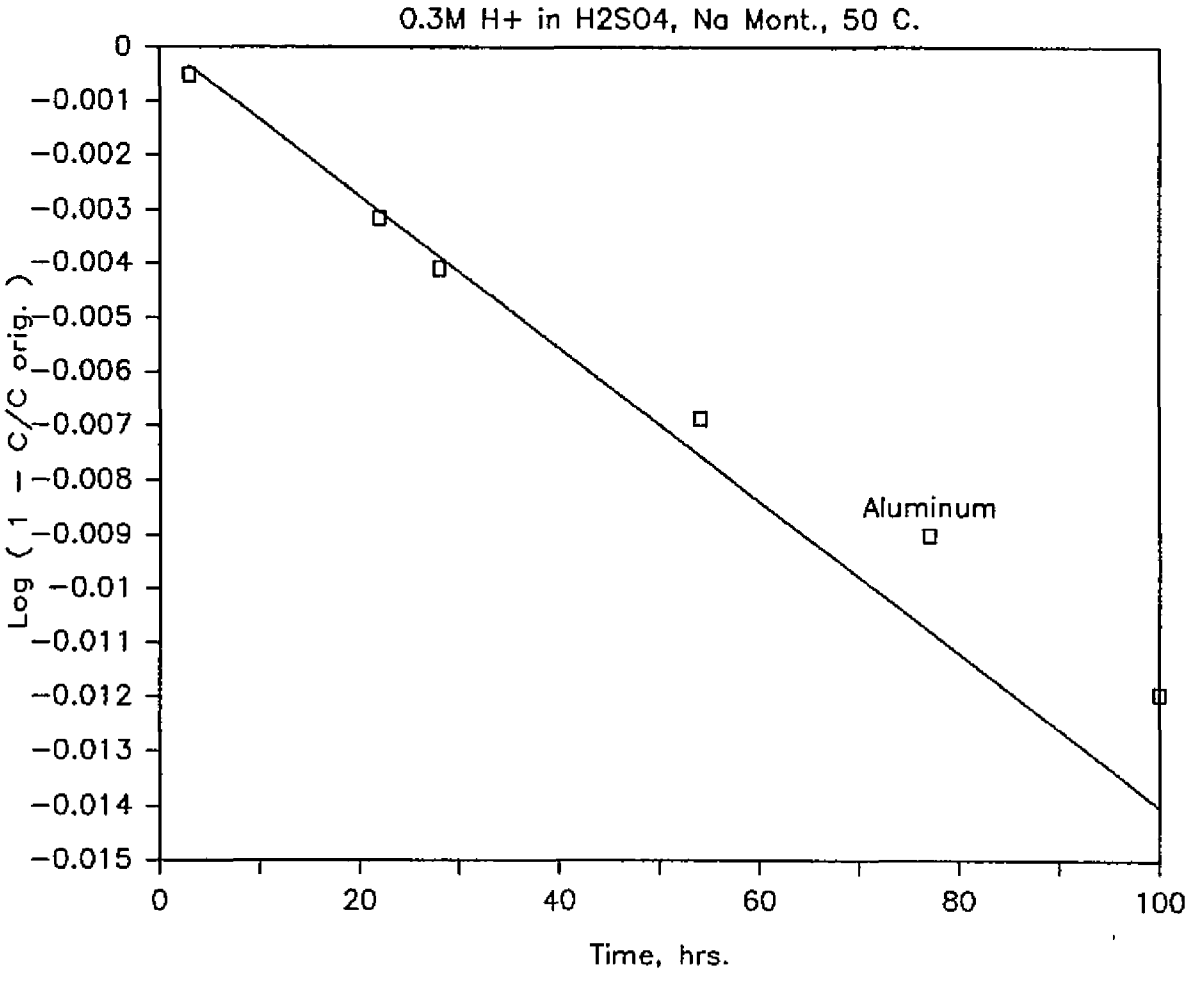
0.3M H+ in H2SO4, Na Mont., 50 C.
0
−0.001
−0.002
−0.003
−0.004
−0.005
−0.006
−0.007
−0.008
−0.009
−0.01
−0.011
−0.012
−0.013
−0.014
−0.015
Log (1 − C/C orig.)
Aluminum
0
20
40
60
80
100
Time, hrs.

Figure B18

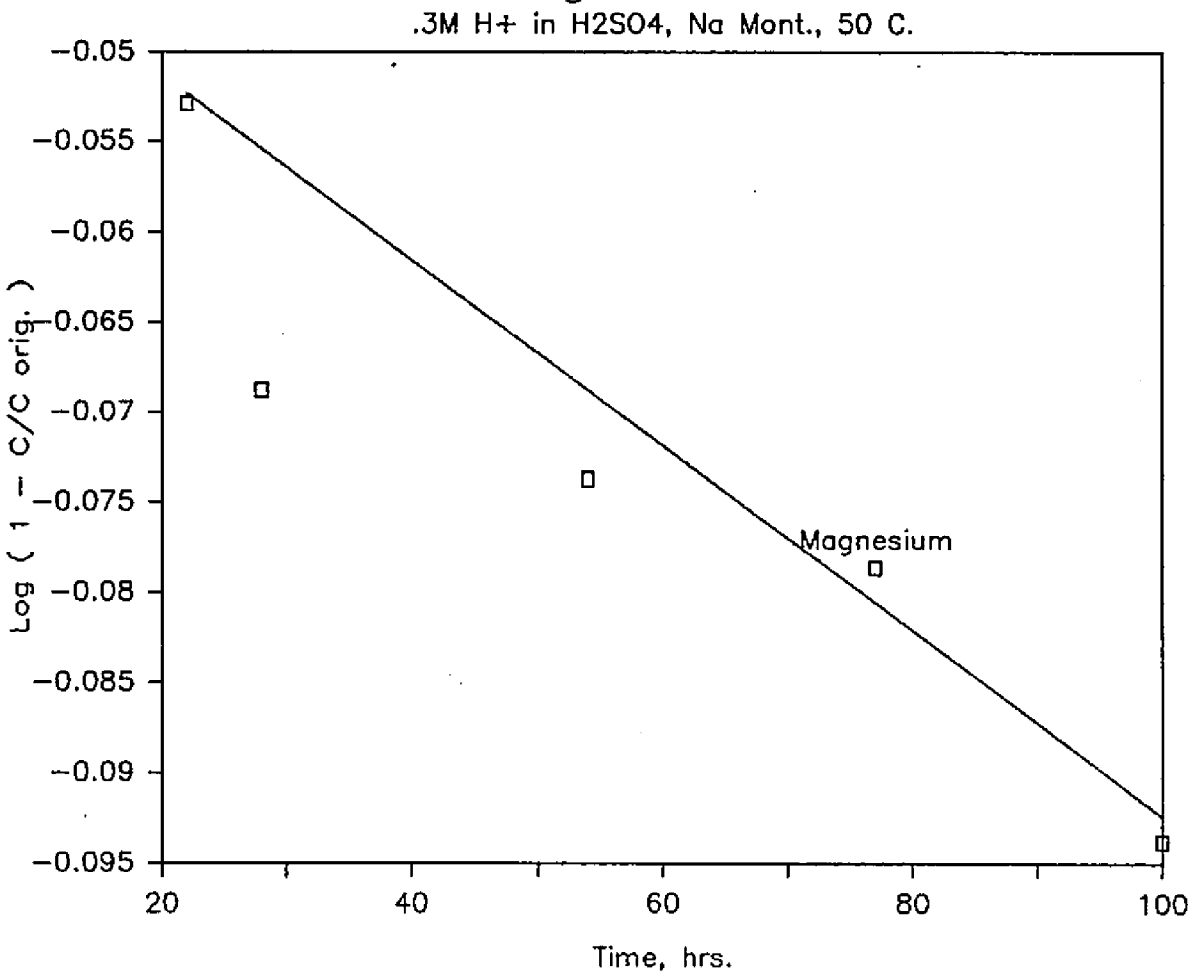
.3M H+ in H2SO4, Na Mont., 50 C.
-0.05
-0.055
-0.06
-0.065
-0.07
-0.075
-0.08
-0.085
-0.09
-0.095
Log (1 - C/C orig.)
Magnesium
20
40
60
80
100
Time, hrs.

Figure B19

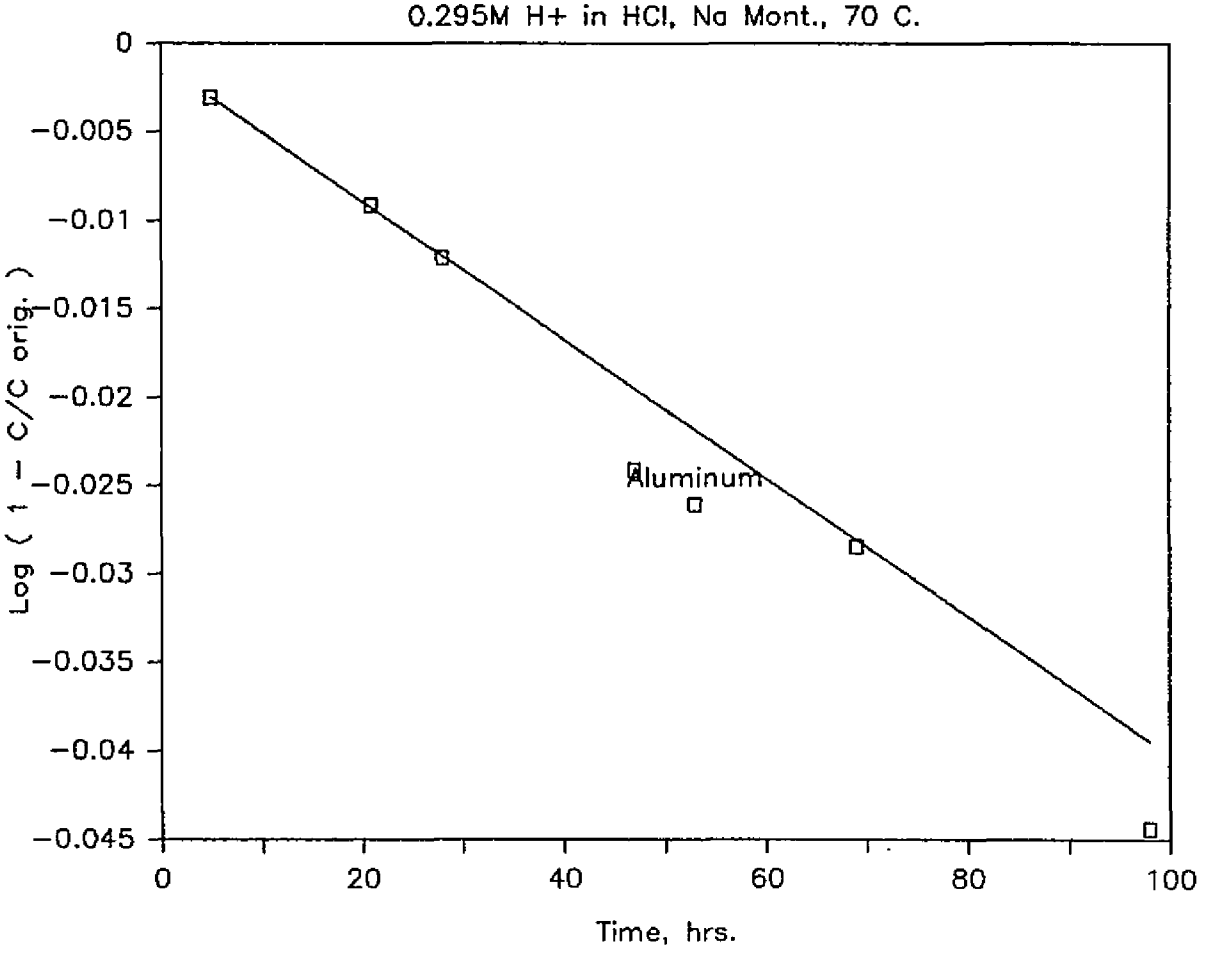
0.295M H+ in HCl, Na Mont., 70 C.
0
−0.005
−0.01
−0.015
−0.02
−0.025
−0.03
−0.035
−0.04
−0.045
Log (1 − C/C orig.)
Aluminum
0
20
40
60
80
100
Time, hrs.

Figure B20

.295M H+ in HCl, Na Mont., 70 C.

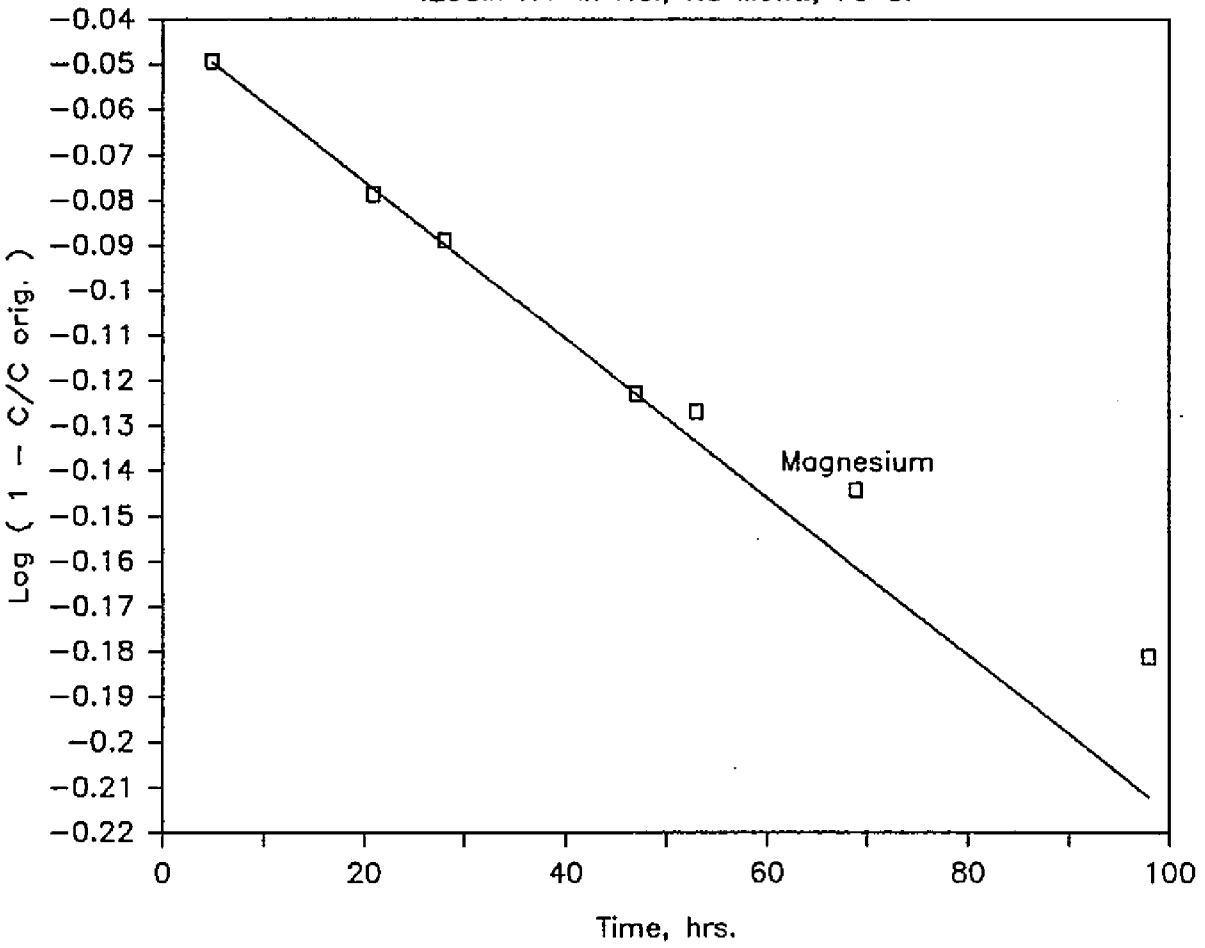

Figure B21

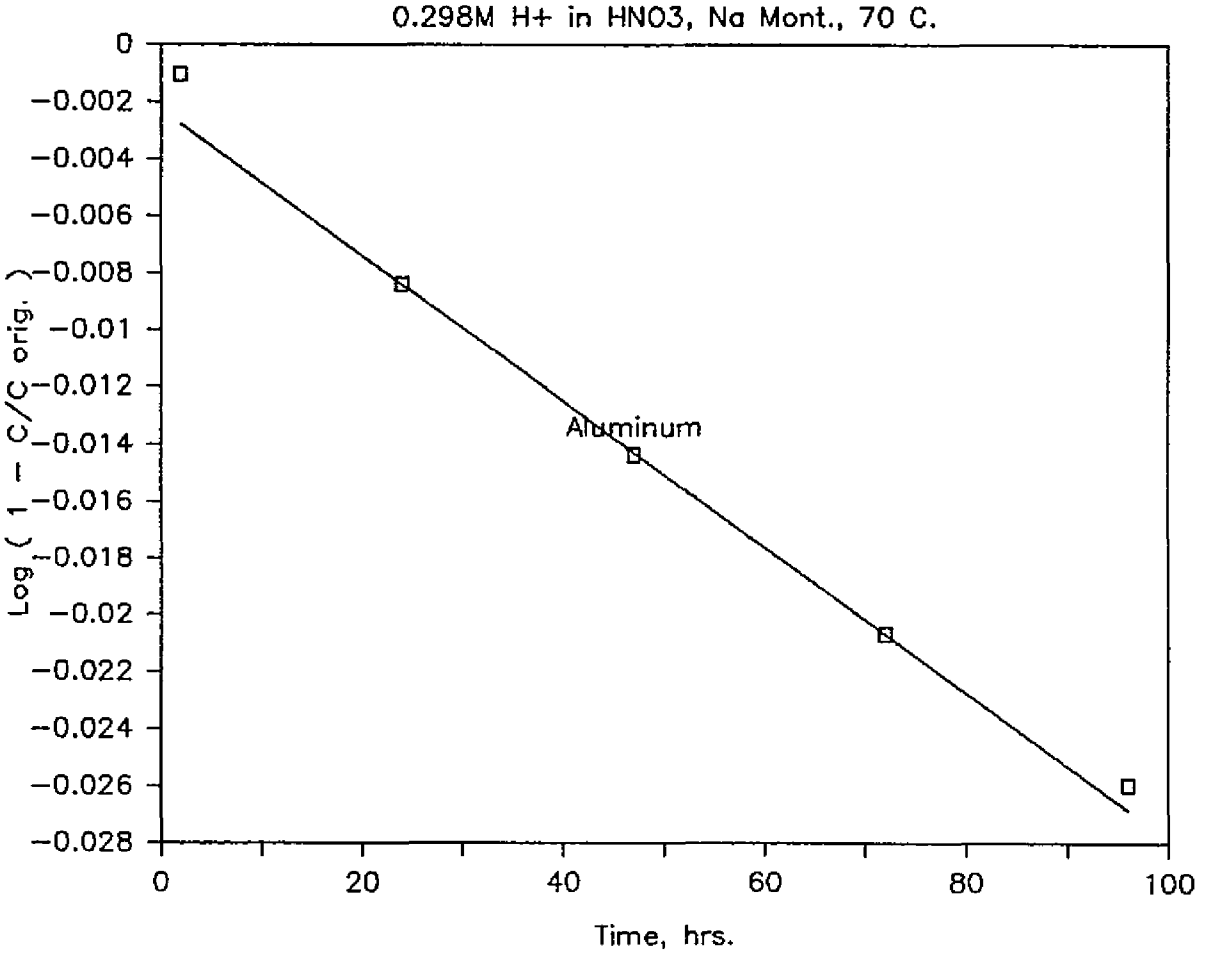
0.298M H+ in HNO3, Na Mont., 70 C.
0
−0.002
−0.004
−0.006
−0.008
−0.01
−0.012
−0.014
−0.016
−0.018
−0.02
−0.022
−0.024
−0.026
−0.028
Log (1 − C/C orig.)
Aluminum
0
20
40
60
80
100
Time, hrs.

Figure B22

.298M H+ in HNO3, Na Mont., 70 C.

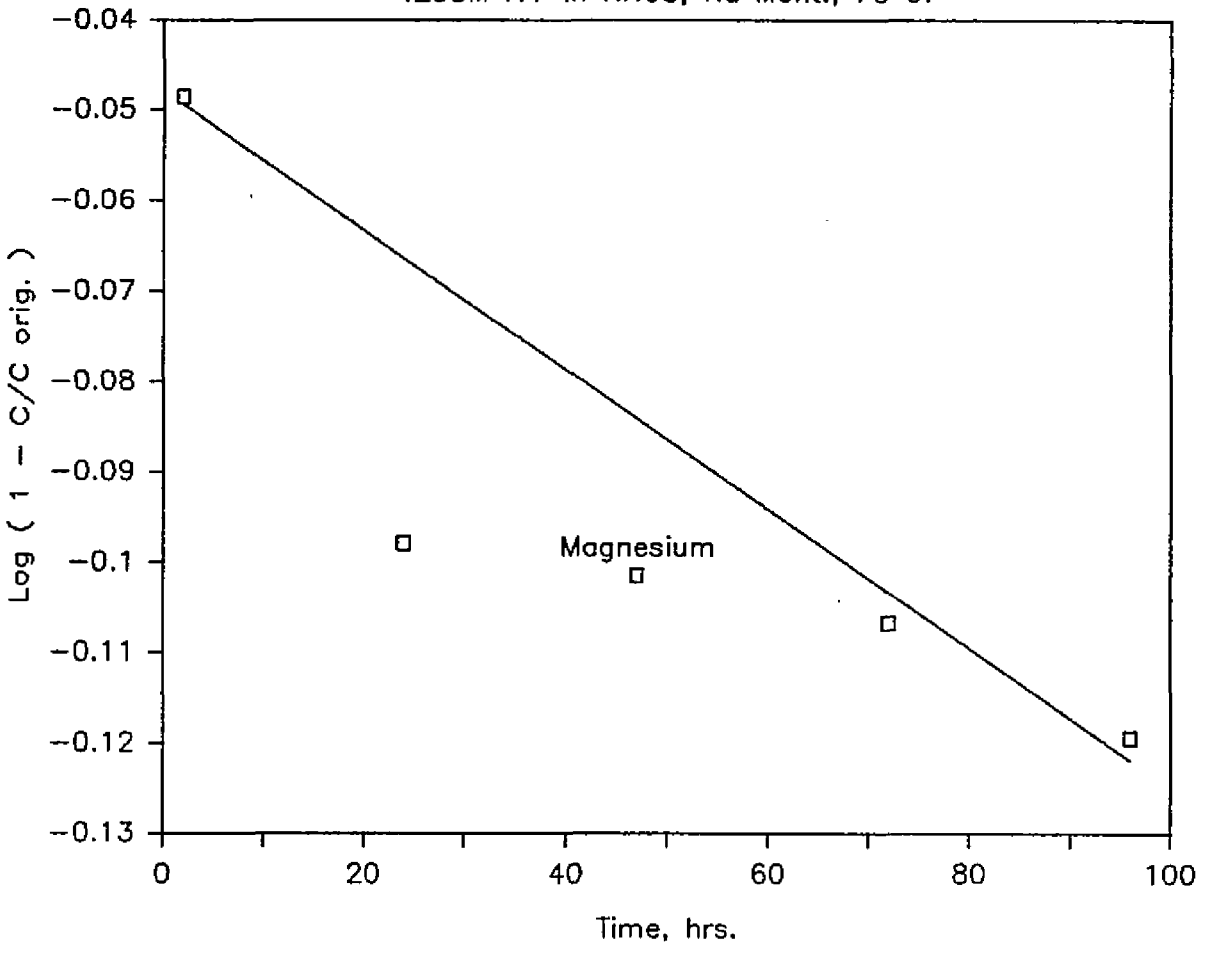

Figure B23

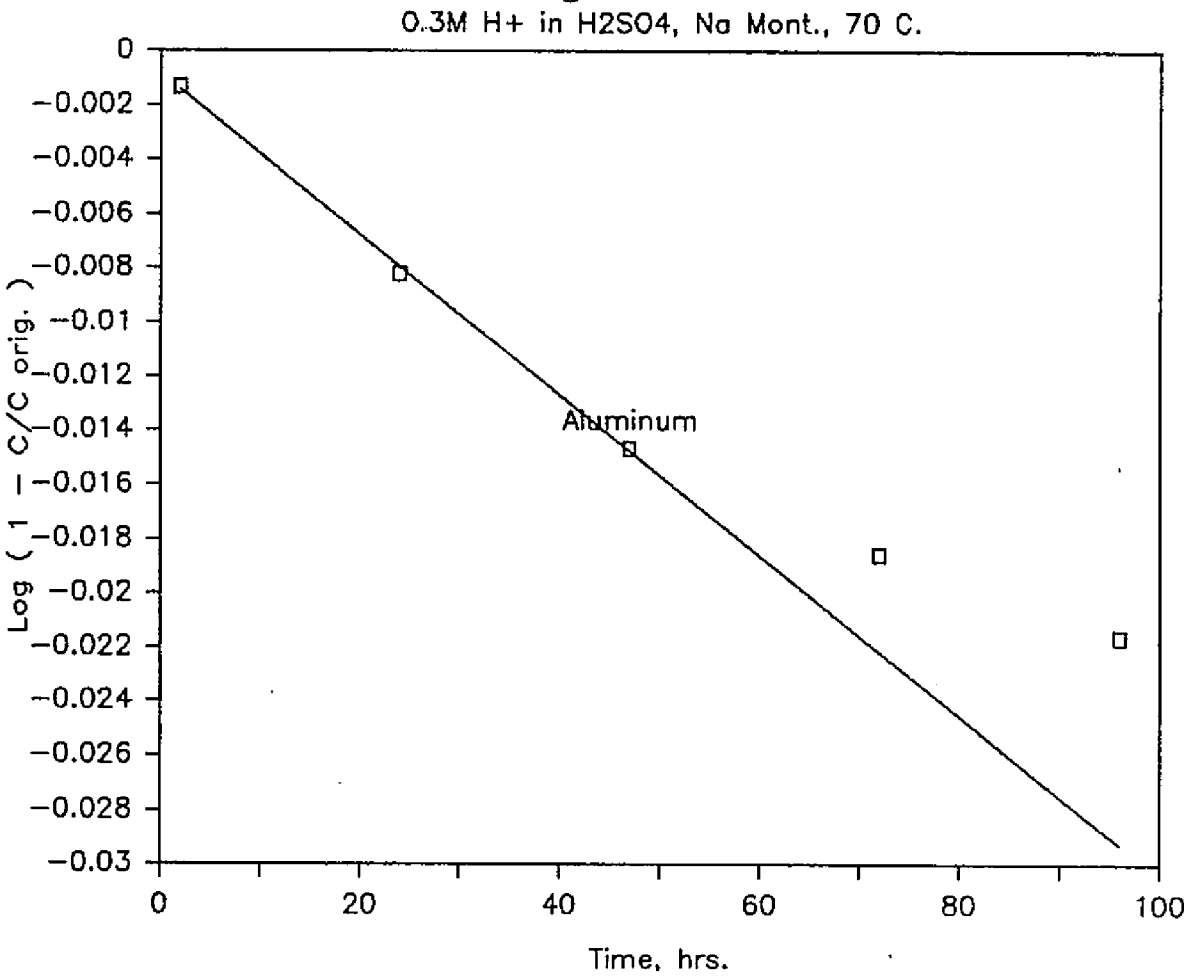
0.3M H+ in H2SO4, Na Mont., 70 C.
Log (1 - C/C orig.)
0
−0.002
−0.004
−0.006
−0.008
−0.01
−0.012
−0.014
−0.016
−0.018
−0.02
−0.022
−0.024
−0.026
−0.028
−0.03
Aluminum
0
20
40
60
80
100
Time, hrs.

Figure B24

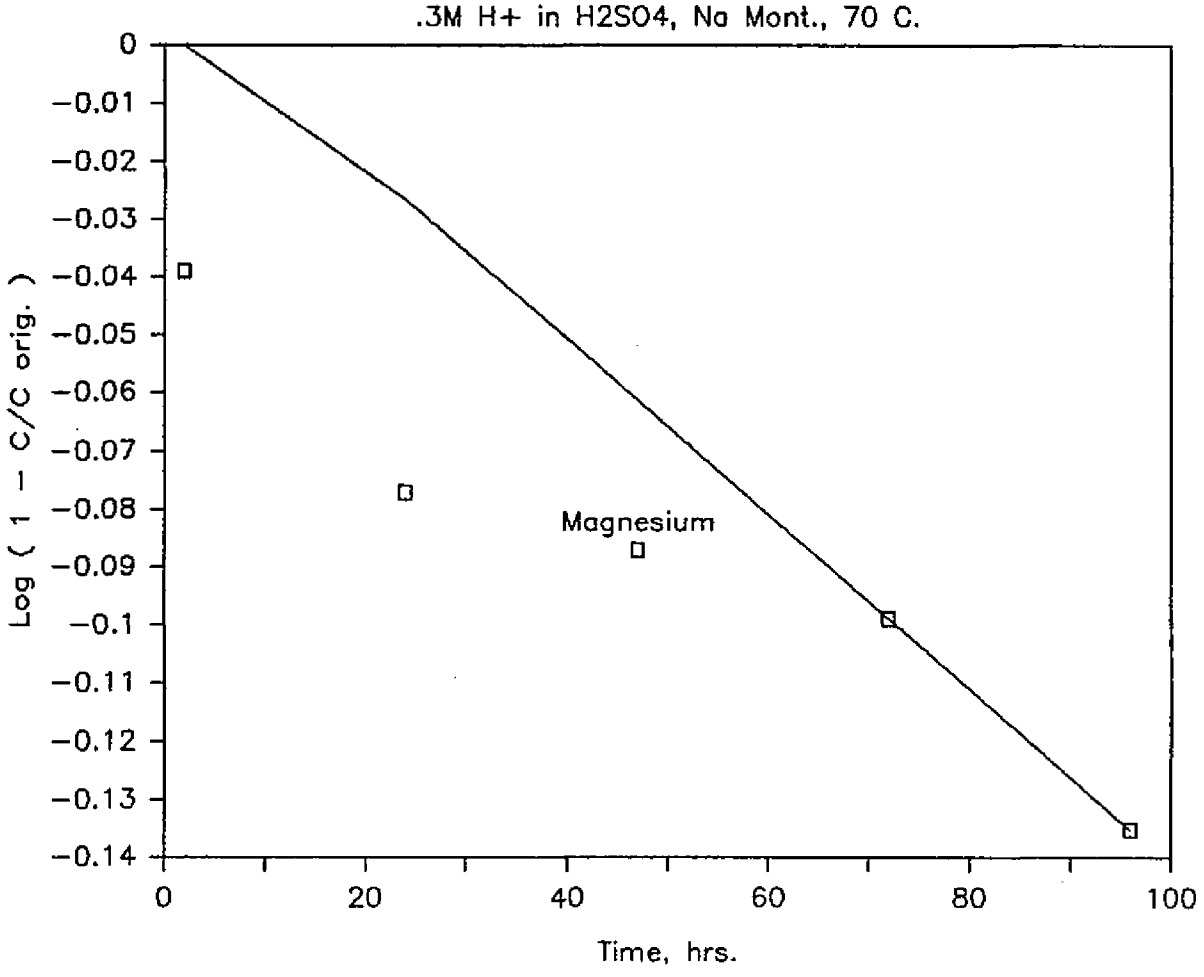
.3M H+ in H2SO4, Na Mont., 70 C.
Log (1 − C/C orig.)
0
−0.01
−0.02
−0.03
−0.04
−0.05
−0.06
−0.07
−0.08
−0.09
−0.1
−0.11
−0.12
−0.13
−0.14
Magnesium
0
20
40
60
80
100
Time, hrs.

Figure B25

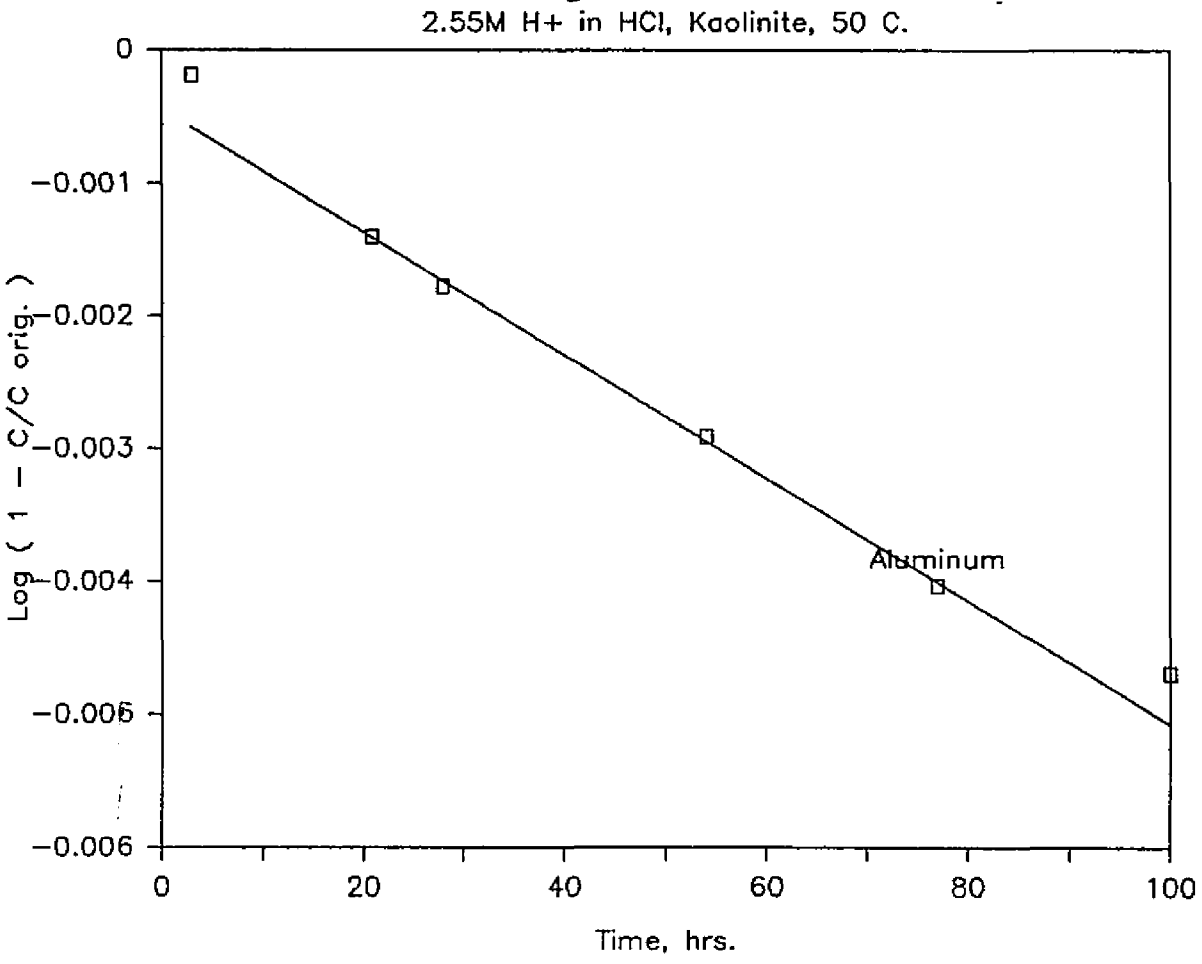
2.55M H+ in HCl, Kaolinite, 50 C.
0
−0.001
−0.002
−0.003
−0.004
−0.005
−0.006
Log (1 − C/C orig.)
Aluminum
0
20
40
60
80
100
Time, hrs.

Figure B26

2.78M H+ in HNO3, Kaolinite, 50 C.

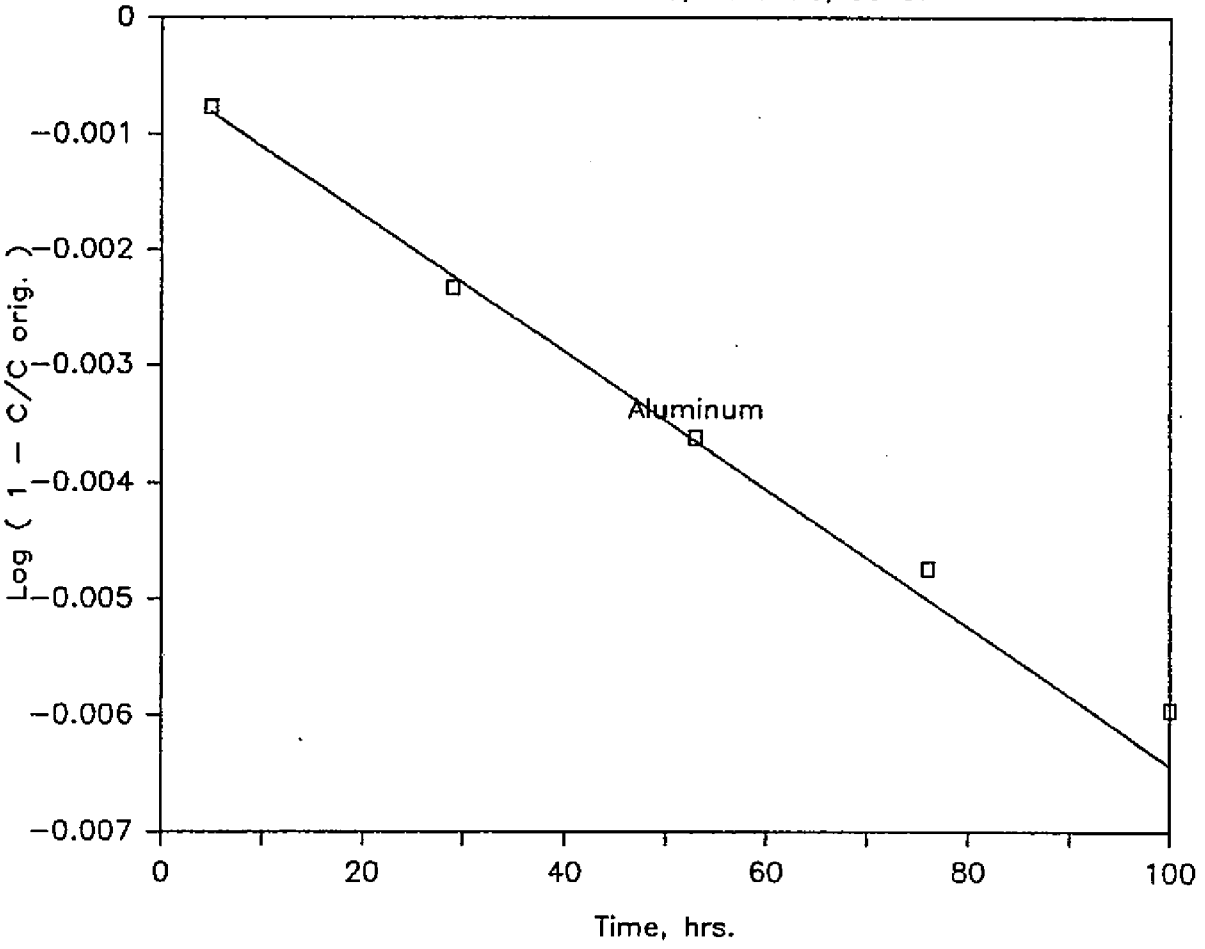

Figure B27

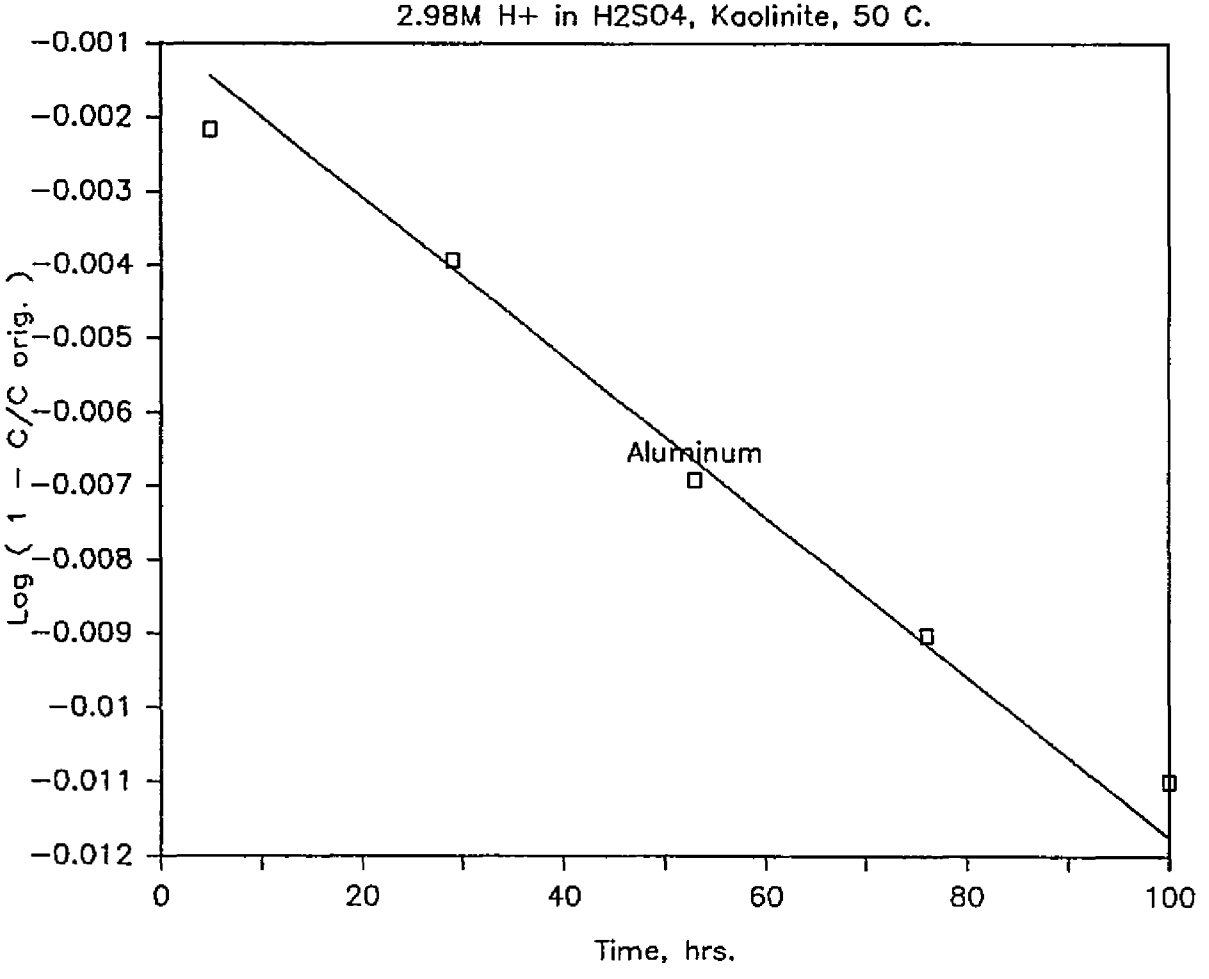
2.98M H+ in H2SO4, Kaolinite, 50 C.
Log (1 - C/C orig.)
-0.001
-0.002
-0.003
-0.004
-0.005
-0.006
-0.007
-0.008
-0.009
-0.01
-0.011
-0.012
Aluminum
0
20
40
60
80
100
Time, hrs.

Figure B28

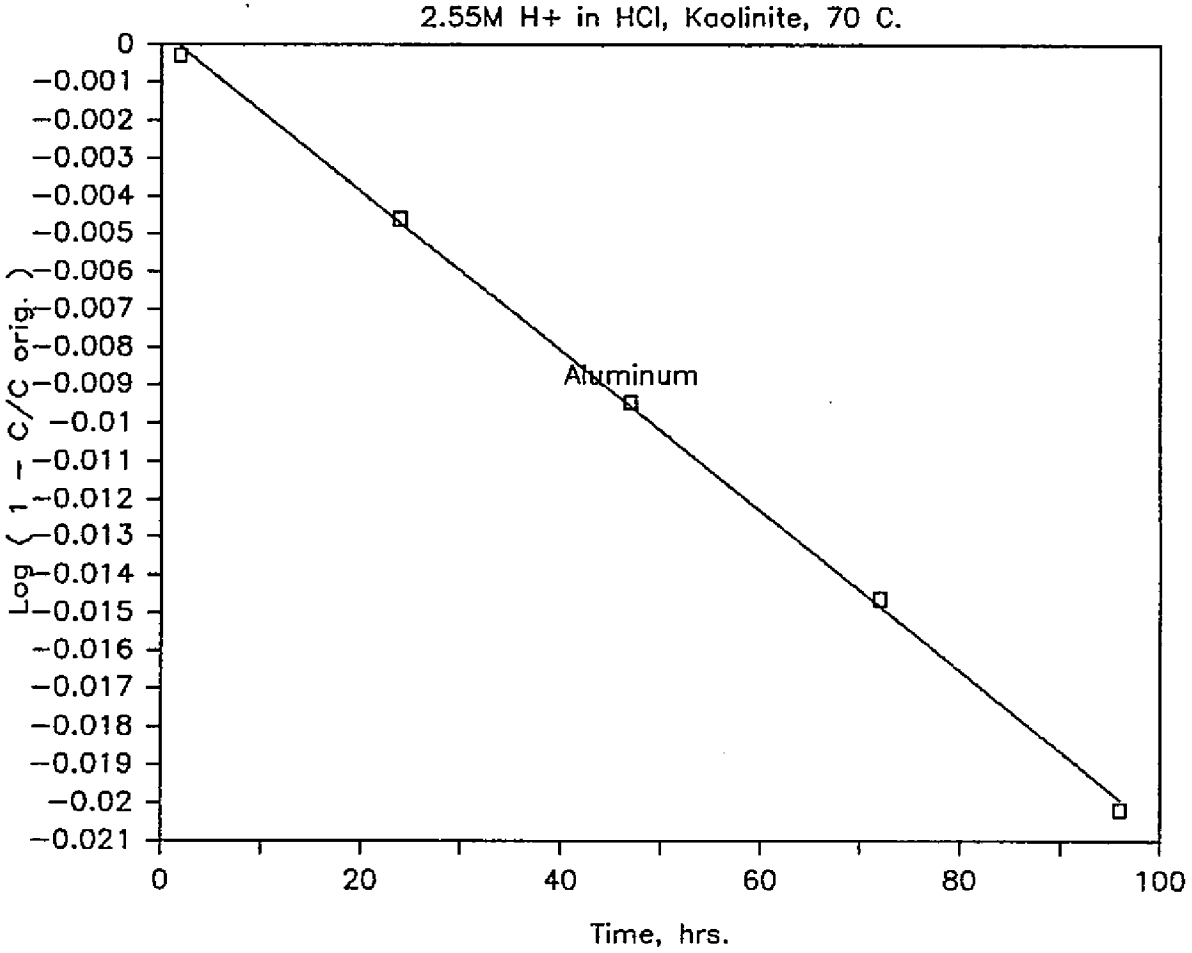
2.55M H+ in HCl, Kaolinite, 70 C.
Log (1 - C/C orig.)
0
−0.001
−0.002
−0.003
−0.004
−0.005
−0.006
−0.007
−0.008
−0.009
−0.01
−0.011
−0.012
−0.013
−0.014
−0.015
−0.016
−0.017
−0.018
−0.019
−0.02
−0.021
Aluminum
0
20
40
60
80
100
Time, hrs.

Figure B29

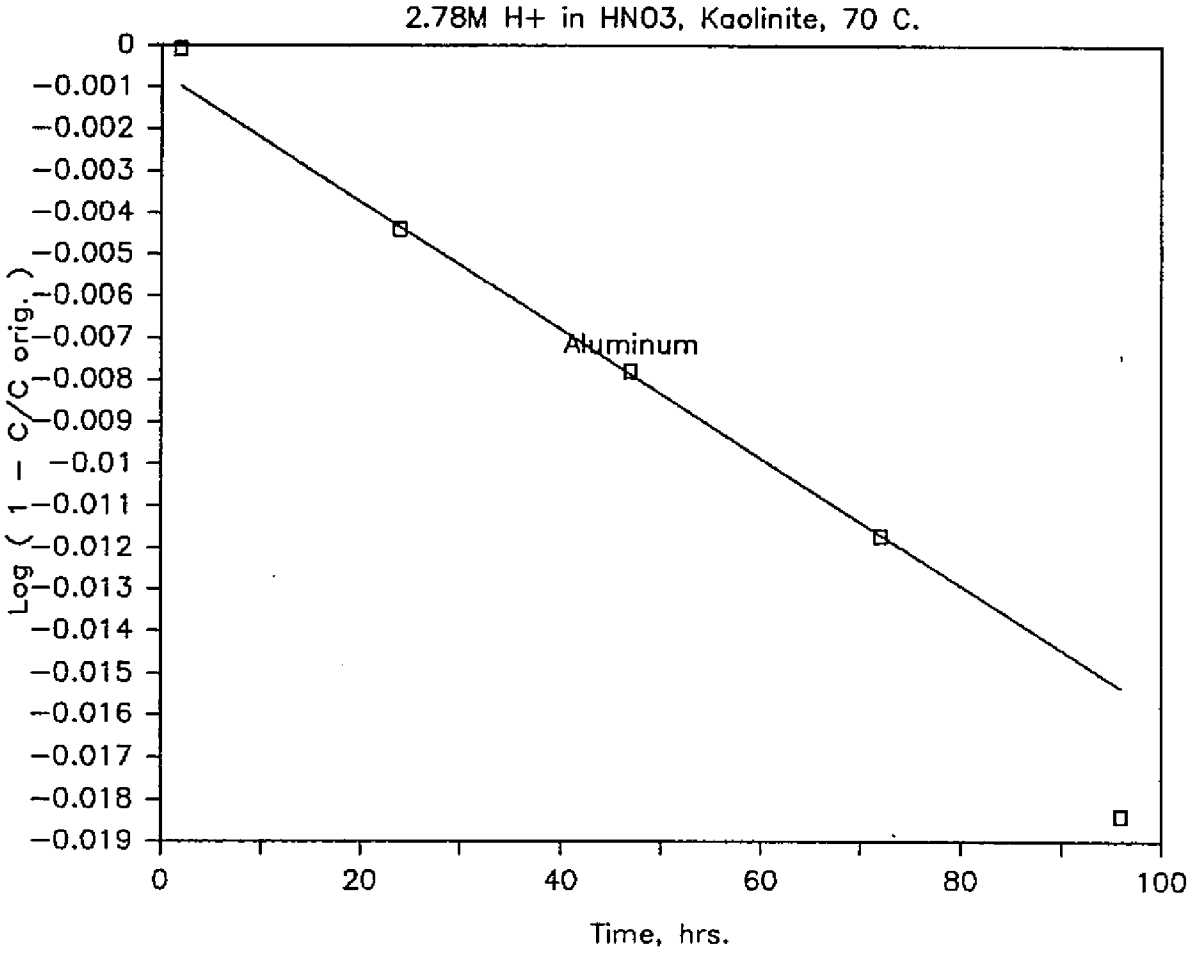
2.78M H+ in HN03, Kaolinite, 70 C.
Log (1 - C/C orig.)
0
−0.001
−0.002
−0.003
−0.004
−0.005
−0.006
−0.007
−0.008
−0.009
−0.01
−0.011
−0.012
−0.013
−0.014
−0.015
−0.016
−0.017
−0.018
−0.019
Aluminum
0
20
40
60
80
100
Time, hrs.

Figure B30

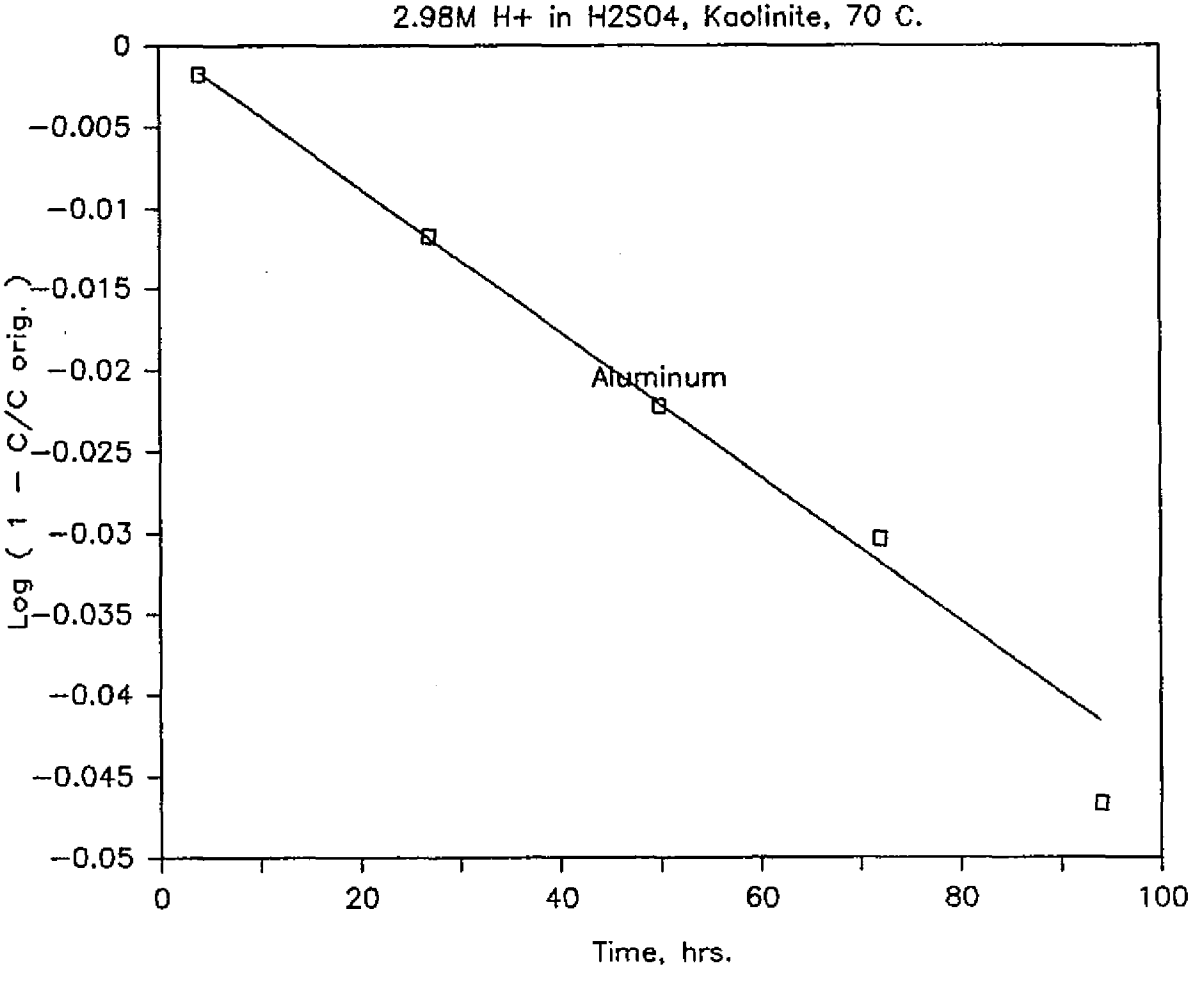
2.98M H+ in H2SO4, Kaolinite, 70 C.
0
−0.005
−0.01
−0.015
−0.02
−0.025
−0.03
−0.035
−0.04
−0.045
−0.05
Log (1 − C/C orig.)
Aluminum
0
20
40
60
80
100
Time, hrs.

Figure B31

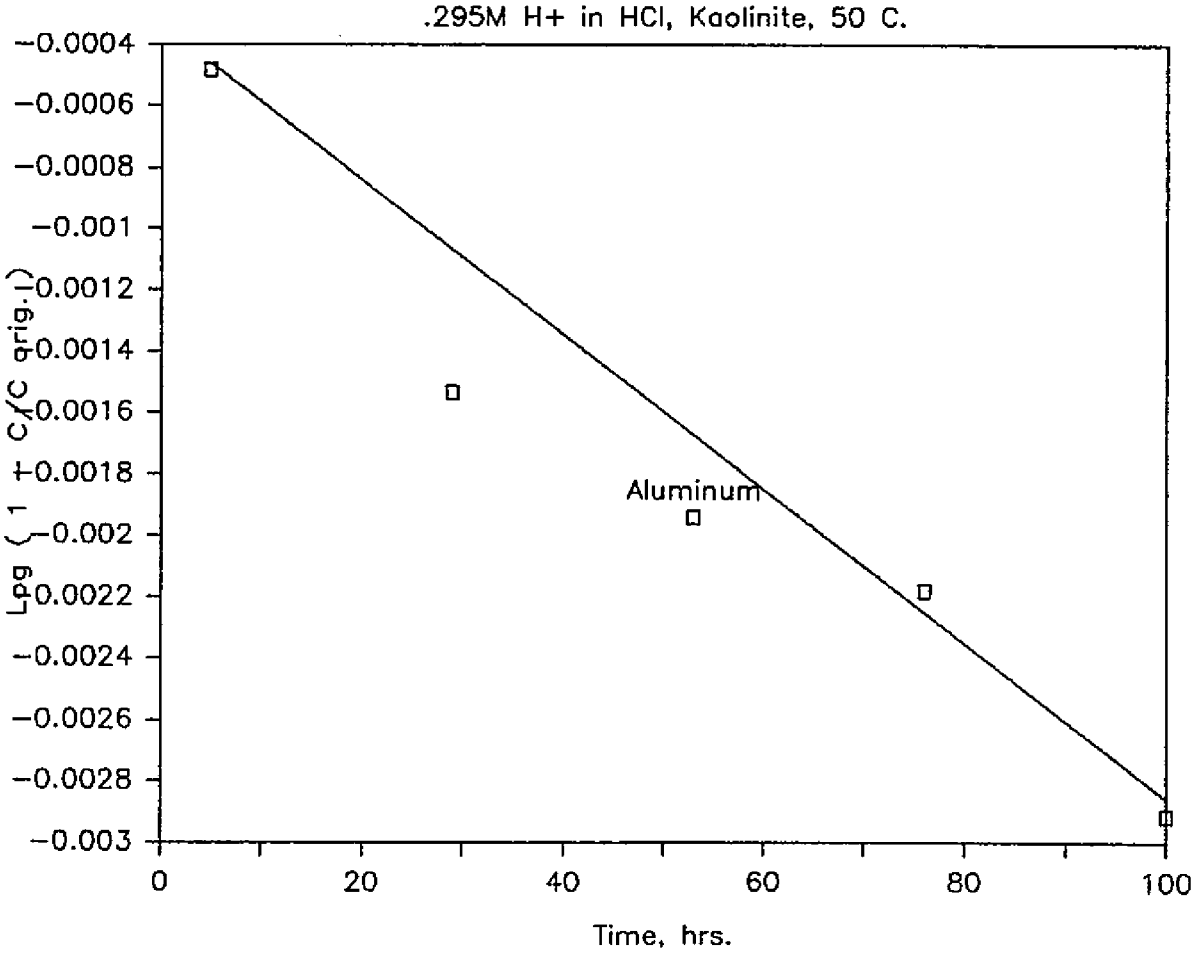
.295M H+ in HCl, Kaolinite, 50 C.
−0.0004
−0.0006
−0.0008
−0.001
−0.0012
−0.0014
−0.0016
−0.0018
−0.002
−0.0022
−0.0024
−0.0026
−0.0028
−0.003
Lpg (1 + C/C orig.)
Aluminum
0
20
40
60
80
100
Time, hrs.

Figure B32

.298M H+ in HNO3, Kaolinite, 50 C.

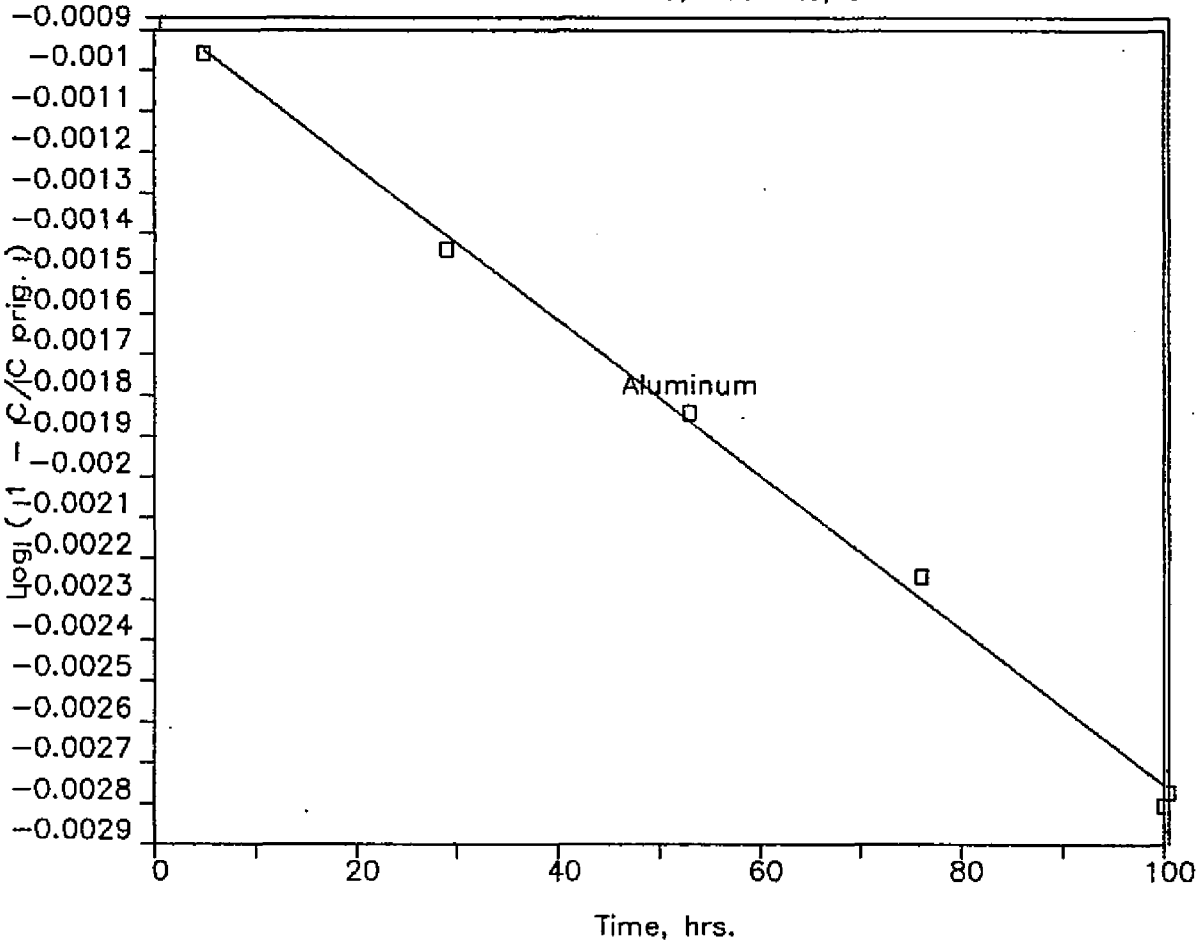

Figure B33

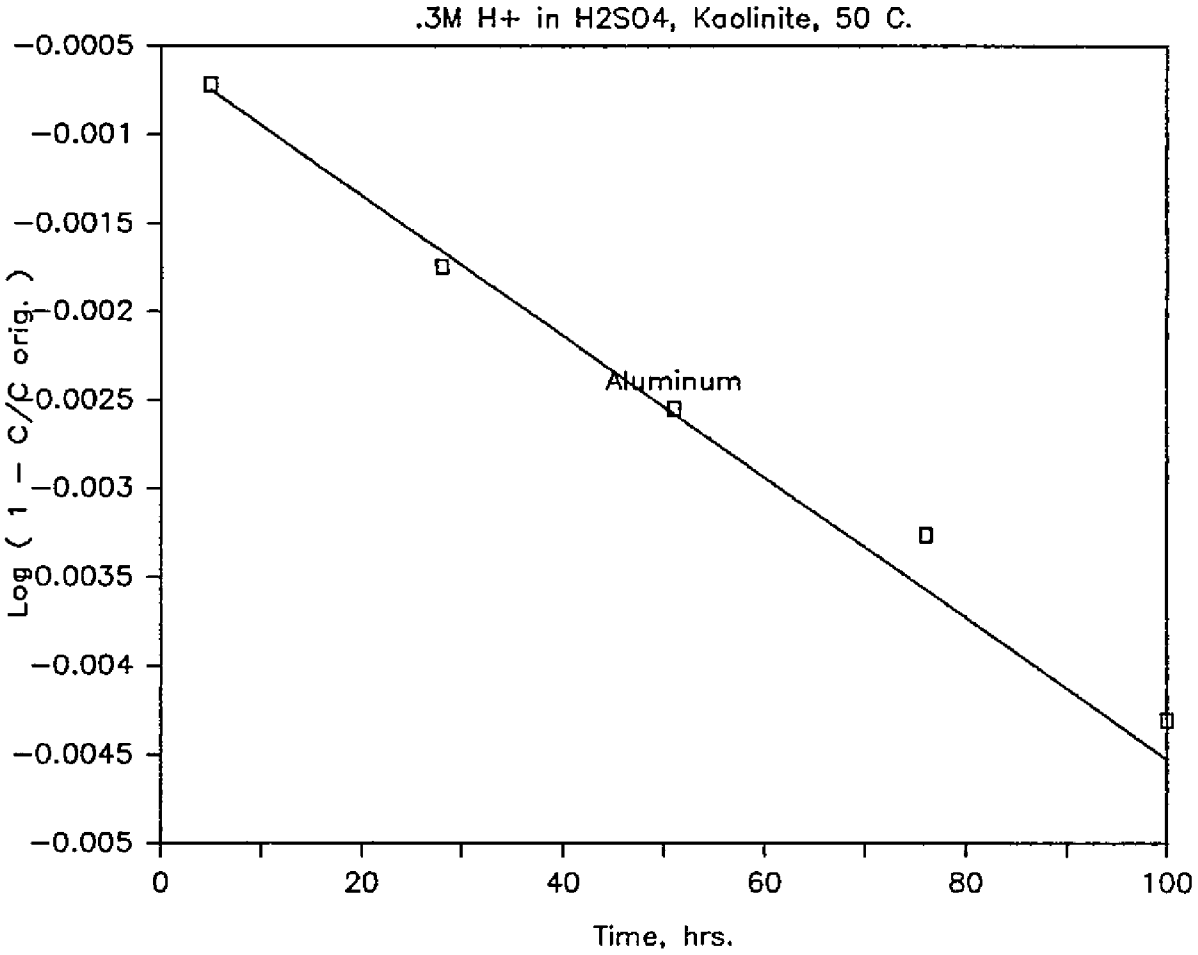
.3M H+ in H2SO4, Kaolinite, 50 C.
Log (1 - C/C orig.)
-0.0005
-0.001
-0.0015
-0.002
-0.0025
-0.003
-0.0035
-0.004
-0.0045
-0.005
Aluminum
0
20
40
60
80
100
Time, hrs.

Figure B34

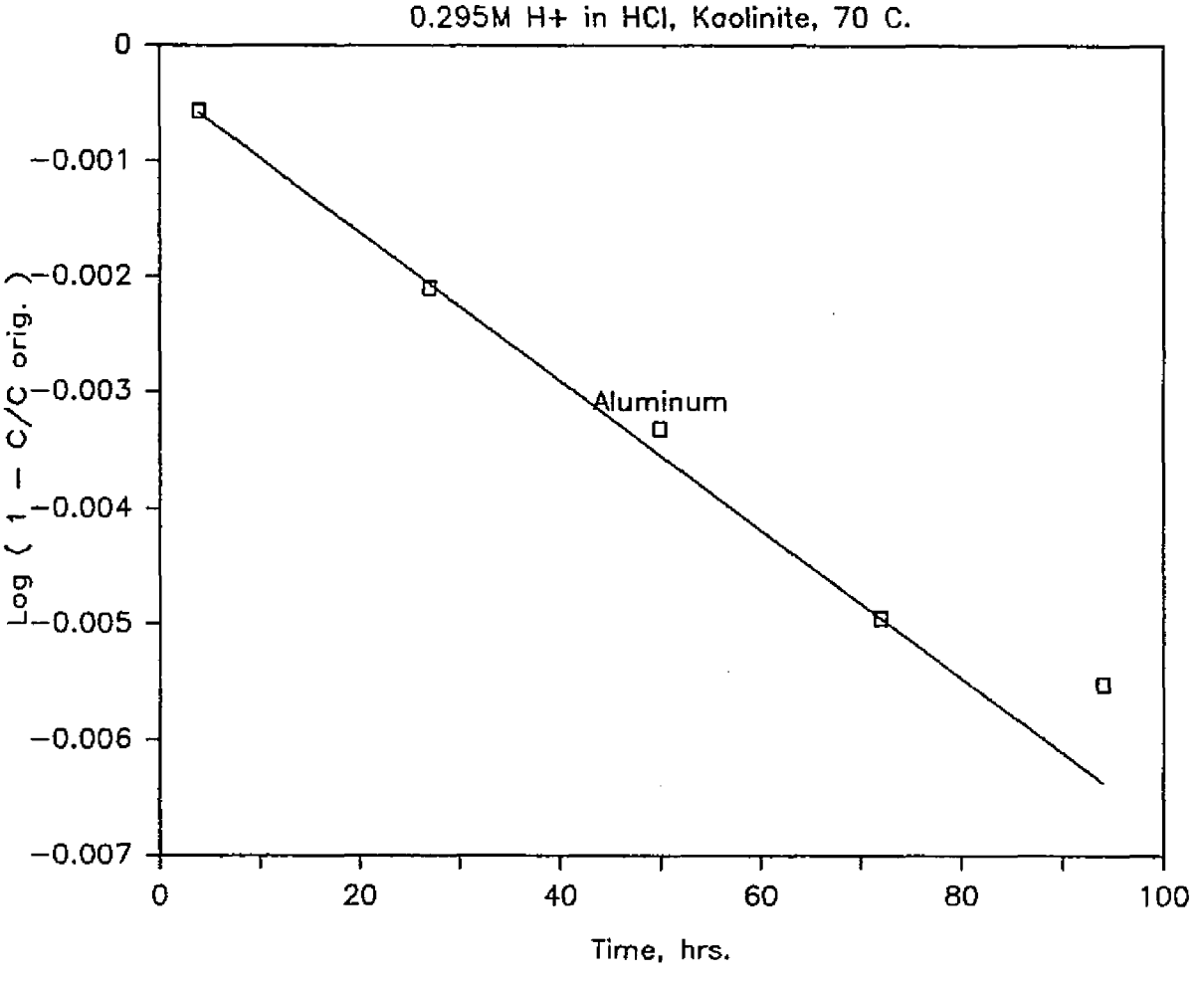
0.295M H+ in HCl, Kaolinite, 70 C.
0
−0.001
−0.002
−0.003
−0.004
−0.005
−0.006
−0.007
Log (1 − C/C orig.)
Aluminum
0
20
40
60
80
100
Time, hrs.

Figure B35

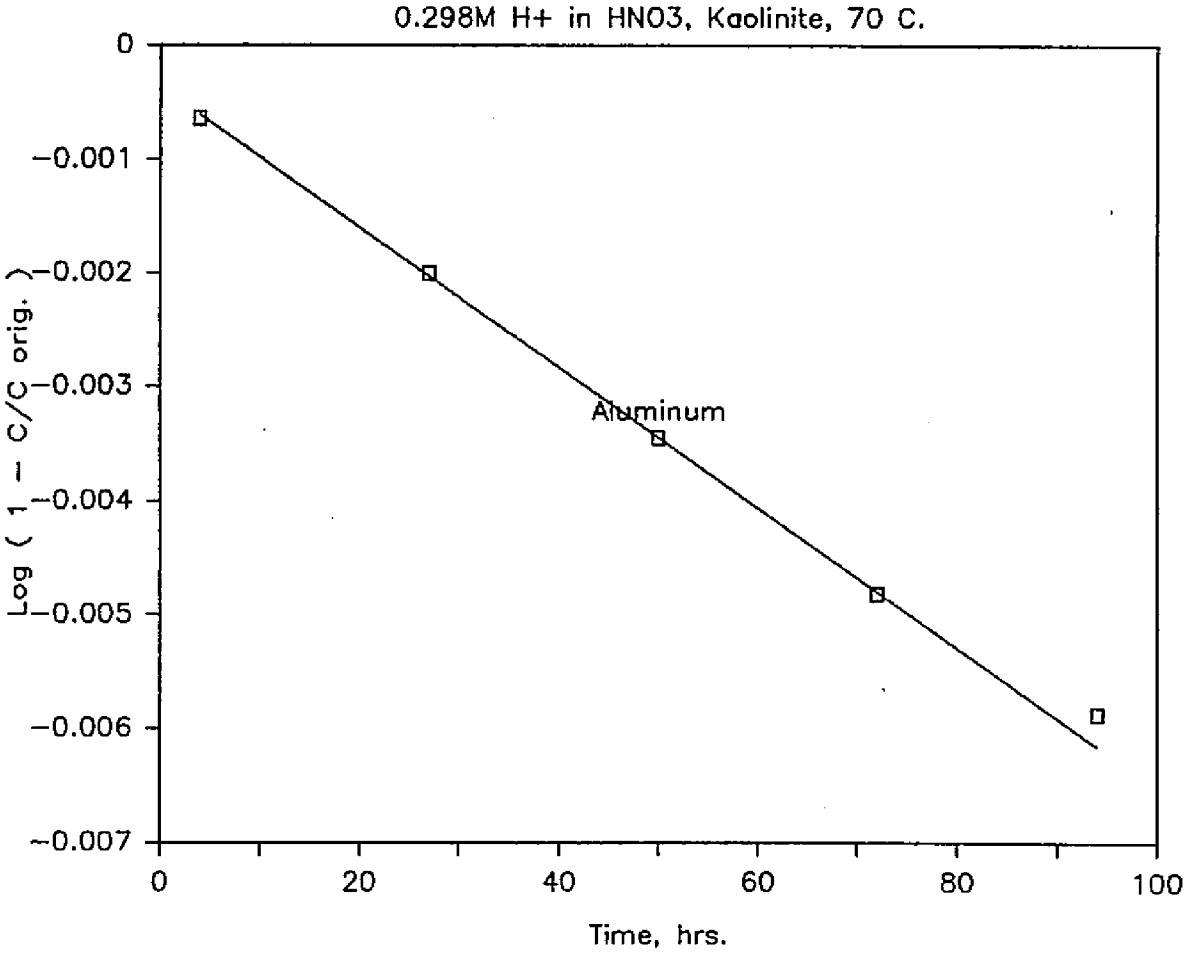
0.298M H+ in HNO3, Kaolinite, 70 C.
0
−0.001
−0.002
−0.003
−0.004
−0.005
−0.006
−0.007
Log (1 − C/C orig.)
Aluminum
0
20
40
60
80
100
Time, hrs.

Figure B36

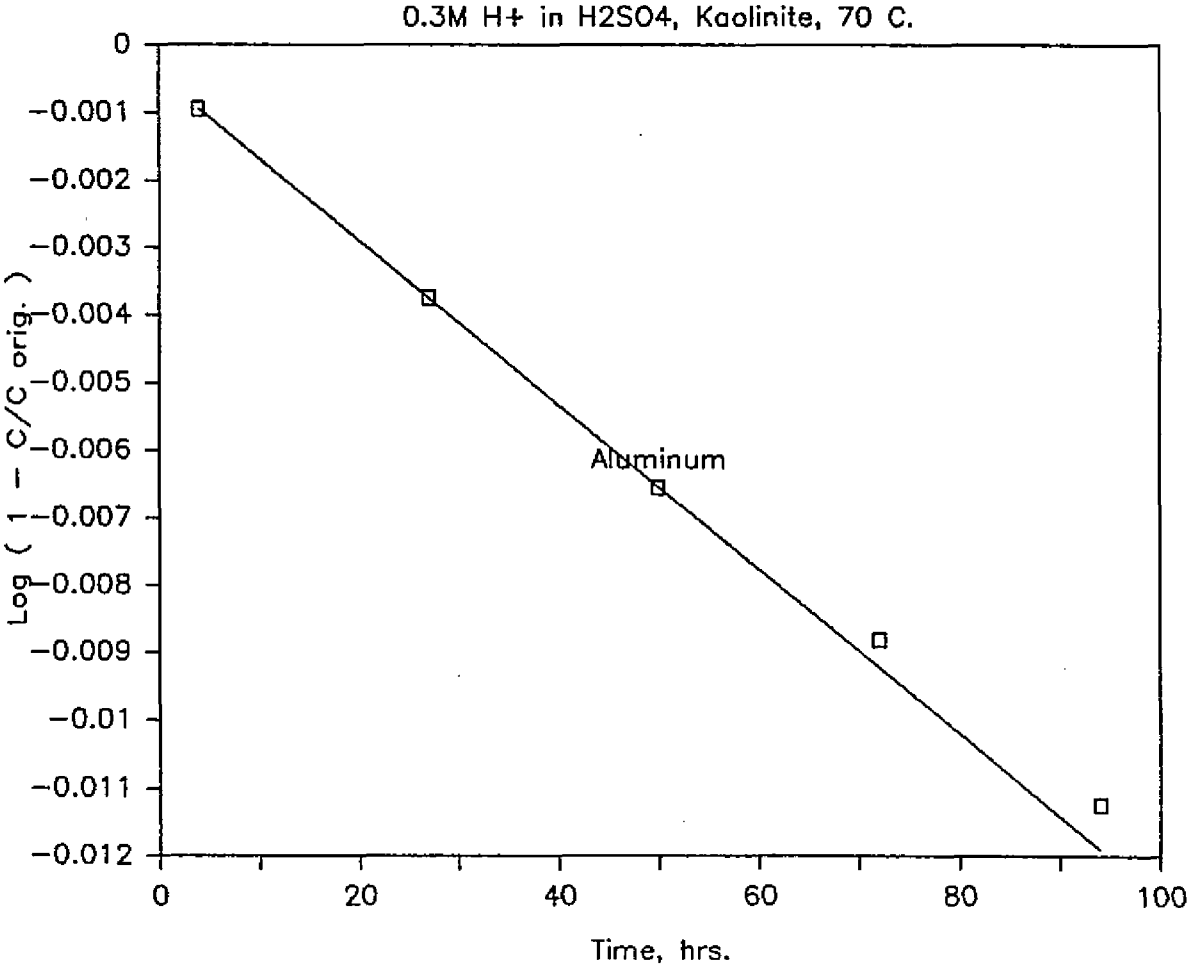
0.3M H+ in H2SO4, Kaolinite, 70 C.
0
−0.001
−0.002
−0.003
−0.004
−0.005
−0.006
−0.007
−0.008
−0.009
−0.01
−0.011
−0.012
Log (1 − C/C orig.)
Aluminum
0
20
40
60
80
100
Time, hrs.

Figure B37

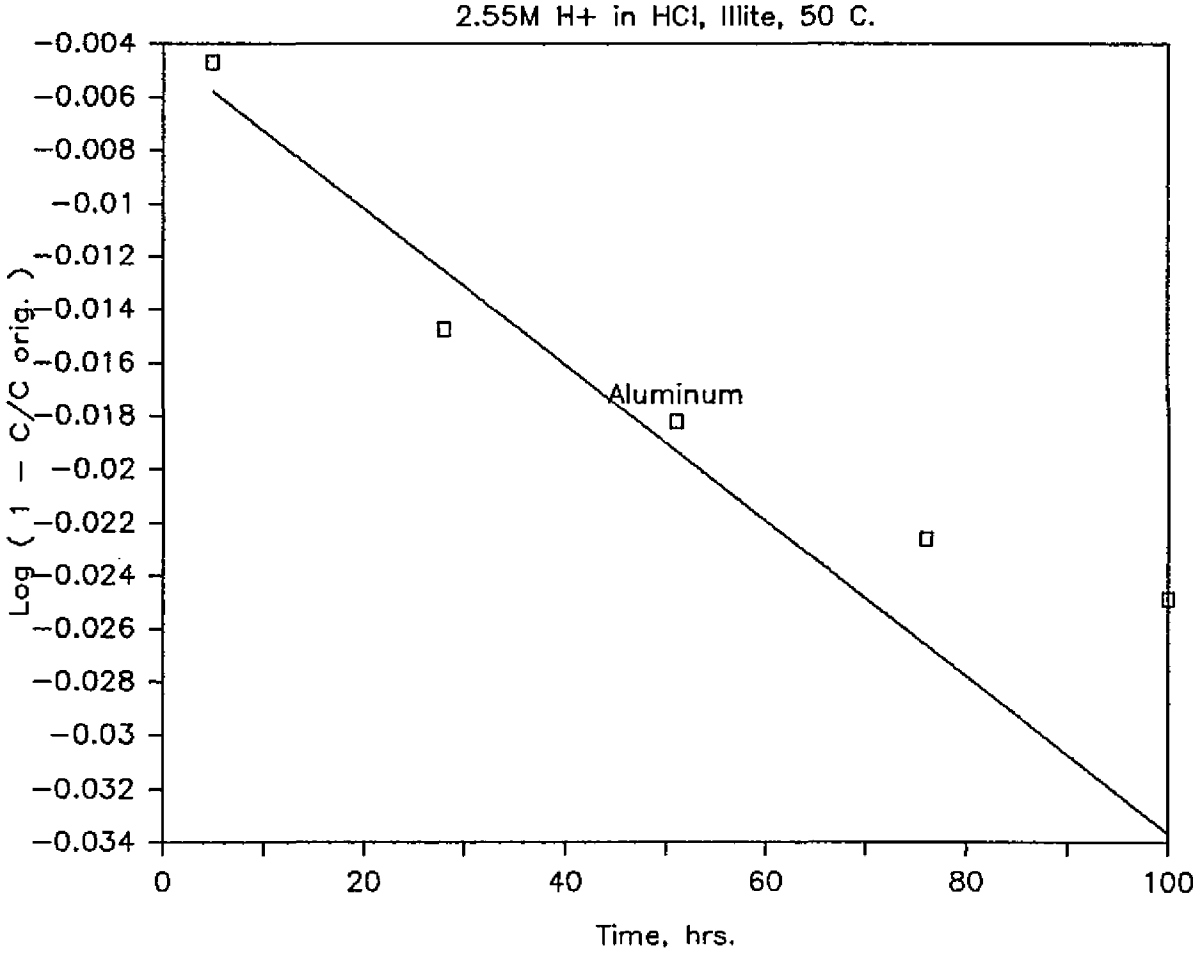
2.55M H+ in HCl, Illite, 50 C.
Aluminum
Log (1 - C/C orig.)
Time, hrs.
-0.004
-0.006
-0.008
-0.01
-0.012
-0.014
-0.016
-0.018
-0.02
-0.022
-0.024
-0.026
-0.028
-0.03
-0.032
-0.034
0
20
40
60
80
100

Figure B38

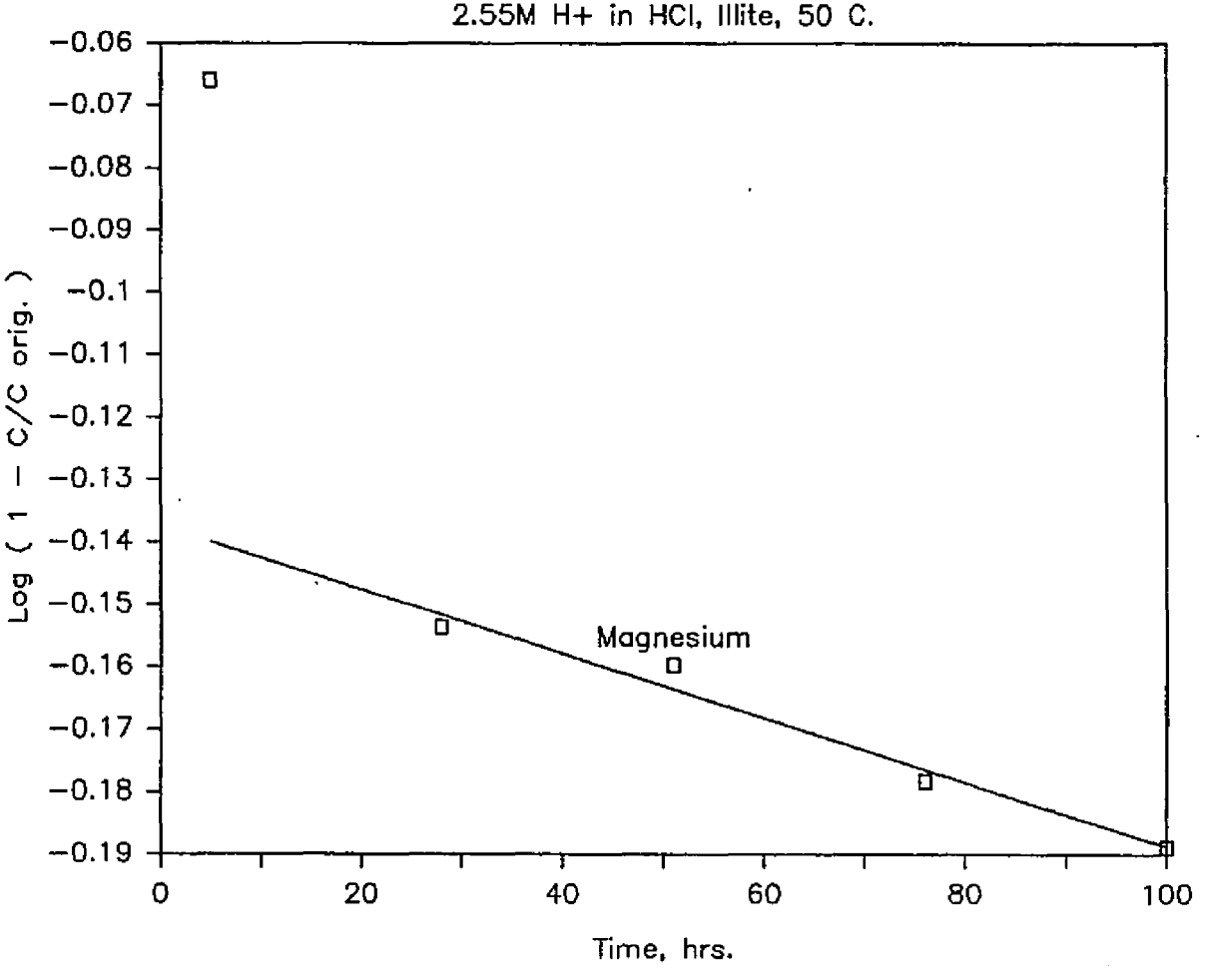
2.55M H+ in HCl, Illite, 50 C.
Log (1 - C/C orig.)
-0.06
-0.07
-0.08
-0.09
-0.1
-0.11
-0.12
-0.13
-0.14
-0.15
-0.16
-0.17
-0.18
-0.19
Magnesium
0
20
40
60
80
100
Time, hrs.

Figure B39

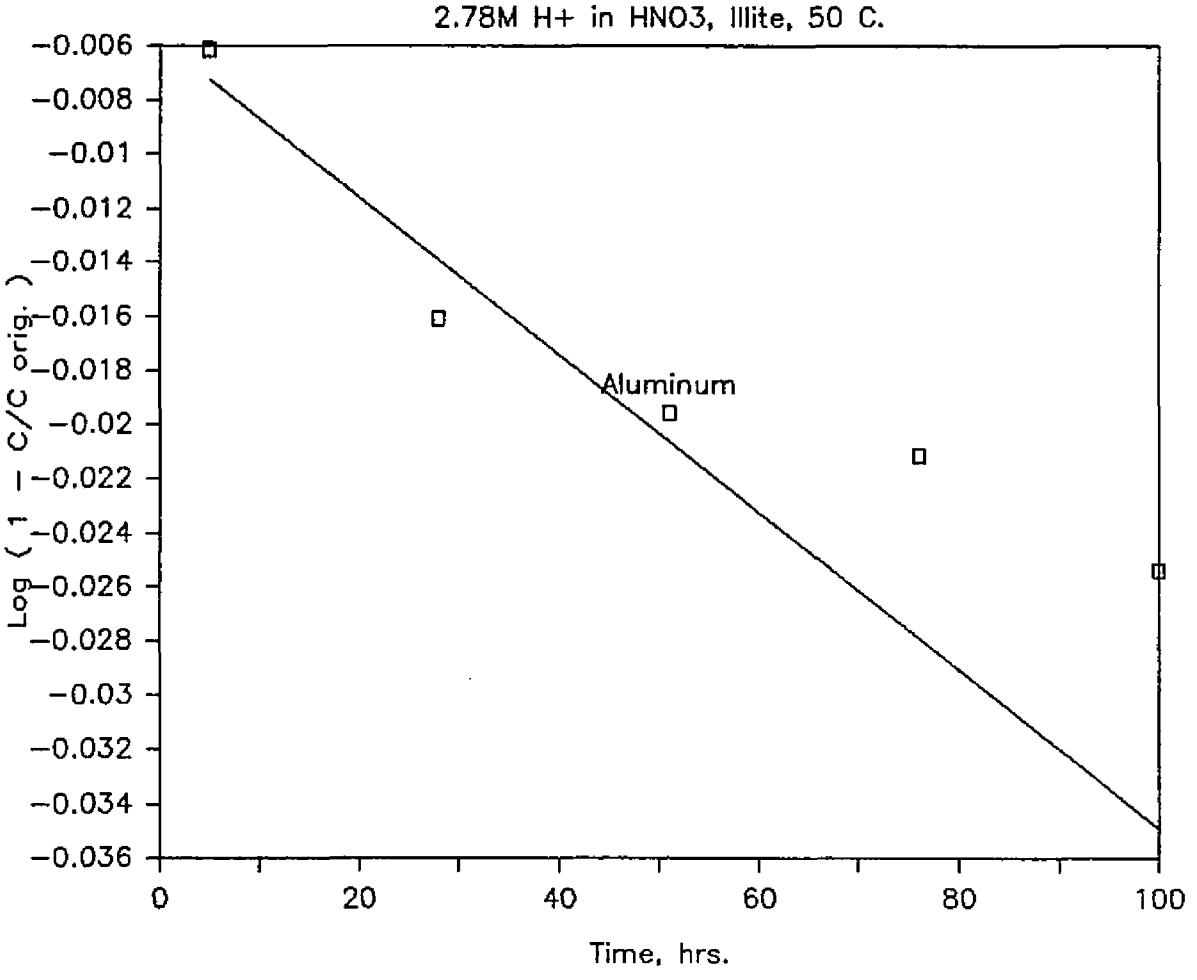
2.78M H+ in HNO3, Illite, 50 C.
Log (1 - C/C orig.)
-0.006
-0.008
-0.01
-0.012
-0.014
-0.016
-0.018
-0.02
-0.022
-0.024
-0.026
-0.028
-0.03
-0.032
-0.034
-0.036
Aluminum
0
20
40
60
80
100
Time, hrs.

Figure B40

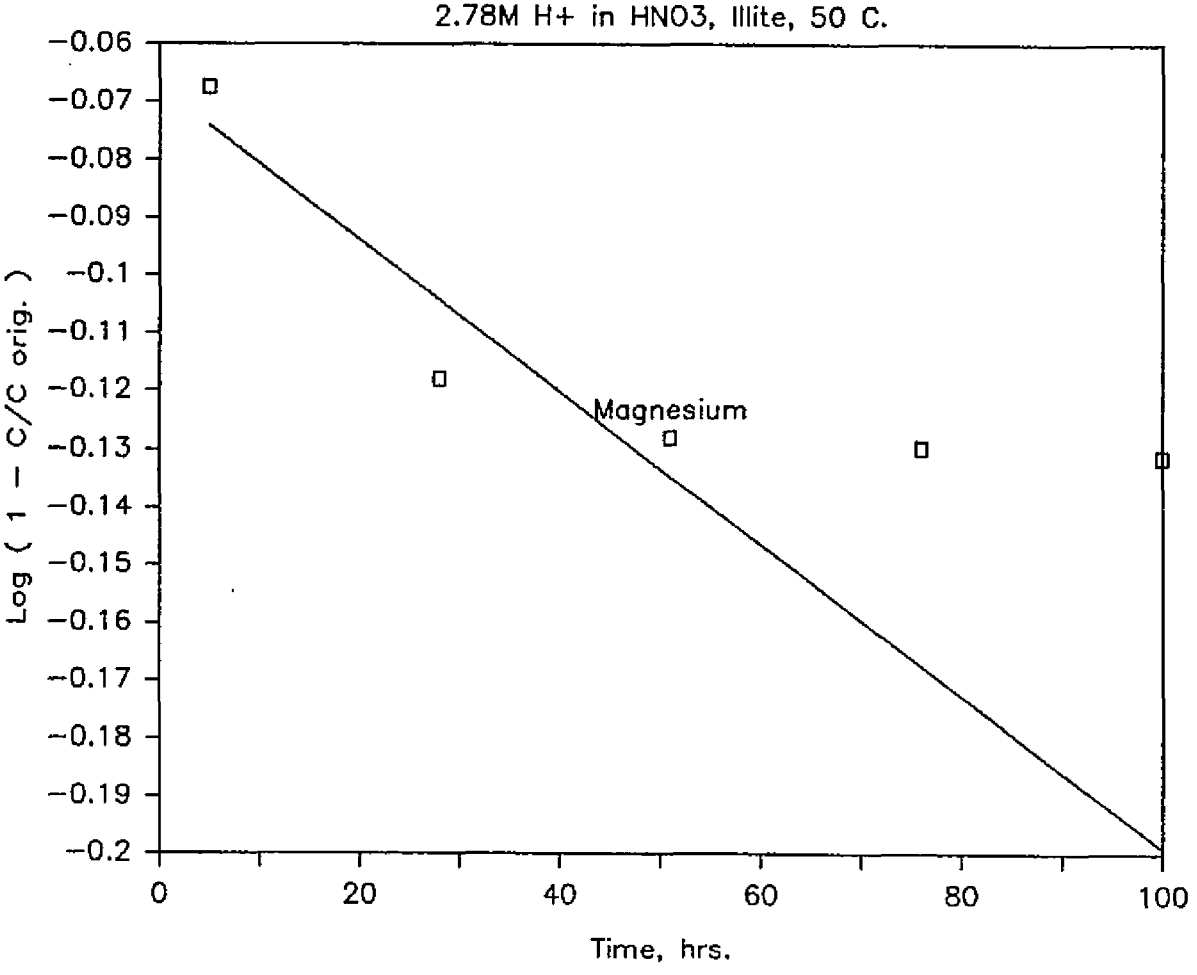
2.78M H+ in HNO3, Illite, 50 C.
Log (1 − C/C orig.)
−0.06
−0.07
−0.08
−0.09
−0.1
−0.11
−0.12
−0.13
−0.14
−0.15
−0.16
−0.17
−0.18
−0.19
−0.2
Magnesium
0
20
40
60
80
100
Time, hrs.

Figure B41

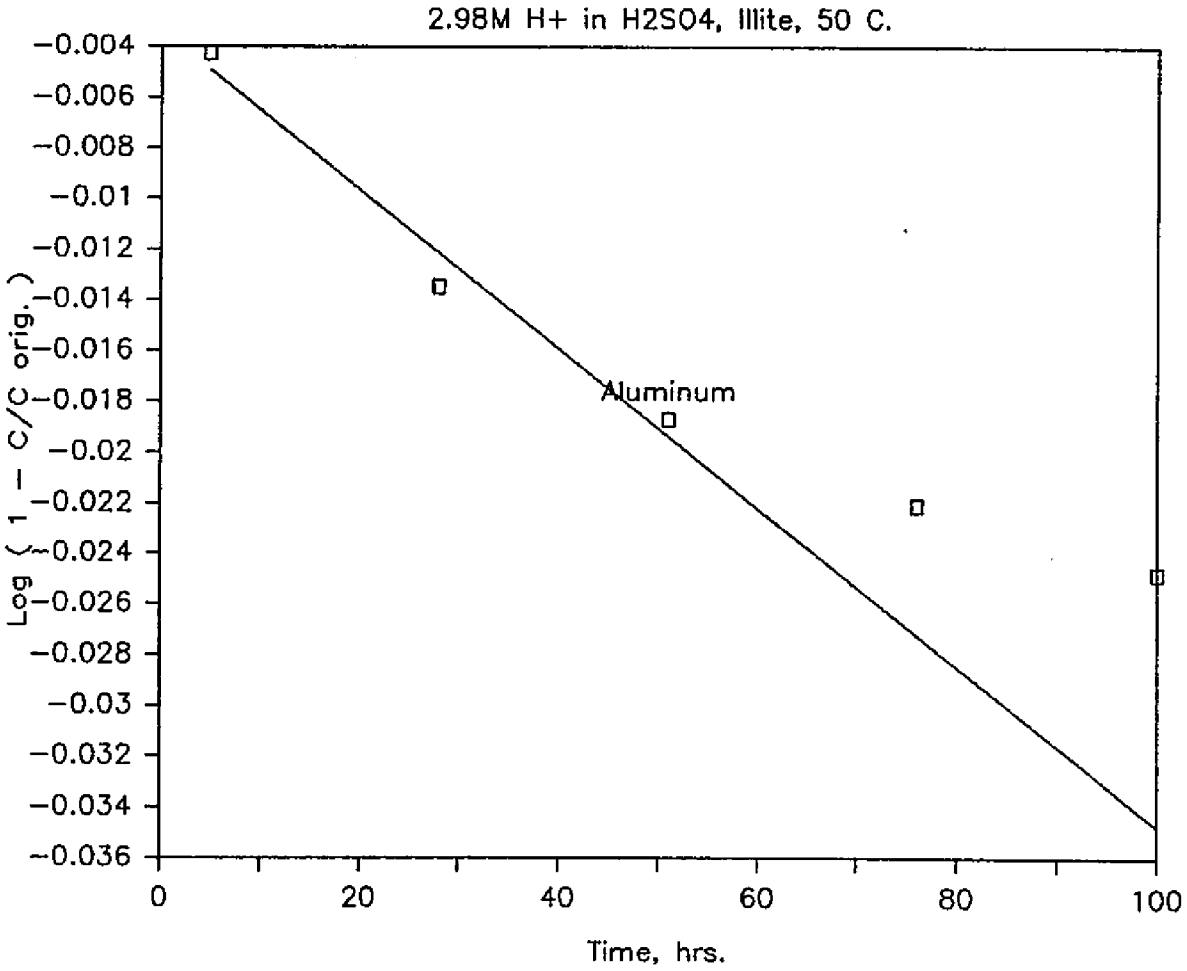
2.98M H+ in H2SO4, Illite, 50 C.
Log (1 - C/C orig.)
-0.004
-0.006
-0.008
-0.01
-0.012
-0.014
-0.016
-0.018
-0.02
-0.022
-0.024
-0.026
-0.028
-0.03
-0.032
-0.034
-0.036
Aluminum
0
20
40
60
80
100
Time, hrs.

Figure B42

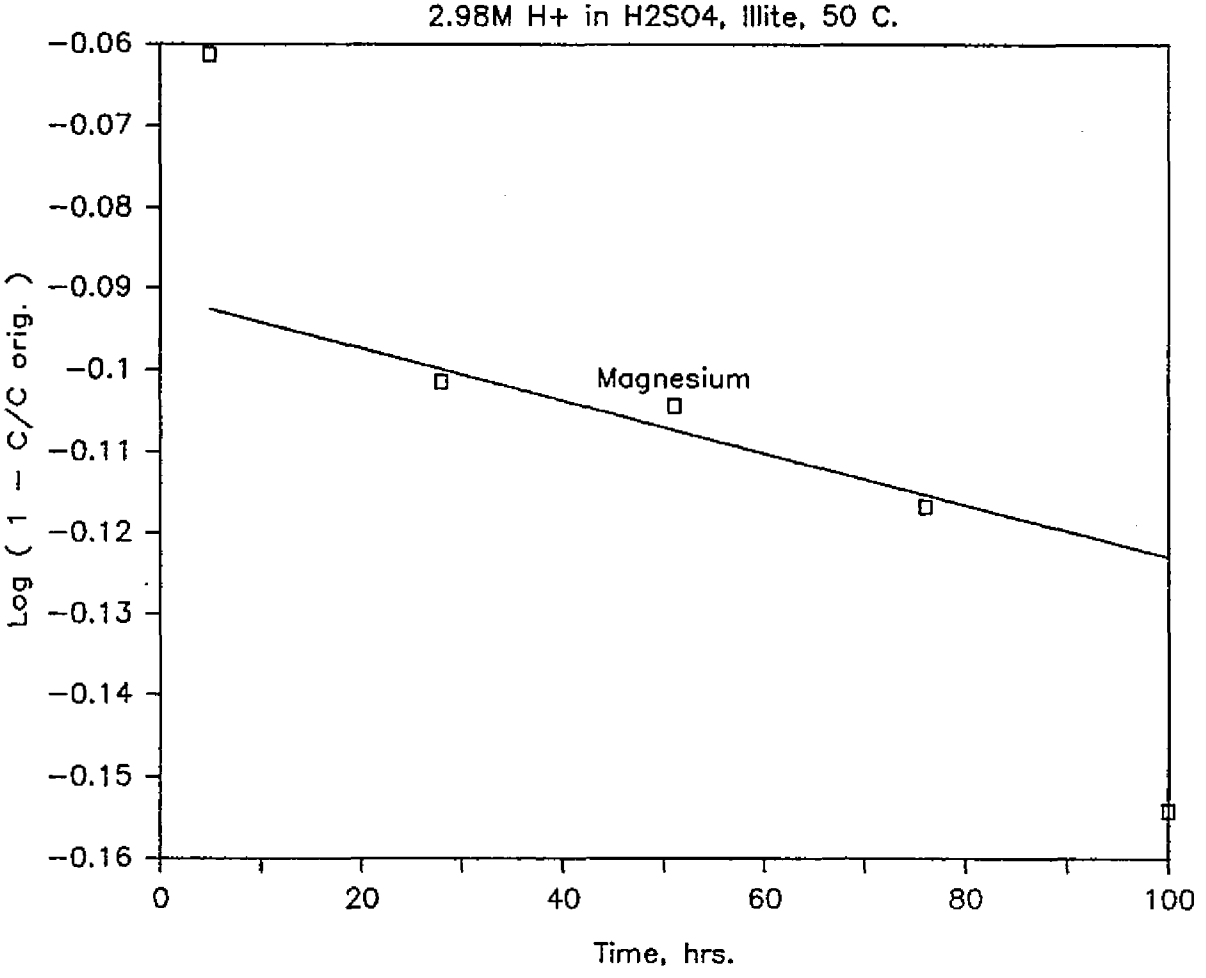
2.98M H+ in H2SO4, Illite, 50 C.
Log (1 - C/C orig.)
-0.06
-0.07
-0.08
-0.09
-0.1
-0.11
-0.12
-0.13
-0.14
-0.15
-0.16
Magnesium
0
20
40
60
80
100
Time, hrs.

Figure B43

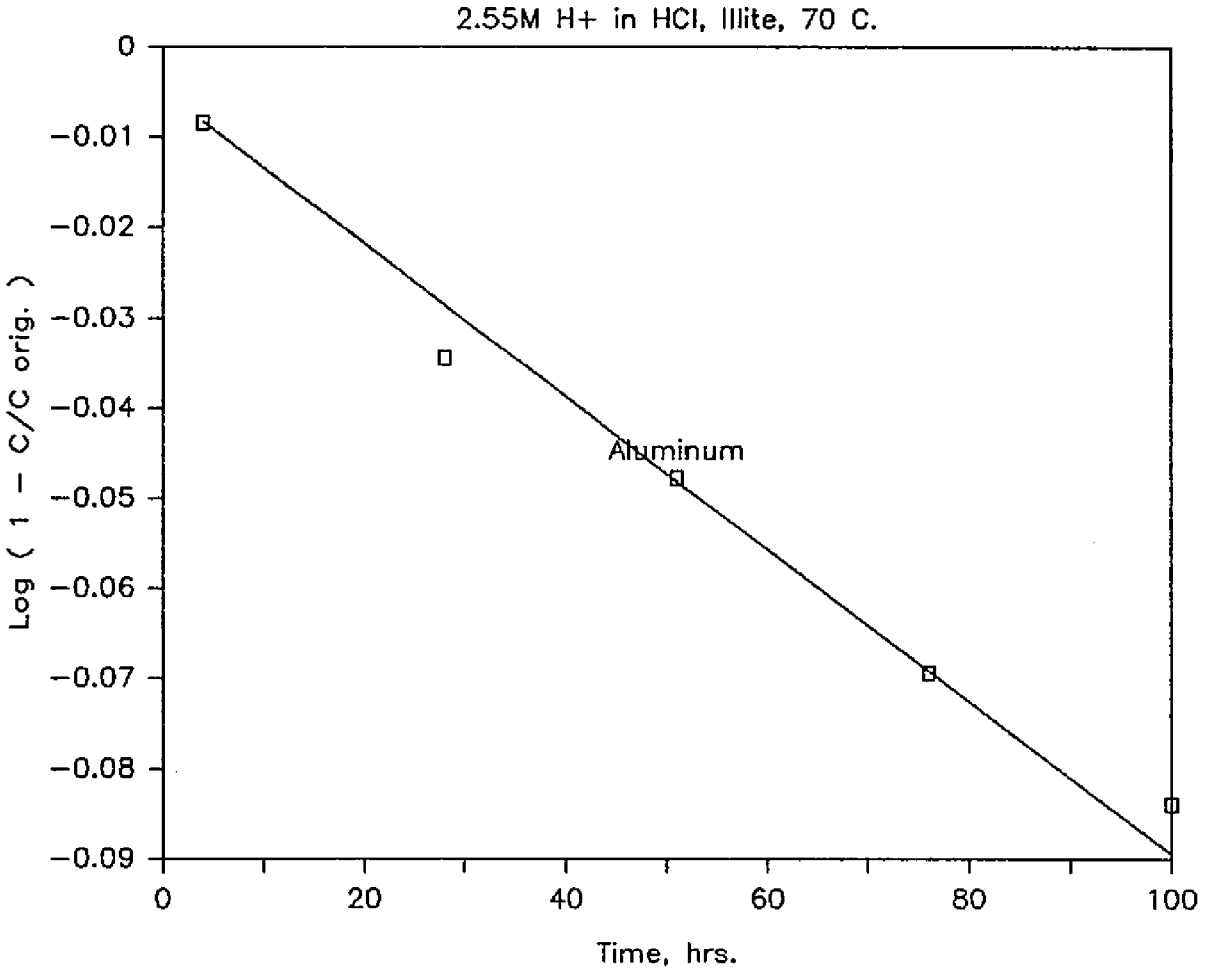
2.55M H+ in HCl, Illite, 70 C.
0
−0.01
−0.02
−0.03
−0.04
−0.05
−0.06
−0.07
−0.08
−0.09
Log (1 − C/C orig.)
Aluminum
0
20
40
60
80
100
Time, hrs.

Figure B44

2.55M H+ in HCl, Illite, 70 C.

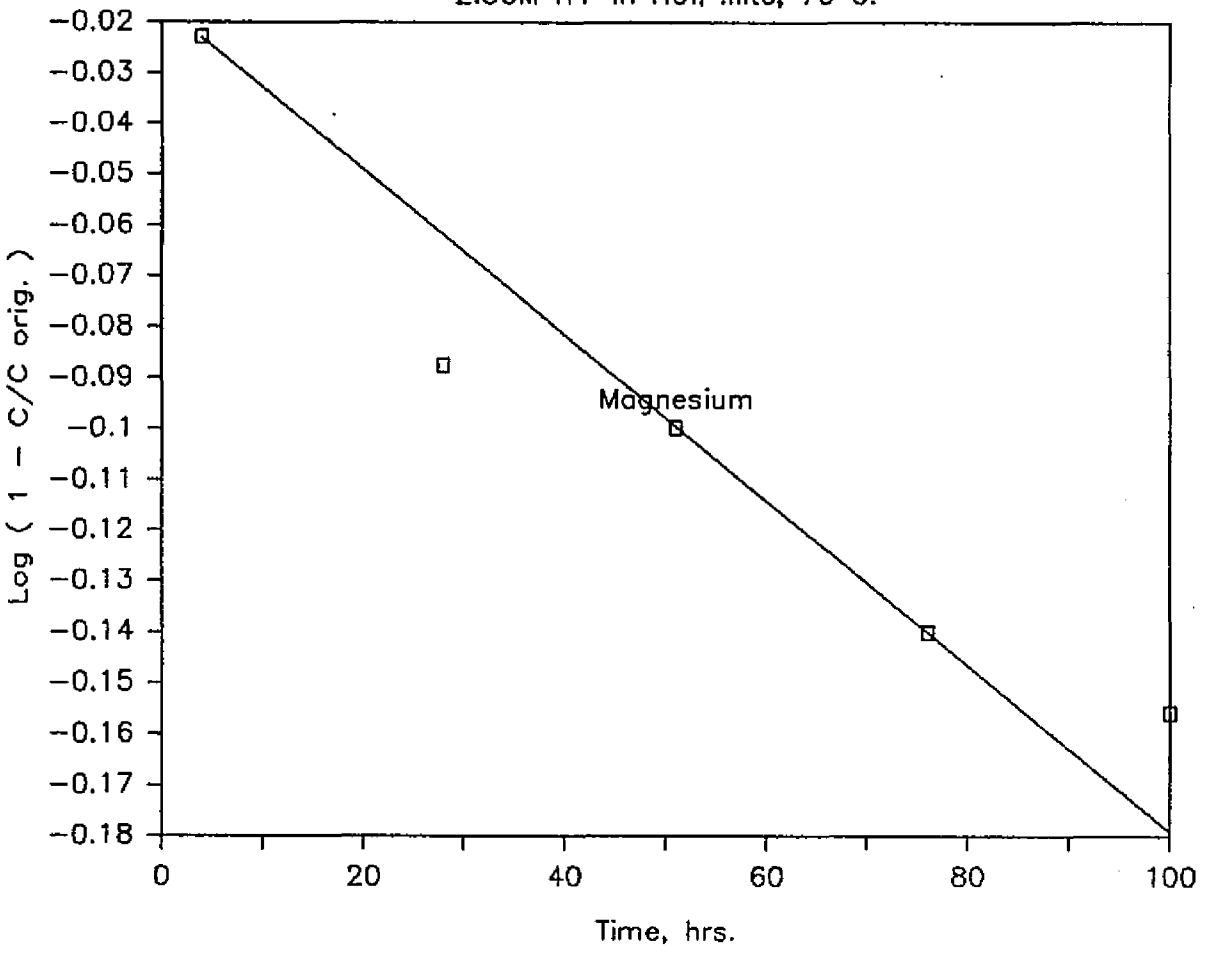

Figure B45

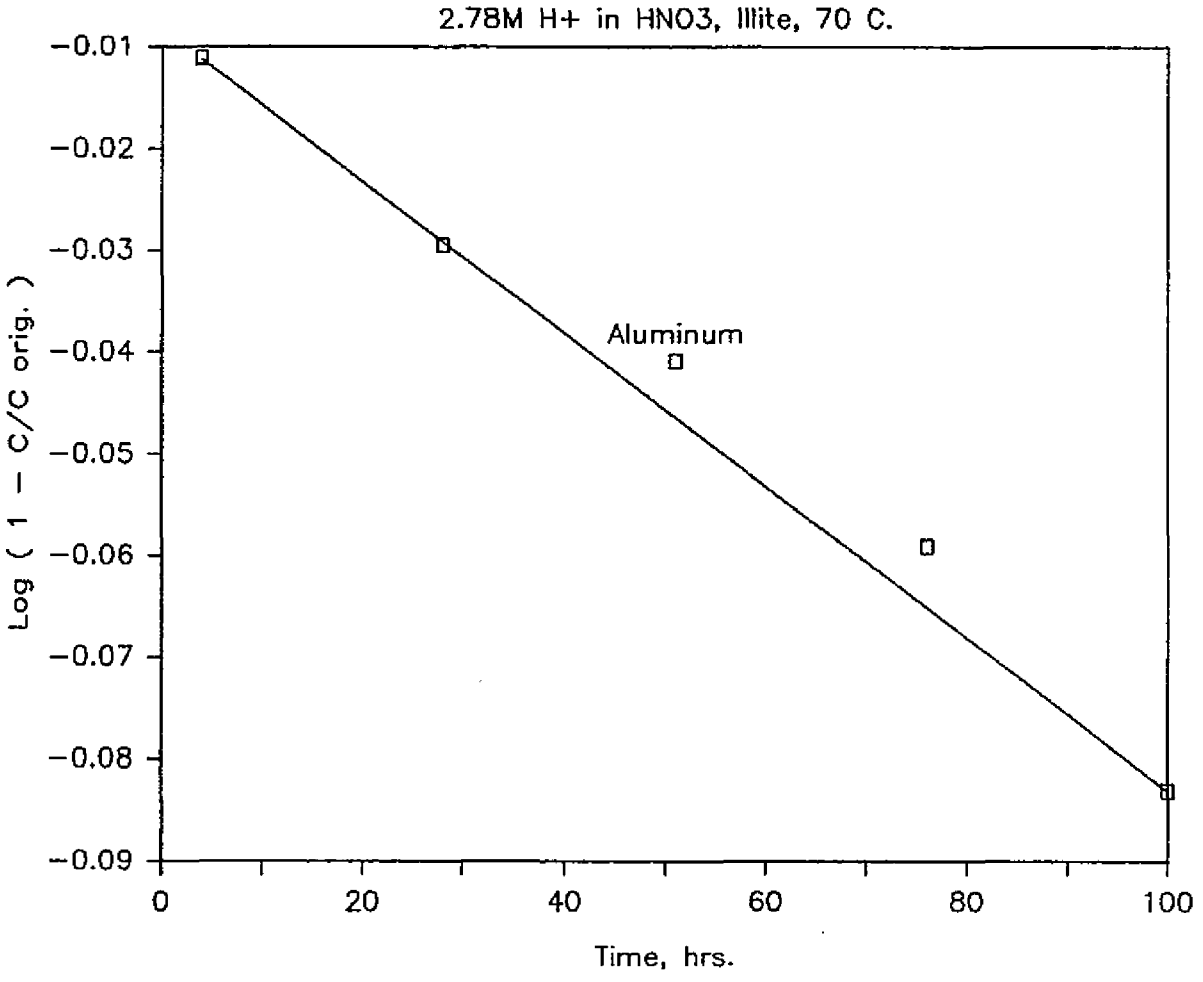
2.78M H+ in HNO3, Illite, 70 C.
Log (1 − C/C orig.)
−0.01
−0.02
−0.03
−0.04
−0.05
−0.06
−0.07
−0.08
−0.09
Aluminum
0
20
40
60
80
100
Time, hrs.

Figure B46

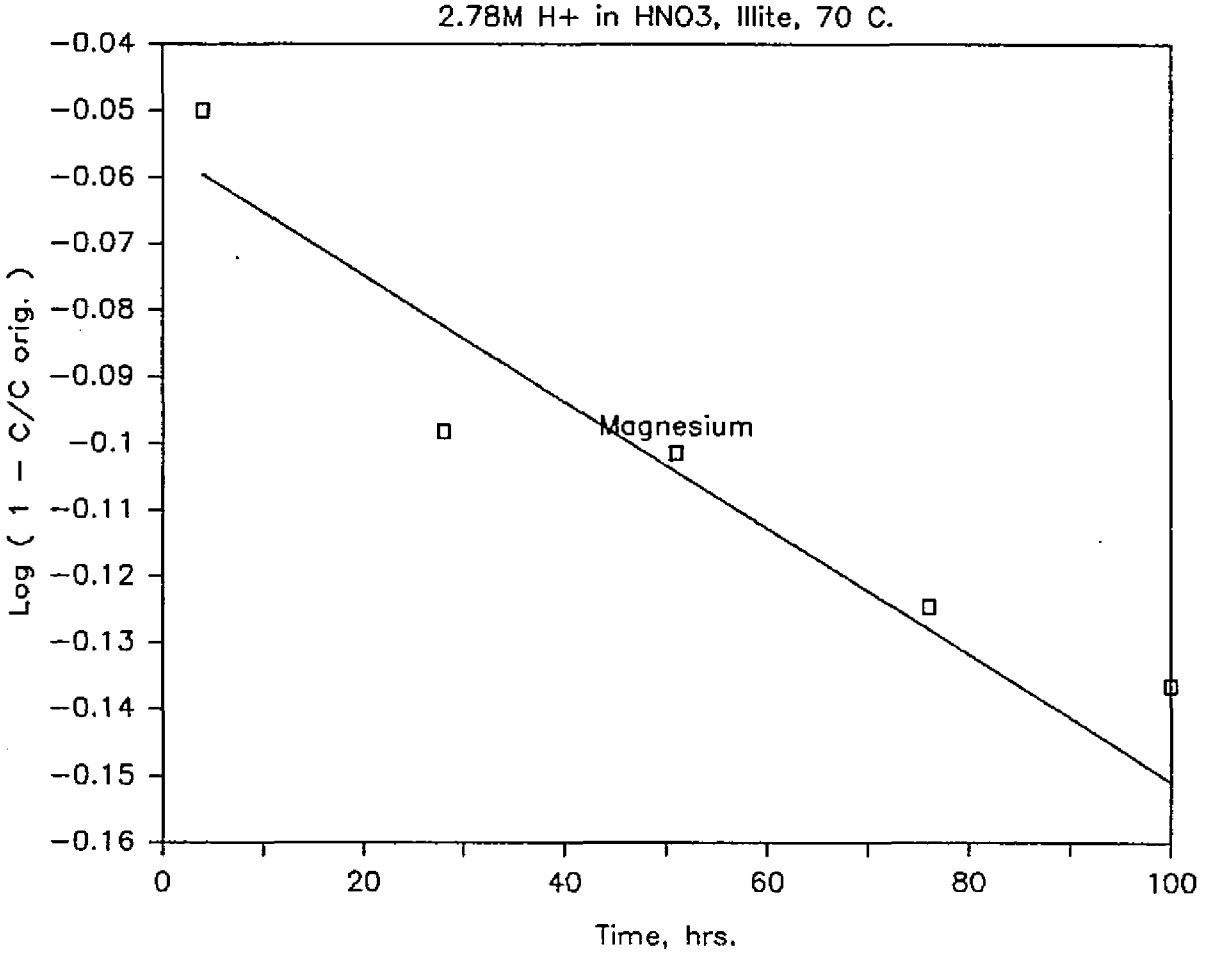
2.78M H+ in HNO3, Illite, 70 C.
Log (1 − C/C orig.)
−0.04
−0.05
−0.06
−0.07
−0.08
−0.09
−0.1
−0.11
−0.12
−0.13
−0.14
−0.15
−0.16
Magnesium
0
20
40
60
80
100
Time, hrs.

Figure B47

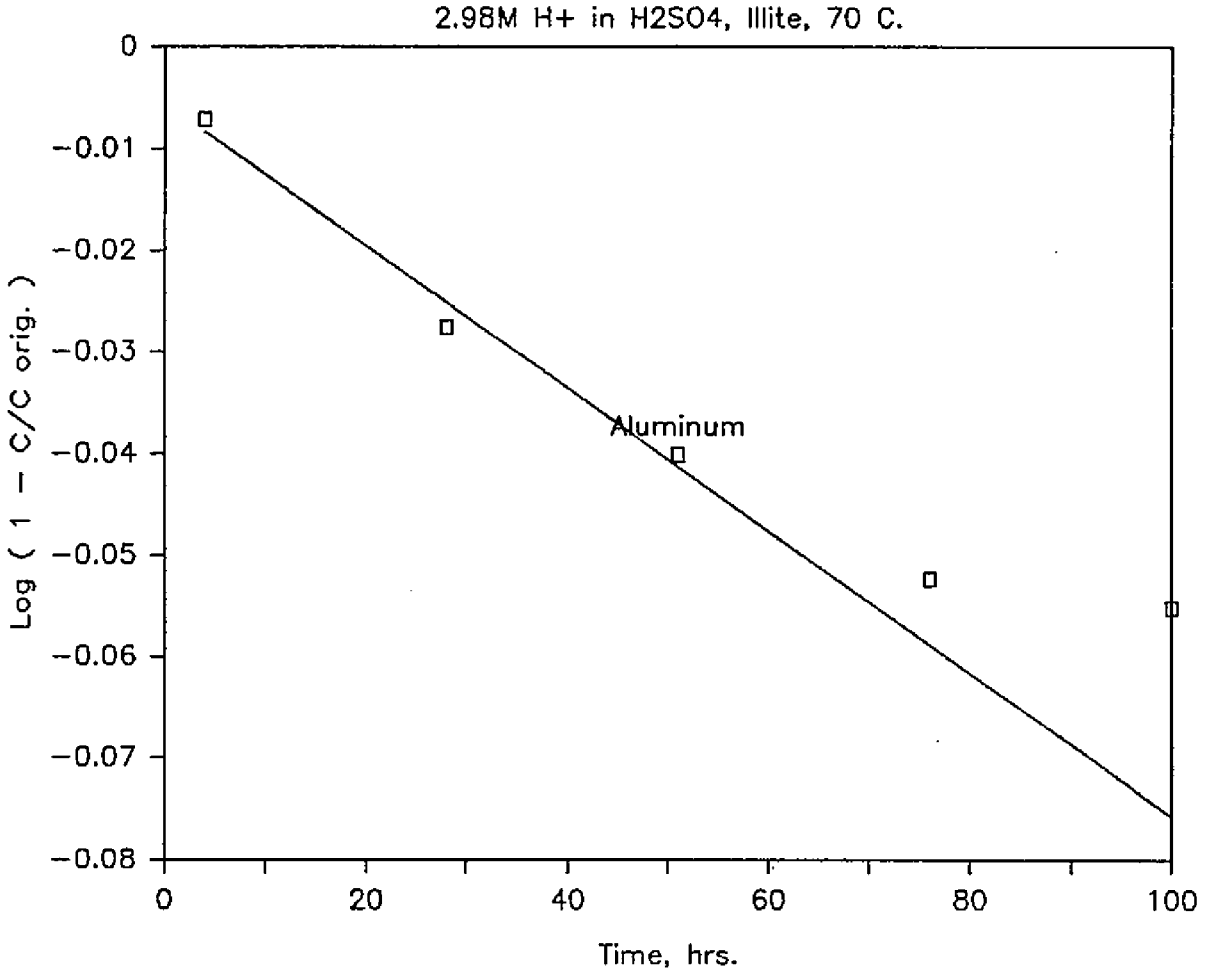
2.98M H+ in H2SO4, Illite, 70 C.
0
-0.01
-0.02
-0.03
-0.04
-0.05
-0.06
-0.07
-0.08
Log (1 - C/C orig.)
Aluminum
0
20
40
60
80
100
Time, hrs.

Figure B48

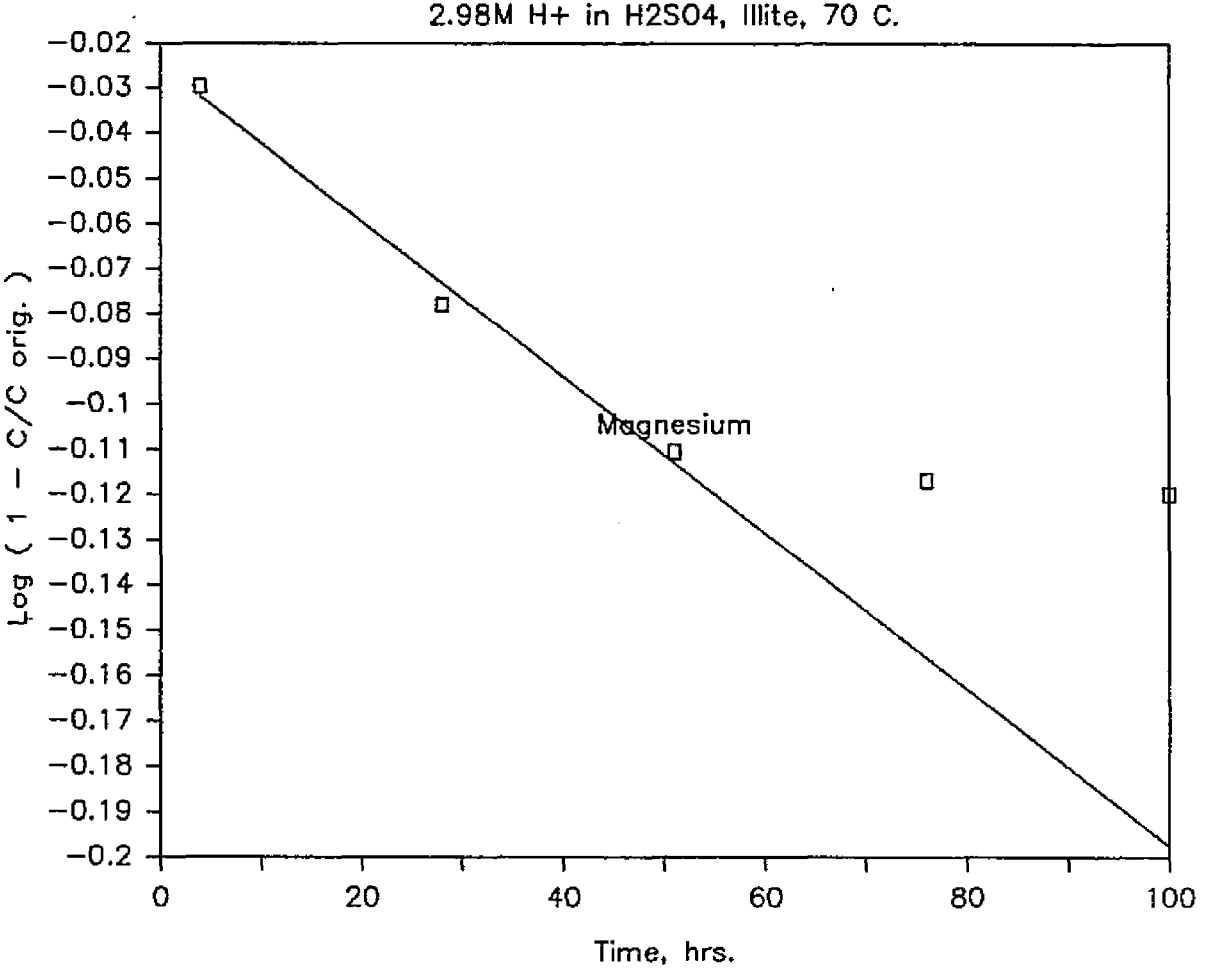
2.98M H+ in H2SO4, Illite, 70 C.
Log (1 − C/C orig.)
−0.02
−0.03
−0.04
−0.05
−0.06
−0.07
−0.08
−0.09
−0.1
−0.11
−0.12
−0.13
−0.14
−0.15
−0.16
−0.17
−0.18
−0.19
−0.2
Magnesium
0
20
40
60
80
100
Time, hrs.

Figure B49

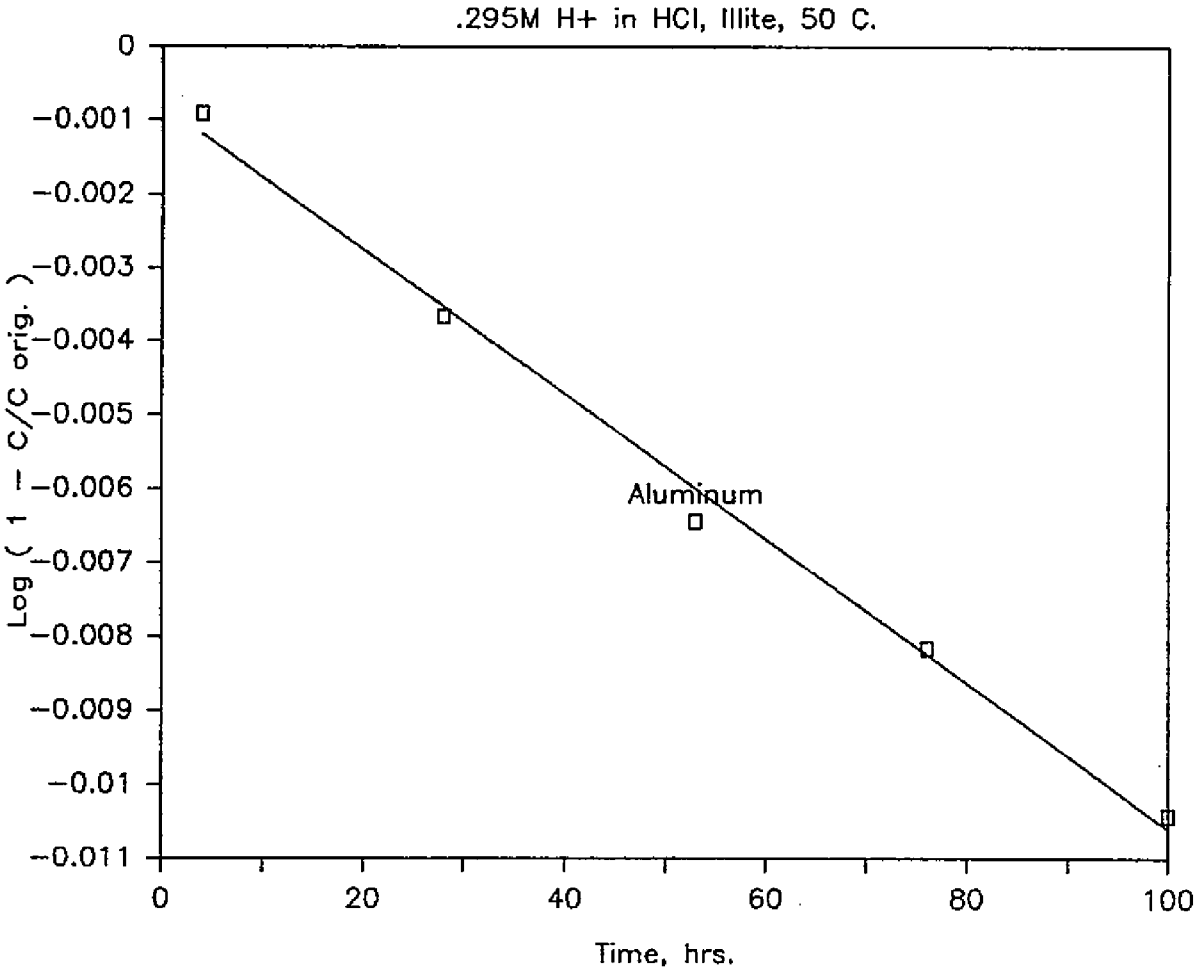
.295M H+ in HCl, Illite, 50 C.
0
−0.001
−0.002
−0.003
−0.004
−0.005
−0.006
−0.007
−0.008
−0.009
−0.01
−0.011
Log (1 − C/C orig.)
Aluminum
0
20
40
60
80
100
Time, hrs.

Figure B50

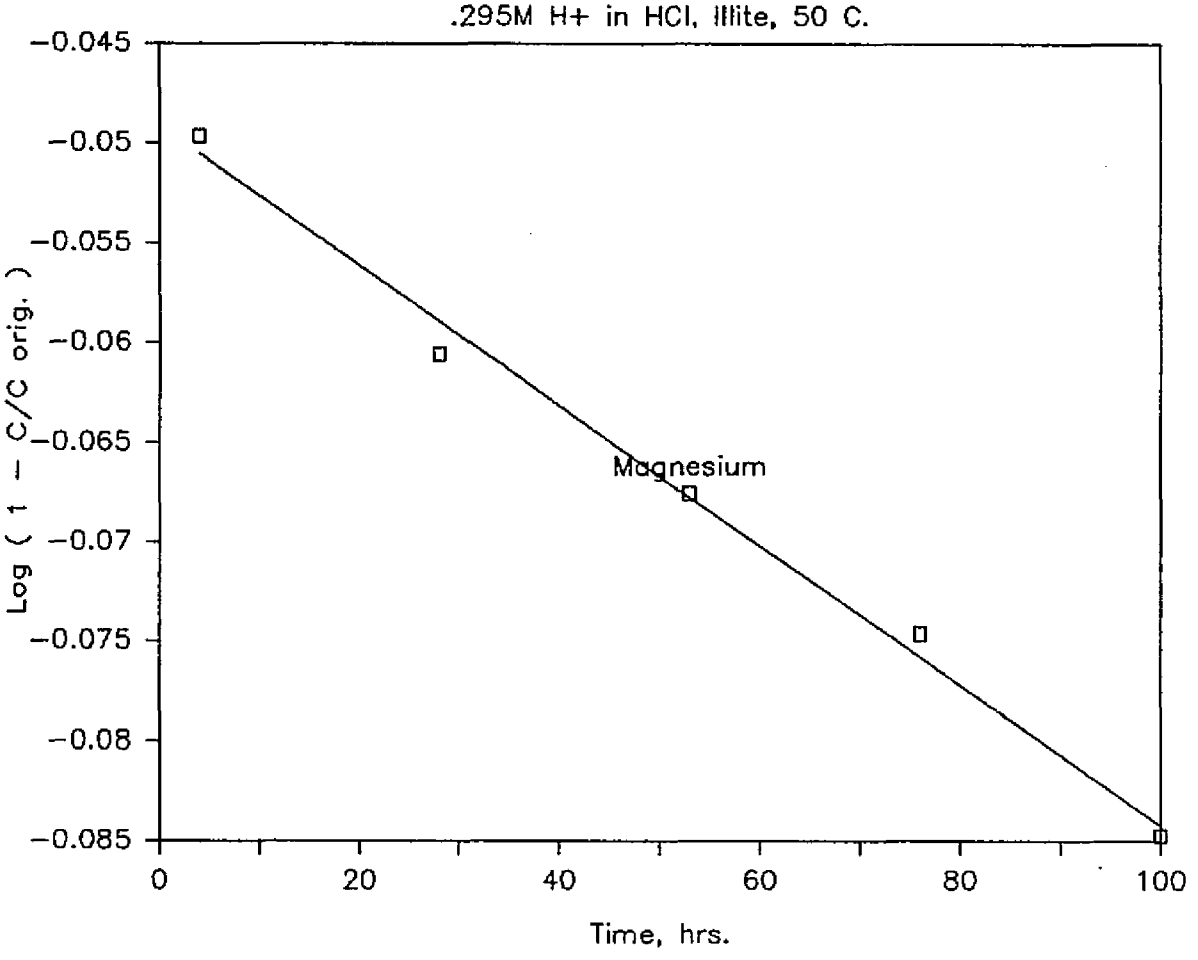
.295M H+ in HCl, Illite, 50 C.
Log (1 - C/C orig.)
-0.045
-0.05
-0.055
-0.06
-0.065
-0.07
-0.075
-0.08
-0.085
Magnesium
0
20
40
60
80
100
Time, hrs.

Figure B51

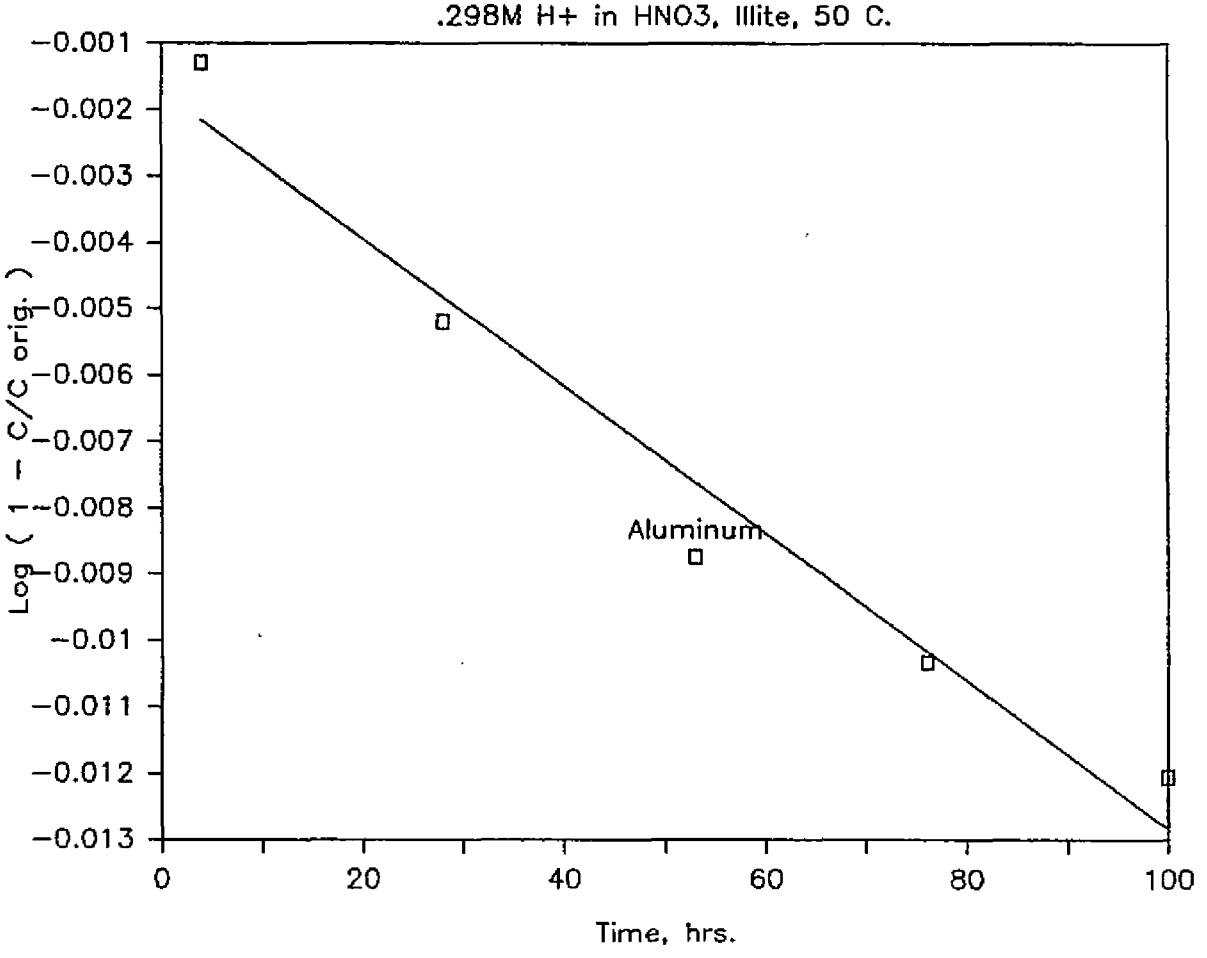
.298M H+ in HNO3, Illite, 50 C.
Log (1 - C/C orig.)
-0.001
-0.002
-0.003
-0.004
-0.005
-0.006
-0.007
-0.008
-0.009
-0.01
-0.011
-0.012
-0.013
Aluminum
0
20
40
60
80
100
Time, hrs.

Figure B52

.298M H+ in HNO3, Illite, 50 C.

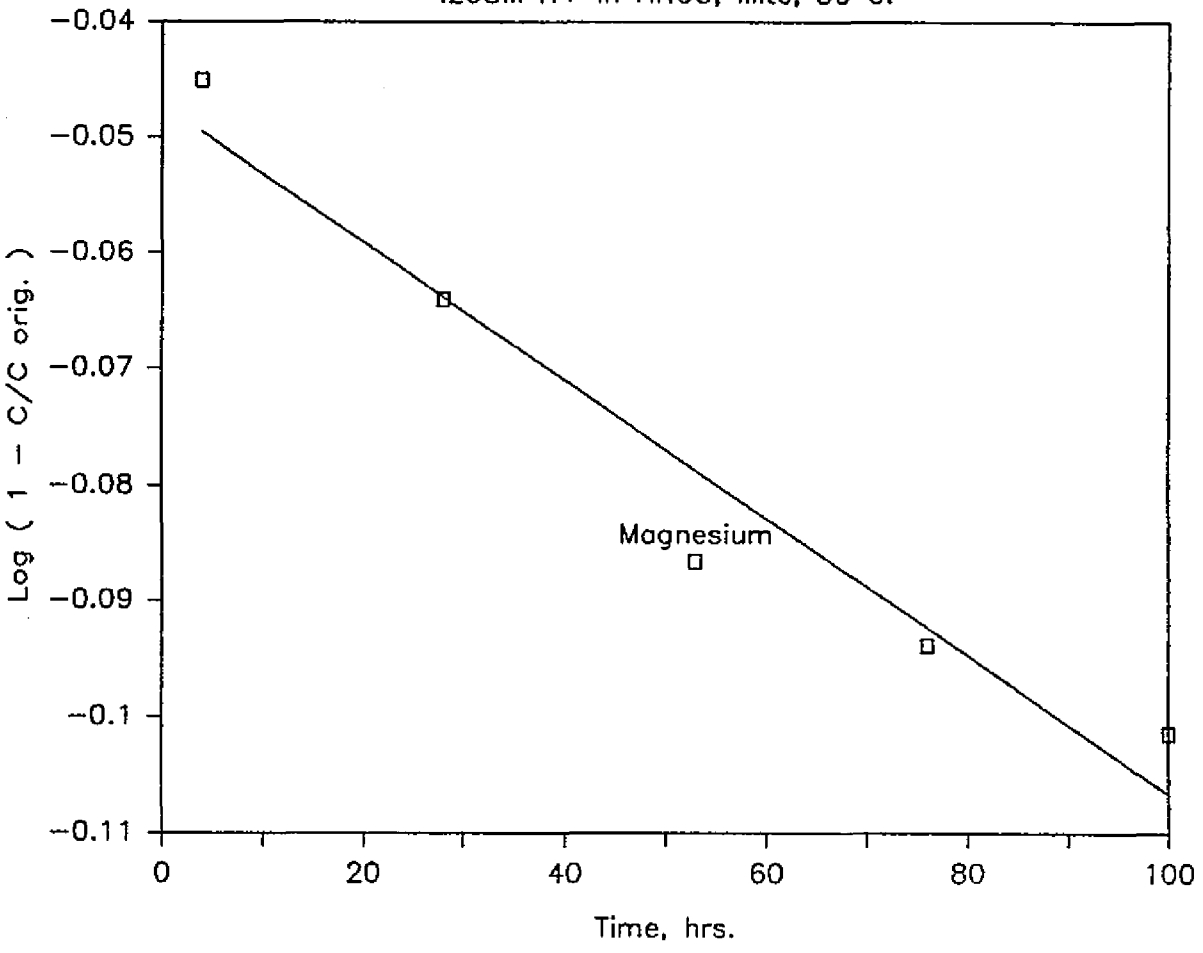

Figure B53

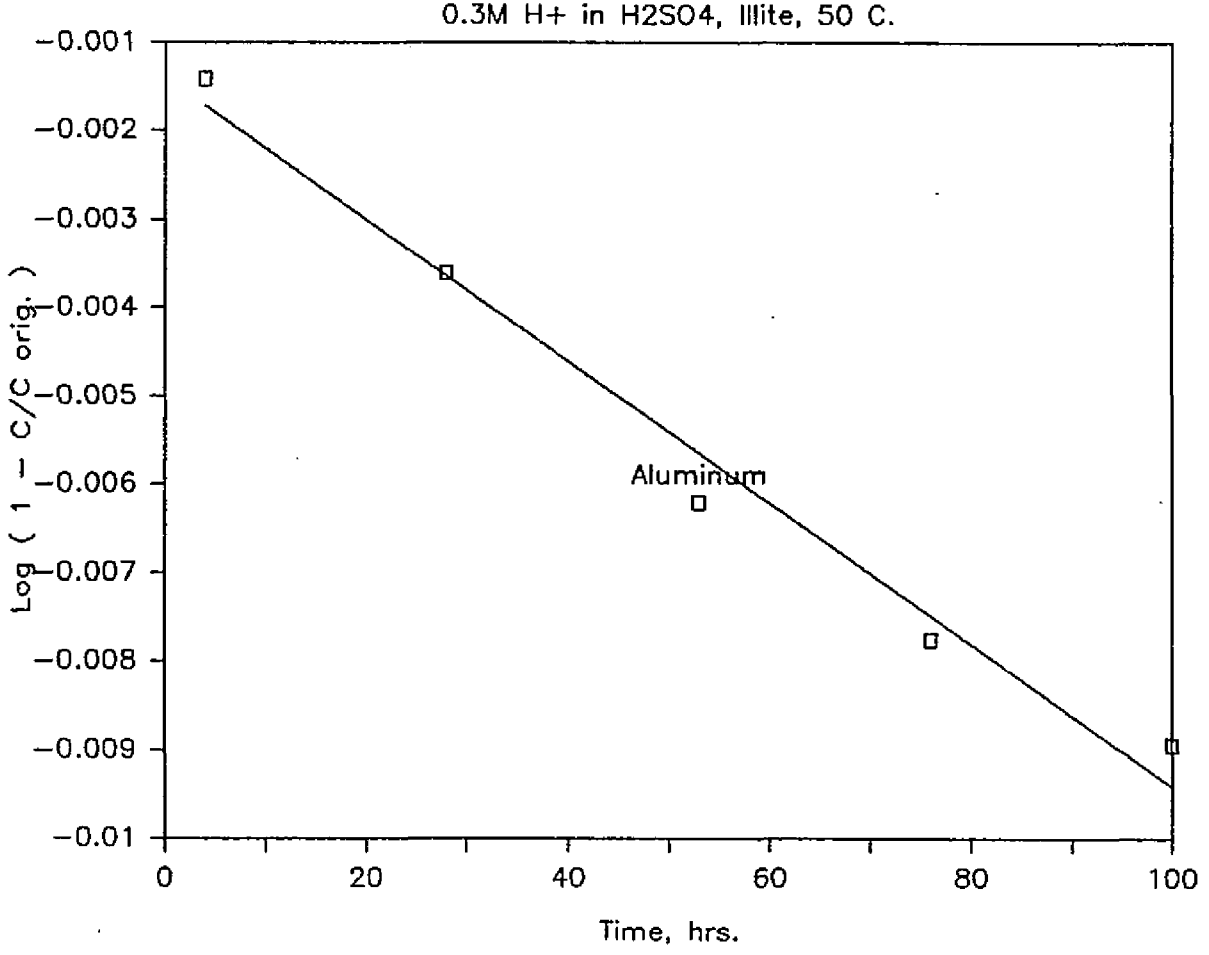
0.3M H+ in H2SO4, Illite, 50 C.
−0.001
−0.002
−0.003
−0.004
−0.005
−0.006
−0.007
−0.008
−0.009
−0.01
Log (1 − C/C orig.)
Aluminum
0
20
40
60
80
100
Time, hrs.

Figure B54

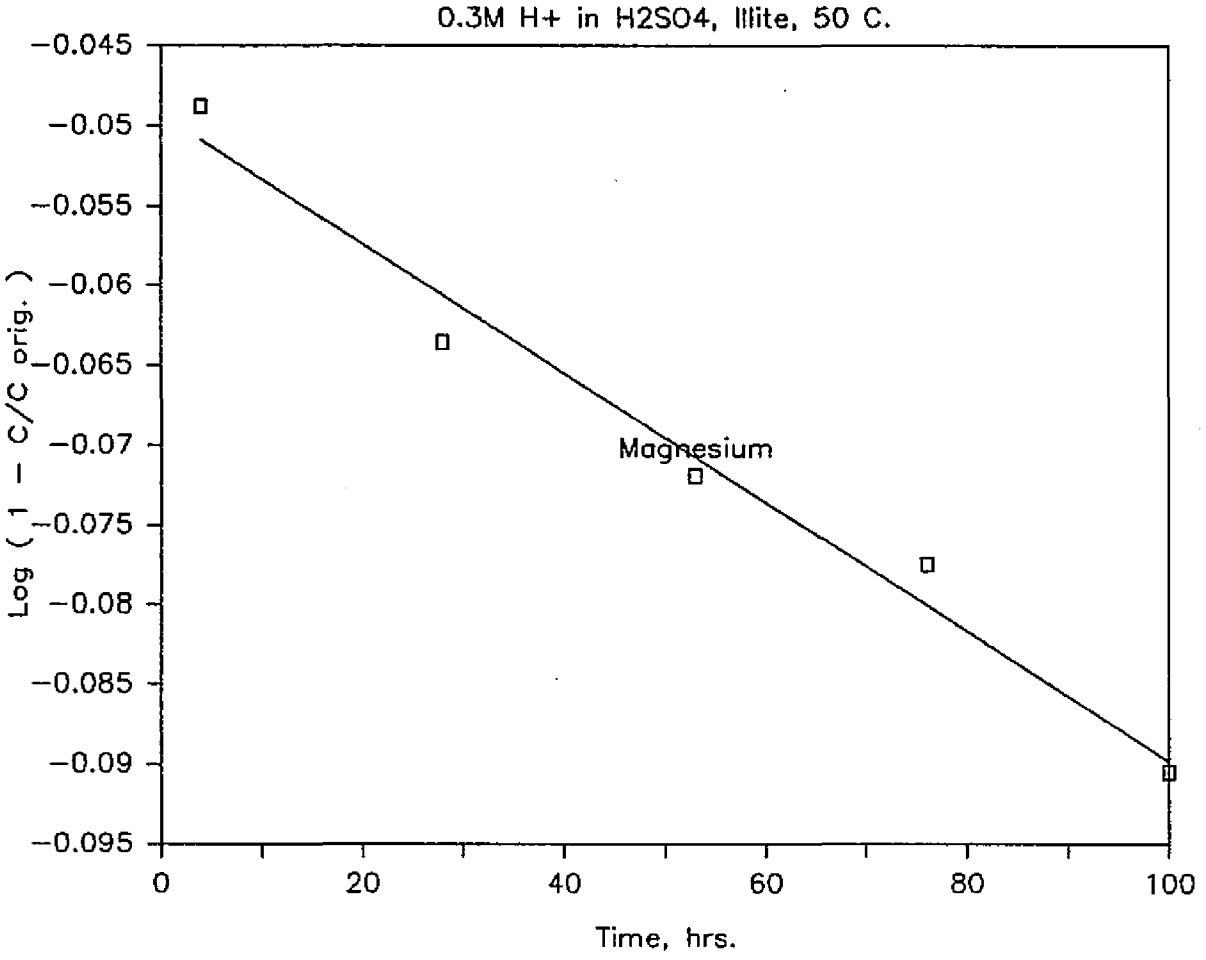
0.3M H+ in H2SO4, Illite, 50 C.
Log (1 - C/C orig.)
-0.045
-0.05
-0.055
-0.06
-0.065
-0.07
-0.075
-0.08
-0.085
-0.09
-0.095
Magnesium
0
20
40
60
80
100
Time, hrs.

Figure B55

.295M H+ in HCl, Illite, 70 C.

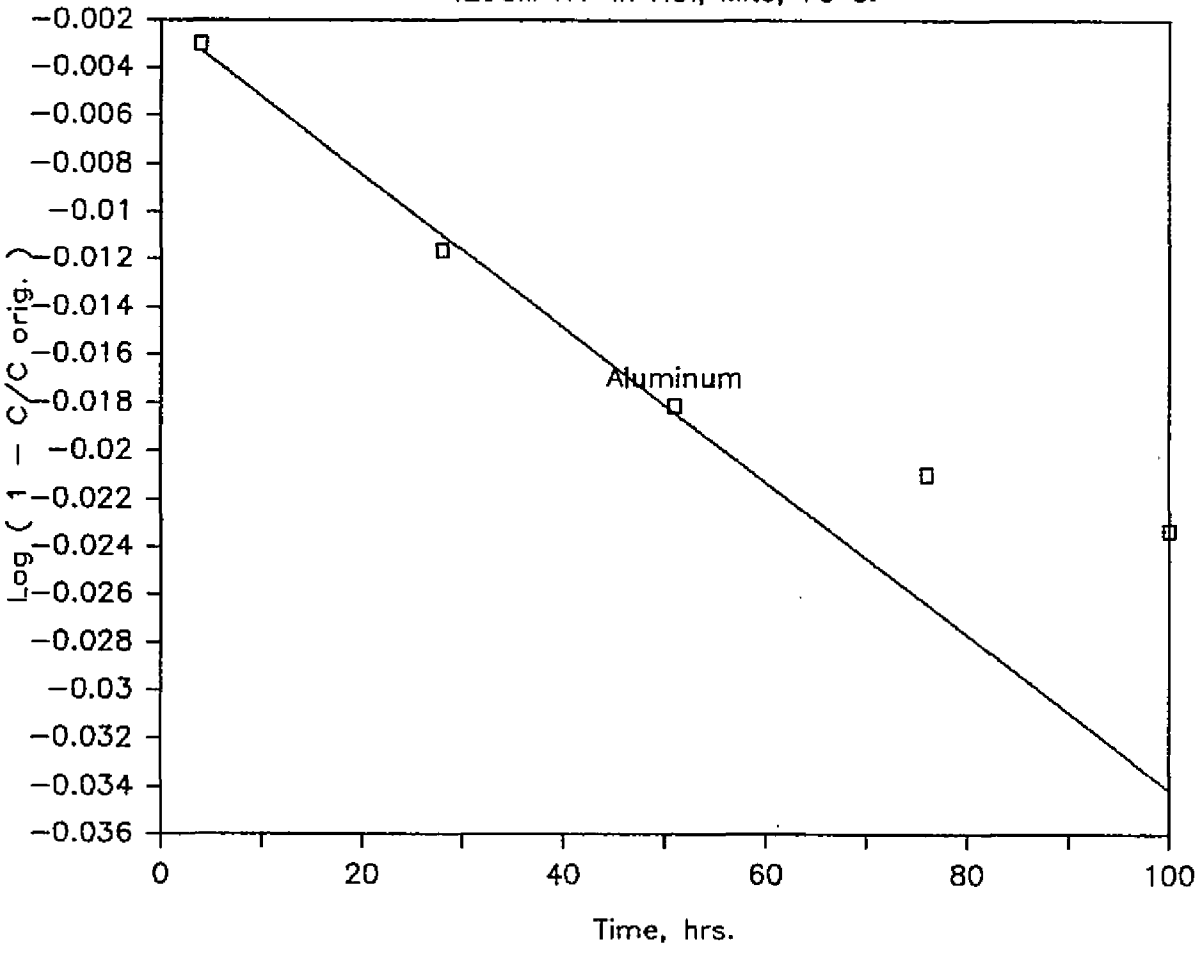

Figure B56

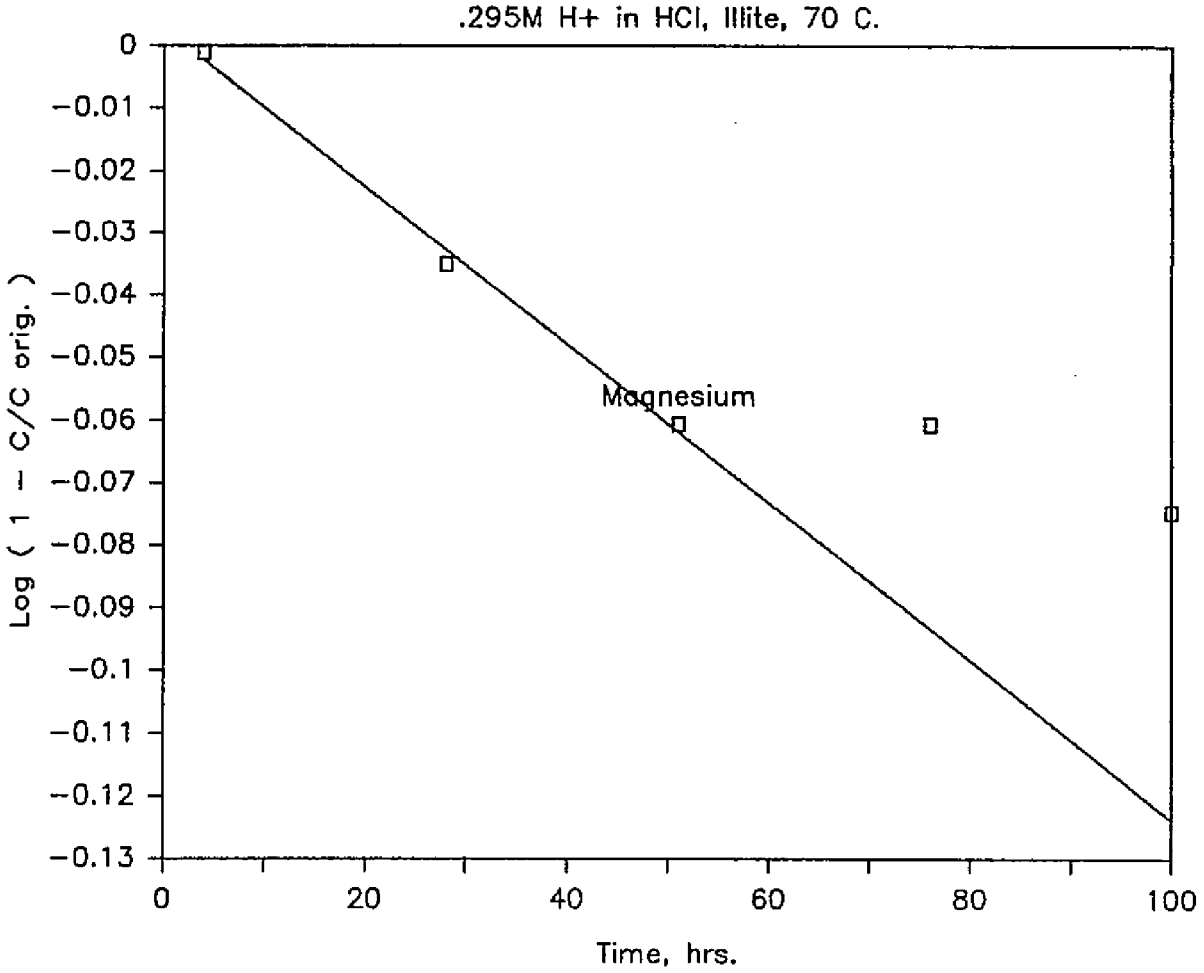
.295M H+ in HCl, Illite, 70 C.
Log (1 - C/C orig.)
0
-0.01
-0.02
-0.03
-0.04
-0.05
-0.06
-0.07
-0.08
-0.09
-0.1
-0.11
-0.12
-0.13
Magnesium
0
20
40
60
80
100
Time, hrs.

Figure B57

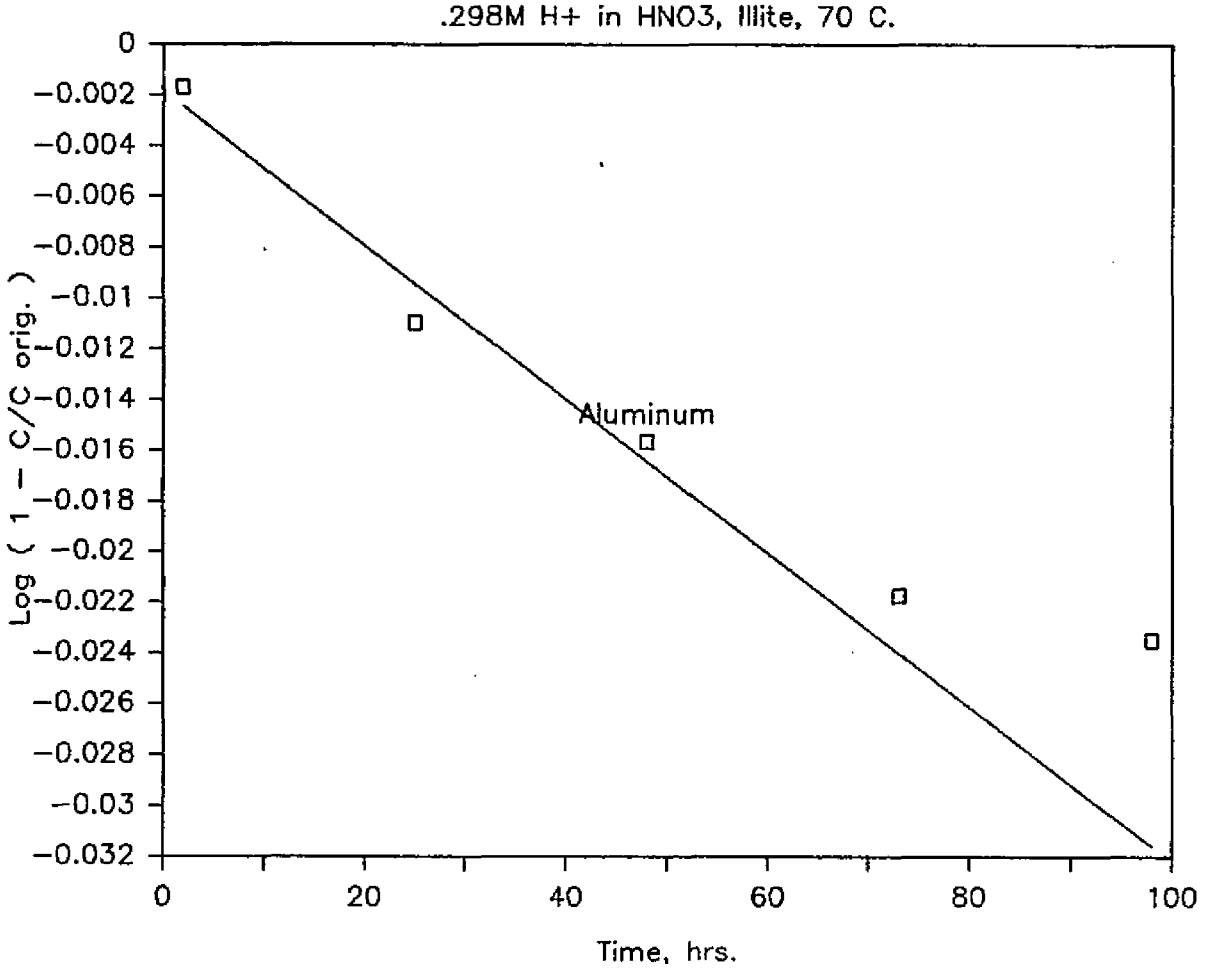
.298M H+ in HNO3, Illite, 70 C.
Log (1 - C/C orig.)
0
-0.002
-0.004
-0.006
-0.008
-0.01
-0.012
-0.014
-0.016
-0.018
-0.02
-0.022
-0.024
-0.026
-0.028
-0.03
-0.032
Aluminum
0
20
40
60
80
100
Time, hrs.

Figure B58

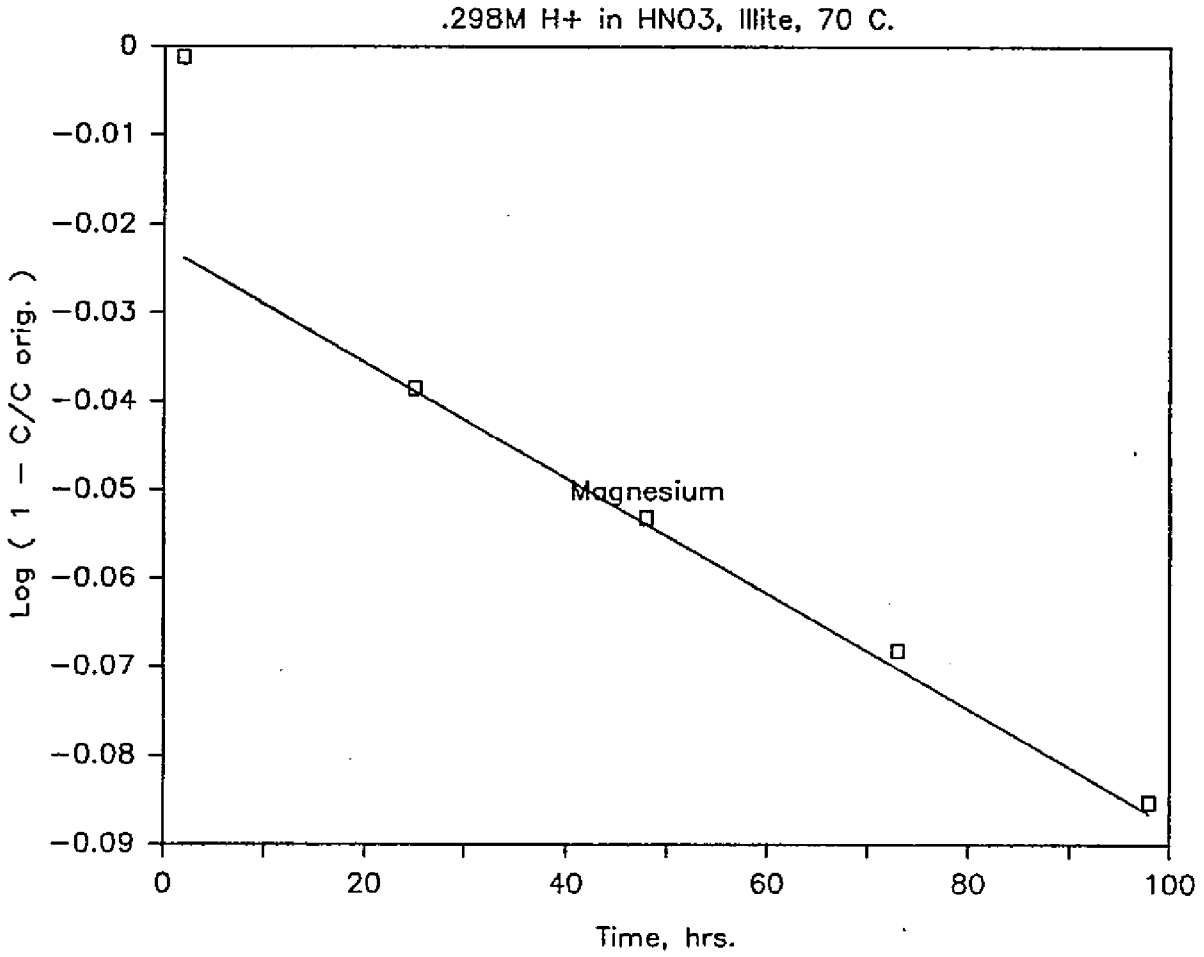
.298M H+ in HNO3, Illite, 70 C.
Log (1 − C/C orig.)
0
−0.01
−0.02
−0.03
−0.04
−0.05
−0.06
−0.07
−0.08
−0.09
Magnesium
0
20
40
60
80
100
Time, hrs.

Figure B59

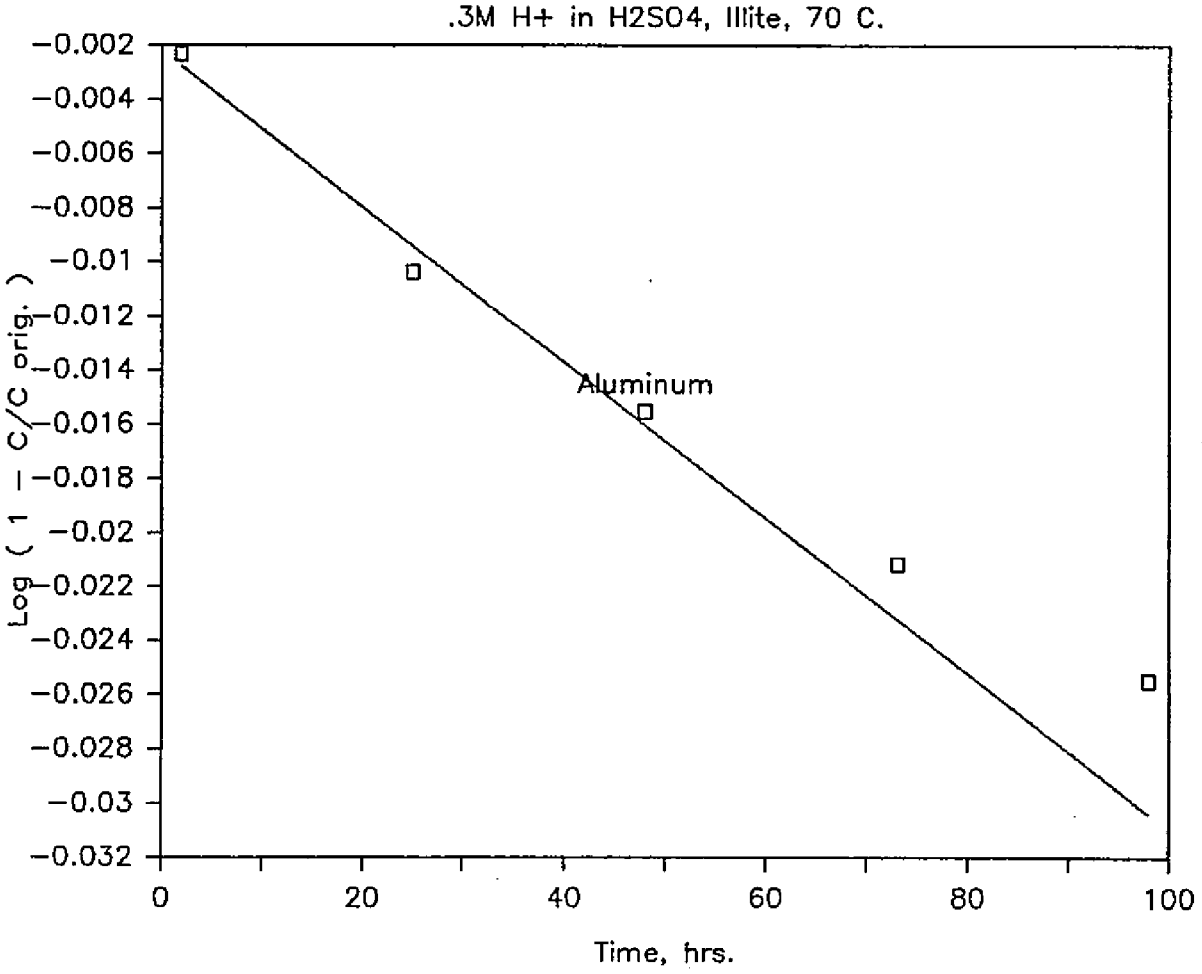
.3M H+ in H2SO4, Illite, 70 C.
Log (1 - C/C orig.)
−0.002
−0.004
−0.006
−0.008
−0.01
−0.012
−0.014
−0.016
−0.018
−0.02
−0.022
−0.024
−0.026
−0.028
−0.03
−0.032
Aluminum
0
20
40
60
80
100
Time, hrs.

Figure B60

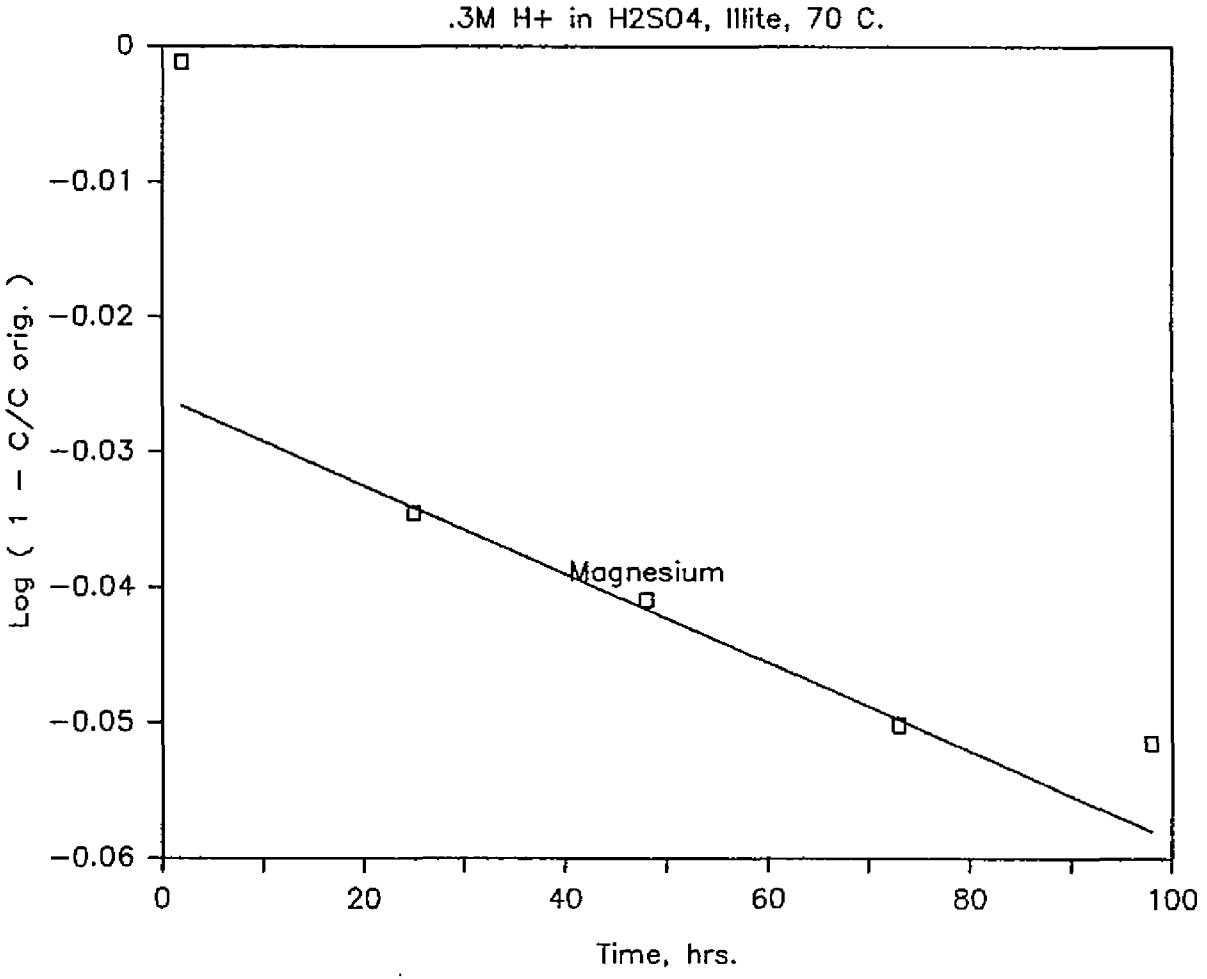
.3M H+ in H2SO4, Illite, 70 C.
0
−0.01
−0.02
−0.03
−0.04
−0.05
−0.06
Log (1 − C/C orig.)
Magnesium
0
20
40
60
80
100
Time, hrs.

APPENDIX C

Energies of activation, E_a, were determined using two measurement temperatures. The values presented should be verified by data from at least one additional temperature. Plots of log (k_T) vs. 1/T are presented in Figures C1 through C18. The slopes of the lines were determined as the first order coefficients of linear least squares curve fit. These values represented E_a/R. Apparent energies of activation were determined by multiplying the values of the slopes by ln(10) and by the gas constant R (1.987 cal/mole-deg. K.)

Figure C1

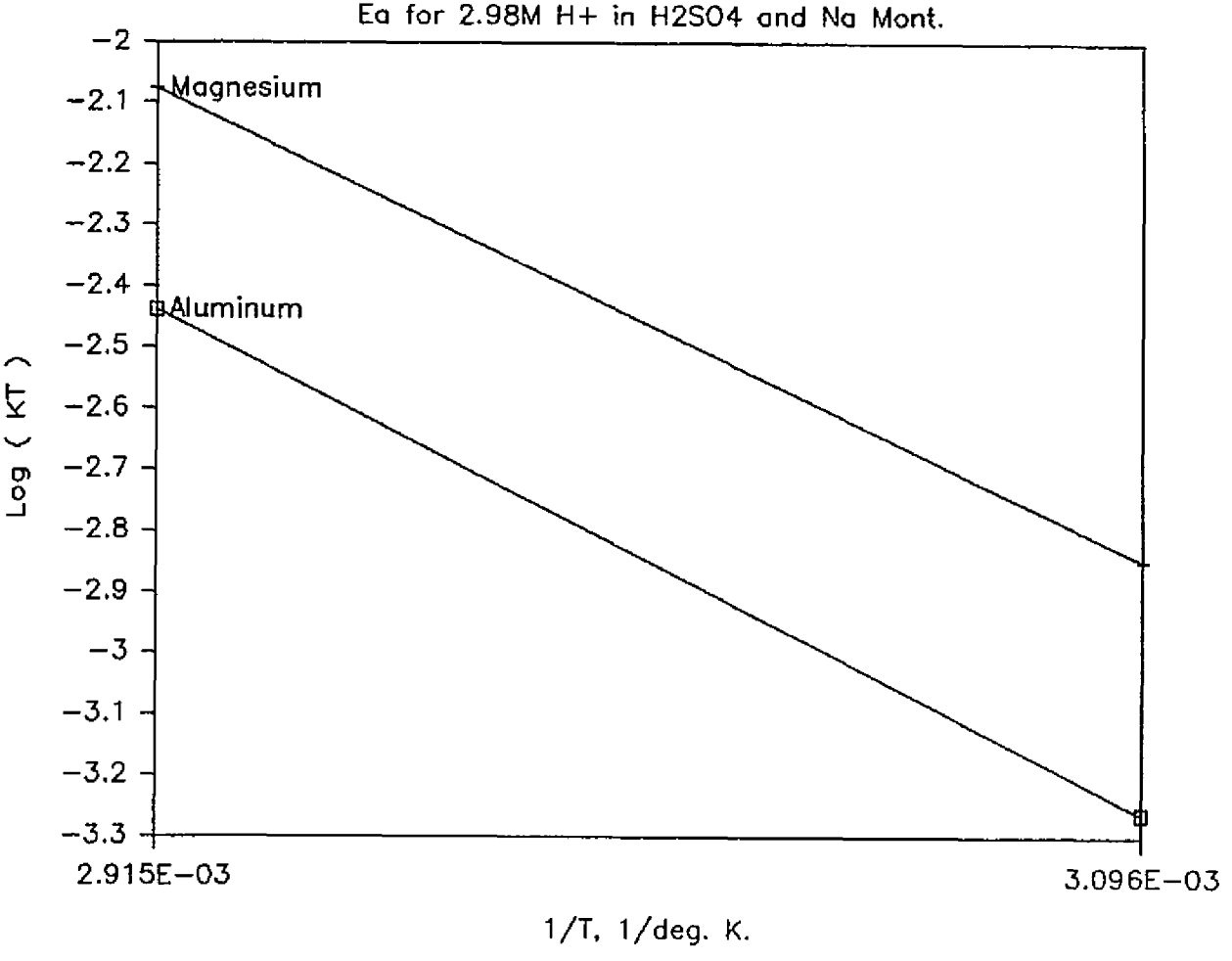
Ea for 2.98M H+ in H2SO4 and Na Mont.
Magnesium
Aluminum
Log (KT)
-2
-2.1
-2.2
-2.3
-2.4
-2.5
-2.6
-2.7
-2.8
-2.9
-3
-3.1
-3.2
-3.3
2.915E-03
3.096E-03
1/T, 1/deg. K.

Figure C2

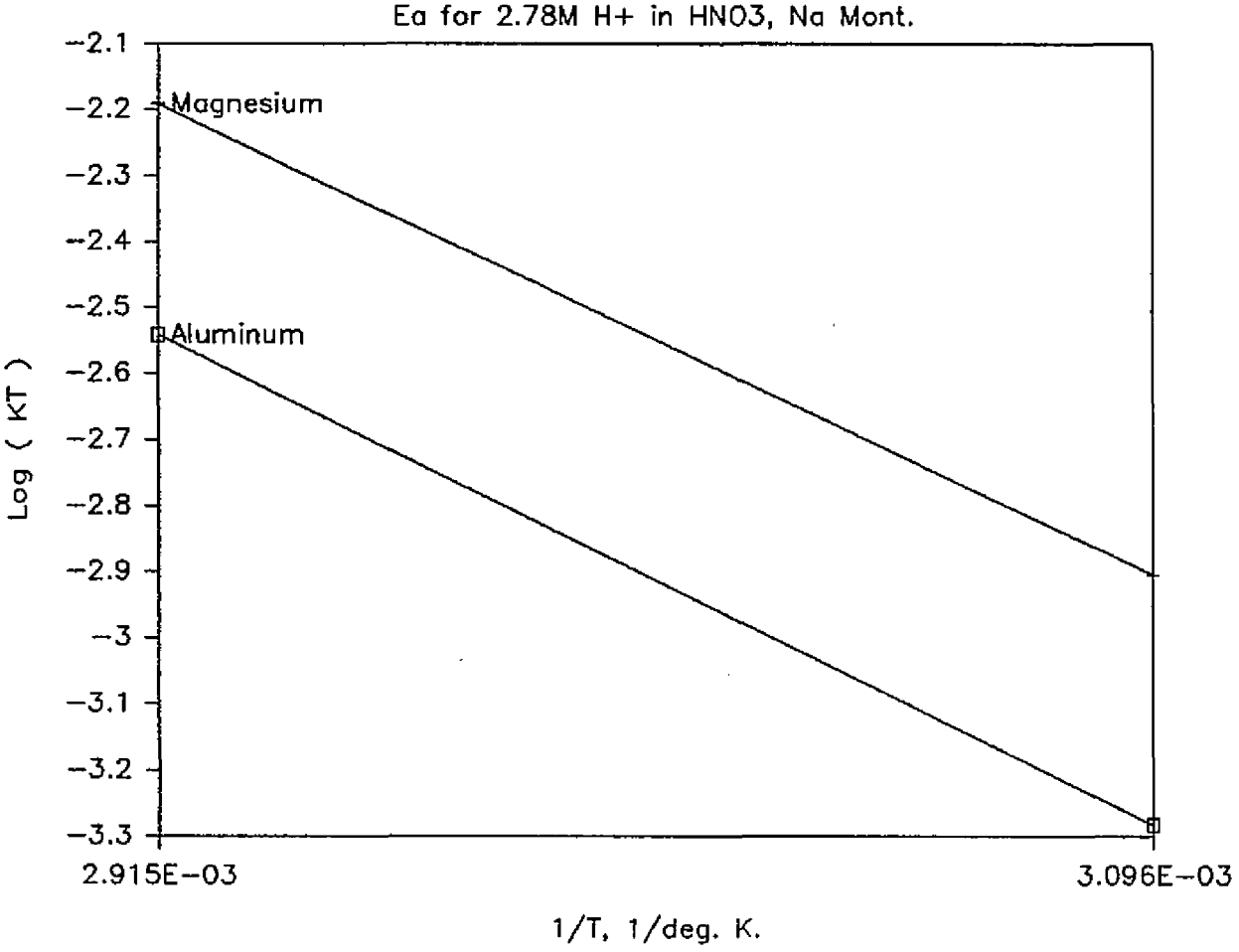
Ea for 2.78M H+ in HNO3, Na Mont.
-2.1
-2.2
-2.3
-2.4
-2.5
-2.6
-2.7
-2.8
-2.9
-3
-3.1
-3.2
-3.3
Log (KT)
Magnesium
Aluminum
2.915E-03
3.096E-03
1/T, 1/deg. K.

Figure C3

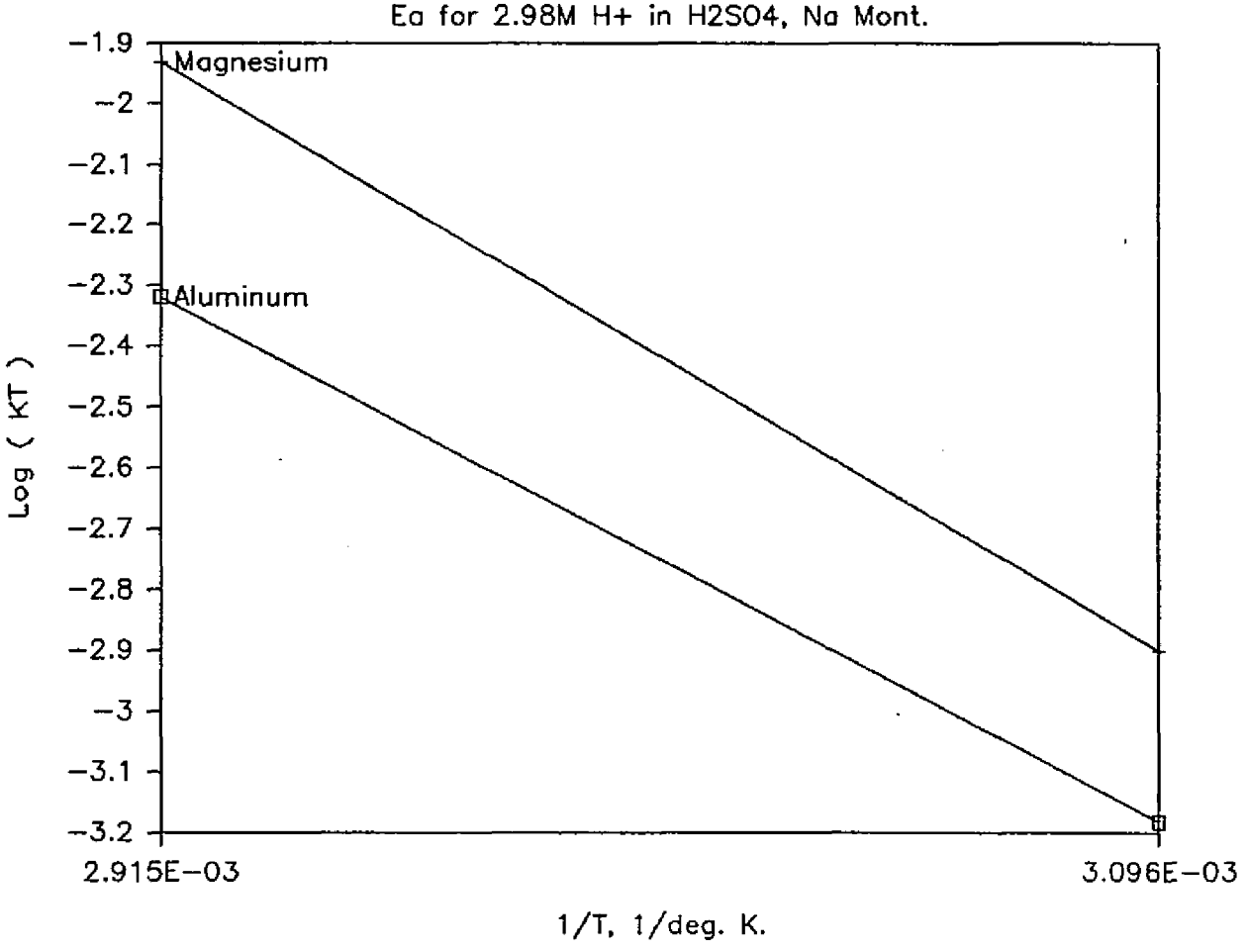
Ea for 2.98M H+ in H2SO4, Na Mont.
Magnesium
Aluminum
-1.9
-2
-2.1
-2.2
-2.3
-2.4
-2.5
-2.6
-2.7
-2.8
-2.9
-3
-3.1
-3.2
Log (KT)
2.915E-03
3.096E-03
1/T, 1/deg. K.

Figure C4

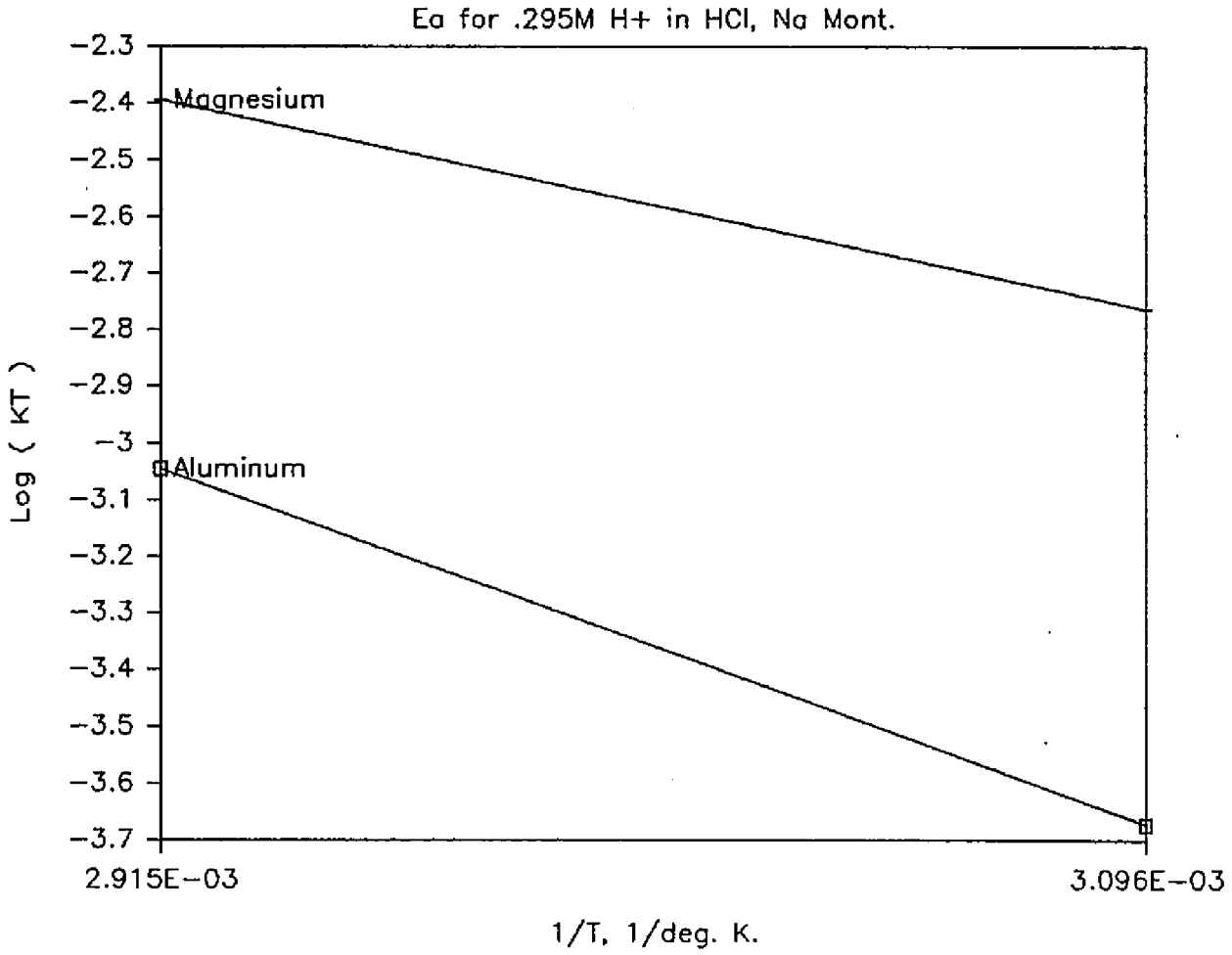
Ea for .295M H+ in HCl, Na Mont.
Magnesium
Aluminum
Log (KT)
-2.3
-2.4
-2.5
-2.6
-2.7
-2.8
-2.9
-3
-3.1
-3.2
-3.3
-3.4
-3.5
-3.6
-3.7
2.915E-03
3.096E-03
1/T, 1/deg. K.

Figure C5

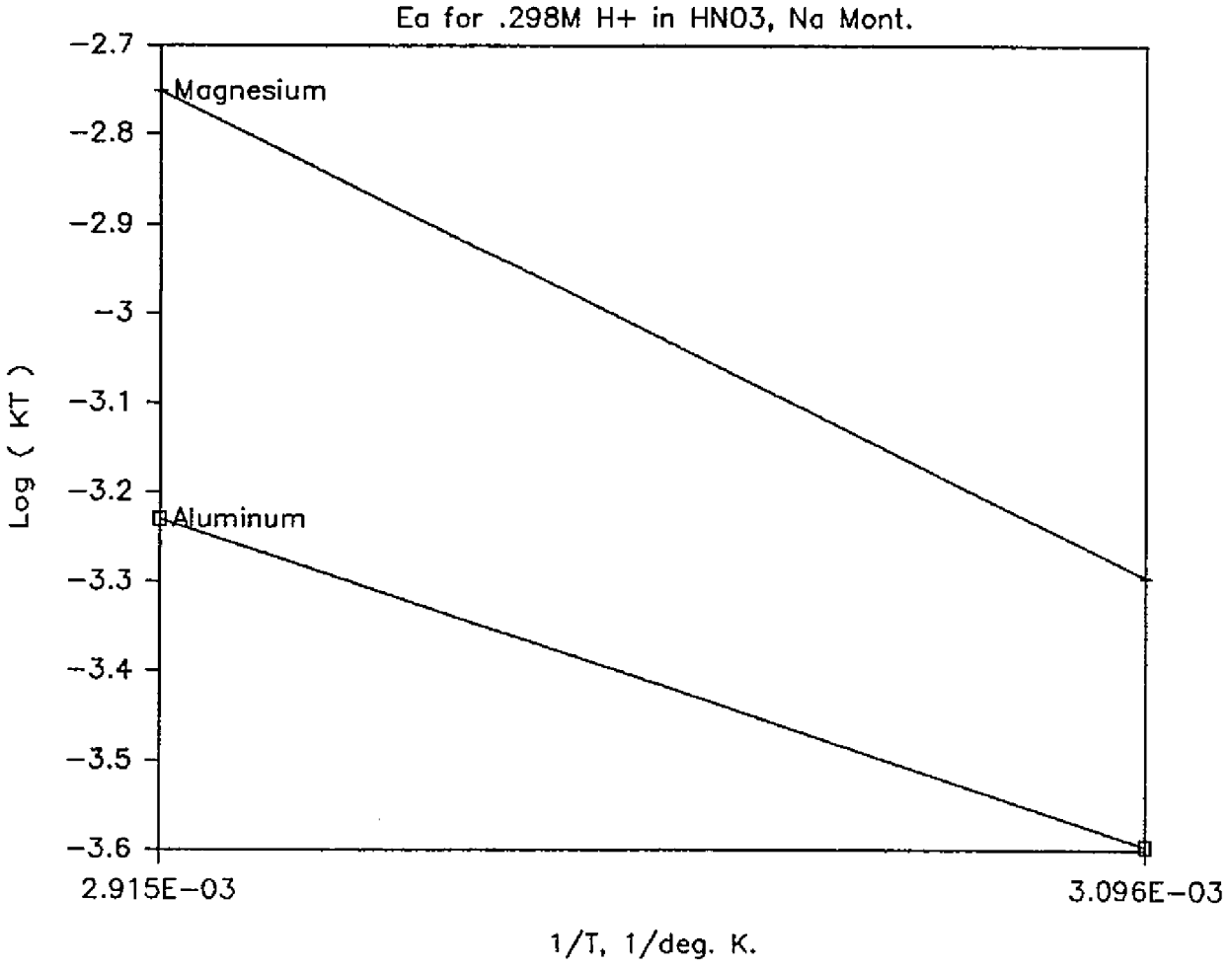
Ea for .298M H+ in HN03, Na Mont.
Magnesium
Aluminum
-2.7
-2.8
-2.9
-3
-3.1
-3.2
-3.3
-3.4
-3.5
-3.6
Log (KT)
2.915E-03
3.096E-03
1/T, 1/deg. K.

Figure C6

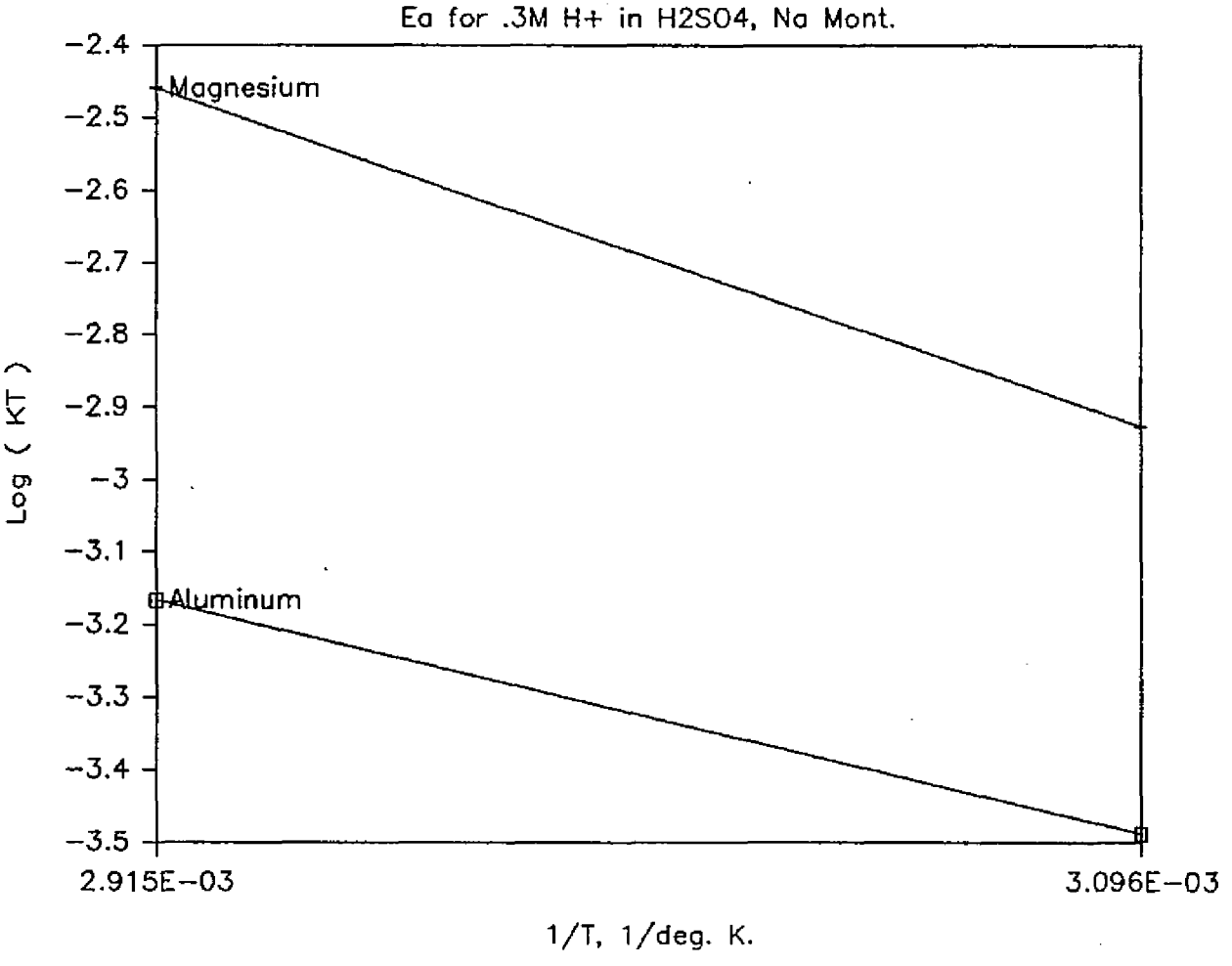
Ea for .3M H+ in H2SO4, Na Mont.
Magnesium
Aluminum
-2.4
-2.5
-2.6
-2.7
-2.8
-2.9
-3
-3.1
-3.2
-3.3
-3.4
-3.5
Log (KT)
2.915E-03
3.096E-03
1/T, 1/deg. K.

Figure C7

Ea for 2.55M H+ in HCl, Kaolinite

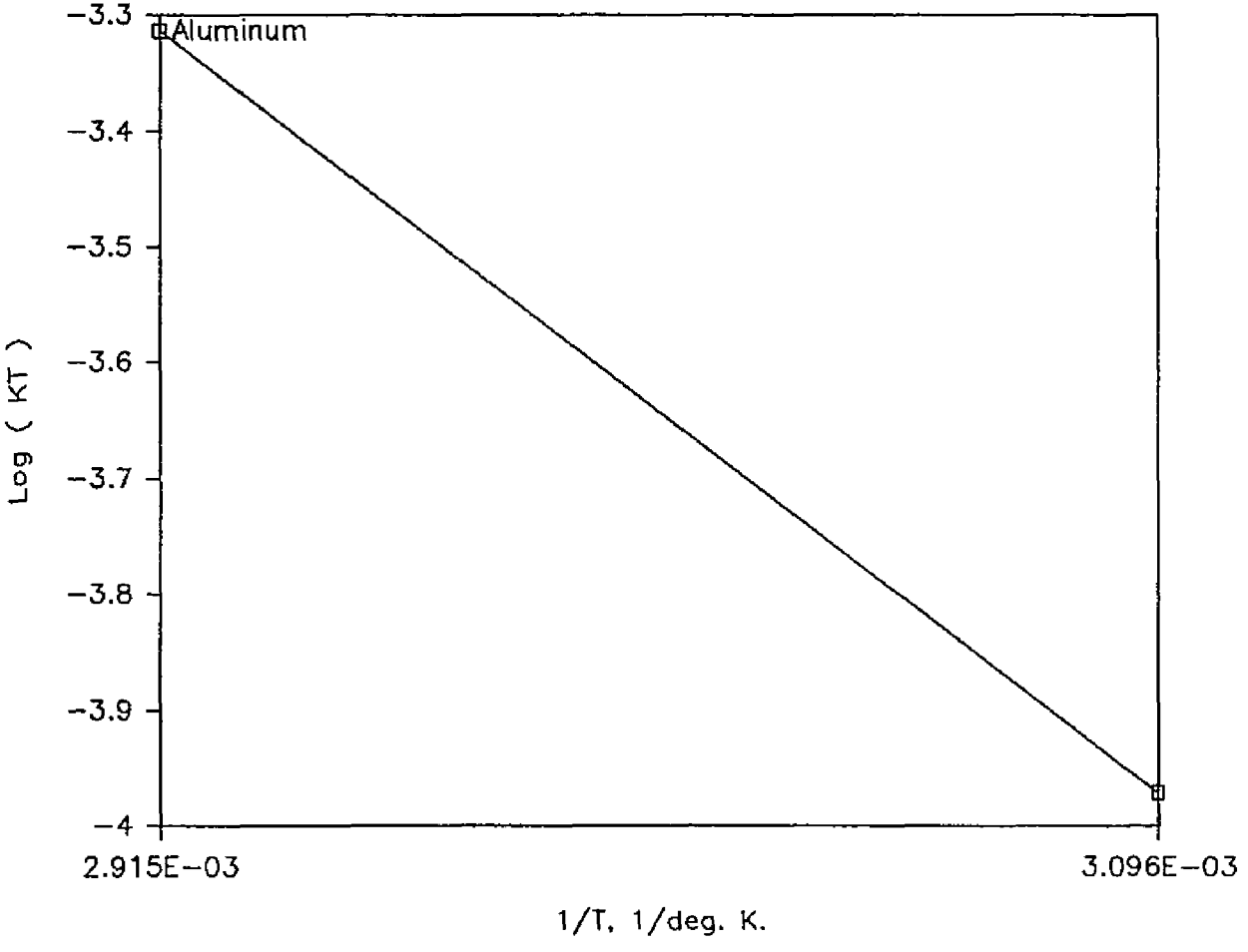

Figure C8

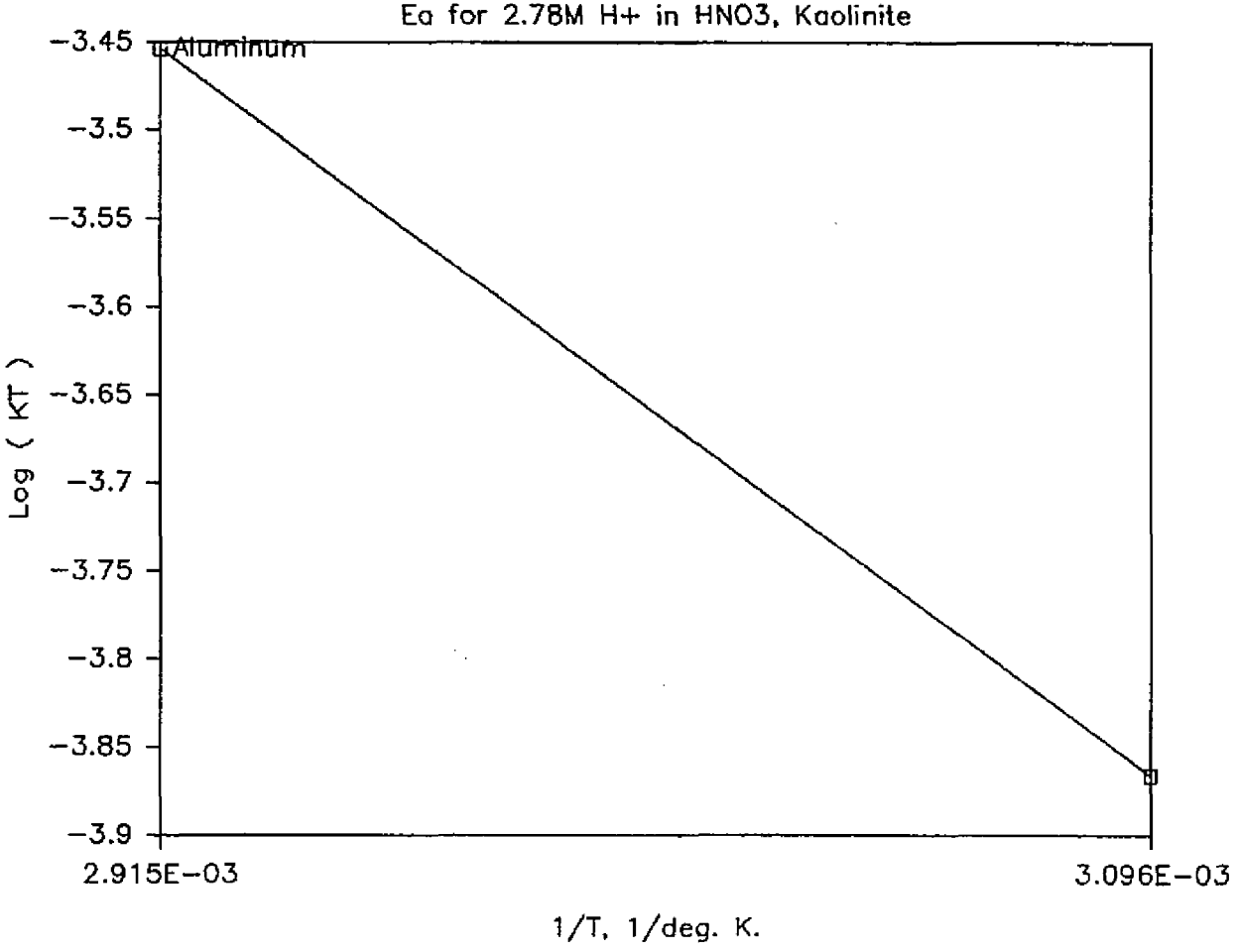
Ea for 2.78M H+ in HNO3, Kaolinite
Aluminum
-3.45
-3.5
-3.55
-3.6
-3.65
-3.7
-3.75
-3.8
-3.85
-3.9
Log (KT)
2.915E-03
3.096E-03
1/T, 1/deg. K.

Figure C9

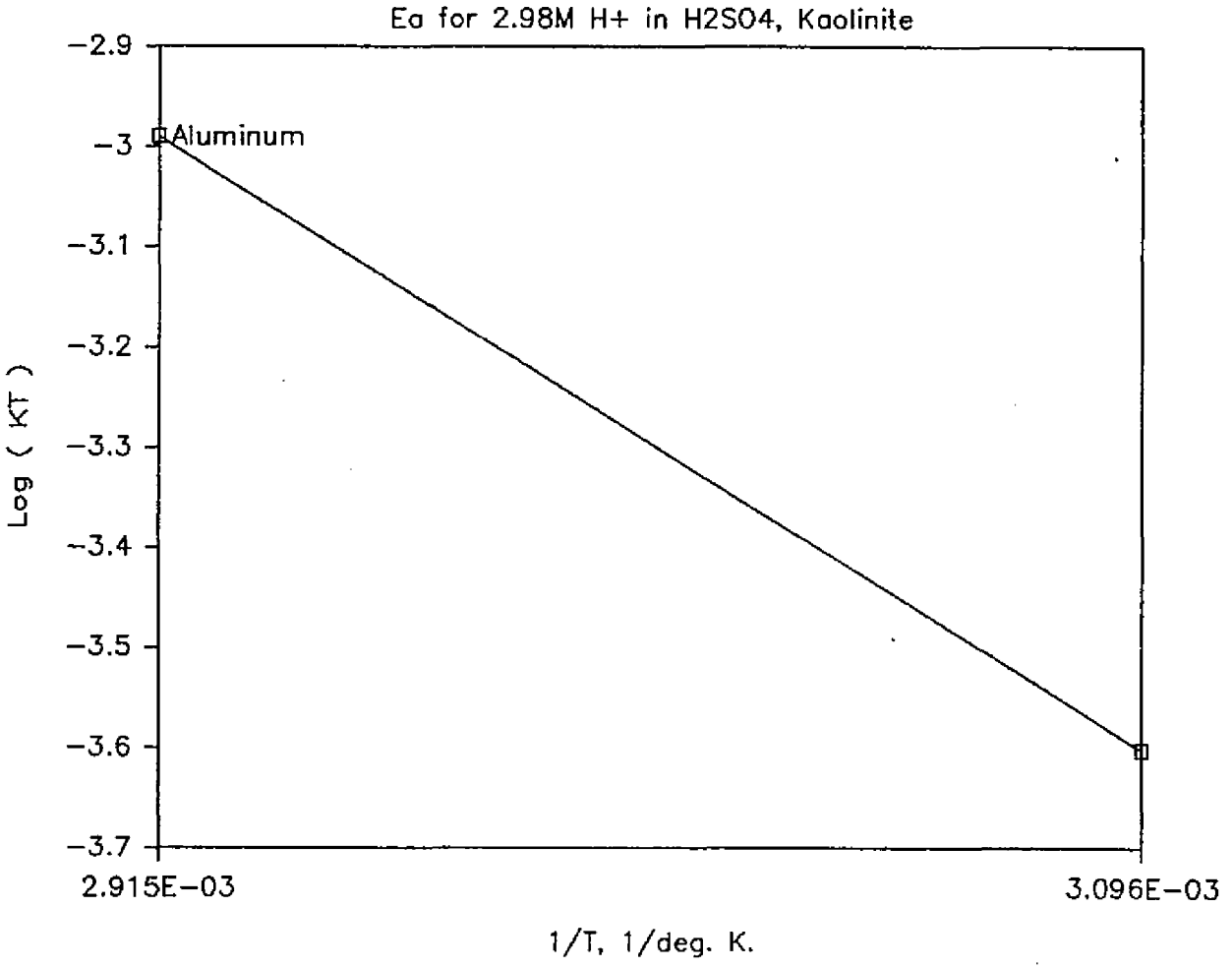
Ea for 2.98M H+ in H2SO4, Kaolinite
-2.9
-3
-3.1
-3.2
-3.3
-3.4
-3.5
-3.6
-3.7
Aluminum
Log (KT)
2.915E-03
3.096E-03
1/T, 1/deg. K.

Figure C10

Ea for .295M H+ in HCl, Kaolinite

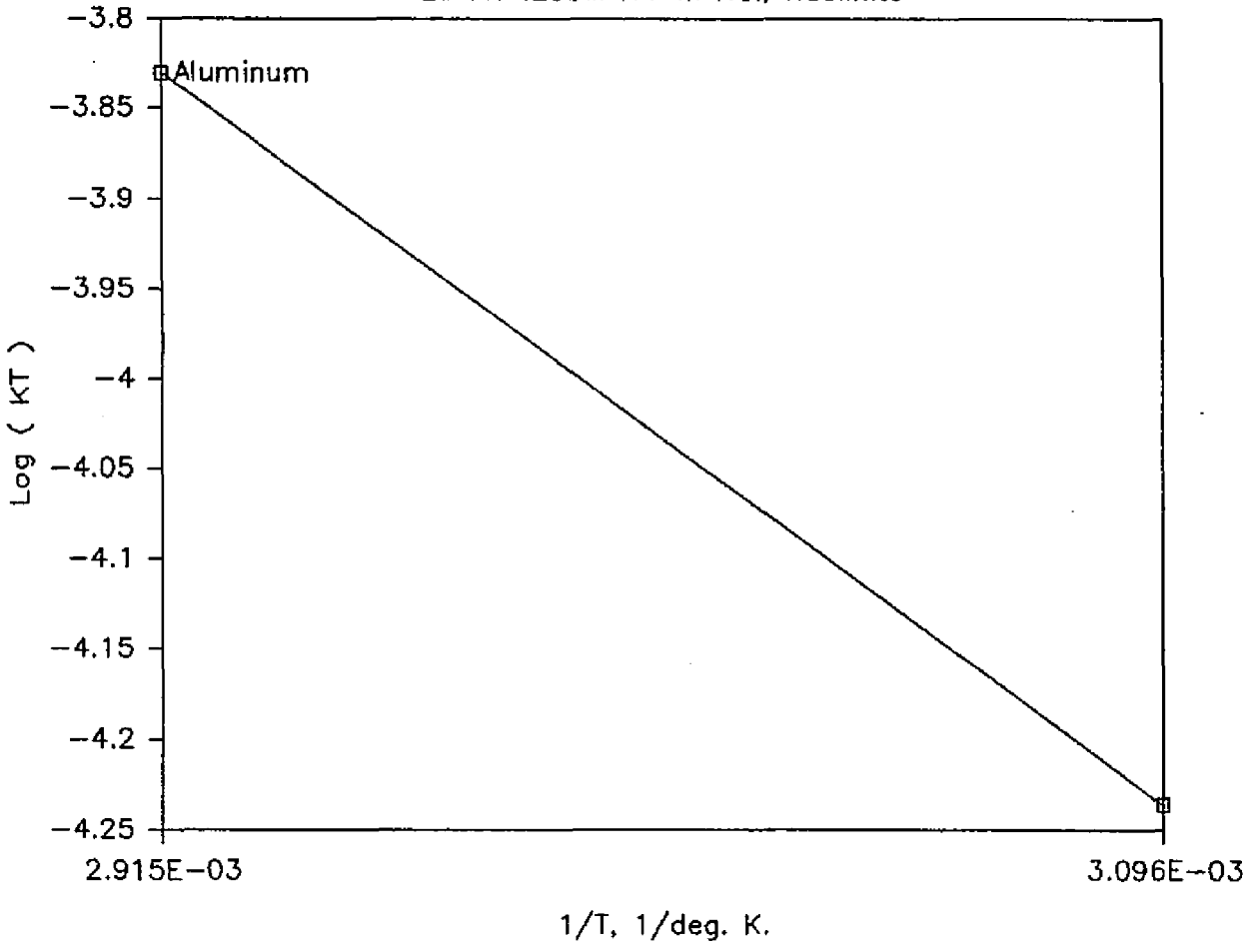

Figure C11

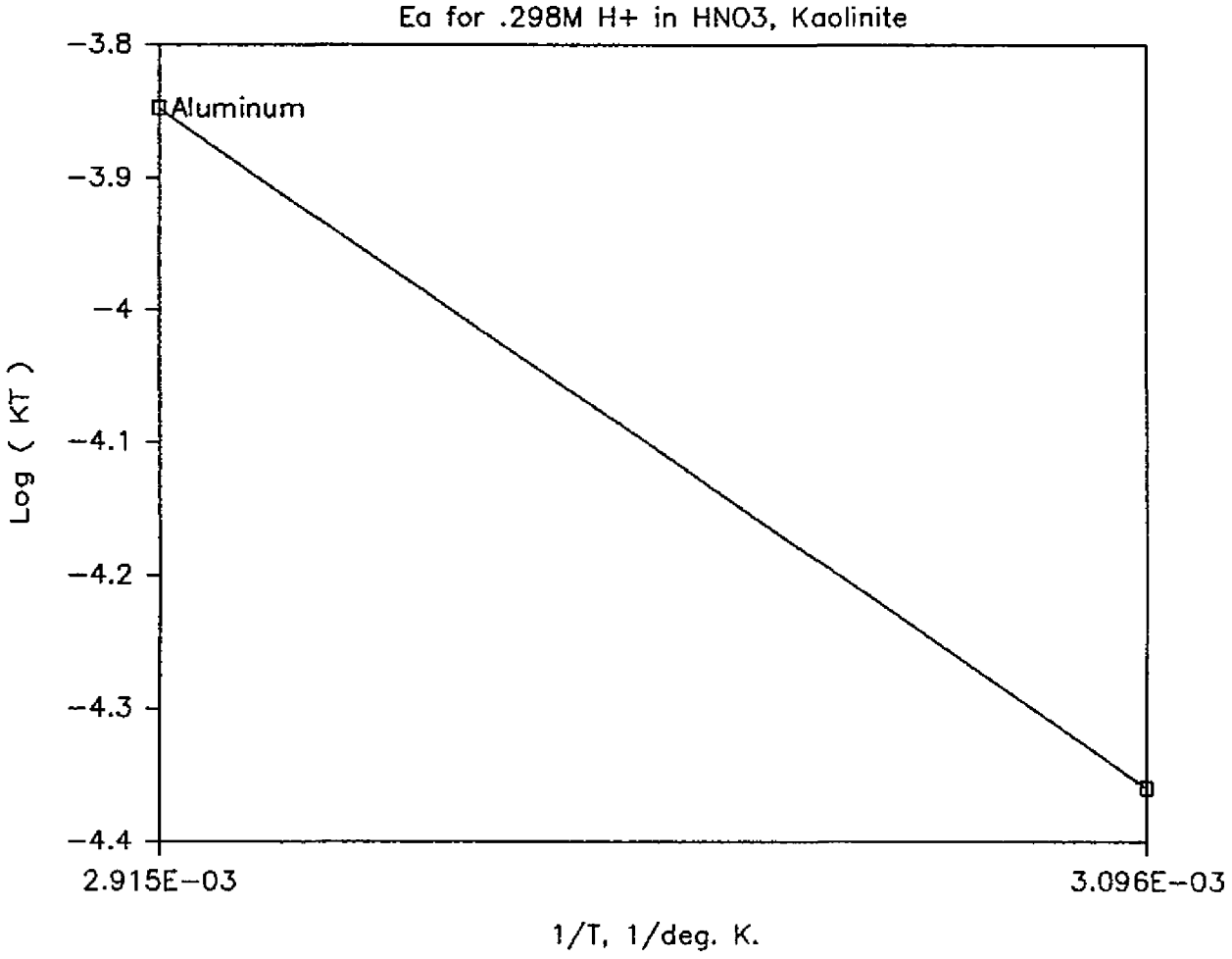
Ea for .298M H+ in HNO3, Kaolinite
Aluminum
-3.8
-3.9
-4
-4.1
-4.2
-4.3
-4.4
Log (KT)
2.915E-03
3.096E-03
1/T, 1/deg. K.

Figure C12

Ea for 0.3M H+ in H2SO4, Kaolinite

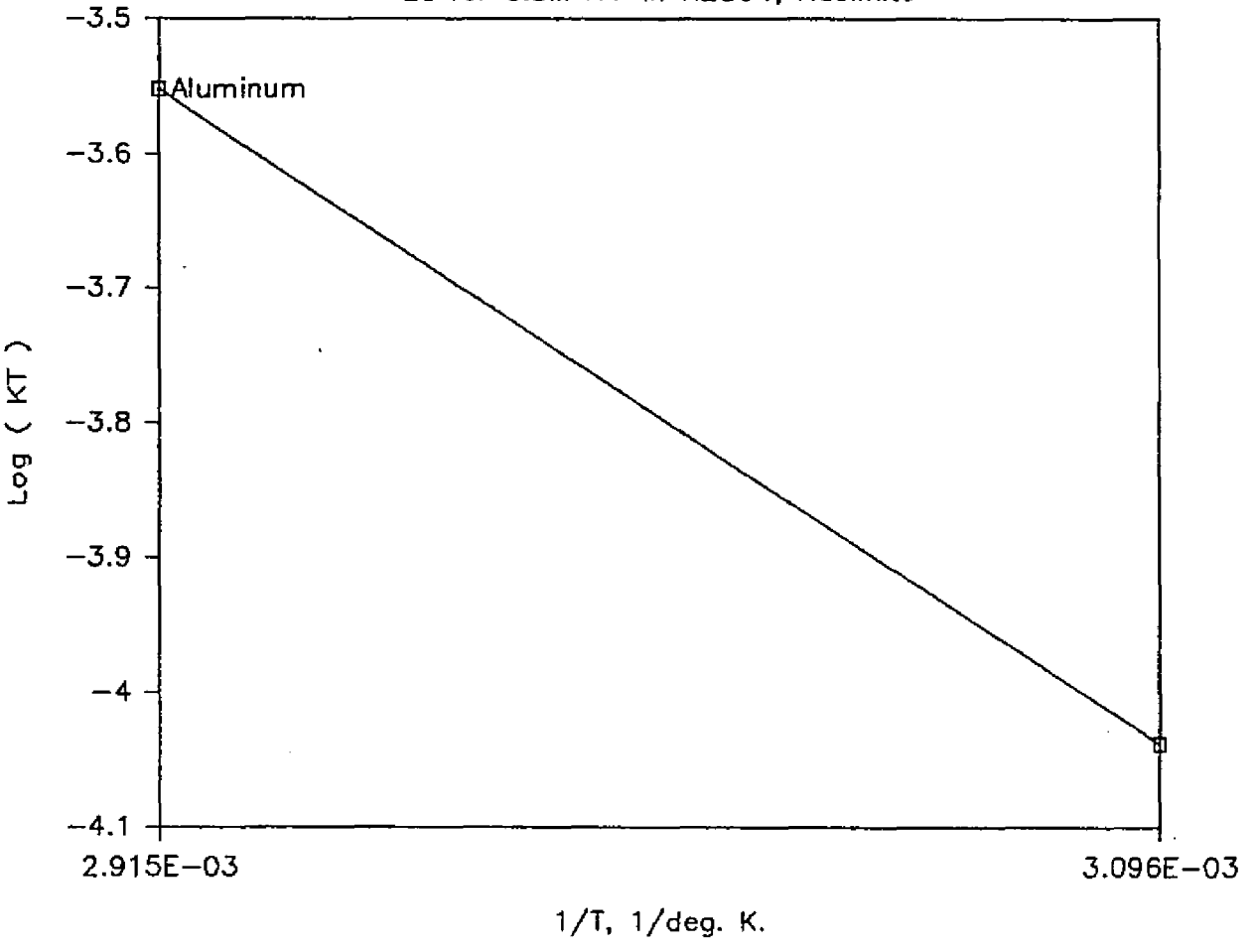

Figure C13

Ea for 2.55M H+ in HCl, Illite

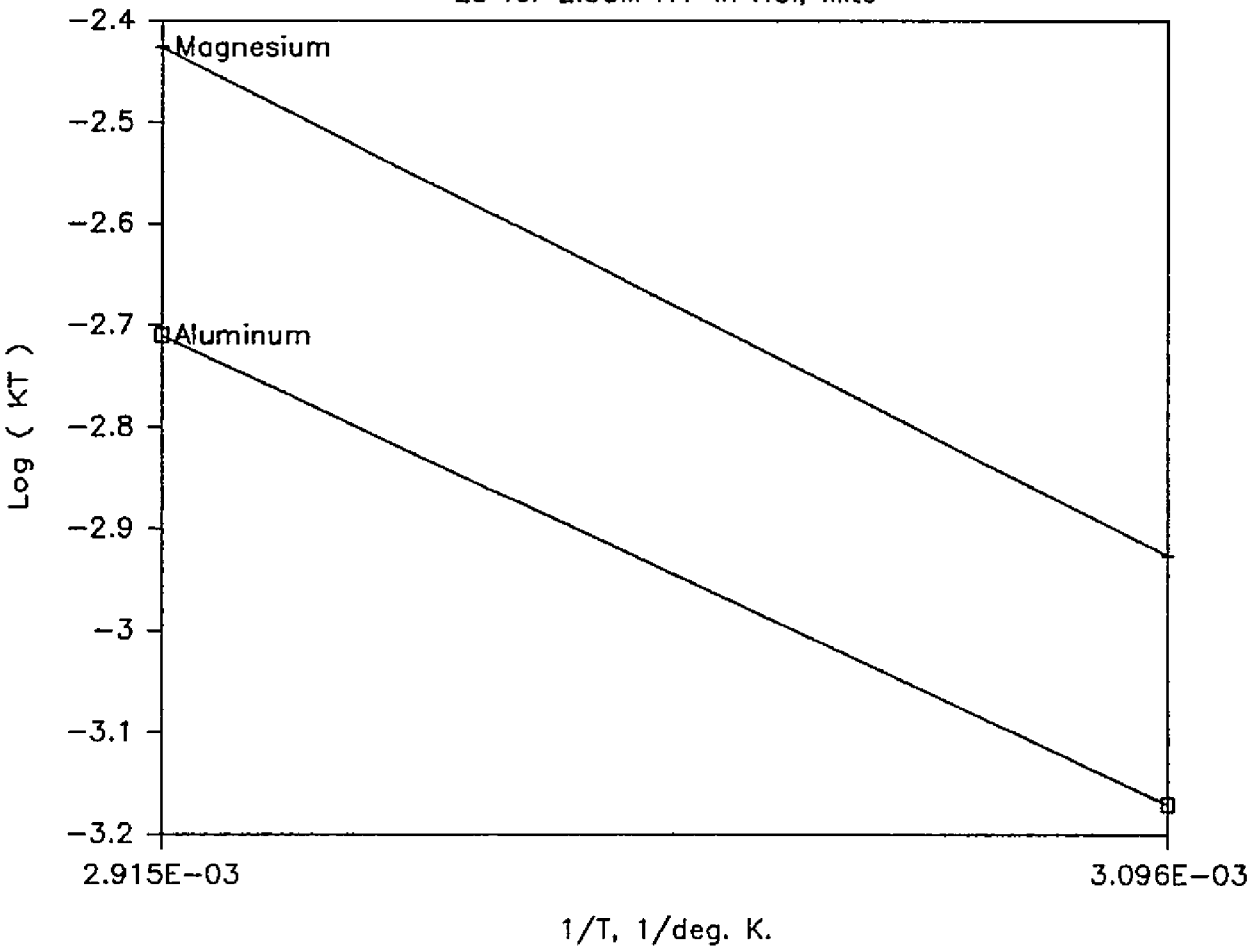

Figure C14

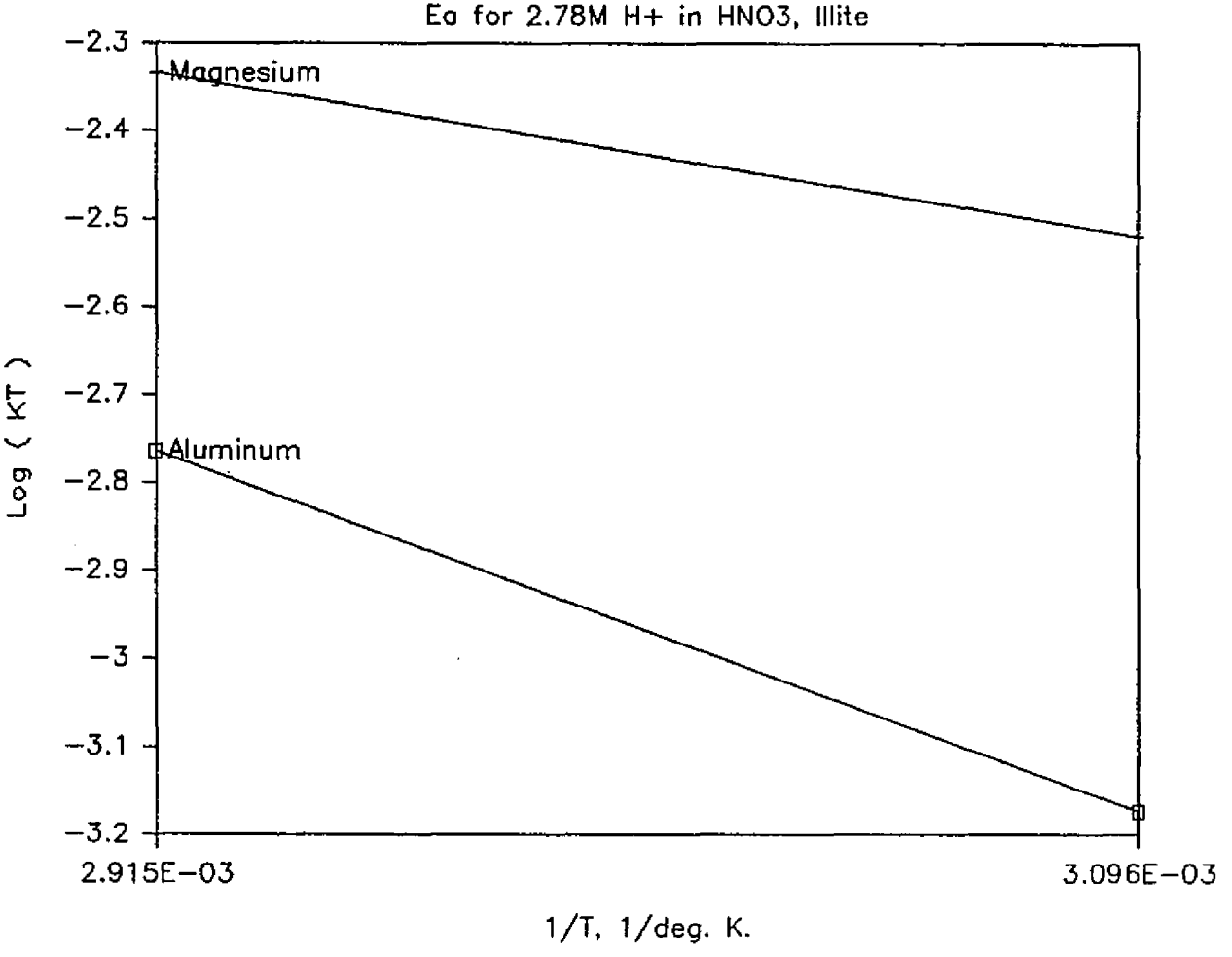
Ea for 2.78M H+ in HNO3, Illite
Magnesium
Aluminum
-2.3
-2.4
-2.5
-2.6
-2.7
-2.8
-2.9
-3
-3.1
-3.2
Log (KT)
2.915E-03
3.096E-03
1/T, 1/deg. K.

Figure C15

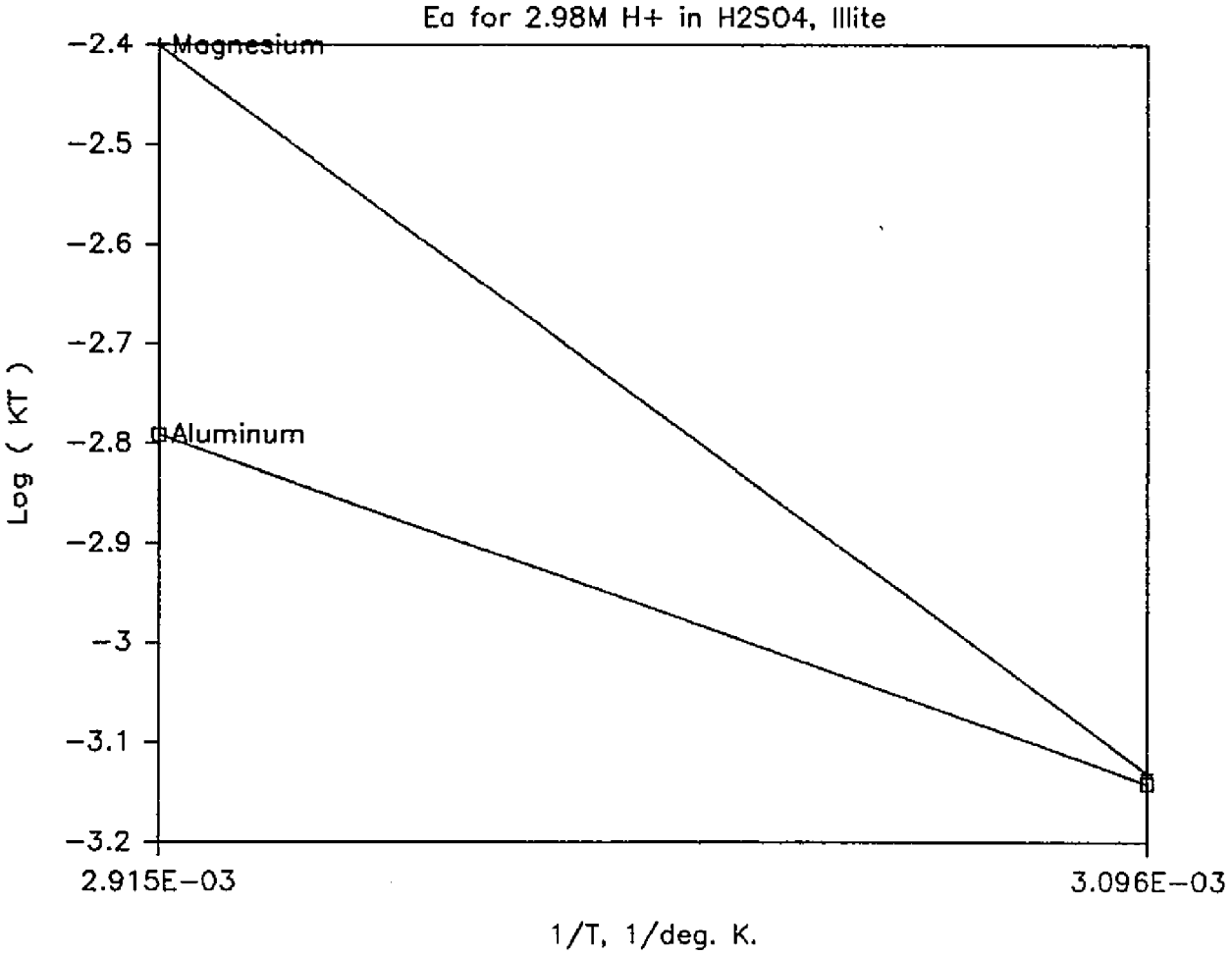
Ea for 2.98M H+ in H2SO4, Illite
Magnesium
Aluminum
-2.4
-2.5
-2.6
-2.7
-2.8
-2.9
-3
-3.1
-3.2
Log (KT)
2.915E-03
3.096E-03
1/T, 1/deg. K.

Figure C16

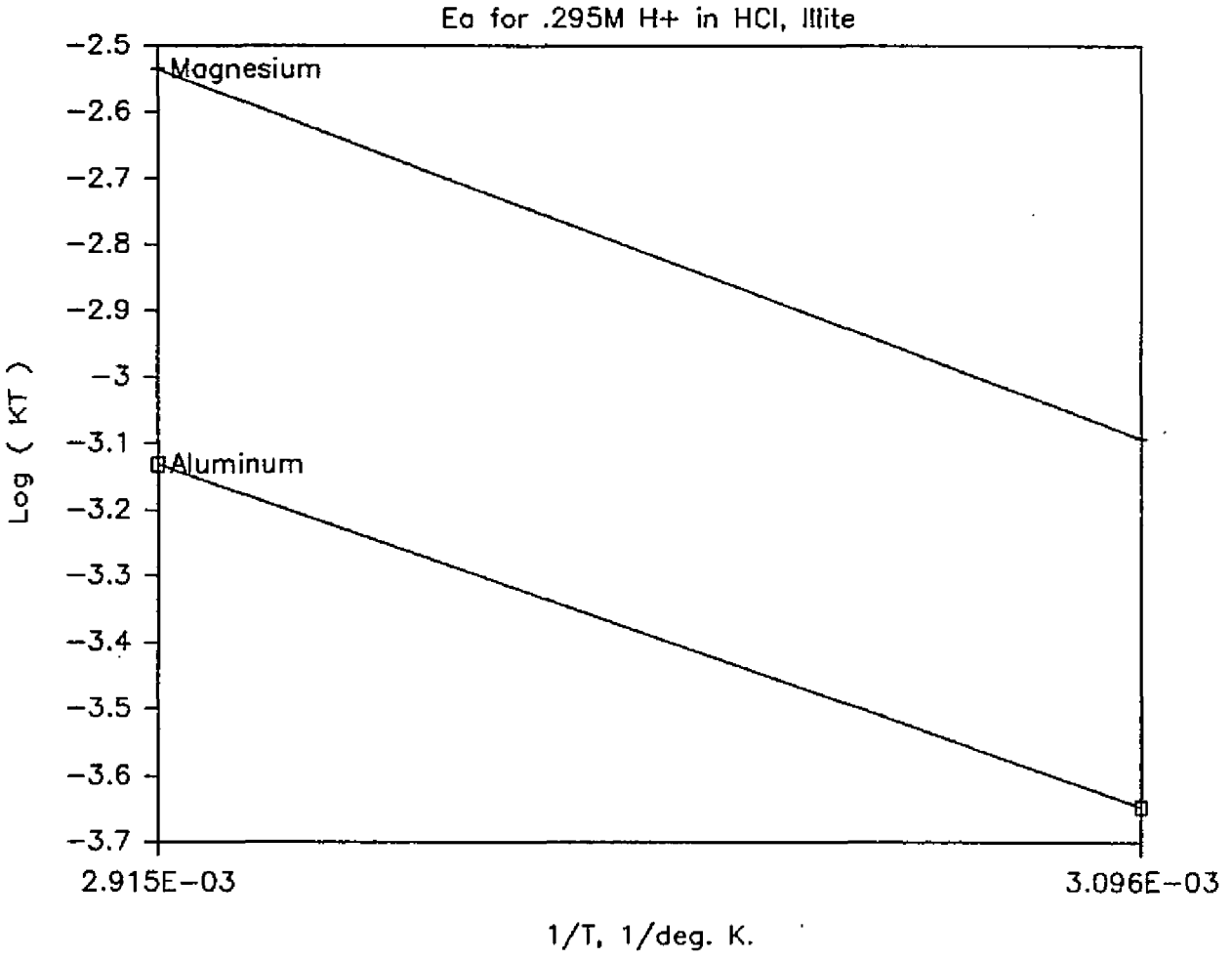
Ea for .295M H+ in HCl, Illite
Magnesium
Aluminum
Log (KT)
-2.5
-2.6
-2.7
-2.8
-2.9
-3
-3.1
-3.2
-3.3
-3.4
-3.5
-3.6
-3.7
2.915E-03
3.096E-03
1/T, 1/deg. K.

Figure C17

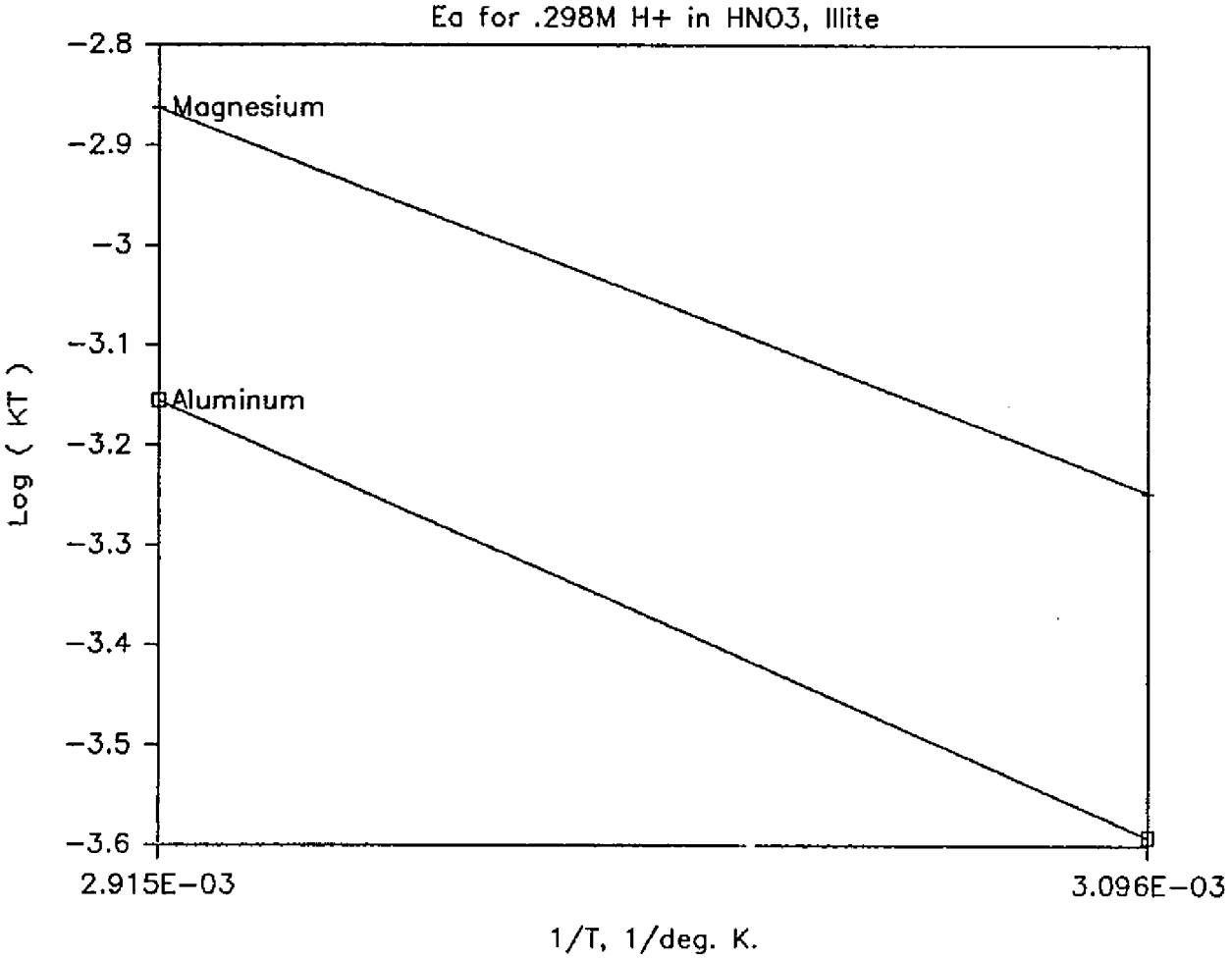
Ea for .298M H+ in HNO3, Illite
Magnesium
Aluminum
Log (KT)
-2.8
-2.9
-3
-3.1
-3.2
-3.3
-3.4
-3.5
-3.6
2.915E-03
3.096E-03
1/T, 1/deg. K.

Figure C18

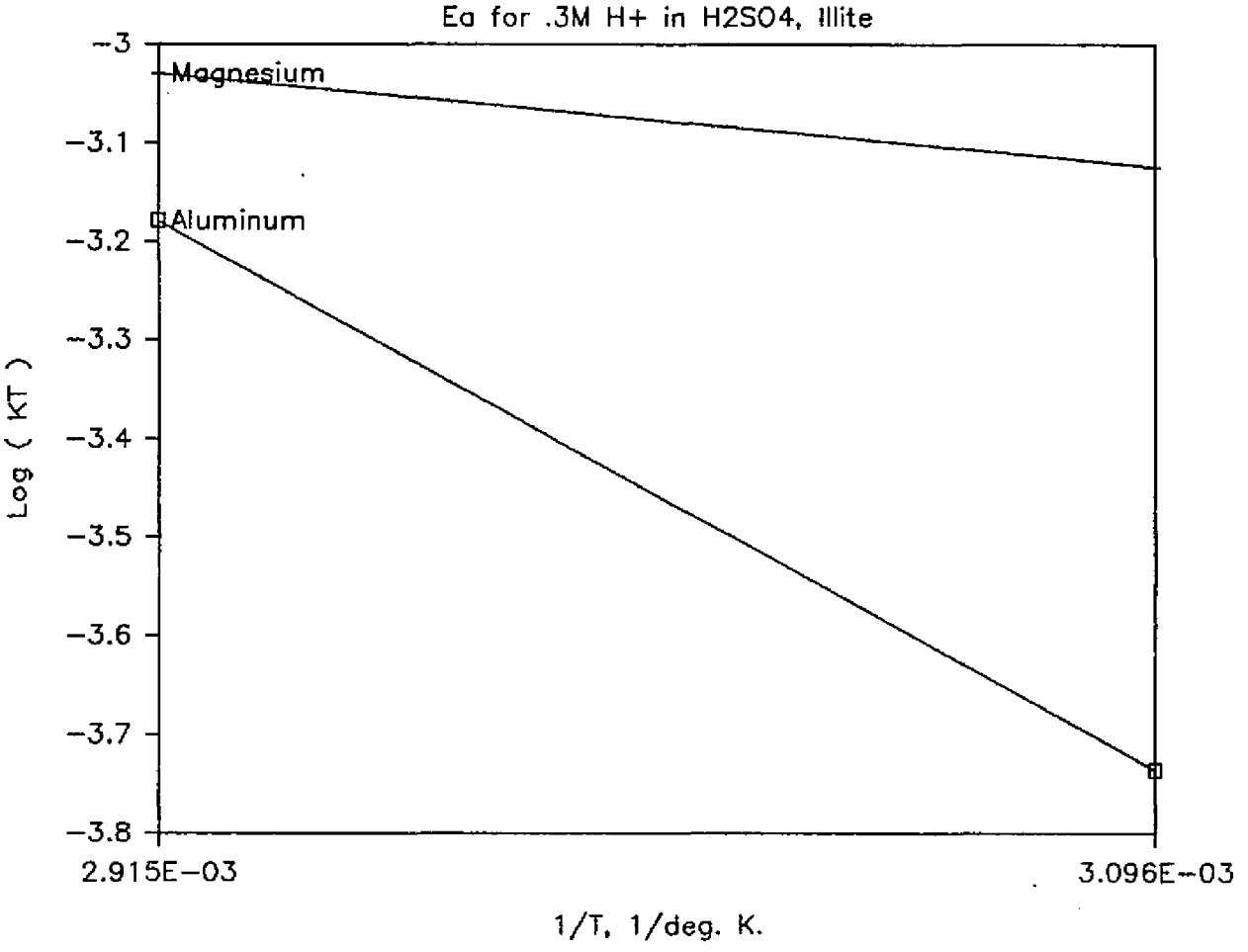
Ea for .3M H+ in H2SO4, Illite
Magnesium
Aluminum
-3
-3.1
-3.2
-3.3
-3.4
-3.5
-3.6
-3.7
-3.8
Log (KT)
2.915E-03
3.096E-03
1/T, 1/deg. K.

VITA

Winton G. Aubert was born in Baton Rouge, Louisiana, on April 10, 1952. He received a B.S. degree in Engineering Science from Louisiana State University (LSU) in 1974, an M.S. degree in Nuclear Engineering from LSU in 1975, and an M.S. degree in Petroleum Engineering from LSU in 1985.

DOCTORAL EXAMINATION AND DISSERTATION REPORT

Candidate: Winton G. Aubert

Major Field: Petroleum Engineering

Title of Dissertation: Fate and Transport of Low-pH Hazardous Materials After Deep Well Disposal

Approved:

Major Professor and Chairman

Dean of the Graduate School

EXAMINING COMMITTEE:

Date of Examination:

December 2, 1986